UNIVERSITEIT VAN PRETORIA
UNIVERSITY OF PRETORIA
YUNIBESITHI YA PRETORIA

A statistical study of the effect of manufacturing methods on the mechanical properties of high-density polyethylene/layered double hydroxide composites

by

Natasha Botha

This thesis is submitted in partial fulfillment of the requirements for the degree

Philosophiae Doctor (Mechanical Engineering)

in the

Department of Mechanical and Aeronautical Engineering
Faculty of Engineering, Built Environment and Information Technology

University of Pretoria
South Africa

2023

ABSTRACT

Title:	A statistical study of the effect of manufacturing methods on the mechanical properties of high-density polyethylene/layered double hydroxide composites
Author:	Natasha Botha
Supervisors:	Dr. H.M. Inglis, Department of Mechanical and Aeronautical Engineering, University of Pretoria Prof. F.J.W.J. Labuschagne, Department of Chemical Engineering, University of Pretoria Dr. R. Coetzer, Department of Statistics, North-West University

Polymer-clay composites have applications in numerous sectors such as packaging, automotive manufacturing and agriculture. A primary focus of polymer composite research is to improve the performance of these composites while also reducing costs. Adding clay to the polymer can enhance the strength and stiffness of the composite. However, adding too much clay can degrade the ductility, hence reducing the usefulness of the material system.

In historical exploratory studies of polymer-clay composites, conducted at the University of Pretoria, it was observed that the mechanical properties were not enhanced as expected by the addition of clay. In fact, the variability observed in the mechanical properties was greater than the effect of increasing the clay weight loading. This could possibly be attributed to manufacturing methods. If polymer-clay composite properties are much more sensitive to manufacturing methods than has been recognised, this is concerning, since bulk manufacturing processes will generally be less tightly controlled than laboratory investigations. By gaining more insight and understanding into the effects of manufacturing variation on the final composite properties it is possible to reduce the issues which inevitably arise when scaling a manufacturing process from a laboratory to an industrial setting.

This study therefore aims to investigate the effects of different manufacturing methods on the statistical variation of the mechanical properties of polymer-clay composites. The mate-

rial system studied is high-density polyethylene (HDPE) filled with layered double hydroxide (LDH), a synthetic clay. A multi-site collaborative study between University of Pretoria (UP, South Africa), Tshwane University of Technology (TUT, South Africa) and Leibniz Institute for Polymer Research (IPF, Germany) was designed. This study is fundamentally interdisciplinary, combining knowledge from polymer materials science, manufacturing, mechanical characterisation and statistics.

A statistical design of experiments was developed using the insights gained from a statistical analysis of historical data and from an in-depth systematic literature review on the effects of manufacturing variation on mechanical properties of HDPE-clay composites. The systematic literature review followed Preferred Items for Systematic Reviews and Meta-Analyses (PRISMA) guidelines. Statistical design of experiments is a robust method to draw reasonable conclusions about the influence of multiple contributing factors on experimental results. The design considered the influence of **manufacturing method** (compression and injection moulding) and **site** (UP, TUT and IPF) in addition to the **clay type** and **clay weight loading** material parameters. Due to the limited mould availability at the South African site, a sub-study considering the influence of the injection moulded **tensile sample mould type** was also included.

A statistical analysis of the experimental results indicated that the moulding method, sample mould type and site (i.e., machine variation) had a larger effect on the mechanical properties then the clay type and clay loading. The effect due to moulding method was expected as it has been documented in literature. The influence of site and sample mould type are important results from this study. The same processing conditions were used at the different sites for both the compression moulding and injection moulding comparisons. The core manufacturing process should not change even when the equipment used is not exactly the same. However, the experimental results demonstrated significant variability as a result of compression moulding on different equipment. The influence of the tensile sample mould type was not expected as the mechanical properties are normalised to the sample geometry, and the comparison was between ISO standard moulds. This raises concerns about the validity of applying experimental test results to predict bulk material performance. This thesis has therefore demonstrated the importance of the consideration of manufacturing variability in studies of polymer-clay composites.

ACKNOWLEDGMENTS

First and foremost I'd like to thank my supervisors, Dr. Helen Inglis, Prof. Johan Labuschagne and Dr. Roelof Coetzer, for their guidance, mentorship and valuable insights throughout this research project.

I'd also like to thank our collaborators for their assistance in the experimental investigation. Dr.-Ing Ines Kühnert and Dr. Andreas Leuteritz from the Institute for Polymer Research in Dresden, Germany; and Dr. Washington Mhike from Tshwane University of Technology in Pretoria, South Africa.

Special thanks to Mr. David Viljoen for his assistance during the systematic literature review and Mrs. Louise Jones for her assistance in compression moulding the samples at the University of Pretoria.

I would also like to mention all the fourth year mechanical engineering students who collected the initial experimental data as part of their final year research projects from 2016 to 2018. The knowledge we gained from this data helped in developing and focussing this research.

I'd like to acknowledge the University of Pretoria Postgraduate Student Fund for providing funding to conduct the experimental work required at the Leibniz Institute for Polymer Research in Dresden, Germany.

And the most important person in my life, my partner, Henriette. She provided me with the necessary emotional support, motivation and space to successfully finish this research.

CONTRIBUTED PUBLICATIONS

Peer-reviewed Conference Publications

1. Botha, N., Inglis, H.M. and Labuschagne, F.J.W.J. (2018). *Analysis of mechanical property degradation in polymer nanoclay composites*, Advances in Composites, Biocomposites and Nanocomposites, vol. 3, pp. 108–120. International Conference on Composites, Biocomposites and Nanocomposites, 7-9 November 2018, Port Elizabeth, South Africa. ISBN: 978-1-9|9858-30-2.

2. Botha, N., Coetzer, R., Inglis, H.M. and Labuschagne, F.J.W.J. (2020). *Understanding the Influence of Manufacturing and Material Parameters on the Mechanical Properties of Polymer-Clay Composites: An Exploratory Statistical Analysis*, AIP Conference Proceedings, vol. 2289, pp. 020061(1–5). Polymer Processing Society Europe-Africa Regional Conference, 18-21 November 2019, Pretoria, South Africa.
DOI: https://doi.org/10.1063/5.0028759.

3. Botha, N., Inglis, H.M., Coetzer, R. and Labuschagne, F.J.W.J. (2021). *Statistical Design of Experiments: An introductory case study for polymer composites manufacturing applications*, MATEC Web of Conferences, Vol. 347, pp. 00028(1–12). 12th South African Conference on Computational and Applied Mechanics, 29 November - 1 December 2021, Cape Town, South Africa. DOI: https://doi.org/10.1051/matecconf/202134700028.

Preprint Publications

1. Botha, N., Coetzer, R., Inglis, H.M. and Labuschagne, F.J.W.J. (2019). *Understanding the Influence of manufacturing and material Parameters on the mechanical properties of polymer-clay composites: An exploratory statistical analysis*, ChemRxiv Preprint. Available from: https://doi.org/10.26434/chemrxiv.10247522.v1.

In Preparation: Peer-reviewed Journal Publications

1. Botha, N., Viljoen, D., Inglis, H.M. and Labuschagne, F.J.W.J. (2022). *A systematic literature review considering the effect of manufacturing variation on the mechanical properties of high-density polyethylene/montmorillonite composites.*

2. Botha, N., Coetzer, R., Inglis, H.M. and Labuschagne, F.J.W.J., *Statistical design of experiments in polymer composite manufacturing applications.*

3. Botha, N., Leuteritz, A., Kühnert, I., Mhike, W., Coetzer, R., Inglis, H.M. and Labuschagne, F.J.W.J., *Influence of tensile sample mould type on the mechanical properties of high-density polyethylene/layered double hydroxides.*

4. Botha, N., Leuteritz, A., Kühnert, I., Mhike, W., Coetzer, R., Inglis, H.M. and Labuschagne, F.J.W.J., *Moulding method and machine variation influence on the mechanical properties of high-density polyethylene/layered double hydroxides.*

CONTENTS

NOMENCLATURE

Roman Symbols

A	Area (mm^2)
d	Displacement (mm)
E	Young's modulus (MPa)
F	Load (N)
k	Design factors or machine stiffness (N/mm)
L	Length (mm)
m	Mass (g)
n	Experimental design point or number of levels
N	Number of experimental runs
p	Model parameters
r	Number of categorical factors or number of replication points
W	Design weight matrix
x	Clay loading (wt%) or Number of continuous factors
X	Model Matrix
y	Response variable
z	Categorical dummy variables

Greek Symbols

α	Distance from the design center
β	Regression model coefficients
σ	Stress (MPa)
ϵ	Strain (mm/mm)
ω	Design weight
ω^2	Descriptive statistical variable denoting proportion of variation in response variable

Statistical Symbols

Df	Degrees of Freedom
F-value	Compares the variability of two groups
MS	Mean square error
p-value	probability that an effect is by chance
Pr(>F)	Accuracy of determination of F-value or p-value
R^2	Explained variation
SE	Estimated standard error which is the standard deviation of the t-value probability distribution
Sum Sq or SS	Sum-of-squares
t-value	Compares the difference in means of two groups
Pr(|t|)	Accuracy of determination of t-value or p-value

Math Symbols

$\sum$	Summation
bold	Matrix
|..|	Determinant
$\underline{\underline{..}}$	Vector
Δ	Change
$..'$	Transpose
$\hat{..}$	Predicted or estimated

Subscripts

between	variability between groups
c	Clay
cat	Categorical variable group
corrected	Corrected value
effect	Between groups
error	Error
f	Failure
FPS	First peak stress (MPa)
gopt	Global D-optimal Design
i	Denotes a number
j	Denotes a number
l	Denotes a number

mean	Mean
measured	Value obtained from machine
o	Original
p	Polymer
total	Total
within	variability within groups

Superscripts

k	Number of factors

Acronymns

ANOVA	Analysis of Variance
ASTM	American Society for Testing and Materials
Ax	Axial Point
BBD	Box-Behnken Design
BK	Buss Kneader
C/C	Clay/Compatibiliser
CCD	Central Composite Design
CI	Confidence Intervals
CO_2	Carbon Dioxide
CP	Center Point
DB	Dry Blending
DM	Direct Mixing
DMA	Dynamic Mechanical Analysis
DoE	Statistical Design of Experiments
EDA	Exploratory Data Analysis
Fac	Factorial Point
FPS	First Peak Stress (MPa)
GDP	Gross Domestic Product
H	High
HDPE	High Density Polyethylene
HSD	Honest Significant Difference
IM	Internal Mixing
IP	In-situ Polymerisation
IPF	Leibniz Institute for Polymer Research
ISO	International Organisation for Standardisation

L	Low
L/D	Length to Diameter ratio
LDH	Layered Double Hydroxide
LDPE	Low Density Polyethylene
LOF	Lack of Fit Point
MDPE	Medium Density Polyethylene
MMT	Montmorillonite
PA	Poly-amide
P/C/C	Polymer/Clay/Compatibiliser
PE	Polyethylene
PP	Polypropylene
PVC	Polyvinyl chloride
PRISMA	Preferred Reporting Items for Systematic Reviews and Meta-Analyses
QA	Quiescent Annealing
R&D	Research and Development
Rep	Replication Point
RSM	Response Surface Methodology
SD	Standard Deviation
SEM	Standard Error of Mean
SI	Solution Intercalation
SPV	Scaled Prediction Variance
SSE	Single-screw Extrusion
SSE EFF	Single-screw Extrusion with Extensional-flow Mixer
TEM	Transmission Electron Microscopy
TSE	Twin-screw Extrusion
TUT	Tshwane University of Technology
UP	University of Pretoria
WA TSE	Water-assisted Twin-screw Extrusion
WAXD	Wide angle X-ray Diffraction
wt%	Weight percentage

LIST OF FIGURES

LIST OF TABLES

CHAPTER 1

INTRODUCTION

1.1 Background

The South African plastics industry contributed 2.3 % to the country's GDP and 18.5 % to the manufacturing GDP in 2019 (Plastics SA, 2020). The largest contributor is the plastics packaging sector (Department of Trade and Industry, 2018; Plastics SA, 2020). Examples include plastic bottles, piping, bags, food storage containers, etc. Some key limitations to South Africa's global competitiveness in the plastics manufacturing industry are high costs and access to raw materials in the plastics value chain, the small local and regional market, the lack of advanced manufacturing practices and downstream focus on R&D, and high logistics costs due to South Africa's geographic location (Department of Trade and Industry, 2018). Several programmes and interventions have been developed in the country with collaboration between the government, industry and academic institutions to address these limitations. To compete on a global level in the plastics manufacturing industry South Africa needs to improve and update its bulk manufacturing processes. Understanding the influences of manufacturing variation on material behaviour in a controlled laboratory setting is a first step towards improving the efficiency of industrial polymer composite manufacturing.

1.1.1 Particulate Composite Materials

Polyethylene-based polymers are popularly used in the plastics industry as they are versatile, cost effective, light weight, ductile and can easily be processed using heat-based techniques such as extrusion and injection moulding (Khanam and AlMaadeed, 2015; Osman and Atallah, 2004). Polyethylene (PE) is a semi-crystalline thermoplastic polymer. Thermoplastics soften when heated and harden when cooled, processes which can be repeated and are reversible (Callister, Jr., 2003), in contrast with thermoset polymers. Crystallinity refers to the level of alignment of the polymer chains, in other words, how the chains are packed together (Callister, Jr., 2003). A semi-crystalline polymer structure is illustrated in Figure 1.1, where

the long polymer chains fold in a regular packing orientation around an amorphous region. The amorphous region is the material that has no crystalline structures (Callister, Jr., 2003). Variants of PE are classified, based on their density and branching, as low-density PE (LDPE), medium-density PE (MDPE) and high-density PE (HDPE). HDPE has long linear chains without any major branching resulting in regular packing with a higher crystallinity. LDPE on the other hand has many long branches resulting in a more irregular packing with low crystallinity. LDPE is more flexible than HDPE with lower tensile and compressive strengths. (Khanam and AlMaadeed, 2015).

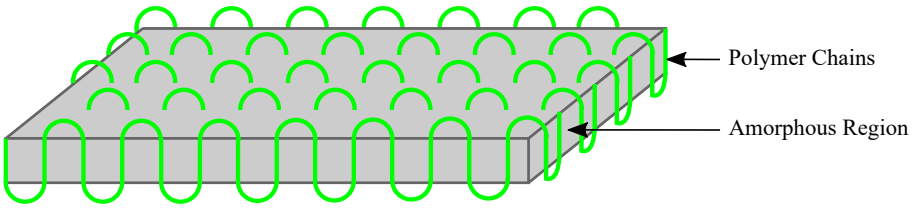

Figure 1.1: Illustration of a semi-crystalline polyethylene structure with folded polymer chains around an amorphous region. [Redrawn from Callister, Jr. (2003)]

To further reduce the cost or improve desired properties of polymer products, fillers — among them micro or nanoclays — are frequently added to form composite materials. Particulate composite materials are a combination of two or more sub-components of materials and consist of a polymer matrix and a filler. Clay particles are a common filler with a layered mineral structure consisting of nanometer-thick silicate layers, and are often referred to as layered silicates (Azeez *et al.*, 2013). By adding these clay fillers the final particulate composite material may have improved material, thermal and electrical properties, as well as a high strength-to-weight ratio at lower costs, all desirable traits for various industrial applications (Gao, 2004; Jordan *et al.*, 2005; Fu *et al.*, 2008; Albdiry *et al.*, 2012; Azeez *et al.*, 2013; El-Sheikhy and Al-Shamrani, 2015; Khanam and AlMaadeed, 2015; Zabihi *et al.*, 2018). However, adding particles to a semi-crystalline polymer such as polyethylene leads to changes within the polymer morphology. In particular the polymer crystallinity is affected, which may result in the degradation of some properties (Osman and Atallah, 2004).

Layered silicates can be dispersed into individual layers, and their surface chemistry can be modified to change the interaction between the clay and polymer (Choudalakis and Gotsis, 2009). The resulting particulate composite material can be classified into one of three different states, dependent on how the polymer matrix and filler are mixed together (Albdiry *et al.*, 2012), referred to as the composite morphology. The three states — immiscible, intercalated and exfoliated — are illustrated in Figure 1.2 and show the degree of dispersion of the filler (represented as lines to reflect the layered structure) in the polymer matrix. An **immiscible** composite, Figure 1.2(a), occurs when the phases remain separate since the chemical bonds within each phase are strong, also known as phase-separated. Figure 1.2(b) shows an **intercalated** state where some polymer chains are located between the filler layers. In **exfoliated** composites, Figure 1.2(c), filler layers are increasingly separated, resulting in random dispersion through the polymer. The level of dispersion of the composite is normally identified using

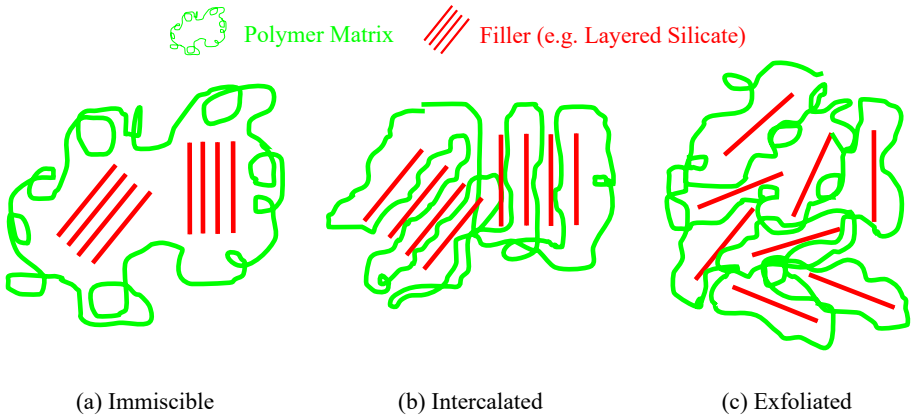

Figure 1.2: Overview of the three states of dispersion in a particulate polymer-clay composite system. [Redrawn from Albdiry *et al.* (2012); Azeez *et al.* (2013); Chen *et al.* (2008, 2013); Fu *et al.* (2019); Paul and Robeson (2008)]

wide angle X-ray diffraction (WAXD) and Transmission Electron Microscopy (TEM) (Azeez *et al.*, 2013; Jordan *et al.*, 2005). The level of dispersion is a critical contributing factor to the properties of the composite. The ideal state for proper dispersion would be exfoliation, which ensures enhanced overall properties of the composite (Nguyen and Baird, 2006; Zabihi *et al.*, 2018). The level of dispersion is dependent on optimisation of the compounding conditions, and it is not always possible to obtain ideal dispersion (Paul and Robeson, 2008). The effects of compounding have therefore been investigated in several studies considering different compounding methods (Boran *et al.*, 2017; Brandenburg *et al.*, 2014; Esteki *et al.*, 2013; Heinemann *et al.*, 1999; Höfler *et al.*, 2018; Merinska *et al.*, 2012; Minkova and Filippi, 2011; Silva *et al.*, 2014) and varying the compounding conditions (Barbosa *et al.*, 2012; Gong *et al.*, 2013; Huang *et al.*, 2015; Lapshin *et al.*, 2008; Li *et al.*, 2007; Mainil *et al.*, 2006; Nguyen and Baird, 2006; Oliveira *et al.*, 2009; Swain and Isayev, 2006, 2007; Ujianto *et al.*, 2018).

The choice of clay is dependent on the desired overall polymer composite properties for a specific application. Montmorillonite (MMT) is a natural clay popularly used due to its unique natural characteristics (high surface area and surface reactivity) which tend to provide improvements to the polymer composite properties (Azeez *et al.*, 2013; Hussain *et al.*, 2006; Kotal and Bhowmick, 2015). The MMT crystal structure consists of two silicate tetrahedral layers with an octahedral layer of aluminum or magnesium sandwiched in between (Fu *et al.*, 2019; Kotal and Bhowmick, 2015; Paul and Robeson, 2008). These layers are stacked in parallel with van der Waals gaps between them, often known as the interlayer or gallery (Azeez *et al.*, 2013; Fu *et al.*, 2019; Kotal and Bhowmick, 2015). MMTs are primarily negatively charged which is characterised by the cation exchange capacity (Paul and Robeson, 2008). A higher cation exchange capacity is indicative of a higher hydration, swelling and dispersion capacity (Azeez *et al.*, 2013). A common alternative to MMT is synthetic clays known as layered double hydroxides (LDH) which are structurally similar with opposite charge of the hydroxide layers (Costa *et al.*, 2005; Kotal and Bhowmick, 2015). LDH has a brucite-like (or hydrotalcite) structure with a single octahedron layer containing Mg^{2+} surrounded by hydroxyl groups (Kotal and Bhowmick, 2015; Labuschagne *et al.*, 2015). LDHs are primarily

positively charged which is characterised by the anion exchange capacity (Dabrowska *et al.*, 2013; Kotal and Bhowmick, 2015). A major advantage of using LDH compared to MMT is the ability to manipulate the clay chemical and physical properties during synthesis to provide improvements on specifically desired properties (Costa *et al.*, 2005; Kotal and Bhowmick, 2015; Moyo *et al.*, 2012, 2013). A disadvantage, however, is that the anion exchange capacity for LDH is quite high compared to the cation exchange capacity for MMT (Kotal and Bhowmick, 2015). Even though MMT-based composites are more likely to provide enhanced mechanical properties with only a small amount, LDH-based composites will have more exfoliated layers per unit amount of filler (Kotal and Bhowmick, 2015). This is due to the crystal structure where each layer of LDH is only composed of a single octahedral sheet, whereas MMT contains multiple octahedral/tetrahedral sheets (Kotal and Bhowmick, 2015). MMT is considered far more often in literature compared to LDH, because it is more familiar (Costa *et al.*, 2005; Dabrowska *et al.*, 2013). LDH is often considered for its enhanced thermal stability and flammability properties (Kotal and Bhowmick, 2015; Labuschagne *et al.*, 2015; Moyo *et al.*, 2012, 2013). Mg-Al LDH is one of the most commonly considered in literature due to its availability, high anion exhange capacity and low charge density (Kotal and Bhowmick, 2015; Moyo *et al.*, 2012). A summary of the key characteristics of both MMTs and LDHs is provided in Table 1.1.

Table 1.1: Summary of key characteristics of montmorillonite (MMT) and layered double hydroxides (LDHs). (Kotal and Bhowmick, 2015; Labuschagne *et al.*, 2015; Moyo *et al.*, 2012, 2013)

Clay	Chemical Formula	Ion Type	Exchange Capacity (mequiv/100 g)
MMT	$(Na,Ca)_{0.33}(Al,Mg)_2(\text{-}Si_4\ O_{10})(OH)_2mH_2O$	Cation	80-150
LDH	$[M^{II}_{1-x}\ M^{III}_x(OH)_2]^{x+}(A^{n-})_{x/n}mH_2O$	Anion	200-400
Mg-Al LDH	$[Mg_{1-x}Al_x(OH)_2]^{x+}(A^{n-})_{x/n}mH_2O$	Anion	200-400

M^{II}: divalent cation (Mg^{2+}, Zn^{2+}, Fe^{2+}, Co^{2+}, Ni^{2+}, Cu^{2+}); M^{III}: trivalent cation (Al^{3+}, Fe^{3+}, Cr^{3+}, Mn^{3+}); A^{n-}: interlayer anion (Cl^-, CO_3^-, NO_3^-, etc.); x: net positive charge where $0.2 \leq x \leq 0.36$; and m: number of co-intercalated water molecules

A challenge to overcome during dispersion is the incompatibility between the hydrophilic clays and the hydrophobic polymers, leading to poor clay-polymer interactions (Rong *et al.*, 2006). This is normally addressed by either modifying the surface of the clay (Azeez *et al.*, 2013; Crosby and Lee, 2007; Fu *et al.*, 2019; Rong *et al.*, 2006) or incorporating a compatibiliser into the composite (Barbosa *et al.*, 2012; Lei *et al.*, 2007; Merinska *et al.*, 2012; Rong *et al.*, 2006). The clay is converted into an organophilic clay by modifying the surface through an exchange of ions (Chen *et al.*, 2013; Kotal and Bhowmick, 2015). Modification of the clay surface ultimately allows for the expansion of the interlayer space, the area between the layered silicate and polymer matrix. Surface modification thus improves diffusion of the polymer into the interlayer space, leading to improved dispersion (Azeez *et al.*, 2013; Fu *et al.*, 2019; Rong *et al.*, 2006). A compatibiliser acts as a lubricant between the clay and polymer increasing their interactions, consequently improving the level of dispersion.

LDH has been used in several industrial applications, both on its own and together with other polymers, and its global market size is expected to reach USD 381.6 million by 2027

(360 Research Reports, 2022). LDH is commercially available from companies such as Kisuma (Kisuma, 2023), Ataman Chemicals (Ataman Chemicals, 2020) and Kyowa Chemical Industry (Kyowa Chemical Industry, 2022). Typical commercial applications of LDH-polymer composites include packaging (e.g., polyolefin films, rigid packaging, thermoforming); and automotive (e.g. thermoplastic compounds, coatings, adhesives, sealants, wires and cables) to name a few (Kisuma, 2023).

1.1.2 Manufacturing: Compounding and Moulding

Particulate polymer composites are manufactured in two stages to produce a testing sample or final component. In some sources these stages are both referred to as processing, with a distinction between primary and secondary processing. In this discussion I will refer to the primary processing as **compounding** and the secondary processing as **moulding**. Compounding is the process in which the powdered mix of polymer and clay is combined into the composite material. Moulding is then applied to form the compounded composite material into the final component. In this thesis, the final component will be a sample which can be tested to characterise the composite mechanical properties.

The choice of compounding method is largely dependent on the desired level of dispersion. An intercalated structure can be obtained by either melt blending (*e.g.* internal mixing or

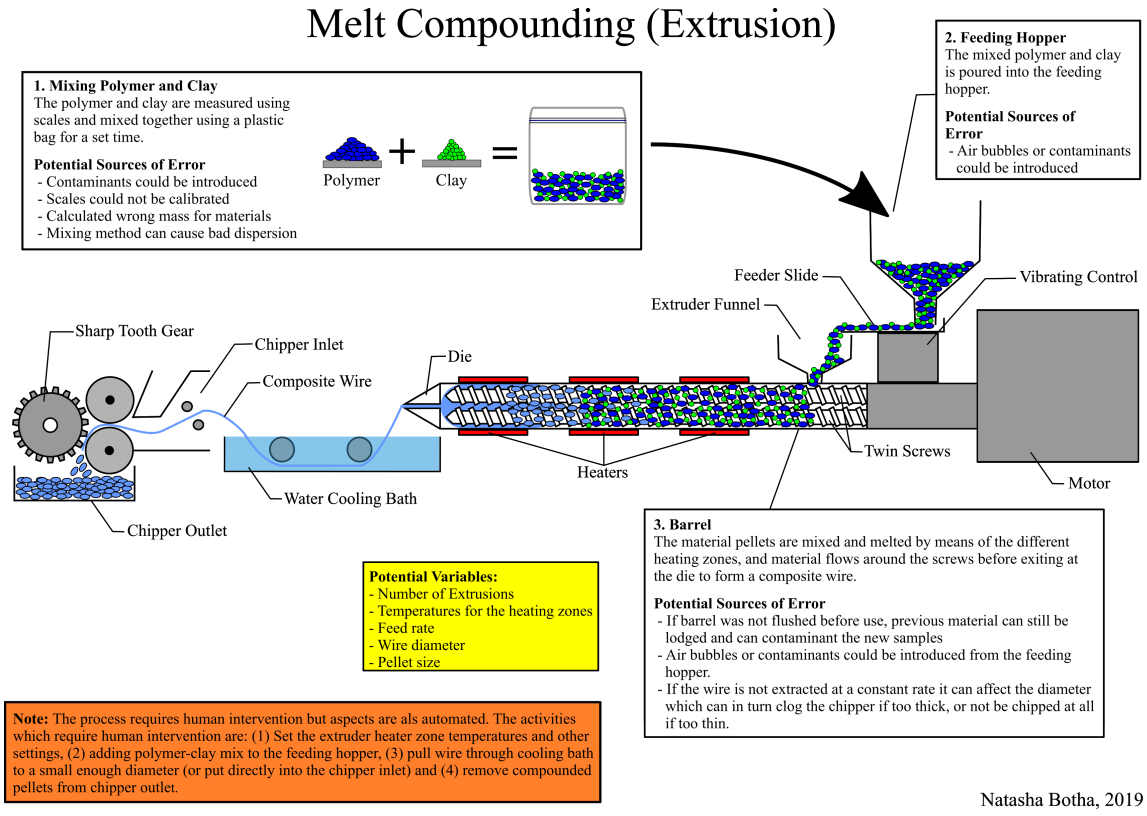

Figure 1.3: Graphical representation of the melt compounding process via extrusion including all the potential sources of error.

extrusion) or in-situ polymerisation, and an exfoliated structure is dependent on the clay, compounding method and any curing agents considered (Jordan *et al.*, 2005). Extrusion is the most popular method of compounding, employing either a single or twin-screw approach, as it is more economical while being flexible for different formulations (Albdiry *et al.*, 2012; Agassant *et al.*, 2017; El-Sheikhy and Al-Shamrani, 2015; Paul and Robeson, 2008). The melt compounding process with a co-rotating twin-screw extruder is illustrated in Figure 1.3. This figure lists potential sources of error that may occur during the process. A twin-screw extruder has two screws that are parallel to one another and rotate in the same direction (Agassant *et al.*, 2017). The extrusion process has three distinct zones: solid-conveying, melting and melt flow (Agassant *et al.*, 2017). During solid-conveying the mixed polymer and clay is first fed into the hopper, before the solid material is conveyed from the feeder to the screws with a fixed feed rate. A positive displacement effect is created by the rotation of the screw which ultimately pushes the solid downstream through the barrel, further mixing the composite. In the melting zone the solid composite melts as it flows over the heating elements with a temperature range between 190 and 230 °C, higher than the melting temperature of the polymer. The melt flow is then pushed through the die end to obtain the desired cross-section, in this case a thin wire (also known as an extrudite), where it solidifies. The extrudite is then quenched in water to cool down before being fed into the chipper to produce pellets. (Agassant *et al.*, 2017; Khanam and AlMaadeed, 2015). Key compounding conditions that can be varied are: barrel heating zone temperature profile, screw speed, feed rate, mixing duration (also referred to as residence time), number of extrusions and die pressure (Albdiry *et al.*, 2012). For example, longer residence times lead to better dispersion while screw configuration also plays a role in achieving better dispersion (Paul and Robeson, 2008).

Once a particulate composite material is compounded it is necessary to shape it into a usable component. For polymer-clay materials this is usually done by means of moulding methods such as injection and compression moulding. Both moulding methods have applications in industry where compression moulding is often used in a high production volume environment requiring high strength components such as the automotive industry; and injection moulding is preferred for higher quality and precision products such as required in the electronics industry (Asim *et al.*, 2017). For commercial production injection moulding is preferred (Agassant *et al.*, 2017; Gao, 2004; Khanam and AlMaadeed, 2015), however Jordan *et al.* (2005) note that researchers prefer compression moulding. The compression moulding process wastes less material compared to injection moulding, and is able to produce larger parts (Tadmor and Gogos, 2006). Both will be discussed here and considered for comparison in this thesis.

The injection moulding process is illustrated in Figure 1.4. Injection moulding primarily consists of two distinct phases: plasticising and moulding. During plasticising the compounded composite pellets are fed through a hopper to a screw that is able to move forwards and backwards through hydraulics, creating the injection pressure. As the screw rotates, the composite solid pellets are fed downstream melting as they move through the heating zone. The molten composite is then forced into the desired mould with an injection pressure created by the hydraulic screw. During moulding a holding pressure and time is applied to the screw until

the injected material solidifies. The temperature of the mould is normally room temperature for thermoplastics, such as HDPE. This temperature is achieved by circulating water through cooling channels around the mould thereby solidifying the composite material. The mould is ejected and final cooling takes place at ambient air temperature. (Agassant *et al.*, 2017; Khanam and AlMaadeed, 2015; Tadmor and Gogos, 2006). Key injection moulding conditions that can be varied are: injection pressure, holding pressure, holding time, cooling time, barrel temperature profile, screw speed and stroke.

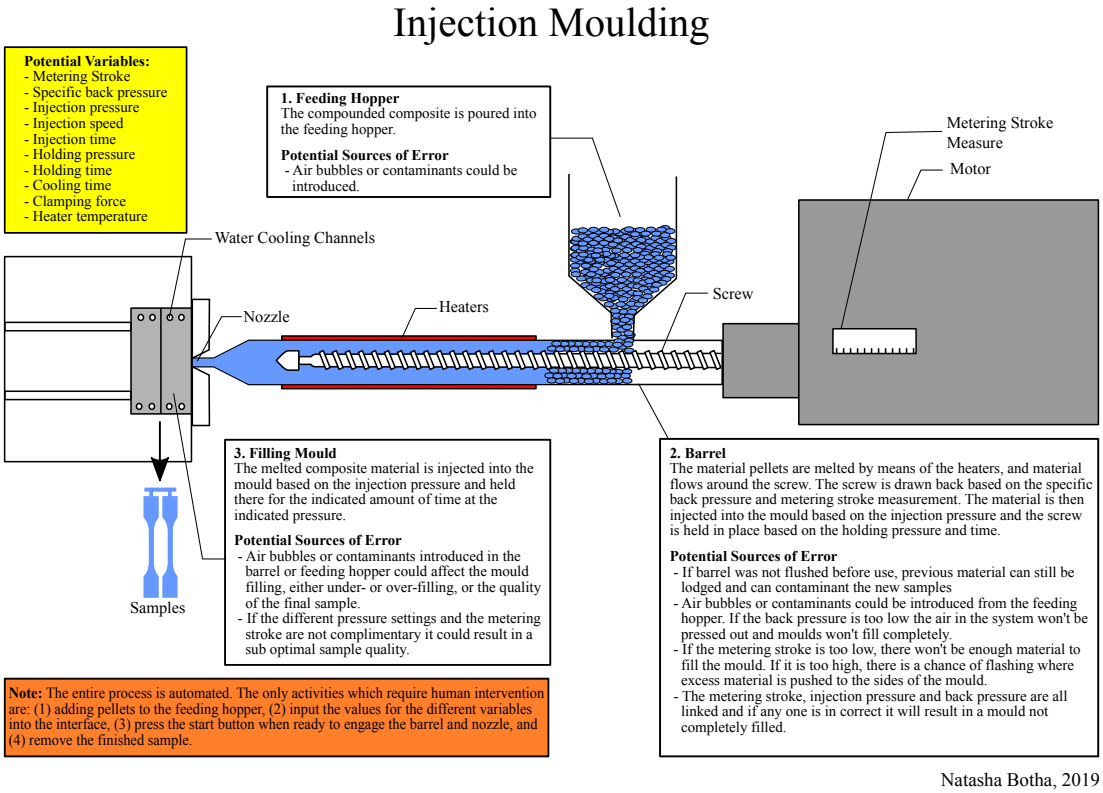

Figure 1.4: Graphical representation of the injection moulding process including all the potential sources of error.

During compression moulding, illustrated in Figure 1.5, the composite pellets are placed in the desired mould before placing it on the bottom pre-heated plate. The bottom heated plate is then hydraulically moved to meet the stationary top plate. At this point a pressure can be applied while the composite material transitions into a molten state. The molten composite flows to fill the mould undergoing complete polymerisation (*i.e.* polymer cross linking) in the process. During polymerisation the pellet skins around the polymer pellets break down with the increased heat. Two polymer pellets then diffuse together to form a new continuous melt. This allows the polymer chains to become mobile in the skin zones to form net chain entanglement (or polymer cross linking). (Bucknall *et al.*, 2020; Raghavan and Wool, 1999; Wool *et al.*, 1989). These polymer pellet boundaries will always be present despite efforts to optimise the process (Bucknall *et al.*, 2020). The temperature and pressure applied during compression moulding are dependent on the properties of the polymer. Once the total press time has been reached, the pressure is released and the bottom heated plate moves back down. The mould is then removed carefully using the correct heat resistant gloves and allowed to

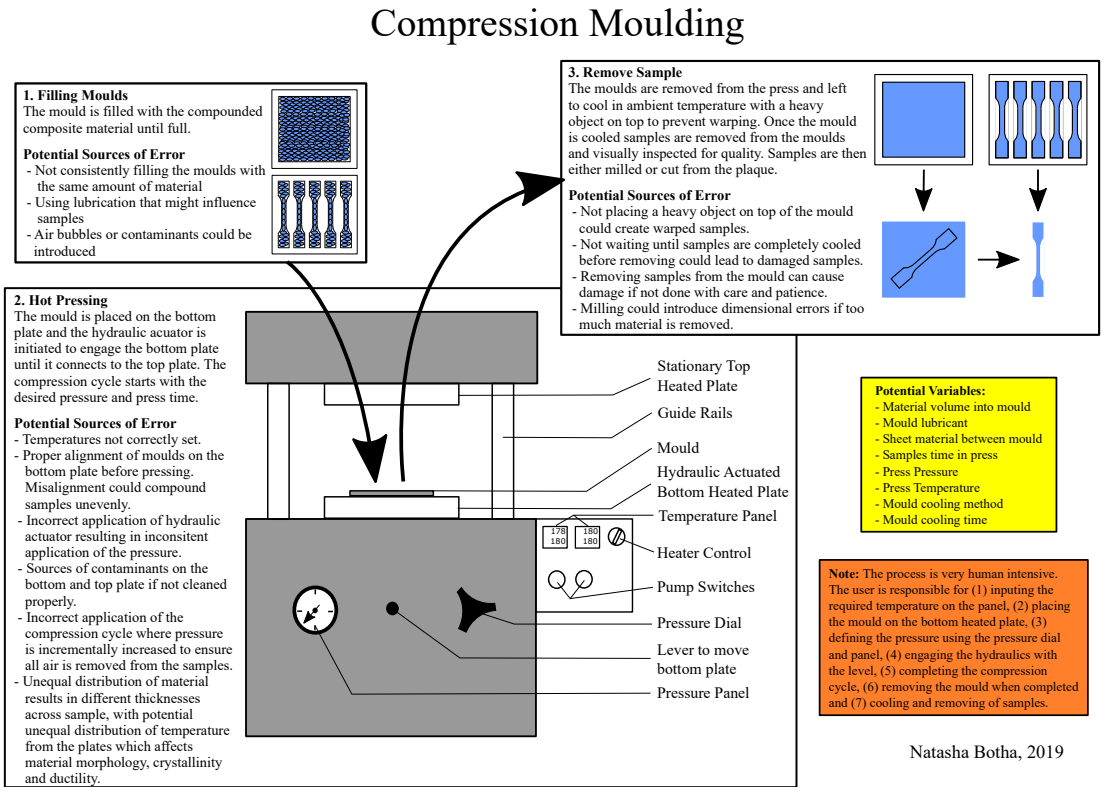

Figure 1.5: Graphical representation of the compression moulding process including all the potential sources of error. Two mould types are considered: a plaque from which the dogbone sample is milled and a mould with five individual dogbone samples.

cool down in ambient air temperature, or some other desired cooling method. (Khanam and AlMaadeed, 2015; Tadmor and Gogos, 2006). Key compression moulding conditions that can be varied are: temperature, press time, press pressure, cooling method and cooling time.

The compounding method plays a prominent role in determining the level of dispersion within the polymer-clay matrix, thereby influencing the composite morphology and overall mechanical properties. Nevertheless, the important role of the moulding method should not be overlooked. Such high temperature and pressure methods result in changes to the composite morphology, such as the crystallinity and polymer chain structure, and consequently affect the final component properties (Shamloo *et al.*, 2017).

1.1.3 Characterisation of Mechanical Properties

The mechanical properties of particulate polymer composites are characterised by tensile and impact tests, among others. Polymer-based composites are very sensitive to the rate of deformation, or strain rate, as shown in Chapter 2 and by Jo and Naguib (2008). Other sensitivities include the temperature and laboratory environment (*e.g.* presence of water, oxygen, etc.) (Callister, Jr., 2003; Grellmann and Seidler, 2013; Khanam and AlMaadeed, 2015). To ensure a standardised approach all tests should follow international standards such as ASTM D638-14 (2014) or DIN EN ISO 527-2 (2012).

During a **uniaxial tensile test** a load is applied to a dogbone sample, shown in Figure 1.6(a), which has wide end sections for clamping, and a narrow uniform central section called the gauge section. The sample is clamped between a fixed bottom clamp and a top clamp attached to the cross-head, which applies a force F to the sample by moving up until the sample fractures or the test is halted. The force applied, measured using a load cell, is normalised by the cross-sectional area of the gauge section to obtain stress, σ. The change in length of the gauge section, normalised by the undeformed length, gives the strain, ε. The mechanical properties are characterised from a tensile stress-strain curve according to an international standard (ASTM D638-14, 2014; DIN EN ISO 527-2, 2012). The cross-head speed is controlled during tensile testing. In the first stage, up until a strain of approximately 1 %, the cross-head speed is slow, 1 mm/min, to allow accurate determination of the Young's modulus. The remaining properties are then determined in the second stage, in which the cross-head speed is specified as 50 mm/min for polymeric materials.

Figure 1.6(b) provides an illustration of a typical polyethylene-based stress-strain curve. The region before the first peak stress is known as the elastic region, where any deformation is still reversible and there is a linear relationship between the stress and strain. The region after the first peak stress is referred to as the plastic region, where the deformation experienced is irreversible.

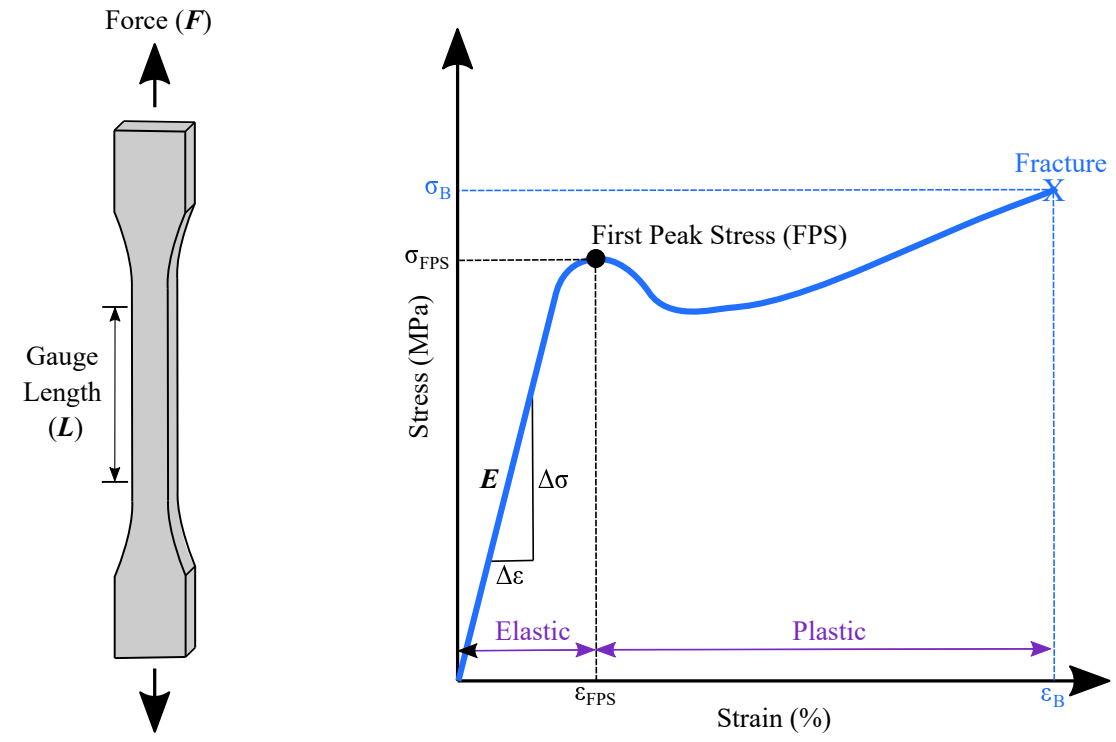

(a) Tensile dogbone sample (b) Definition of mechanical properties

Figure 1.6: Illustration of a typical polyethylene-based stress-strain curve showing ho the mechanical properties are determined. [Redrawn from Callister, Jr. (2003) and Grellmann and Seidler (2013)]

The following mechanical properties can be determined:

- **Young's modulus (MPa):** Determined using Hooke's law to find the gradient in the linear elastic region. It represents the material stiffness and is shown as E on Figure 1.6.
- **First Peak Stress (MPa):** The first maximum stress which is achieved. In the case where this corresponds to an increase in strain without an increase in stress, this is equivalent to the yield stress, at which the material transitions from elastic to plastic deformation. In the case where the sample fractures before the stress begins to decrease, this will be equivalent to the maximum stress. As seen in Figure 1.7(a), polymers under tensile testing display a wide variety of possible material responses. The First Peak Stress (FPS) offers a general and unambiguous definition of the onset of first failure, either by yield or by fracture.
- **Elongation at FPS (%):** The strain corresponding to the first peak stress.
- **Tensile stress at break (MPa):** The tensile stress where the sample fractures. This can be identical to the maximum stress as is the case in the Figure 1.6.
- **Elongation at break (%):** The total strain corresponding to the point of fracture.

Both the stress and strain at break usually do not provide any physically meaningful values. In addition, the elongation at break tends to exhibit high statistical variation, while the stress at which fracture is identified to have occurred is dependent on the testing software. (Grellmann and Seidler, 2013).

Various different possible stress-strain curves for polymer-based materials are shown in Figure 1.7(a). Curve A (red) represents a brittle polymer which fractures while still deforming elastically. Curve B (blue) shows a ductile polymer with the maximum stress above the yield point, typical for softer polymers where work hardening occurs after the first peak stress. A ductile material with no work hardening is shown by curve C (green). Here the polymer undergoes elastic deformation before reaching the first peak stress (or yield point) thereafter undergoing plastic deformation before reaching fracture.

Figure 1.7(b) shows the material behaviour for a semi-crystalline polymer, such as HDPE, and illustrates the sample appearance at different stages. Before any load is applied, the sample is undeformed (1). In the linear region uniform elastic deformation occurs with an increase in load (2). In this elastic region deformation is largely due to the movement of polymer chains, which are randomly oriented, relative to one another. Just after the first peak stress is reached the material softens, resulting in a localised reduction of the sample cross-section which is commonly referred to as necking (3). The material softens due to the rupture of weak intermolecular bonds between the chains, which then begin to straighten, resulting in extensive plastic deformation. Strain hardening, in which the stress begins to

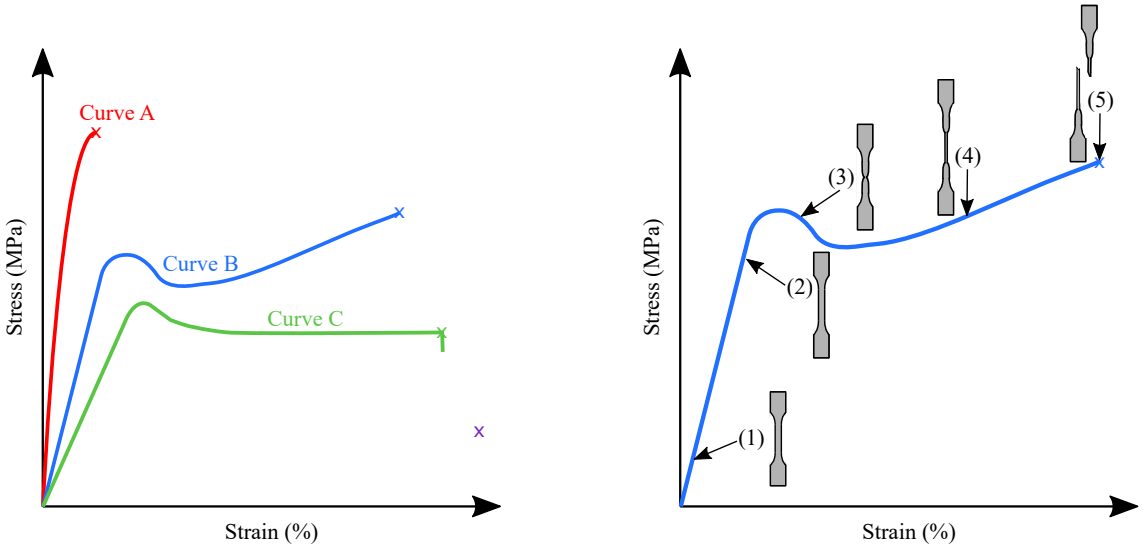

(a) Typical tensile curves

(b) Typical polyethylene material behaviour

Figure 1.7: Illustration of (a) typical stress-strain curves for polymer materials and (b) typical material behaviour for polyethylene-based materials during tensile testing. [Redrawn from Callister, Jr. (2003) and Grellmann and Seidler (2013)]

increase, is caused by the stretching of polymer chains (4). With further increases in loading, the polymer chains will begin to break, at which point sample fracture will occur (5).

Another important mechanical property test is a **Charpy impact test** to determine the fracture characteristics by measuring the impact energy (Grellmann and Seidler, 2013; Khanam and AlMaadeed, 2015). The international standards to consider for a Charpy impact test are ASTM D6610-18 (2018) and DIN EN ISO 179-1 (2010). An illustration of the Charpy impact test is shown in Figure 1.8. For a notched Charpy impact test a small notch is milled into the sample. The sample is then placed, notch down, between two supports. A pendulum, with an energy of 0.5 to 50 J, then hits the sample first creating a crack by transferring energy to the sample, thereafter enlarging the crack with additional hits until it fractures. The impact strength is then calculated by dividing the absorbed energy with the smallest initial cross-section of the sample under the notch. (Grellmann and Seidler, 2013; Khanam and AlMaadeed, 2015)

1.1.4 Influences on Mechanical Properties

Mechanical properties of polymer composites are affected either by changing the polymer composite material system or the manufacturing approach (Boran *et al.*, 2017; Chen *et al.*, 2017). Good interaction between the clay and polymer and good dispersion within the composite are important factors to consider when trying to improve the mechanical properties (Albdiry *et al.*, 2012; Jordan *et al.*, 2005; Khanam and AlMaadeed, 2015; Paul and Robeson, 2008).

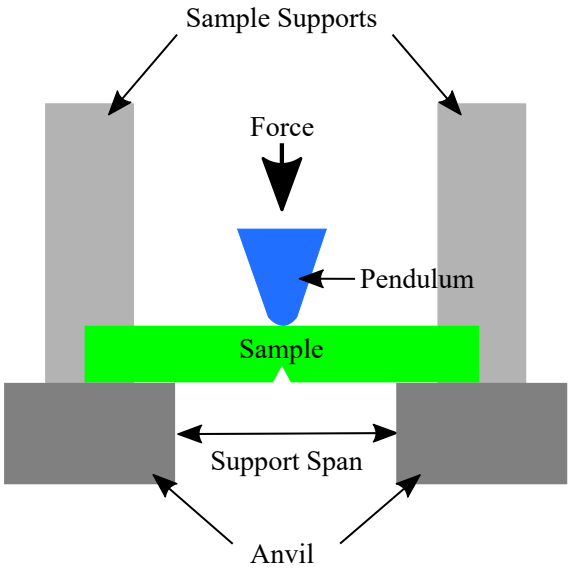

Figure 1.8: Illustration of the Charpy impact test focusing on the sample configuration. [Redrawn from Grellmann and Seidler (2013) and ASTM D6610-18 (2018)]

Influence of Material System

The influence of the polymer-clay material system (*e.g.* clay and polymer type, clay loading, dispersion and the interaction between the clay and polymer) on the mechanical properties have been the subject of much research (Crosby and Lee, 2007; Fu *et al.*, 2008; Azeez *et al.*, 2013; Albdiry *et al.*, 2012; Kotal and Bhowmick, 2015). Thermo-mechanical properties are dependent on the interactions between the clay particles and the polymer matrix which include the type of clay, compatibiliser or surface treatment used and its dispersion in the matrix (Albdiry *et al.*, 2012; Paul and Robeson, 2008; Zabihi *et al.*, 2018). As a result, much research has focused on finding the clay loading that will yield the optimum thermo-mechanical properties for a desired application. The desired improvement of the mechanical properties is most often obtained at a relatively low clay loading (≤ 5 wt%) (Jordan *et al.*, 2005; Azeez *et al.*, 2013; Quaresimin *et al.*, 2016; Romo-Uribe, 2017; Rueda *et al.*, 2017; Mittal *et al.*, 2018; Zabihi *et al.*, 2018). As such, most experimental studies normally only investigate low clay loadings of, for example, 3 wt% (Romo-Uribe, 2017), 5 wt% (Lim *et al.*, 2017; Nevalainen *et al.*, 2009; Nunes *et al.*, 2016) and 7 wt% (Heydari-Meybodi *et al.*, 2015). Heydari-Meybodi *et al.* (2015) concluded in their study that the Young's modulus decreased with an increase in clay loading from 5 wt% to 7 wt%. Romo-Uribe (2017) mentioned that a clay loading of 10 wt% or more only results in small improvements of some of the mechanical properties. Zabihi *et al.* (2018) mentioned that when the clay loading is increased beyond the threshold limit value, the Young's modulus will level off. They attribute this to a change in the clay-polymer interaction. It has been observed that while including clay fillers may increase the Young's modulus and tensile strength of the nanocomposite, other important mechanical properties such as elongation to failure and impact fracture toughness often decrease (Chen *et al.*, 2008; Lim *et al.*, 2017; Nevalainen *et al.*, 2009). This degradation in mechanical performance is an important variable to understand when designing a composite material system (Fechter, 2016;

Fechter *et al.*, 2018). Despite this there are few reports from literature on the threshold clay loading beyond which the mechanical properties start to degrade. I have shown in Chapter 2 and Botha *et al.* (2018) that by adding too much clay ($\geq$ 10 wt%) we mitigate and even reverse the initial improvements in the mechanical properties.

Jordan *et al.* (2005) provides a comprehensive review on the experimental trends of polymer composites which includes a detailed discussion on the influence of mechanical properties. They extracted general behavioural trends based on the nature of the polymer matrix (crystalline or amorphous) and the clay-polymer interactions:

- **Young's Modulus:** Increases with the addition of clay, especially at lower clay loadings. However, there is a critical loading where aggregation occurs resulting in a decrease in Young's modulus. The Young's modulus was not found to be dependent on the nature of the polymer matrix or the clay-polymer interactions.
- **Yield Stress (First Peak Stress in the thesis):** Increases with an increase in clay loading. If there is poor interaction between the clay and polymer the yield stress decreases regardless of the clay loading.
- **Ultimate Tensile Stress:** Increases when there is good clay-polymer interaction, without a uniform trend as the clay loading increases.
- **Elongation at Break:** Decreases with an increase in clay loading, especially for semi-crystalline or crystalline polymers.

Based on the observations from Jordan *et al.* (2005) it is clear that the interaction between the polymer and clay plays a larger role with regards to the mechanical properties. When there is greater adhesion between the polymer and clay it results in less debonding with an applied stress, leading to an improvement in both Young's modulus and tensile strength (Jordan *et al.*, 2005; Paul and Robeson, 2008).

Influence of Manufacturing

In addition to the material system, the manufacturing process has an influence on the composite morphology and consequently the thermo-mechanical properties (Albdiry *et al.*, 2012; Chen *et al.*, 2017; El-Sheikhy and Al-Shamrani, 2015; Khanam and AlMaadeed, 2015). Albdiry *et al.* (2012) compared various experimental studies, each using different manufacturing methods, and concluded that the mechanical properties of the resulting polymer-clay composites are affected by the manufacturing method. This is largely due to the change in polymer-clay morphology (*i.e.* degree of dispersion, polymer chain formation, crystallinity, ductility, etc.) which is dependent on the manufacturing procedure (Albdiry *et al.*, 2012; El-Sheikhy and Al-Shamrani, 2015; Khanam and AlMaadeed, 2015). It is theoretically possible to tailor the mechanical properties of polymer-clay composites by controlling the manufacturing

process and hence change the composite morphology. For example, increases in crystallinity generally accompany an increase in stiffness in high-density polyethylene (HDPE) (Ferhoum *et al.*, 2014), while a decrease in the size of the crystallites (regions of crystallinity) results in increased impact strength and stiffness (Leephakpreeda, 2001). Both of these factors can be controlled, for example through variation of the cooling rate and time. It is possible to increase the polymer-clay stiffness by increasing the exofliation of clay within the polymer (Luo and Daniel, 2003; Sheng *et al.*, 2004). Clay agglomerates — a collection of clay particles which forms a larger group — may be formed with a reduction in dispersion of the clay particles. These agglomerates reduce the overall matrix-filler contact area thereby acting as stress concentrators, leading to reduced overall mechanical properties (Tolinski, 2015; Zare, 2016; Zare and Rhee, 2019). By increasing the shear in the polymer melt (for example through higher rotational speeds during extrusion, a reduction in melt temperature, or change in screw design) the degree of dispersion is increased and the prevalence of agglomerates reduced. This may result in increased exfoliation (Tolinski, 2015; Cho and Paul, 2001; Zhang *et al.*, 2017). It is important to note that the agglomeration encountered in polymer-clay composites is typically soft agglomeration, rather than the reinforcing hard agglomeration or aggregation found in some composites with nanoparticles (Dorigato *et al.*, 2013; Nichols *et al.*, 2002).

To this effect the choices made during manufacturing — that is either the method or conditions — clearly have an effect on the resulting mechanical properties (Albdiry *et al.*, 2012; Boran *et al.*, 2017; Chen *et al.*, 2017). However, before the desired manufacturing process can be successfully controlled it is first necessary to understand the effects of manufacturing on the composite morphology and mechanical properties. Two important review articles consider the effects of compounding on the composite properties of polymer-clay composites. Modesti *et al.* (2010) focused on the effects of compounding of polypropylene (PP) and polyamide (PA6) based composites and how these affect the composite morphology and overall composite properties. The review also included the consideration of additional techniques added to the compounding process in an attempt to improve clay dispersion, for example ultrasound, water and supercritical CO_2. In their review they discussed the effects due to variation in temperature, shear (by changing the extruder screw speed), residence time, extruder configuration, extruder screw profiles and processing route (or blending protocol). They concluded that it is difficult to compare and generalise observations from different studies, despite the importance of the effects due to compounding conditions. Albdiry *et al.* (2012) focused on the effects of different compounding methods and their influence on the polymer-clay composite properties. They provide a detailed review of the polymer-clay composite morphology and how the clay dispersion is affected by the compounding method. This is followed by a discussion on the resulting effects on various properties, including mechanical properties, by means of selected examples from literature. Specifically regarding the mechanical properties, Albdiry *et al.* (2012) investigated 8 studies (none PE-based composites) and found that the properties significantly change depending on the compounding method and conditions employed. They briefly discuss the effect of different moulding methods, indicating that the Young's modulus for compression moulded samples are much lower than those of injection moulded samples.

General behavioural trends for the different mechanical properties due to compounding based on the review article from Albdiry *et al.* (2012) are summarised below:

- **Young's Modulus:** Mechanically mixed composites show good exfoliation and therefore have a larger Young's modulus than shear mixed composites. Injection moulded samples have higher Young's modulus than compression moulded samples, which is attributed to a greater shear history. During mixing of the composite the Young's modulus increases with an increase in mixing time. This is attributed to the a good dispersion and compatiblisation effect of the clay in the polymer matrix.
- **Ultimate Tensile Stress:** Shear mixed composites have a higher strength than mechanically mixed composites. Similar to Young's modulus, an increase in mixing time increases the tensile strength.
- **Stress at Break:** For the mechanically and shear mixed composites there is no clear behavioural trend. This behaviour is attributed to the mobility restrictions of the polymer chains during tensile testing.
- **Elongation at Break:** Similar behaviour to the stress at break for the mechanically and shear mixed composites.

Barrel temperature and screw configuration during extrusion are shown to have little influence on the tensile properties or the impact strength (Albdiry *et al.*, 2012; Modesti *et al.*, 2010). These observations clearly show that the mechanical properties are dependent on the changes in compounding.

To date there are no review articles that discuss the effects of moulding, or secondary processing, methods or conditions. To this end, select studies are briefly discussed to illustrate the importance of understanding the influence of moulding method on the composite morphology and final component properties. Both Chu *et al.* (2007) and Mistretta *et al.* (2018) considered the effect of compression and injection moulding on HDPE-based composites. Chu *et al.* (2007) found Young's modulus to be higher for injection moulded samples compared to compression moulded samples. This increase was attributed to the injection moulding process which imparts a greater shear history and the orientation of the clay particles in the flow direction. Similarly, Mistretta *et al.* (2018) found injection moulded samples to have much higher Young's modulus, tensile strength and elongation at break than compression moulded samples. They attributed this improvement to better material compactness and homogeneity regarding the distribution of the clay in the polymer that is obtained during injection moulding. Injection moulding also reduces thermal degradation effects with lower residence times. Xiang *et al.* (2009) and Gao *et al.* (2012) investigated the differences between traditional injection moulding and dynamic packing injection moulding (DPIM). DPIM induces shear during the moulding phase dramatically changing the composite structure by changing the orientation of the clay in the polymer matrix compared to the isotropic orientation in conventional injection moulding. Xiang *et al.* (2009) and Gao *et al.* (2012) observed that

DPIM provides a significant improvement in both the Young's modulus and tensile strength compared to conventional injection moulding. Xiang *et al.* (2009) more interestingly showed that DPIM samples exhibit a brittle behaviour compared to the more ductile behaviour of conventional injection moulded samples. The behaviour of the mechanical properties is indicative of the prolonged shear that samples experience during DPIM improving the orientation and interfacial adhesion between the clay and polymer. Dabrowska *et al.* (2013) investigated two different manufacturing routes: (1) internal mixing followed by compression moulding to manufacture plates and (2) twin-screw extrusion and spinning to manufacture fibers. Young's modulus and tensile strength at yield for the plates was higher than for the fibers. The crystallinity for the plates was higher than the fibers, although the stiffness and strength for both correlated well as a function of crystallinity. The main differences observed are therefore due to the differences in the manufacturing route as this affects the crystallinity. Stress at break was on average higher for the fibers compared to the plates, in fact it was almost double. This is attributed to the polymer chain orientation during the spinning process to create the fibers. The elongation at break showed similar ductile behaviour. The fiber samples had lower mechanical properties compared to the compression moulded samples.

Most of the studies that do consider the influence of compounding and moulding on mechanical properties focus on MMT as the clay, purely because it is more well known and widely used. Far fewer consider the effects when using LDH as a filler. There is a clear gap in the knowledge base concerning the effect of manufacturing on the mechanical properties of HDPE/LDH composites. This is corroborated in Chapter 3 where I identified 33 studies from an initial 1633 (2 % of the total literature identified) investigating the effects of manufacturing on the mechanical properties of HDPE/MMT composites. From the initial search only Dabrowska *et al.* (2013), which used LDH, was identified as a candidate for inclusion. It was excluded on the basis that one of the manufacturing routes only produced a fiber, which is not considered to be a useful end product.

Based on these discussions it is evident that moulding plays a vital role in the final composite mechanical properties, particularly as this is the method used to produce a final component. This is an especially important step in the manufacturing process for bulk manufacturing where the aim is a suitable end product with the desired properties. Despite the clear importance of moulding on the final component mechanical properties there have been far fewer studies investigating these effects compared to compounding (Modesti *et al.*, 2010; Shamloo *et al.*, 2017).

1.1.5 Statistical Design of Experiments

Traditionally, especially when designing polymer-clay composite experiments, a one-factor-at-a-time approach is considered. In this approach one factor is varied while the other factors of interest are fixed. This ultimately results in a large number of experiments, often time consuming and costly. Alternatively, when confronted with an experiment containing a number of different factors, while accounting for all the potential sources of error, a more systematic

and scientifically rigorous approach should be considered. This is especially important in a field such as polymer-clay composites where there are numerous complex interactions between the material system, manufacturing, composite morphology and mechanical properties. To save on time and cost it is ideal to design an experiment that is able to evaluate multiple factors simultaneously. One such approach is from the field of statistics known as a statistical design of experiments (DoE).

Statistical design of experiments (DoE) is a collection of statistical optimisation techniques used to plan an experiment that is able to consider the effects of multiple factors with a sufficient number of experiments (Montgomery, 2013). The aim of a DoE is to optimise the experimental design by minimising the number of required experimental runs, while still investigating the full experimental design space. Box and Liu (1999) refer to DoE as the catalyst for scientific learning and discovery. They used a paper helicopter to illustrate using DoE for screening of the most influential variables, understanding the variable effects and optimising the flight time of the helicopter from a fixed height. Coetzer *et al.* (2008) illustrated the optimisation of a catalyst system through the sequential application of the design of experiments and response surface models. They engaged in four rounds of statistical experimental design and analysis to reduce the amount of co-catalyst required by 12 times, which made the process economically feasible. DoE has excellent inductive power if employed correctly and provides a scientific paradigm for learning sequentially more about the process or product development, and for discovering optimal conditions and formulations.

This approach has been considered in polymer composites to find the optimum manufacturing conditions (Ramachandran *et al.*, 2012; Campos-Requena *et al.*, 2014; Ibrahim *et al.*, 2014; Moghri *et al.*, 2016; Ujianto *et al.*, 2018) for a range of polymer-clay composite systems. The different DoE designs fall into two classes: factorial designs and response surface method (RSM) designs. As the name implies, factorial designs take a factorial approach by considering all possible combinations of the factors and their variations. Factorial designs normally require a large number of experiments and are used to screen potential factors of interest. RSM designs use an assumed response surface (*e.g.* linear, two-order interactions or quadratic) to optimise a design. Commonly considered RSM designs in polymer composites include Taguchi (Ibrahim *et al.*, 2014), Box-Behnken (Moghri *et al.*, 2016; Ramachandran *et al.*, 2012; Ujianto *et al.*, 2018), central composite design (Campos-Requena *et al.*, 2014) and D-optimal designs (Mohamadi *et al.*, 2014, 2016). RSM designs are ideal for the field of polymer composites where the aim of an experiment is often to optimise the material system or the manufacturing conditions.

It is clear that DoE has many benefits over the traditional one-factor-at-a-time approach designing a more efficient and optimal experimental study. However, there is very little information available in literature on how to choose the most appropriate design for the desired application. In fact, there are limited resources available that provide an introductory level knowledge of DoE and its application (Gündoğdu *et al.*, 2014; Montgomery, 2013; Lundstedt *et al.*, 1998; Telford, 2007; Wang and Wan, 2009). Tanco *et al.* (2009) has emphasised the importance of choosing the correct design and knowing how to apply it properly. If not

applied properly the data obtained from the study would have no statistical relevance and the researcher would be unable to infer any sound conclusions. This highlights the importance of increasing the knowledge base for experimental designs in the field of polymer composites.

1.1.6 Historical Experiments

LDH as a filler has been the focus of research at the University of Pretoria, as its structure can easily be manipulated to provide improvements to desired properties. Several studies (Moyo *et al.*, 2012, 2013; Labuschagne *et al.*, 2015; Fechter, 2016; Fechter *et al.*, 2018) have focused on better understanding the effect of LDH in different polymeric matrices and how the composite properties are affected, especially thermal stability and flammability. However, the enhancements observed in the thermal properties were at the cost of the mechanical properties (Fechter, 2016; Fechter *et al.*, 2018). This prompted further research into the effect of adding LDH to a polymer on the mechanical properties in an attempt to identify the optimum clay loading.

In addition to the effect of the material system (*i.e.*, clay loading, clay type and polymer grade) variations in manufacturing were investigated to better understand the effect on the composite morphology (*e.g.* level of clay dispersion) (Parschau, 2016; Ellis, 2017; Braun, 2018; Heymans, 2018; Botha *et al.*, 2018). The LDH used in these studies is chemically modified with a surface treatment to assist in better dispersion, and for this reason the addition of a compatibiliser is unnecessary. Two LDH clays were considered, namely DHT4-A, because of its compatiblity with polyolefins such as polyethylene, and Alcamizer 1 which is not compatible with polyolefins but specifically designed for polyvinyl chloride (PVC). Both are Mg-Al LDHs with similar chemical formulations to Mg-Al LDH in Table 1.1. The effect of the surface treatment was also studied by removing it from some of the Alcamizer 1. The mechanical properties of interest were the Young's modulus and ultimate tensile strength (equivalent to the first peak stress) as they are indicative of mechanical improvements. It was observed that low clay loadings (2.5 wt%, 5 wt% and 7.5 wt%) do not provide any conclusive results to determine an optimum clay loading. There was no clear influence due to the surface treatment, indicating that it did not increase the affinity of the clay to bond with the polymer matrix. This led to a new question in which the aim was to determine the limits of adding clay loading, and whether the mechanical properties degrade (Botha *et al.*, 2018). In addition to the first peak stress, the percentage elongation was determined, as it is a measure of the material ductility and therefore an indicator of material property degradation. The ultimate tensile strength for higher clay loadings (10 wt%, 15 wt% and 20 wt%) provided no further insights. However, the percentage elongation at failure showed clearly the onset of material property degradation for clay loadings above 10 wt%.

The lack of any observable influence due to clay loading prompted a more detailed analysis of all the historical data by means of an exploratory data and statistical analysis (see Chapter 2). This analysis corroborated the initial findings where clay loading was determined to have no statistically significant effect on the mechanical properties. This could be attributable

to a lack of good dispersion or clay-polymer interaction, both of which are required for enhancements in mechanical properties (Albdiry *et al.*, 2012; Jordan *et al.*, 2005; Khanam and AlMaadeed, 2015; Paul and Robeson, 2008). Scanning electron microscopy results suggested that intercalation and exfoliation were not achieved, resulting in a less advantageous composite morphology. The level of dispersion of the filler in the polymer matrix cannot be directly controlled thus an ideal level of exfoliation cannot be guaranteed even when the compounding conditions are optimised (Paul and Robeson, 2008).

The results indicated that there is no statistically significant difference between Alcamizer 1 and Uncoated Alcamizer 1 (*i.e.*, Alcamizer 1 without any surface treatment). This additional chemical modification therefore played no role in the clay-polymer interaction. Another unexpected observation was that Alcamizer 1 provided better overall mechanical properties than DHT4-A, even though Alcamizer 1 is less compatible with the polymer matrix. Overall, there was significant variability in the data, in fact, this variability far exceeded the effect due to an increase in clay weight loading. The statistical variability observed in the historical experimental data could be attributed to human error, to manufacturing or could be inherent in the material system.

The motivation for designing this study was therefore to understand why we did not see the expected enhancements in mechanical properties due to clay loading that were expected from the literature. It is hypothesised that the property enhancements are potentially sensitive to manufacturing. This becomes a crucial problem once tightly controlled laboratory investigations are upscaled for bulk manufacturing operations.

1.2 Thesis Aim and Scope

The aim of this study is to investigate the sensitivity of HDPE/LDH composite properties to manufacturing variations, comparing the two most common moulding methods, compression and injection moulding. To understand the effect of manufacturing variation on the composite mechanical properties this thesis will further compare manufacturing performed on university equipment with manufacturing performed on state-of-the-art equipment. Clay type and clay loading will be studied to quantify the relative impacts of material composition and manufacturing variation for this material system through proper statistical analysis. As far as possible the same moulding conditions will be implemented at the different sites to minimise statistical differences.

This is a multi-site collaborative study between two South African universities, University of Pretoria and Tshwane University of Technology; and an international state-of-the-art facility, Leibniz Institute for Polymer Research (Germany). The polymer is high-density polyethelene (HDPE) grade C7260. The LDH clays that will be compared are DHT4-A and Alcamizer 1, which were chosen based on the difference in their compatibility with polyethylene. No compatibiliser is included as both clays are already surface treated which will aid their dispersion into the polymer matrix (Azeez *et al.*, 2013; Fu *et al.*, 2019; Rong *et al.*, 2006). The

HDPE/LDH composites will be compounded using co-rotating twin-screw extrusion before dividing the material according to a statistical design of experiments.

To address the thesis aim, this study will answer the following research question: *How do variations in manufacturing influence the mechanical properties of polymer-clay composites?* This is inherently an interdisciplinary study requiring knowledge from polymer composites, manufacturing, mechanical characterisation and statistics.

The specific study research objectives are listed below.

1. **Gain insight into the historical tensile data for HDPE/LDH using statistical tools.** This will provide an overall sense of the influence of the material and manufacturing systems, and their resulting effect on the mechanical properties. (Chapter 2)

2. **Perform an in-depth systematic literature review on the influence of manufacturing variations on mechanical properties of polymer-clay composites.** Following the PRISMA (Preferred Reporting Items for Systematic Reviews and Meta-Analyses) guidelines allows for a transparent and reproducible review. Only behavioural trends will be considered as it is difficult to compare and generalise observations from studies where different composite systems are considered (Modesti *et al.*, 2010). Note, for the review HDPE/MMT is considered as opposed to HDPE/LDH. This is purely because MMT is considered far more often in literature (Costa *et al.*, 2005; Dabrowska *et al.*, 2013) and will therefore yield a larger dataset to review. As LDH is the synthethic alternative to MMT, it is theoretically possible to extrapolate the observations to HDPE/LDH. (Chapter 3)

3. **Compare statistical design of experiments techniques through two case studies.** This will allow me to select an appropriate design method to develop an efficient experimental design. (Chapter 4)

4. **Design the experimental studies to investigate the influence of material and manufacturing systems on the tensile and impact properties of HDPE/LDH composites.** The potential sources of error discussed in Figures 1.3 to 1.5 will be taken into account during the design. The design will be informed by discussions with collaborators to standardise the manufacturing conditions. (Chapter 5)

5. **Use statistical analysis to analyse the experimental data.** This will allow identification of parameters which have a statistically significant effect and a quantification of their relative importance. (Chapter 6)

There are two limitations in this study, namely the polymer grade and the tensile sample mould types. The HDPE C7260 polymer grade was discontinued by the supplier. As a consequence the study was limited to the amount of polymer acquired based on the statistical design of experiments. Another limitation is the availability of the tensile sample mould types

for the equipment in use. The compression moulding equipment only has moulds available for ISO Type 1BA. However, the injection moulding university equipment only has a ISO Type 1A mould available, whereas the state-of-the-art equipment has both a ISO Type 1A and ISO Type 1BA mould available. This study will therefore also investigate the influence of tensile sample mould type.

It should be noted that compounding and testing are outside the scope of the analysis of this thesis. Compounding of the HDPE/LDH composites were done at the National Centre for Nano-structured Material at the Council for Scientific and Industrial Research (CSIR). The impact and tensile testing were both conducted at the Leibniz Institute for Polymer Research, which is an internally accredited facility in Germany, complying with the relevant ISO standards. All testing was done at this single site using equipment specifically set up for testing of polymer specimens. The testing equipment is calibrated and validated according to the required standards.

1.3 Significance

The South African Industrial Policy Action Plan highlights the lack of advanced manufacturing practices and downstream R&D focus as key constraints in the plastics manufacturing industry (Department of Trade and Industry, 2018). The knowledge gained through this research can support researchers and industry in making more informed decisions on the design and manufacturing of their polymer-clay composite systems. This is especially vital when considering the scalability of the manufacturing process which inevitably has new challenges not necessarily observed in controlled laboratory investigations.

All the published literature regarding the effects of manufacturing variation is based on experiments conducted in a controlled laboratory environment. There is a disconnect between academia and what the resulting product performance would be in an industrial manufacturing operation. This research therefore has important implications for applying research done on sample scale, in a controlled laboratory environment, to predict performance of bulk polymer composites.

Many concepts covered in this thesis will be familiar or intuitive to experienced practitioners in the field of polymer science. The significance of my research is to investigate these concepts through an interdisciplinary study. My training as a mechanical engineer means I have approached polymer science as an outsider, a perspective which has allowed me to question the tacit knowledge in the field. The PRISMA guidelines (originating in medical science) establish a systematic and replicable methodology for reviewing the published literature. Statistical Design of Experiments allows robust and efficient investigation of a multi-factorial design space, and ensures that the inferences which are drawn from the experimental data are reliable. The specific novel contributions of this thesis, never previously reported in literature, are: the investigation of the influence of manufacturing machine variation on the mechanical

properties of polymer-clay composites; and the discovery of a size effect for tensile sample moulds.

CHAPTER 2

ANALYSIS OF HISTORICAL TENSILE DATA

From 2016 to 2018 a number of experimental studies were conducted as part of the mechanical engineering undergraduate research project module at the University of Pretoria. Each study considered different material, manufacturing and testing conditions. Before conducting any future experimental studies it is necessary to get an overall sense of this historical data. The aim of this chapter is to gain insight into the effect of various manufacturing and composite material parameters on the mechanical properties based on historical tensile data. This will be done in two stages:

1. Investigate and understand the data set to identify any main characteristics, patterns or anomalies. This process is referred to as an exploratory data analysis (EDA).
2. Once we have a better understanding of the data a statistical analysis will be conducted to quantify the observed effects.

Sections of the work discussed in this chapter, along with additional statistical analysis, have been presented as full length conference articles at two peer reviewed conferences (Botha *et al.*, 2018, 2020) and as a preprint on ChemRXiv (Botha *et al.*, 2019).

2.1 Introduction

The experimental data considered here were collected from 2016 to 2018 as part of a larger study to better understand the composite material system and manufacturing procedure and how the mechanical properties are affected by these. This was done by focussing on different aspects of the system as part of the final year undergraduate mechanical engineering research projects at the University of Pretoria. In 2016, the aim was to investigate the influence of the number of extrusion passes and clay loading on HDPE A7260 and Alcamizer 1 (Parschau, 2016). With the number of extrusions fixed, in 2017 the aim was to find the mechanism which causes changes in the mechanical properties by investigating different polymer grades, clay

types, clay loading and varying the vertex hot press time (Ellis, 2017). Following this, in 2018 the number of extrusions and press time were fixed along with the clay type and polymer grade. Two research projects were defined. The first investigated the effects of higher clay loadings and again considered the influence of the number of extrusions at these higher loads (Heymans, 2018). The second investigated the effects of the sample cooling method and the strain rate during tensile testing (Braun, 2018). Clay loading as a design variable is the only commonality between the experimental studies, with the exception of the second study in 2018 which only considered neat HDPE.

It should be mentioned that in each year a statistical design of experiments (DoE) was conducted where Parschau (2016) considered a Box-Behnken design, Ellis (2017) a full factorial design and Braun (2018) a Taguchi design. During 2018 there were complications with the equipment and only 18 % of the total samples were manufactured.

The composite material, manufacturing and testing system parameters considered in the historical studies are summarised in Table 2.1. The total number of samples include the five repeated test specimens for each case investigated as per the requirements of ASTM D638-14 (2014) to ensure statistical significance. Strain rate, press time, number of extrusions and sample cooling method are constant variables in at least three of the four experimental studies.

Table 2.1: Summary of the historical experimental studies conducted by the students indicating the design and constant variables considered.

Year	Experiment	Design Variable		Constant Variable		Total Samples
2016	Influence of the number of extrusions and clay loading	Clay loading Nr of extrusions	0, 5, 10 wt% 1, 2, 3	Press Time Sample Cooling Strain Rate Clay Type Polymer Type	20 min Air 5 mm/min Alcamizer HDPE A7260	79
2017	Influence of the material system and press time	Polymer Type Clay Type Clay loading Press Time	HPDE B7750, C7260, D7255 Alcamizer, DHT4A, Uncoated Alcamizer 0, 2.5, 5, 7.5 wt% 25, 30, 35, 45 min	Nr of extrusions Sample Cooling Strain Rate	2 Air 5 mm/min	538
2018	Influence of extrusions and higher clay loadings	Clay loading Nr of extrusions	10, 15, 20 wt% 1, 2	Press Time Sample Cooling Strain Rate Clay Type Polymer Type	25 min Air 5 mm/min DHT4-A HDPE B7750	20
2018	Influence of sample cooling method and strain rate	Sample Cooling Strain Rate	Air, Quenched, Furnace 5, 100, 500 mm/min	Polymer Type Clay Type Clay loading Nr. of Extrusions Press Time	C7260 None 0 wt% 2 25 min	65

2.2 Materials and Methods

Melt-mixing combined with extrusion is a simple, cost-effective method for producing thermoplastic polymers while providing sufficient clay dispersion (Jordan *et al.*, 2005; Azeez *et al.*,

2013; El-Sheikhy and Al-Shamrani, 2015; Albdiry *et al.*, 2012). The polymer-clay composite systems in the historical experiments were compounded using a TX28P CFAM 28 mm 18 L/D twin-screw extruder before applying a compression moulding technique (using a Vertex Hot Press) to manufacture the tensile test samples (Parschau, 2016; Ellis, 2017; Heymans, 2018; Braun, 2018).

2.2.1 Materials

One of the most versatile and widely used thermoplastics is polyethylene because of its toughness, near-zero moisture absorption, chemical inertness, low coefficient of friction, ease of processing and electrical properties (Khanam and AlMaadeed, 2015; Osman and Atallah, 2004). High density polyethylene (HDPE) was chosen for the polymer matrix, with different grades considered during the different experimental studies. The polymer was procured in pellet form by Safripol, South Africa.

To better understand the effects of the clay filler three fillers were considered, (1) Alcamizer 1, which is developed for polyvinyl chloride (PVC) compatibility, (2) DHT4-A which is designed for poly-olefin compatibility and (3) an uncoated Alcamizer 1 to determine the effect of surface coating which was obtained by removing the surfactant using a solvent. All clays were obtained from Kisuma Chemicals, The Netherlands. Literature has shown that we can expect an improvement in mechanical properties at relatively low levels of clay loading (≤ 5 wt%) (Jordan *et al.*, 2005; Azeez *et al.*, 2013; Quaresimin *et al.*, 2016; Romo-Uribe, 2017; Rueda *et al.*, 2017; Mittal *et al.*, 2018; Zabihi *et al.*, 2018). For this reason the historical experimental studies mainly focused on clay loadings of 2.5, 5 and 7.5 wt%. However, as we are interested in better understanding the relationship between clay loading and degradation of mechanical properties, higher clay loadings of 10, 15 and 20 wt% were considered in a later study.

2.2.2 Manufacturing

An overview of the manufacturing process considered for the collection of the historical data is provided in Figure 2.1. The manufacturing process is divided into two phases.

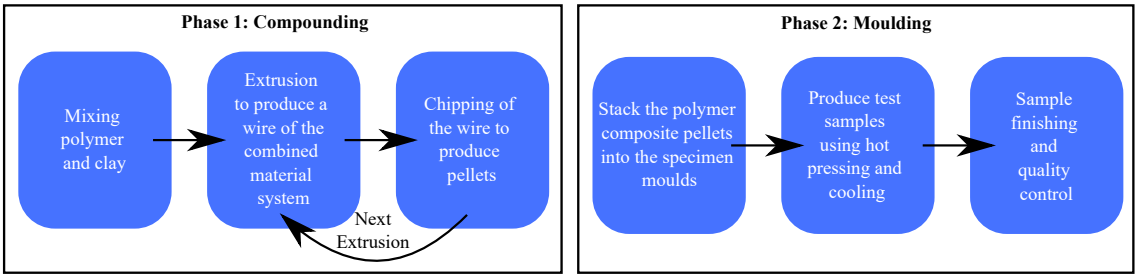

Figure 2.1: Overview of the manufacturing process divided into a compounding phase and a moulding phase.

The first phase is the compounding process. HDPE is pulverised into a fine powder and tumble mixed with the required clay loading in a bag for 45 min to ensure dispersion (El-Sheikhy and Al-Shamrani, 2015). A mathematical relation is used to determine the required mass of clay (m_c) for a specified mass of the polymer (m_p) given a specified clay weight loading (x):

$$x = \frac{m_c}{m_p + m_c} \quad \text{or} \quad m_c = m_p \left(\frac{x}{1 - x} \right) \tag{2.1}$$

The polymer-clay mixture is then extruded into a long wire using a TK28P CFAM twin screw extruder after which the wire is fed through a chipper to obtain pellets. This process was repeated a second time when two extrusions were required and a third time for three extrusions. The heating zone temperatures for the extruder were set to 105 °C (heating zone 1), 165 °C (heating zone 2), 195 °C (heating zone 3) and 185 °C (die heating zone).

In the second phase, the tensile testing samples are created by stacking the polymer composite pellets into specimen moulds designed and manufactured by Parschau (2016) based on the ASTM D638-14 (2014) Type I dimensions as shown in Figure 2.2. The specimens were then compression moulded using a vertex hot press at a fixed temperature of 180 °C and a pressure of 15 MPa applied in increments for the total press time specified in Table 2.1. The pressure increments were applied from 0 to 7.5 MPa and held for 30 s before increasing the pressure to 15 MPa for 5 min. The pressure is then dropped back to 0 MPa where it is increased to 7.5 MPa and held for 30 s before increasing it to 15 MPa and holding for the remainder of the press time. The pressure is released back to 0 MPa before removing the mould from the vertex hot press. This incremental pressure increase and reduction is done to ensure that any air trapped in the mould is released to prevent air bubbles from forming in the final sample.

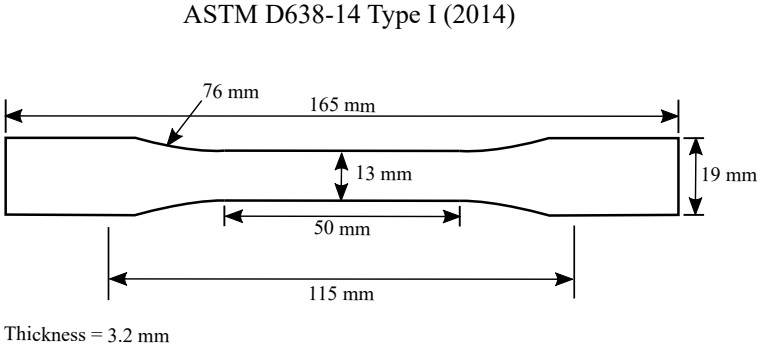

Figure 2.2: Tensile dogbone sample with dimensions for ASTM D638-14 (2014) Type I.

Finally, specimens were cured using one of three sample cooling methods, (1) air cooled at room temperature by placing the mould in the laboratory until the mould was cool enough to touch, (2) quenched by placing the mould immediately after removal from the press into cold water or (3) furnaced by placing the moulds into a furnace which was heated to 60 °C before switching it off. Once the moulds were cooled, the samples were removed and the surfaces finished using a carpenters knife and fine grade sanding paper. This is done to remove any excess material or impurities due to the pressing procedure that could potentially influence the tensile testing results.

2.2.3 Mechanical Characterisation

To obtain the desired mechanical properties a tensile test was conducted using a Lloyd Instruments LRX Plus 5 kN Tensile Machine according to ASTM D638-14 (2014). For each case investigated an average of 5 repeated samples were tested. Tensile tests were conducted at a strain rate of 5, 100 or 500 mm/min depending on the study as described in Table **??**.

Ellis (2017) noted that the 5 kN Tensile Machine is adequate to determine the ultimate tensile strength, but does not provide the 0.2 % offset Yield Strength and Elastic Modulus. A clip gauge was therefore used with the collection of the 2016 and 2017 data to measure the specimen displacement to obtain a more accurate representation of the composite strain. However, during the 2018 tensile tests the clip gauge continued to slip and was therefore not used (Heymans, 2018). The elastic modulus and yield stress are not considered as no strain gauges were used during the 2018 tensile tests and as a result these cannot be determined with any measure of accuracy from the resulting stress-strain curves.

2.2.4 Data Processing

Unprocessed data files were obtained from the tensile testing process for all cases considered, except for the 2016 data investigating the number of extrusions. The data for the 2016 study were digitised (using G3Data, Frantz (2000)) from the report of Parschau (2016) as the unprocessed data files were no longer available. Parschau (2016) conducted tensile testing up to the ultimate tensile strength (UTS) without a clip gauge. The unprocessed tensile data files for the experimental tests conducted in 2017 and 2018 require post processing and correction before the mechanical properties of interest can be estimated from the tensile curve.

An experimental tensile test provides a text file containing the applied force and resulting specimen or machine displacement (depending on whether a clip gauge was used or not) over time until failure occurs. This data set is first converted to the more commonly used stress-strain curve using the following relations:

$$\sigma = \frac{F}{A} \quad \text{and} \quad \epsilon = \frac{\Delta L}{L_o} \tag{2.2}$$

where L_o is either the gauge length (if a clip gauge was used) or the distance between the grips (if no clip gauge was used). The stress-strain curve is then processed to remove any abnormalities in the curve according to ASTM D638-14 (2014):

1. Correct the toe region (caused due to takeup of slack and alignment of the sample) by first determining the maximum linear gradient (also known as Young's modulus) in the elastic region and then applying the maximum linear gradient to the curve.
2. If a clip gauge was used there is the potential for slippage of either the sample or clip gauge. In such cases the negative strain is zeroed before enforcing linear elasticity on the vertical strain and correcting the toe region as discussed in step 1.

3. In the rare case where there is an abnormality in the data due to incorrect computer settings and the relative displacement is presented, the average linear gradient for other curves in that set is determined and then applied to the abnormal dataset to correct the linear region.

4. In cases where a clip gauge was not used, the machine displacement is recorded and it is normally required to account for the machine stiffness. However to accurately determine the machine stiffness a few samples would need to be tested with a clip gauge. This step is only relevant to the 2018 dataset and is shown to be unnecessary in Appendix A.1. It has no effect on the first peak stress and corrects the elongation to failure with an average error of 3.75 %. This error is much lower than the observed variation in the elongation to failure data as seen in the exploratory data analysis.

5. In general some data cleaning steps are required such as enforcing a positive increasing strain, removing any NaN values from the dataset and correcting any large horizontal steps in the linear region.

Figure 2.3 illustrates these correction steps through examples from the overall dataset. Figure 2.3(a) considers a normal data set (HDPE B7750 with 15 wt% DHT4-A, 2018) with no clip gauge where only a toe correction is required. Figure 2.3(b) shows a data set (Neat HDPE B7750, 2017) where the clip gauge slipped, both an increase in strain and linear elasticity were enforced. Figure 2.3(c) is one of six cases (HDPE B7750 with 2.5 wt% Uncoated Alcamizer, 2017) where incorrect computer settings resulted in a lower gradient than observed in the remaining data. The unprocessed and processed stress-strain curves for all cases considered can be viewed in Appendix A.

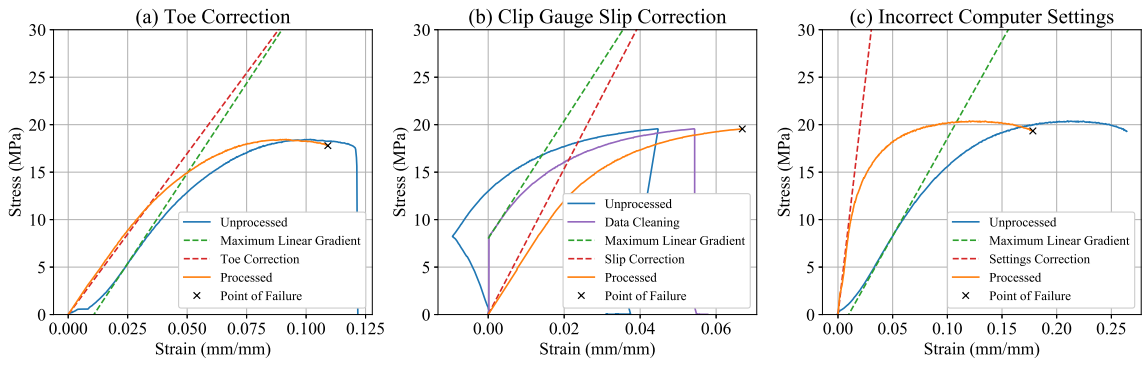

Figure 2.3: Examples to illustrate the data processing steps correcting for (a) the toe region, (b) clip gauge slippage and (c) incorrect computer settings.

The mechanical properties of interest are then determined from the processed stress-strain graphs as shown in Figure 2.4 where the First Peak Stress (σ_{FPS}) is defined as the first peak stress the material can achieve, the percentage elongation at the first peak stress (ϵ_{FPS}) is the strain measured at σ_{FPS} and the percentage elongation to failure (ϵ_f) is the strain measured at the recorded point of failure. As the tensile testing conditions for each of the experimental studies were different, ϵ_f is merely considered to give an indication of the material ductility

and potential material property degradation. To this end, ϵ_f is normalised using ϵ_{FPS} to obtain the normalised ϵ_f which can be compared across the different experimental studies. A normalised ϵ_f of 1 would indicate a sample which failed at the first peak stress (ϵ_{FPS}). Based on this definition, it is not possible to obtain a normalised ϵ_f value below 1. This would assume that ϵ_{FPS} is higher than ϵ_f, which is an unlikely occurrence in any material as the first peak stress will at the very least equal the point of failure if failure was reached before yield. An example of calculating the normalised ϵ_f is shown in Figure 2.4.

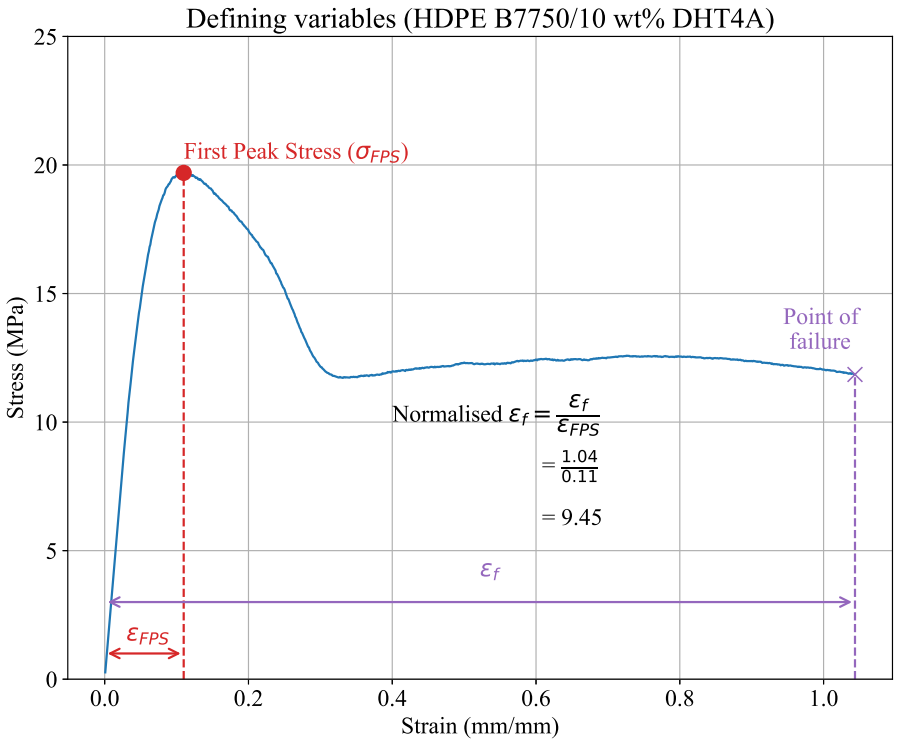

Figure 2.4: Defining the variables used in this chapter with HDPE B7750/10 wt% DHT4A case as an example.

Following the determination of σ_{FPS} and normalised ϵ_f, Table 2.2 provides the summary statistics for the different combinations of the experimental variables, reporting the mean, standard deviation (SD) and the standard error of the mean (SEM) for each of the experimental conditions. In statistics the SD indicates the variation in the data from the mean. A lower SD therefore indicates that the data are clustered around the mean, where a high SD indicates that the data are spread out. The SEM provides an indication of how far the sample mean of the data is from the true population mean and will always be smaller than SD. A SEM value close to 0 will indicate that the sample mean is accurate.

For the historical data the SD for σ_{FPS} ranges from 0.237 to 7.713 which indicates that some cases are clustered around the mean, while others are more spread out. We observe similar behaviour for normalised ϵ_f with a range of 0.029 to 5.885. In both instances the SEM is rather small compared to the SD and provides a good indication that the sample mean is accurate. The mean for σ_{FPS} ranges between 15.267 and 31.730 MPa and for normalised ϵ_f between 1.026 and 11.316 %. In both instances this is quite a large variation across the

Table 2.2: Summary statistics of the σ_{FPS} and normalised ϵ_f responses for the different combinations of experimental variables, where SD is the standard deviation and SEM is the standard error of the mean.

Clay Loading	Strain Rate	Extru-sions	Clay Type	Polymer Grade	Press Time	Sample Cooling	Nr. of Observations	σ_{FPS} (MPa) Mean	SD	SEM	Normalised ϵ_f Mean	SD	SEM
0	5	1	Neat	A7260	20	Air	7	18.801	1.533	0.579			
0	5	2	Neat	A7260	20	Air	11	21.538	2.812	0.848			
0	5	2	Neat	B7750	25	Air	5	22.275	3.430	1.534	2.152	0.787	0.352
0	5	2	Neat	B7750	30	Air	8	21.086	1.497	0.529	1.709	0.874	0.309
0	5	2	Neat	B7750	35	Air	5	23.874	2.954	1.321	2.662	0.953	0.426
0	5	2	Neat	B7750	45	Air	5	22.491	2.992	1.338	2.903	1.086	0.485
0	5	2	Neat	C7260	25	Air	20	22.395	1.964	0.439	11.316	5.604	1.253
0	5	2	Neat	C7260	25	Furnace	9	16.729	7.713	2.571	6.504	5.885	1.962
0	5	2	Neat	C7260	25	Quenched	11	18.778	2.669	0.805	10.719	3.346	1.009
0	5	2	Neat	C7260	30	Air	5	21.563	3.478	1.555	2.522	0.728	0.326
0	5	2	Neat	C7260	35	Air	5	21.240	1.992	0.891	3.431	0.407	0.182
0	5	2	Neat	C7260	45	Air	5	20.395	2.977	1.331	2.543	1.420	0.635
0	5	2	Neat	D7255	25	Air	5	20.145	2.130	0.952	3.153	0.696	0.311
0	5	2	Neat	D7255	30	Air	5	19.913	2.428	1.086	2.551	0.651	0.291
0	5	2	Neat	D7255	35	Air	5	18.758	3.560	1.592	2.195	0.825	0.369
0	5	2	Neat	D7255	45	Air	5	19.643	3.437	1.537	2.892	0.127	0.057
0	5	3	Neat	A7260	20	Air	10	21.725	3.086	0.976			
0	100	2	Neat	C7260	25	Air	14	26.486	3.436	0.918	2.478	0.774	0.207
0	100	2	Neat	C7260	25	Quenched	1	25.373			6.818		
0	500	2	Neat	C7260	25	Air	15	31.730	1.236	0.319	1.067	0.073	0.019
2.5	5	2	Alcamizer 1	B7750	25	Air	5	20.822	3.343	1.495	3.047	0.320	0.143
2.5	5	2	Alcamizer 1	B7750	30	Air	5	19.360	1.700	0.760	3.025	0.148	0.066
2.5	5	2	Alcamizer 1	B7750	35	Air	5	20.545	1.150	0.514	2.976	0.029	0.013
2.5	5	2	Alcamizer 1	B7750	45	Air	5	19.122	2.644	1.183	2.371	1.004	0.449
2.5	5	2	Alcamizer 1	C7260	25	Air	5	22.147	2.361	1.056	2.936	0.565	0.253
2.5	5	2	Alcamizer 1	C7260	30	Air	5	22.581	2.941	1.315	2.991	1.041	0.466
2.5	5	2	Alcamizer 1	C7260	35	Air	5	23.491	1.224	0.547	3.199	1.175	0.526
2.5	5	2	Alcamizer 1	C7260	45	Air	5	22.393	1.233	0.551	3.245	0.181	0.081
2.5	5	2	Alcamizer 1	D7255	25	Air	5	17.708	1.802	0.806	3.280	0.540	0.242
2.5	5	2	Alcamizer 1	D7255	30	Air	5	19.583	1.515	0.677	2.424	1.060	0.474
2.5	5	2	Alcamizer 1	D7255	35	Air	5	17.077	0.832	0.372	2.783	0.887	0.397
2.5	5	2	Alcamizer 1	D7255	45	Air	5	18.177	1.034	0.463	2.409	0.820	0.367
2.5	5	2	DHT4-A	B7750	25	Air	5	17.374	1.344	0.601	1.713	0.553	0.247
2.5	5	2	DHT4-A	B7750	35	Air	5	20.054	1.418	0.634	2.016	0.244	0.109
2.5	5	2	DHT4-A	C7260	25	Air	5	20.860	1.452	0.649	2.437	0.825	0.369
2.5	5	2	DHT4-A	C7260	35	Air	5	20.134	0.878	0.393	4.103	2.288	1.023
2.5	5	2	DHT4-A	D7255	25	Air	5	18.111	2.320	1.038	2.537	0.799	0.357
2.5	5	2	DHT4-A	D7255	35	Air	5	17.806	2.076	0.928	2.728	0.100	0.045
2.5	5	2	Uncoated Alcamizer 1	B7750	25	Air	5	19.345	1.048	0.469	2.146	0.539	0.241
2.5	5	2	Uncoated Alcamizer 1	B7750	35	Air	5	19.904	3.108	1.390	1.692	0.282	0.126
2.5	5	2	Uncoated Alcamizer 1	C7260	25	Air	5	18.934	3.090	1.382	1.406	0.245	0.109
2.5	5	2	Uncoated Alcamizer 1	C7260	35	Air	5	21.414	2.410	1.078	1.385	0.420	0.188
2.5	5	2	Uncoated Alcamizer 1	D7255	25	Air	5	18.886	1.310	0.586	1.075	0.124	0.055
2.5	5	2	Uncoated Alcamizer 1	D7255	35	Air	5	17.429	1.557	0.696	1.729	0.445	0.199
5	5	1	Alcamizer 1	A7260	20	Air	8	22.284	0.596	0.211			
5	5	2	Alcamizer 1	A7260	20	Air	9	22.693	0.803	0.268			
5	5	2	Alcamizer 1	B7750	25	Air	5	19.121	0.816	0.365	2.730	0.530	0.237
5	5	2	Alcamizer 1	B7750	30	Air	5	19.079	2.365	1.058	2.650	0.879	0.393
5	5	2	Alcamizer 1	B7750	35	Air	5	18.625	1.869	0.836	2.561	1.316	0.588
5	5	2	Alcamizer 1	B7750	45	Air	5	20.976	2.210	0.989	2.196	1.025	0.458
5	5	2	Alcamizer 1	C7260	25	Air	4	20.431	3.025	1.512	3.053	0.658	0.329
5	5	2	Alcamizer 1	C7260	30	Air	6	20.027	1.318	0.538	3.463	1.228	0.501
5	5	2	Alcamizer 1	C7260	35	Air	5	21.037	1.308	0.585	3.427	0.386	0.173
5	5	2	Alcamizer 1	C7260	45	Air	5	20.809	1.345	0.602	3.188	0.868	0.388
5	5	2	Alcamizer 1	D7255	25	Air	5	20.560	1.803	0.806	2.773	0.993	0.444
5	5	2	Alcamizer 1	D7255	30	Air	5	20.640	3.205	1.433	3.249	0.348	0.156
5	5	2	Alcamizer 1	D7255	35	Air	5	18.935	2.455	1.098	2.279	0.826	0.369
5	5	2	Alcamizer 1	D7255	45	Air	5	17.872	1.667	0.745	2.741	1.254	0.561
5	5	2	DHT4-A	B7750	25	Air	5	19.361	1.298	0.581	2.131	1.068	0.478
5	5	2	DHT4-A	B7750	35	Air	5	18.917	2.375	1.062	2.954	0.085	0.038
5	5	2	DHT4-A	C7260	25	Air	5	17.427	1.193	0.534	2.963	0.557	0.249
5	5	2	DHT4-A	C7260	35	Air	4	17.074	1.321	0.661	4.282	4.997	2.499
5	5	2	DHT4-A	D7255	25	Air	5	18.521	2.381	1.065	2.595	0.749	0.335
5	5	2	DHT4-A	D7255	35	Air	5	19.738	1.133	0.507	2.842	0.343	0.153
5	5	2	Uncoated Alcamizer 1	B7750	25	Air	5	16.878	5.030	2.249	1.037	0.052	0.023
5	5	2	Uncoated Alcamizer 1	B7750	35	Air	4	20.563	1.240	0.620	1.026	0.436	0.218
5	5	2	Uncoated Alcamizer 1	C7260	25	Air	5	20.295	3.019	1.350	1.682	0.697	0.312
5	5	2	Uncoated Alcamizer 1	C7260	35	Air	5	21.346	2.104	0.941	1.624	0.554	0.248
5	5	2	Uncoated Alcamizer 1	D7255	25	Air	5	15.267	3.612	1.615	1.851	0.410	0.183
5	5	2	Uncoated Alcamizer 1	D7255	35	Air	5	18.987	2.161	0.966	2.277	0.798	0.357
5	5	3	Alcamizer 1	A7260	20	Air	8	22.844	0.790	0.279			
7.5	5	2	Alcamizer 1	B7750	25	Air	5	19.210	1.280	0.573	3.410	2.216	0.991
7.5	5	2	Alcamizer 1	B7750	30	Air	5	19.385	1.593	0.712	2.214	1.388	0.621
7.5	5	2	Alcamizer 1	B7750	35	Air	5	20.847	1.656	0.740	3.412	0.241	0.108
7.5	5	2	Alcamizer 1	B7750	45	Air	5	19.463	1.442	0.645	1.937	1.721	0.769

Table 2.2 continues on the following page.

Table 2.2 continues from the previous page.

Clay Loading	Strain Rate	Extru-sions	Clay Type	Polymer Grade	Press Time	Sample Cooling	Nr. of Observations	σ_{FPS} (MPa) Mean	SD	SEM	Normalised ϵ_f Mean	SD	SEM
7.5	5	2	Alcamizer 1	C7260	25	Air	4	20.920	0.940	0.470	2.342	3.359	1.679
7.5	5	2	Alcamizer 1	C7260	30	Air	5	21.470	0.597	0.267	1.681	1.315	0.588
7.5	5	2	Alcamizer 1	C7260	35	Air	5	20.094	2.495	1.116	2.497	1.026	0.459
7.5	5	2	Alcamizer 1	C7260	45	Air	5	20.232	2.975	1.330	5.424	4.983	2.228
7.5	5	2	Alcamizer 1	D7255	25	Air	5	16.999	1.537	0.687	3.024	0.552	0.247
7.5	5	2	Alcamizer 1	D7255	30	Air	5	18.024	2.353	1.052	2.747	0.610	0.273
7.5	5	2	Alcamizer 1	D7255	35	Air	5	18.762	1.132	0.506	2.504	0.921	0.412
7.5	5	2	Alcamizer 1	D7255	45	Air	5	17.515	0.737	0.330	2.610	0.487	0.218
7.5	5	2	DHT4-A	B7750	25	Air	5	18.295	1.161	0.519	1.652	0.300	0.134
7.5	5	2	DHT4-A	B7750	35	Air	5	16.640	2.885	1.290	1.987	1.045	0.467
7.5	5	2	DHT4-A	C7260	25	Air	5	19.258	1.430	0.639	1.595	0.385	0.172
7.5	5	2	DHT4-A	C7260	35	Air	5	19.854	1.330	0.595	1.995	0.294	0.132
7.5	5	2	DHT4-A	D7255	25	Air	5	18.901	2.297	1.027	2.635	0.812	0.363
7.5	5	2	DHT4-A	D7255	35	Air	5	18.880	2.495	1.116	2.971	0.294	0.132
7.5	5	2	Uncoated Alcamizer 1	B7750	25	Air	4	16.469	3.887	1.943	2.434	2.178	1.089
7.5	5	2	Uncoated Alcamizer 1	C7260	25	Air	4	20.505	4.973	2.486	2.620	1.592	0.796
7.5	5	2	Uncoated Alcamizer 1	C7260	35	Air	4	21.082	2.869	1.435	1.621	0.449	0.224
7.5	5	2	Uncoated Alcamizer 1	D7255	25	Air	5	17.096	1.689	0.755	1.380	0.428	0.191
7.5	5	2	Uncoated Alcamizer 1	D7255	35	Air	5	18.747	3.967	1.774	1.108	0.159	0.071
10	5	1	Alcamizer 1	A7260	20	Air	7	18.736	0.636	0.241			
10	5	1	DHT4-A	B7750	25	Air	5	17.747	0.358	0.160	3.581	1.326	0.593
10	5	2	Alcamizer 1	A7260	20	Air	9	21.337	0.435	0.145			
10	5	2	DHT4-A	B7750	25	Air	5	19.001	0.587	0.263	3.589	3.761	1.682
10	5	3	Alcamizer 1	A7260	20	Air	10	21.425	0.754	0.238			
15	5	2	DHT4-A	B7750	25	Air	5	18.448	0.344	0.154	1.070	0.059	0.027
20	5	2	DHT4-A	B7750	25	Air	5	18.001	0.237	0.106	1.078	0.085	0.038

data set which provides an initial indication that the variables do have an influence on the mechanical responses. The number of observations for the different combinations of experimental conditions are very different. This is partly due to the fact that the experiments were conducted across three years. This is a clear indication that the experimental conditions are unbalanced. In a balanced design we would expect the number of observations to be almost the same for all the different conditions considered.

2.3 Exploratory Data Analysis

The exploratory data analysis (EDA) investigates the effect of the different manufacturing (number of extrusions, press time and sample cooling method), testing (strain rate) and material parameters (polymer grade, clay type and clay weight loading) on the mechanical properties of interest, *i.e.* σ_{FPS} and ϵ_f.

According to literature we expect to observe an increase in σ_{FPS} if there is a good interaction between the filler and polymer (Fu *et al.*, 2008; Azeez *et al.*, 2013; El-Sheikhy and Al-Shamrani, 2015) and a decrease if the interaction between the filler and polymer is poor (Jordan *et al.*, 2005; Fu *et al.*, 2008). HDPE is a semi-crystalline polymer (Osman and Atallah, 2004) and it has been reported that, in general, with the addition of clay particles a decrease in ϵ_f is observed regardless of the interaction between the clay and polymer (Jordan *et al.*, 2005).

2.3.1 Material System Influence

The influence of the material system on σ_{FPS} and ϵ_f was the focus of the 2017 data set (Ellis, 2017) as described in Table 2.1. This dataset is visually explored in scatter plots, where each data point for the mechanical properties is plotted as a function of clay weight loading for the different HDPE grades and clay types as shown in Figure 2.5. There is a lot of variation in the ϵ_f data and as a result it is difficult to draw any sensible conclusions.

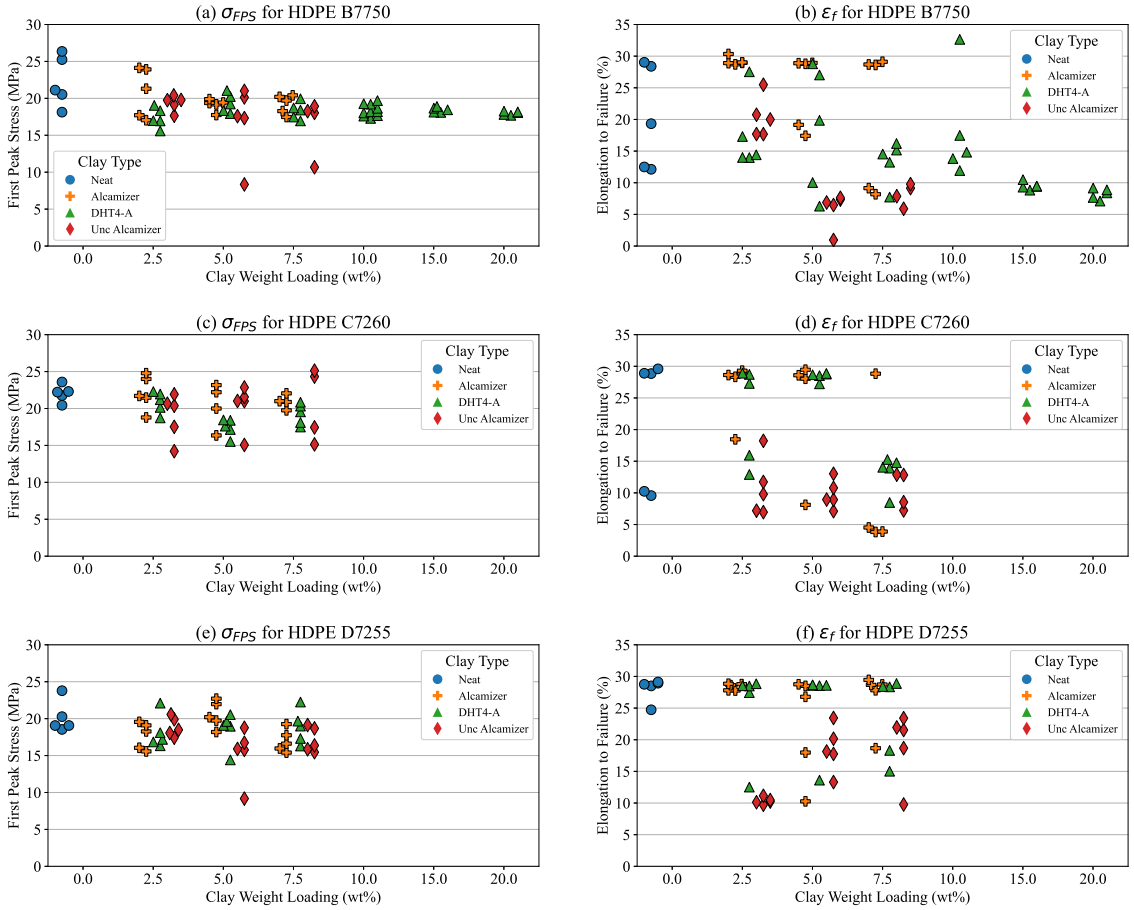

Figure 2.5: Influence of the material system variables on σ_{FPS} and ϵ_f. Each HDPE grade is in a new row of the figure and the clay types are represented by different markers and Unc Alcamizer refers to Uncoated Alacamizer.

Clay Loading

A general observation from Figure 2.5 is that as clay is added to the polymer system, there is a decrease in σ_{FPS} from the neat case for all polymer grades and clay types, which indicates a poor interaction between the polymer and clay (Jordan *et al.*, 2005). Depending on the HDPE/clay system, either an increase or further decrease is observed at higher clay loadings (≥ 5 wt%). σ_{FPS} for HDPE B7750 is less variable than for HDPE C7260 and HDPE D7255. For example, referring to the HDPE B7750/DHT4-A composite system, the largest difference in σ_{FPS} between two consecutive clay loadings is 3.55 MPa which was the initial decrease from

neat to a loading of 2.5 wt%. There is at most a 0.55 MPa change in σ_{FPS} for clay loadings larger than 10 wt%. Similar observations are made for the other HDPE/clay composite systems. We can therefore conclude that the difference in σ_{FPS} due to clay loading is not meaningful enough to determine either an optimum clay loading or the point at which the material strength starts to degrade.

There is a general decrease in ϵ_f with the addition of clay. This is to be expected for a semi-crystalline polymer. For the HDPE B7750/DHT4A composite system it is clear from Figure 2.5(b) that there is a degradation in the material ductility as the ϵ_f mean decreases from 39.91 % at 10 wt% to 9.50 % and 8.24 % for 15 and 20 wt%, respectively. This degradation in material properties is potentially due to an increase of particle agglomeration (Azeez *et al.*, 2013). There is a lot of variability in ϵ_f for clay loadings below 10 wt% even within individual clay types. This indicates that even though the manufacturing process is kept constant, the possibility for variability within the composite morphology exists, most likely due to the polymer-clay interaction.

Polymer Grade

For the influence of the polymer grade, it is observed from the σ_{FPS} mean in Table 2.2 that neat HDPE B7750 has the highest mean with 22.26 MPa compared to HDPE C7260 (20.38 MPa) and HDPE D7260 (19.61 MPa). With the inclusion of clay we note that, in general, HDPE C7260 has a higher σ_{FPS} mean irrespective of clay type.

There appears to be no noticeable trend for ϵ_f between the different HDPE grades as the mean values are within 1% or less of one another.

Clay Type

Alcamizer 1 provides a higher σ_{FPS} followed by DHT4-A and Uncoated Alcamizer. This is surprising, since Alcamizer 1 is known to be designed for compatibility with PVC (a highly polar polymer). The surface treatment of Uncoated Alcamizer 1 does little to improve mechanical properties, as the means of σ_{FPS} for Alcamizer 1 and Uncoated Alcamizer 1 are very close. The variability in the results for Uncoated Alcamizer 1 is larger than Alcamizer 1 and DHT4-A, with DHT4-A providing the least variability.

From Figure 2.5, we see that Alcamizer 1 and DHT4-A tend to have larger values for ϵ_f than Uncoated Alcamizer 1. Alcamizer 1 and DHT4-A are treated with a surface coating, whereas the surface coating was removed for Uncoated Alcamizer 1. This clearly indicates that clay surface coating has a noticeable influence on the material ductility.

The variability in both σ_{FPS} and ϵ_f highlights the inconsistent interaction between the polymer and clay, especially in the cases where there is no surface coating (*e.g.* Uncoated Alcamizer 1). This surface coating normally acts as a lubrication to improve polymer-clay interaction.

2.3.2 Manufacturing and Testing System Influence

The influence of the manufacturing and testing system variables on the mechanical properties of interest (*i.e.* σ_{UTS} and ϵ_f) is shown in Figure 2.6.

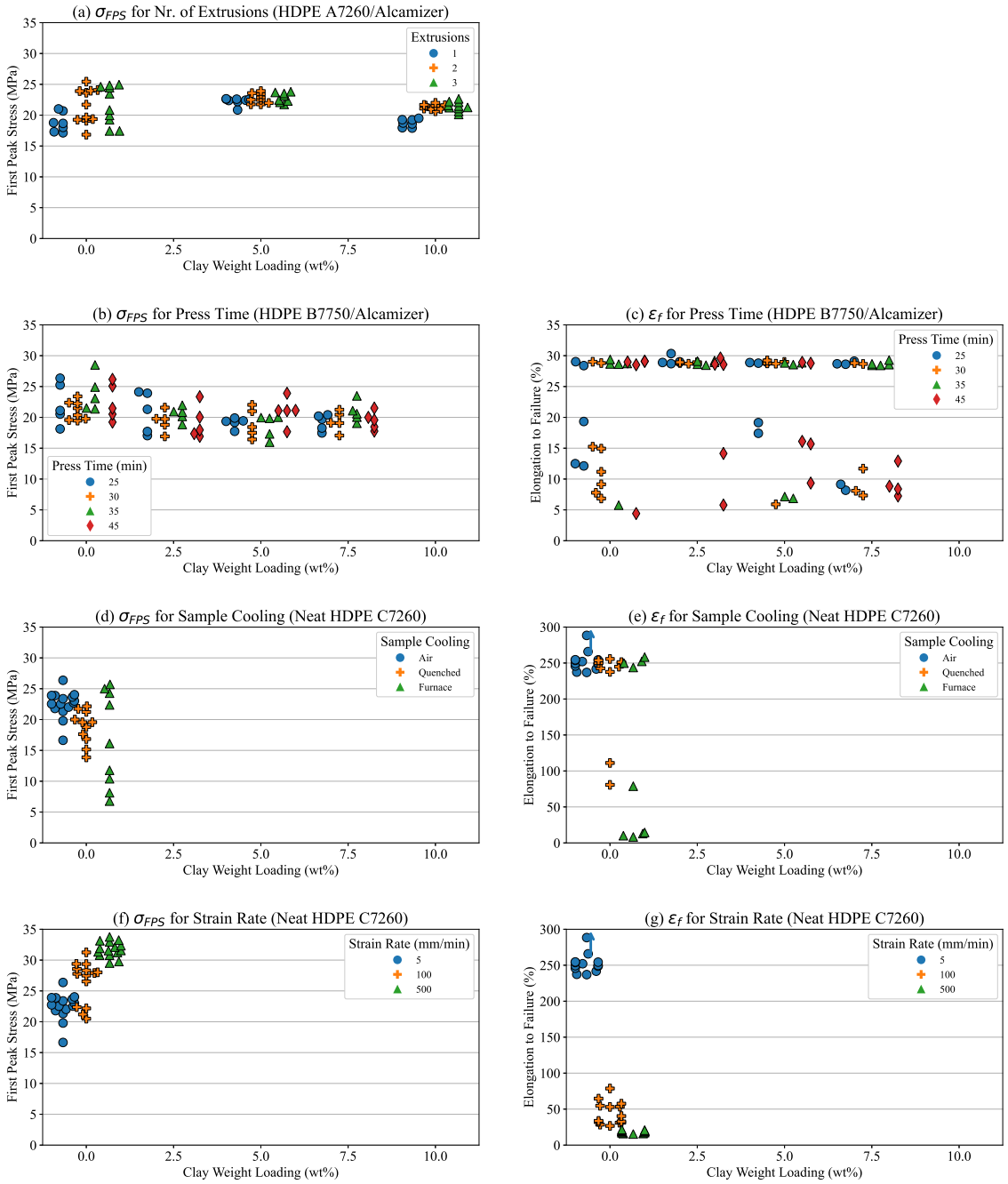

Figure 2.6: Influence of the material system variables on σ_{FPS} and ϵ_f. Each row in the figure represents a manufacturing condition where (a) is the number of extrusions (HDPE A7260/Alcamizer 1), (b)-(c) the press time (HDPE B7750/Alcamizer 1), (d)-(e) the sample cooling method (Neat HDPE C7260) and (f)-(g) the strain rate (Neat HDPE C7260). Markers denote each of the variations within a manufacturing condition and an up arrow denotes more data points outside the y-axis limit.

Number of Extrusions

From Figure 2.6(a) there is a definite influence from 1 to 2 extrusions, where σ_{FPS} increases with an increase in the number of extrusions. This is expected due to better mixing of the clay in the polymer, but not too much to degrade material. However, when increasing the number of extrusions to 3 there is no significant enhancement in σ_{FPS}. Generally an increase in the number of extrusions causes a material to become more brittle which will influence its processability (Azeez *et al.*, 2013). This could lead to the sample experiencing failure before yielding occurs, consequently decreasing σ_{FPS}.

Press Time

In Figure 2.6(b) there is a decrease in σ_{FPS} as the clay weight loading increases, but σ_{FPS} appears to be constant from about 5 wt%. The maximum mean σ_{FPS} enhancement is found to be 6.67 % for neat HDPE and 4.9 % for 2.5 wt% at a 35 min press time; and 12.06 % for 5 wt% and 1.85 % for 7.5 wt% at a press time of 45 min. This enhancement in mean σ_{FPS} is not considered enough of an improvement to warrant the additional time and effort required to press the tensile samples during manufacturing. The variability in press time across the different clay types is rather large. This is likely due to the compression moulding process itself which is known to have a non-uniform heating distribution. This inconsistent heating process affects the composite morphology, consequently affecting the mechanical response which could explain the observed variations (Chu *et al.*, 2007; Mistretta *et al.*, 2018).

ϵ_f in Figure 2.6(c) does not provide additional insight into the influence of press time as there is no observable trend in the data. Most of the samples reached the prescribed elongation of 30 %, with a number of samples failing before then. This could be attributed to the changes in composite morphology (*i.e.* an increase in clay agglomerates and therefore material brittleness) due to the inconsistent heating process in compression moulding.

Sample Cooling Method

As noted in Figure 2.6(d) the furnaced samples had the largest variance within the data set and provided the lowest mean σ_{FPS} (16.73 MPa), whereas the air cooled samples provided the highest σ_{FPS} (22.51 MPa) and the quenched sample mean σ_{FPS} was 19.33 MPa.

The air cooled samples were highly ductile with ϵ_f higher than 200 % as seen in Figure 2.6(e). The level of ductility decreased for the quenched and furnaced samples. This is to be expected as the method of cooling the tensile samples influences the material crystallinity which consequently influences its ductility.

Strain Rate

In Figure 2.6(f) a linear increase in σ_{FPS} is observed with an increase in strain rate where the mean σ_{FPS} is 20.38 MPa for 5 mm/min, 26.41 MPa for 100 mm/min and 31.73 MPa for 500 mm/min.

The material ductility decreases as ϵ_f decreases with an increase in strain rate as shown in Figure 2.6(g). The strain rate clearly has an influence on the mechanical properties. During tensile testing as the sample is pulled in tension the polymer chains extend. For a low strain rate the polymer chains have ample time to extend and therefore tend to exhibit more ductile behaviour. On the other hand at higher strain rates the polymer chains don't have enough time to extend and tend to break quickly resulting in brittle behaviour.

2.4 Statistical Analysis

In any manufacturing process we expect a degree of variability and uncertainty and the aim of the statistical analysis is to quantify the sources of this variability. That is, the percentage of variability attributable to the material system, the manufacturing methodology or random error.

From the summary statistics shown in Table 2.2 it is clear that the number of observations per case is fairly large, and the standard error of the mean is quite small compared to the mean for each response. This provides an indication that it should be possible to quantify statistically significant effects of the experimental variables, and significant differences between the levels of the variables of interest. The effects of polymer grade, clay type, clay loading, number of extrusions, press time and strain rate on the responses, σ_{FPS} and ϵ_f, were of interest.

For the statistical analysis normalised ϵ_f is considered due to the large variability observed for ϵ_f in the EDA. Sample cooling is not considered as there are fewer data points for furnaced and quenched samples (9 furnaced and 12 quenched) compared to the 555 air cooled data points. In the normalised ϵ_f analysis will exclude the 2016 data as results are only up to FPS.

Due to the unbalanced nature of the historical experimental study, only the main or linear effects of the variables could be statistically quantified, and no two-order interactions are considered. The statistical analysis was conducted using Python's statistical modelling module, statsmodels (Perktold *et al.*, 2010).

2.4.1 Analysis of Variance (ANOVA)

The effects of the variables on σ_{FPS} and normalised ϵ_f are quantified through the analysis of variance (ANOVA) (Montgomery, 2013). ANOVA is a statistical procedure used to determine

whether several population means are equal. This is done using an F-test which simply compares the variability between two or more groups (Montgomery and Runger, 2007):

$$F = \frac{SS_{between}/Df_{between}}{SS_{within}/Df_{within}}, \tag{2.3}$$

where SS is the sum of squares which describes the total variability of the data from the mean for a specific variable group. The subscript *between* refers to the variability between groups and is indicated by the variable name in the ANOVA table (c.f. Table 2.3) for each variable. The subscript *within* refers to the variability within the groups and is indicated by the "Residual" row in the ANOVA table. To yield significance, $SS_{between}$ must be greater than SS_{within}. Df denotes the degrees of freedom and is dependent on the number of levels within each variable (*e.g.*, clay type has 3 levels: Alcamizer 1, DHT4-A and Uncoated Alcamizer 1) and the number of repeated sample points (*i.e.*, the number of observations listed in Table 2.2).

The p-value is the probability of obtaining an F-value with the specified degrees of freedom that is greater than the calculated F-value. That is, the probability that the calculated value follows the F-distribution under the null hypothesis, which indicates the means of the groups are equal. It is therefore represented as Pr(>F) in the ANOVA table (c.f. Table 2.3) and indicates the probability that the effect of the variable on the response is only by chance. Therefore, the smaller the p-value the greater the probability that the variable has an effect on the response. For example, a p-value smaller than 0.05 indicates that the variable has a significant effect on the response with more than 95 % confidence.

The different computations mentioned here are used to populate the ANOVA tables that will be discussed in this subsection. The significance level of the p-value is indicated with a set of codes below the table, where only those with a '*' indicating statistical significance (*e.g.*, '*', '**' or '***'). In the tables the first row refers to Intercept which is the value of the intercept for a linear model as the ANOVA is performed for the linear model discussed in the following subsection.

First Peak Stress (σ_{FPS})

The validity of the ANOVA F-test is based on the assumptions of constant variance between the populations compared and whether the data originated from simple random sampling *i.e.*, residuals are normally distributed approximately. Therefore, for the ANOVA analysis it is good practice to first determine if the assumptions of constant variance and random distribution of the errors hold. The results for the ANOVA analysis of σ_{FPS} are shown in Figure 2.7. From Figure 2.7(a) the variability of the residuals are within an acceptable range varying at most 3 units from the mean. The residuals versus predicted results in Figure 2.7(b) indicates randomness which confirms simple random sampling. It can therefore be concluded that the ANOVA assumptions are upheld.

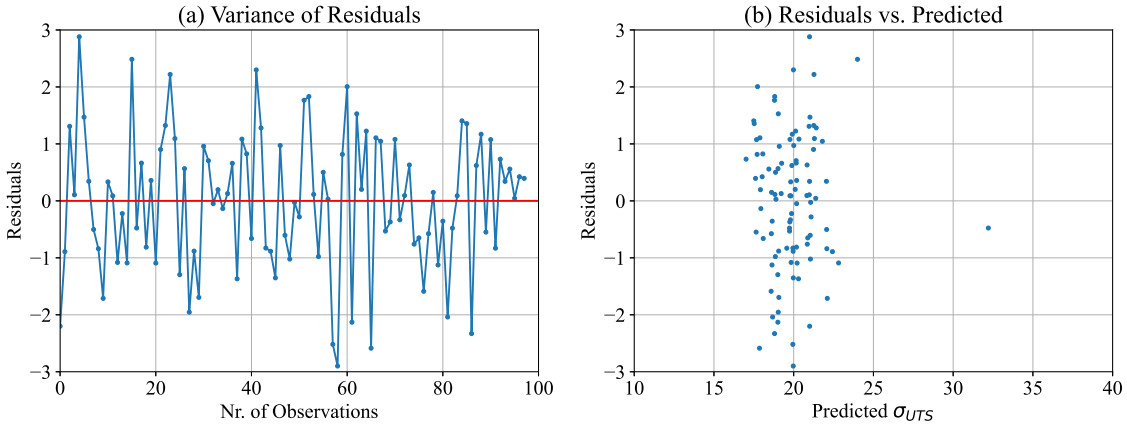

Figure 2.7: ANOVA assumptions for (a) variance of the residuals and (b) residuals vs. predicted values for σ_{FPS}.

Table 2.3: Analysis of variance for σ_{FPS}. A significant effect is when Pr(>F) (p-value) < 0.05.

	Df	Sum Sq	F-value	Pr(>F)	
Intercept	1.0	839.24	512.54	$5.43e^{-38}$	***
PolymerGrade	3.0	77.35	15.75	$3.03e^{-08}$	***
ClayType	3.0	24.98	5.09	$2.74e^{-03}$	**
Extrusions	2.0	7.36	2.25	0.112	
ClayLoading	1.0	4.44	2.71	0.103	
StrainRate	1.0	92.91	56.74	$4.62e^{-11}$	***
PressTime	1.0	0.027	0.017	0.90	
Residual	86.0	140.82			

Significance Codes: '***': 0-0.001, '**': 0.001-0.01, '*': 0.01-0.05, '.':0.05-0.1, ' ': 0.1-1.0

The ANOVA results are given in Table 2.3 for σ_{FPS}. It is clear that polymer grade, clay type and strain rate have a statistically significant effect on σ_{FPS}. All these variables have a p-value of less than 0.05 which indicates a statistically significant effect. On the other hand, number of extrusions, clay loading and press time have p-values larger than 0.05 which indicate that they have no statistically significant effect σ_{FPS}.

Normalised Elongation at Failure (normalised ϵ_f)

The residual analysis results for the ANOVA analysis of normalised ϵ_f are shown in Figure 2.8. From Figure 2.8(a) the variability of the residuals are within an acceptable range varying approximately 1 unit from the mean except for a few outliers. The residuals versus predicted values for the normalised ϵ_f in Figure 2.8(b) is random indicating simple random sampling. The ANOVA assumptions are verified for normalised ϵ_f.

The ANOVA results for the normalised ϵ_f are shown in Table 2.4. Note that all variables have a statistically significant effect (p-value < 0.05) on the normalised ϵ_f except for press time (p-value > 0.05). The most surprising result here is that clay loading is deemed to have no statistically significant effect on σ_{UTS}. It is a well known fact from literature that clay loading

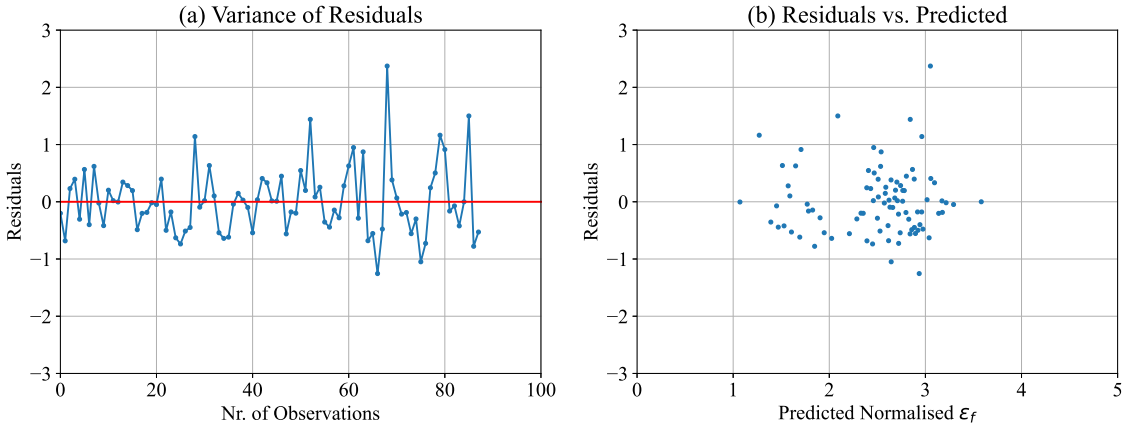

Figure 2.8: ANOVA assumptions for (a) variance of the residuals and (b) residuals vs. predicted for normalised ϵ_f.

does influence the properties of a polymer-clay composite system. The EDA corroborated this influence where we observed a decrease in both σ_{UTS} and ϵ_f with an increase in clay loading.

Table 2.4: Analysis of variance for normalised ϵ_f. A significant effect is when Pr(>F) (p-value) < 0.05.

	Df	Sum Sq	F-value	Pr(>F)	
Intercept	1.0	18.64	66.36	$4.90e^{-12}$	***
PolymerGrade	2.0	2.30	4.10	$2.02e^{-02}$	*
ClayType	3.0	20.55	24.39	$3.11e^{-11}$	***
Extrusions	1.0	4.88	17.37	$7.88e^{-05}$	***
ClayLoading	1.0	2.69	9.58	$2.74e^{-03}$	**
StrainRate	1.0	2.32	8.27	$5.21e^{-03}$	**
PressTime	1.0	0.34	1.20	0.28	
Residual	78.0	21.90			

Significance Codes: '***': 0-0.001, '**': 0.001-0.01, '*': 0.01-0.05, '.':0.05-0.1, ' ': 0.1-1.0

2.4.2 Linear (or Regression) Model

Now that we know which experimental variables have a statistically significant effect, the next step is to determine whether there are any statistically significant differences between the different levels of each experimental variable. To achieve this, a linear (or regression) model is developed as a function of the experimental variables using the least squares method. The linear model fitted for this work is defined as:

$$\hat{y} = \hat{\beta}_0 + \hat{\beta}_1 z_{1,B7750} + \hat{\beta}_2 z_{1,C7260} + \hat{\beta}_3 z_{1,D7255} + \hat{\beta}_4 z_{2,DHT4-A} + \hat{\beta}_5 z_{2,Neat} + \hat{\beta}_6 z_{2,UncAlc} + \hat{\beta}_7 z_{3,extr2} + \hat{\beta}_8 z_{3,extr3} + \hat{\beta}_9 x_{loading} + \hat{\beta}_{10} x_{strain} + \hat{\beta}_{11} x_{press}. \quad (2.4)$$

The response variable is represented by y, with the fitted or predicted value denoted by $\hat{y}$, and is either σ_{FPS} or normalised ϵ_f. The estimated regression coefficients are represented by $\hat{\beta}_i$ and shown in the "Estimate" column in the linear regression table (c.f. Table 2.5). Parameter

estimates are obtained with least squares minimisation of the residuals *i.e.*, $\sum_i (y - \hat{y})^2$. Categorical dummy variables are denoted with $z_{i,level}$ indicating the second and third levels of the variable as $\hat{\beta}_0$, the intercept, captures the first levels. The dummy variable is set to either 0 or 1 depending on which level is active.

For a linear regression model the R^2 value provides an indication of the proportion of total variability in the response variable explained by the model. The adjusted R^2 is a variation on the R^2 value which adjusts for the number of terms in the regression model. This value reduces as the number of unnecessary terms in the model is increased (Montgomery, 2013). A value closer to 1 is indicative of good model predictability as it would fit the observed data well. For this study, a minimum value of 0.7 is arbitrarily considered to represent a good model. Residual standard error indicates the standard error of the model, and provides an indication of the model's ability to quantify statistically significant effects. This value should ideally be very small when compared to the overall mean of the model. The linear regression model considers a t-statistic to determine the p-value, which determines the difference between the means of two groups. In regression, the t-value is determined from (Montgomery and Runger, 2007):

$$t = \frac{\hat{\beta}_i - \beta_i}{SE(\hat{\beta}_i)}. \tag{2.5}$$

Under the null hypothesis $\beta_i = 0$, the numerator is just the estimated regression coefficient, $\hat{\beta}_i$. The denominator is the standard error (SE) of the parameter estimate. It is denoted by "Std. Error" in the linear model table (c.f. Table 2.5). Similar to the ANOVA, the p-value is the probability to obtain a t-distribution value with specified degrees of freedom which is greater than the calculated t-value. It is therefore represented as Pr(>|t|) in the linear model table (c.f. Table 2.5) and indicates the probability that the effect of the variable on the response is only by chance. The significance level of the p-value is indicated with a set of codes below the table, where only those with a '*' indicate significance (*e.g.*, '*', '**' or '***').

First Peak Stress (σ_{FPS})

It is good practice to first determine if the assumption of normal distribution of residual holds. This is visually observed by means of a probability plot where the percentiles of the residuals would approximate the percentiles of the standard normal distribution and the points will fall on a straight line, approximately (Montgomery, 2013). The probability plot for the linear regression model of σ_{FPS} is shown in Figure 2.9. The residuals follow a standard normal distribution approximately. Both the R^2 and adjusted R^2 values are close to one another which indicates that the model can provide good predictability.

The linear regression model results are shown in Table 2.5 for σ_{FPS}. Note that the first level of the variable is used for comparison which is why Polymer Grade [T.A7260], Clay Type [T.Alcamizer] and Extrusions [T.1] do not appear in Table 2.5. Similary, Polymer Grade [T.B7750] and Clay Type [T.Alcamizer] do not appear in Table 2.6. Note that for the

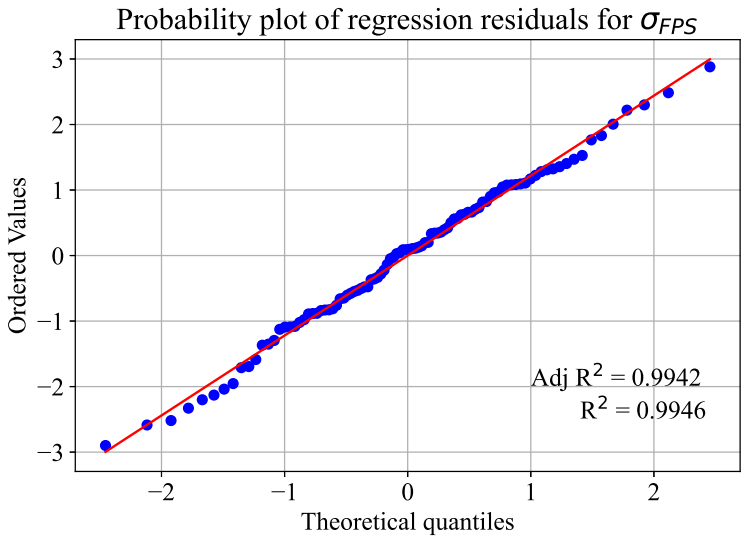

Figure 2.9: Probability plot of the residuals for σ_{FPS}.

linear model the statistical significance is quantified by comparing the ratio of the estimate to its standard error for the variable to a t-distribution with specified degrees of freedom (Montgomery, 2013).

Table 2.5: Linear model for σ_{FPS}, where a significant effect is when Pr(> |t|) (p-value) < 0.05.

Nr. Observations	98	R-squared		0.702	
Df Residuals	86	Adjusted R-squared		0.664	
Df Model	11	F-statistic		18.46	
		Residual Standard Error		1.28	
	Estimate	Std. Error	t-value	Pr(> |t|)	
Intercept	20.2450	0.894	22.639	0.000	***
PolymerGrade[T.B7750]	-1.4766	0.755	-1.955	0.054	.
PolymerGrade[T.C7260]	-0.3909	0.772	-0.506	0.614	
PolymerGrade[T.D7255]	-2.6314	0.775	-3.396	0.001	***
ClayType[T.DHT4-A]	-1.0894	0.364	-2.990	0.004	**
ClayType[T.Neat]	0.5988	0.470	1.275	0.206	
ClayType[T.Uncoated Alcamizer 1]	-0.9418	0.384	-2.451	0.016	*
Extrusions[T.2]	1.4276	0.822	1.737	0.086	.
Extrusions[T.3]	1.8135	0.994	1.825	0.071	.
ClayLoading	-0.0836	0.051	-1.647	0.103	
StrainRate	0.0205	0.003	7.533	0.000	***
PressTime	0.0028	0.021	0.129	0.898	

Significance Codes: '***': 0-0.001, '**': 0.001-0.01, '*': 0.01-0.05, '.':0.05-0.1, ' ': 0.1-1.0

From Table 2.5 we note that the adjusted R^2 of 0.664, *i.e.* relatively close to 0.7 which is the minimum threshold, and the model will be able to predict σ_{FPS} with relative accuracy. The residual standard error of the model is 1.28, which is very small compared to the overall mean of 20.245 (Estimate value for Intercept in Table 2.5) and indicates that statistically significant effects of the variables on σ_{FPS} can be quantified.

The values in the Estimate column is the average change in σ_{FPS} for the specific level of the variable compared to its first level given in alphabetical order. Note that a variable is always compared to its first entry which is not shown in the table (*i.e.* Polymer Grade [T.A7260], Clay Type [T.Alcamizer] and Extrusions [T.1]). For example, the σ_{FPS} of HDPE B7750 is on average 1.4766 MPa lower than the σ_{FPS} of HDPE A7260. Again, the p-value ($\Pr(>|t|)$), indicates the probability that the effect is only by chance and a statistically significant effect is when the p-value is less than 0.05.

We note that polymer grade has on average a negative effect on σ_{FPS}. Only HDPE D7255 has a statistically significant effect when compared to HDPE A7260 with a p-value lower than 0.05. The effect on σ_{FPS} due to clay type is more varied, with a negative effect for DHT4-A and Uncoated Alcamizer and a positive effect for neat HDPE when compared to Alcamizer. Both DHT4-A and Uncoated Alcamizer have a statistically significant effect when compared to Alcamizer with p-values less than 0.05. Strain rate has a positive effect on σ_{FPS} and increases on average by 0.0205 units for a one mm/min increase in strain rate. Strain rate is statistically significant with a p-value less than 0.05.

Normalised Elongation at Failure (normalised ϵ_f)

To determine if the normalised ϵ_f follows a normal distribution a probability plot of the regression residuals is illustrated in Figure 2.10. From Figure 2.10 the residuals follow an approximately normal distribution. Both the R^2 and adjusted R^2 values are close to one another which indicates that the model can provide good predictability.

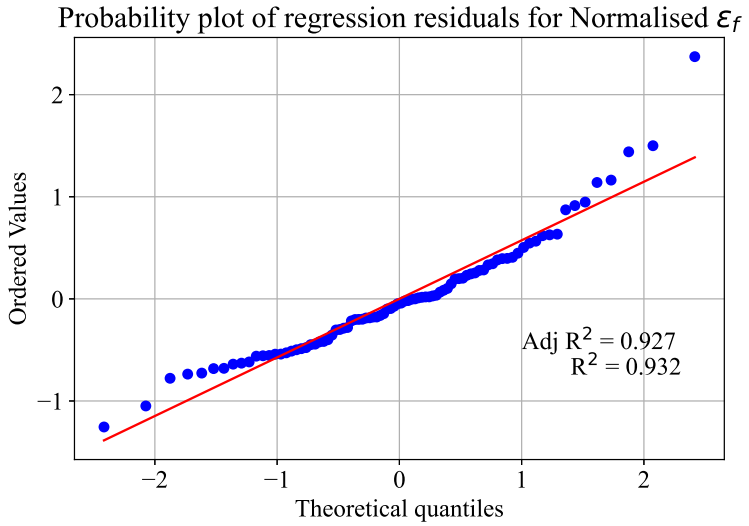

Figure 2.10: Probability plot of the residuals for normalised ϵ_f.

The linear regression model results for normalised ϵ_f are shown in Table 2.6. From Table 2.6 we note that the adjusted R^2 value is 0.554, *i.e.* the model will therefore struggle to predict the normalised ϵ_f. The residual standard error is 0.530 which is smaller than the overall mean of 4.2949, indicating that statistically significant effects of the variables on the normalised ϵ_f can be quantified.

Table 2.6: Linear model for normalised ϵ_f, where a significant effect is when Pr(> |t|) (p-value) < 0.05.

Nr. Observations	88	R-squared		0.600	
Df Residuals	78	Adjusted R-squared		0.554	
Df Model	9	F-statistic		13.03	
		Residual Standard Error		0.530	
	Estimate	Std. Error	t-value	Pr(> |t|)	
Intercept	4.2949	0.527	8.146	0.000	***
PolymerGrade[T.C7260]	0.3972	0.142	2.796	0.007	**
PolymerGrade[T.D7255]	0.2737	0.142	1.933	0.057	.
ClayType[T.DHT4-A]	-0.2546	0.155	-1.648	0.103	
ClayType[T.Neat]	-0.5108	0.210	-2.430	0.017	*
ClayType[T.Uncoated Alcamizer 1]	-1.3475	0.160	-8.406	0.000	***
Extrusions[T.2]	-1.6989	0.408	-4.168	0.000	***
ClayLoading	-0.0684	0.022	-3.094	0.003	**
StrainRate	-0.0033	0.001	-2.875	0.005	**
PressTime	0.0098	0.009	1.094	0.277	

Significance Codes: '***': 0-0.001, '**': 0.001-0.01, '*': 0.01-0.05, '.':0.05-0.1, ' ': 0.1-1.0

Polymer grade has on average a positive effect on the normalised ϵ_f. We note that only HDPE C7260 is statistically significantly different (p-value < 0.05) when compared to HDPE A7260. Neat HDPE and Uncoated Alcamizer both have a statistically significant effect (p-value < 0.05) from Alcamizer and have on average a negative effect. The number of extrusions, clay loading and strain rate have on average a negative effect on the normalised ϵ_f, and are statistically significant.

2.4.3 Tukey Honest Significant Difference (HSD)

The linear model in Tables 2.5 and 2.6 does not provide a statistical comparison of all the variable levels with each other, only to the first level (listed alphabetically, *e.g.* HDPE A7260 for polymer grade, Alcamizer 1 for clay type and 1 extrusion for number of extrusions). The Tukey Honest Significant Difference (HSD) test is used to provide multiple comparisons between all the levels of the variables of interest (Montgomery, 2013); and is based on the Studentised Range Statistic to provide a family-wise true significant difference test. The studentised range statistic is simply the difference between the minimum and maximum data point within a group and is normalised using the group's standard deviation.

The Tukey HSD test results are shown in Figure 2.11 for both σ_{UTS} and normalised ϵ_f. These are for all experimental variables which consist of more than one level, namely the polymer grade and clay type; and were found to have statistical significance from the ANOVA results. The intervals on the graph represent 95 % confidence intervals (CI) for the mean difference in the response variable between the two levels of interest. If the confidence interval does not contain zero, the two levels of interest are statistically significantly different with 95 % confidence. Note these are family wise 95 % confidence intervals adjusted for the number of

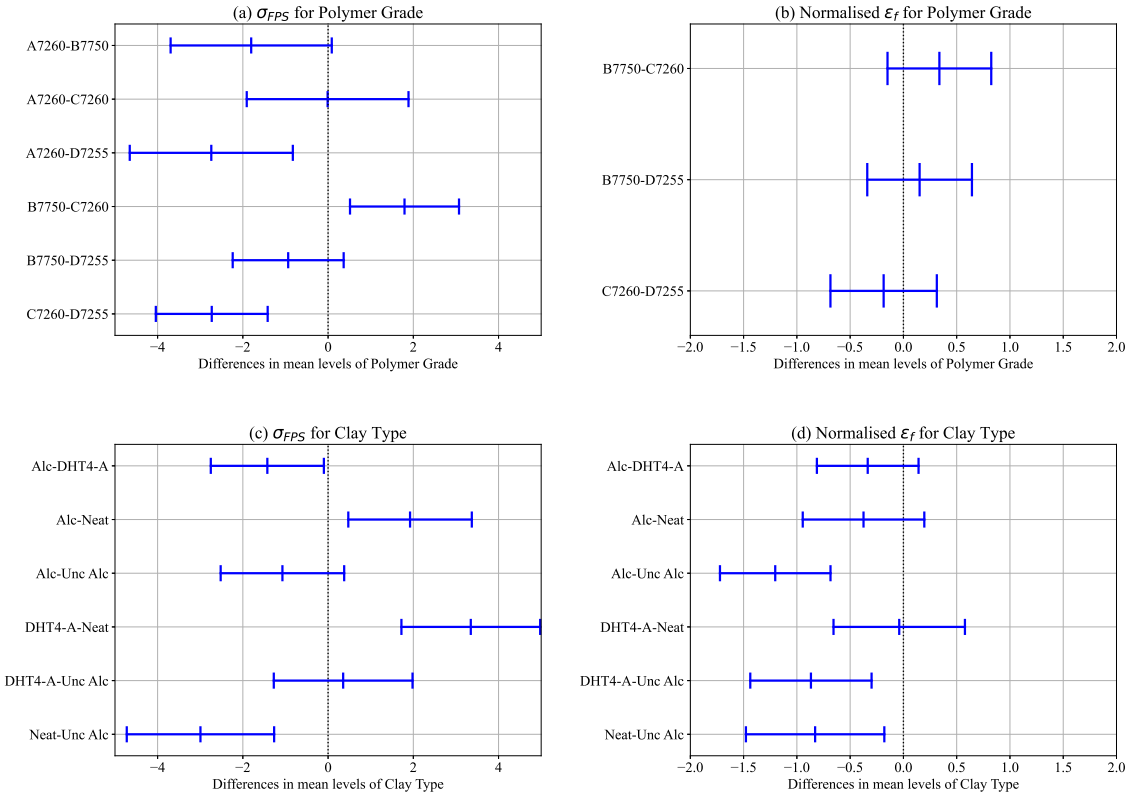

Figure 2.11: Tukey HSD test to determine the statistical significance of (a) σ_{FPS} for Polymer Grade, (b) Normalised ϵ_f for Polymer Grade, (c) σ_{FPS} for Clay Type and (d) Normalised ϵ_f for Clay Type. In (b) and (c) UAlc refers to Uncoated Alcamizer 1 and Alc refers to Alcamizer 1.

levels being compared.

From Figure 2.11(a) we note that three levels of polymer grade are statistically significantly different from each other for σ_{FPS}, namely HDPE A7260-D7255, HDPE B7550-C7260 and HDPE C7260-D7255. HDPE A7260-B7750, HDPE A7260-C7260 and HDPE B7550-D7255 were not statistically significantly different (zero on the x-axis is within the 95 % CI band). For normalised ϵ_f in Figure 2.11(b) we note that none of the polymer grades are statistically significantly different from one another.

For clay type all levels are statistically significantly different for σ_{FPS} except for Uncoated Alcamizer (UAlc in Figure 2.11(c)) which is not statistically significantly different from Alcamizer or DHT4-A (zero on the x-axis is within the 95 % CI band). For normalised ϵ_f (c.f. Figure 2.11(d)) Alcamizer is not statisically significantly different from DHT4-A or Neat HDPE and Neat HDPE is not statisically significantly different from DHT4-A. This is unexpected since Alcamizer 1 is less compatible with HDPE, while DHT4-A is.

2.5 Conclusion

Over the past few years a number of experiments were performed by mechanical engineering undergraduate students during their final year research project. These projects considered

different HDPE/clay composite systems and manufacturing parameters.

An exploratory data analysis (EDA) was considered to explore the historical data and to gain potential insight for the direction of future experimental work. The EDA has shown that the material and testing system parameters have an influence on the mechanical properties of interest (σ_{FPS} and ϵ_f). The results indicated that there is a poor interaction between the polymer and clay as σ_{FPS} tends to decrease with the addition of clay. A decrease in ϵ_f was observed with an increase in clay loading. These observations correspond with what was expected based on literature (Jordan *et al.*, 2005; Fu *et al.*, 2008; Azeez *et al.*, 2013). It was observed that low clay loadings ($\leq$ 7.5 wt%) do not provide any conclusive results to determine an optimum clay loading. This observation is contrary to literature (Jordan *et al.*, 2005; Azeez *et al.*, 2013; Quaresimin *et al.*, 2016) which has indicated that improvements can be obtained with clay loadings $\leq$ 5 wt%. For higher clay loadings ($\geq$ 10 wt%) σ_{FPS} provided no further insights, however the ϵ_f indicated an onset of material property degradation. This initial observation should be supplemented with other measurements such as toughness and impact resistance in future studies. The manufacturing parameters have slight influences but the small improvements in mechanical properties do not outweigh the substantial investment in time and resources required to achieve the improved properties. The strain rate had an observable influence on both the response variables.

Initial observations in the statistical analysis indicated that due to the different experimental designs considered, only main or linear effects between variables could be quantified. The statistical analysis for σ_{FPS} and normalised ϵ_f considered Analysis of Variance (ANOVA) and linear regression models. The ANOVA results indicated that polymer grade, clay type and strain rate had a statistically significant effect on σ_{FPS}. Similarly, clay type, number of extrusions, clay loading and strain rate had a statistically significant effect on the normalised ϵ_f. An interesting result for σ_{FPS} was that clay loading has no statistically significant effect, which is in contrast to what we expect from literature. The linear regression model indicated polymer grade, clay type and clay loading have a negative effect on σ_{FPS}, while the number of extrusions, strain rate and press time had a positive effect. For normalised ϵ_f the linear model indicated a positive effect due to polymer grade and press time, and a positive effect due to clay type, clay loading and strain rate. Only the linear model for σ_{FPS} can be used to predict the response variable of interest. However, both linear models indicated that statistically significant effects are quantifiable.

From the EDA we noticed a lot of variability in the results for both σ_{FPS} and ϵ_f. This variability can either be inherent in the material system, due to the manufacturing process or something else entirely. Despite this variability it was possible to conduct a statistical analysis on the σ_{FPS} and normalised ϵ_f to quantify some of these effects which seem primarily to be influenced by the material system with polymer grade and clay type identified as statistically significant. Based on the observations of both the EDA and statistical analysis it is recommended that the following material, manufacturing and testing conditions are considered for future studies:

- **Polymer Grade:** The influence of polymer grade observed in the EDA is due to the different grades having different neat properties. The statistical analysis indicated that there is no difference between the HDPE A7260-HDPE B7750, HDPA A7260-HDPE C7260 and HDPE B7550-HDPE D7255 grades for σ_{FPS}. The EDA indicated that HDPE B7750 provides the highest mean σ_{FPS}. However, Safripol South Africa no longer manufactures this polymer grade. As a consequence, HDPE C7260, with the second highest mean σ_{FPS}, will be considered for this thesis. Unfortunately, HDPE C7260 has been discontinued since the completion of this thesis and future studies will therefore not be able to replicate the work presented in this thesis.

- **Clay Type:** The EDA indicated that Alcamizer 1 resulted in higher σ_{FPS} compared to DHT4-A which was unexpected as Alcamizer 1 is not ideal for poly-olefins. There is statistical significance for clay type for both response variables of interest. It should therefore be investigated further in future studies.

- **Clay Loading:** Clay loading should always be considered during a polymer clay study as it does have a known effect on the mechanical properties. Based on the EDA it is suggested that clay loadings considered not exceed 10 wt% as material degradation sets in. Higher clay loadings is dependent on the focus of the study, however it will add another level of uncertainty. The concerning statistical observations should be further investigated.

- **Number of Extrusions:** There is no statistical significance for σ_{FPS}, while statistical significance was indicated for normalised ϵ_f. During the EDA it was determined that 2 extrusions is sufficient, as more does not provide additional improvements and requires more resources (*i.e.* cost and time).

- **Press Time:** No statistical significance was found and the EDA indicated that the σ_{FPS} improvement from 25 to 45 min does not warrant the additional manufacturing time and cost. A press time of 25 min is therefore adequate.

- **Sample Cooling:** The EDA indicated that air cooled samples provide the highest mechanical properties.

- **Strain Rate:** Both analyses indicated a clear influence due to strain rate which should be investigated further.

An unexpected result from the historical data analysis is the lack of any statistical significant effect due to the clay loading. This is especially evident for σ_{FPS} where no increase was observed once clay is introduced into the polymer matrix. This is counter to what is expected based on literature. Generally, there were difficulties in obtaining consistent and significant results, with large variations observed in both mechanical responses. Based on the historical data, it was not possible to determine the origin of these variations. This ambiguity is the fundamental motivation for the research conducted in this thesis.

These results have highlighted the need for a better approach to designing the experimental studies required to better understand and quantify the effects on the mechanical properties of the HDPE/clay composites. The conclusions and recommendations from this chapter will be used to determine the parameters and ranges of interest in the thesis experimental design.

CHAPTER 3

SYSTEMATIC LITERATURE REVIEW

The historical data analysis clearly indicated that changes in the manufacturing conditions do have an influence on the mechanical properties of high-density polyethylene/layered double hydroxide (HDPE/LDH). A natural next step is to interrogate the research landscape to gain a better understanding of the variation in manufacturing and their influence on mechanical properties.

The purpose of this chapter is therefore to analyse and compare the behavioural trends of the different manufacturing considerations and their effects on the mechanical properties, with a specific focus on HDPE and montmorillonite (MMT) composites. It was decided to focus on MMT for this review as it is more commonly used in literature compared to LDH (Costa *et al.*, 2005; Dabrowska *et al.*, 2013). This will ensure that there is ample data to conduct a proper review, which is not guaranteed when only considering LDH. For example, the current keywords do include "layered silicate" finding 7 studies where LDH was considered. Ding and Qu (2006); Costache *et al.* (2007); Ardanuy *et al.* (2009); Dabrowska *et al.* (2013); Peng *et al.* (2017) and El-Fattah and ElKader (2018) were excluded as they didn't conform to the eligibility criteria. One study (Botha *et al.*, 2020) is based on the work presented in Chapter 2 and was therefore not included in this chapter. It is safe to assume that the observed behavioural trends in this chapter can be directly applied to LDH as it is structurally similar and a common alternative to MMT.

In this review, I followed the PRISMA (Preferred Reporting Items for Systematic Reviews and Meta-Analyses) guidelines, aiming to provide a comprehensive overview of the current literature on the influence of manufacturing variation on the mechanical properties. PRISMA requires investigator triangulation, meaning that more than one investigator should work on deciding whether a study conforms to the eligibility criteria. The initial database search and study selection was performed in January 2020, with updated searches conducted in September 2021 and June 2022 to ensure no recent publications were omitted.

3.1 Introduction

A number of review papers have been published, discussing the processing, characterisation and properties of polymer nanocomposites (Fu *et al.*, 2019; Hetzer and Kee, 2008; Hussain *et al.*, 2006; Jordan *et al.*, 2005; Khanam and AlMaadeed, 2015; Kotal and Bhowmick, 2015; Mittal *et al.*, 2018; Müller *et al.*, 2017), and providing an overview of the polymer nanocomposite components (Crosby and Lee, 2007) and the synthesis and properties of nanoparticles (Hanemann and Szabo, 2010). These reviews usually discuss a wide range of polymer-clay systems and the different techniques used to manufacture these composites. The paper by Khanam and AlMaadeed (2015) is narrower in scope, in that it only considered polyethylene-based (PE) nanocomposite systems. The authors provide a discussion on the various compounding and processing methods and the types of analyses that may be performed, but do not compare the effects of manufacturing variations on mechanical properties. The reviews by Albdiry *et al.* (2012) and Modesti *et al.* (2010) investigate the effects of manufacturing, specifically compounding, on the mechanical properties of polymer-clay composites. Albdiry *et al.* (2012) compare seven experimental studies with diverse manufacturing methods and composites. The material systems studied did not include PE. They concluded that the mechanical properties of the resulting polymer-clay composites are affected by the manufacturing method. Modesti *et al.* (2010) provide a review investigating how different blending protocols, compounding methods and conditions, and compounding treatments (for example, supercritical CO_2 and ultrasound) affect the mechanical properties of nanocomposites. They did not compare different studies, but rather provided an analysis and understanding of the specific factors and the relationships that exist between manufacturing factors and composite morphology by discussing selected works.

A drawback of reviews that follow an ad-hoc search strategy is that they only provide an overview of a part of the literature, and don't necessarily include all the available literature on the topic or research question. For this reason, I will pursue a systematic literature review to ensure a prescribed methodology is used to collect, evaluate, identify and select the literature to review. By following such a predefined systematic methodology, the process minimises any potential bias while being repeatable (Moher *et al.*, 2009, 2015). The PRISMA (Preferred Reporting Items for Systematic Reviews and Meta-Analyses) guidelines define a systematic literature review as an 'attempt to collate all relevant evidence that fit pre-specified eligibility criteria to answer a specific research question" (Moher *et al.*, 2015). The PRISMA guidelines provide a checklist of recommended items to include in a systematic review, including details on the method such as eligibility criteria, information sources, search strategy, data collection and synthesis; and the synthesis of the results either considering a quantitative or qualitative analysis depending on the data (Moher *et al.*, 2009, 2015). This is a beneficial approach to reporting literature reviews as it highlights the transparency of the research process while ensuring the quality, reliability and reproducibility of the review (Moher *et al.*, 2015). These types of reviews are considered the reference standard in the health care industry (Moher *et al.*, 2009, 2015). Only a limited number of systematic reviews have been published in the field

of polymer-clay composites (Maniar, 2004; Mochane *et al.*, 2018; Mishra *et al.*, 2019; Sapuan *et al.*, 2016).

At present, there are no general or systematic literature reviews that provide a comprehensive overview of the published literature focusing on the effects of manufacturing on the mechanical properties of high-density polyethylene (HDPE)/montmorillonite (MMT) composites. This is largely due to the difficulty in comparing and generalising observations from different sources (Modesti *et al.*, 2010). The purpose of this chapter is to provide an example of a systematic literature review following the PRISMA guidelines (Moher *et al.*, 2009, 2015) while addressing the gap in the current knowledge base with regards to the influence of manufacturing variation on mechanical properties. I will do this by following the systematic literature review methodology to compare and assess the available evidence with the aim of answering the following research question: *How do variations in manufacturing influence the mechanical properties of HDPE/MMT composites?*

3.2 Methods

This systematic literature review is performed in accordance with the PRISMA (Preferred Reporting Items for Systematic Reviews and Meta-Analyses) guidelines (Moher *et al.*, 2009, 2015).

3.2.1 Eligibility criteria

To be included in this review, a study had to meet the following eligibility criteria based on the stated research question:

- The study considers any **high-density polyethylene-based (HDPE) polymer** which includes **blends with or without compatibiliser** as long as HDPE is the primary polymer component. For polymer blends the **secondary component should aid processing**, for example through reducing melt viscosity.
- The composite system contains **any type of silicate layered clay** either modified or not, as long as it is the primary filler. Examples include montmorillonite, mica, halloysite and vermiculite.
- The study investigates **change or variation in the manufacturing conditions of a specific method** or there is a **comparison of two or more manufacturing methods**.
- The final processing step should result in a **useful end product** that can be used for **bulk material testing** (*i.e.*, not an extrudite or fiber).

- **The influence on the mechanical properties is reported**. This will include studies where the mechanical properties are reported as a function of either clay or compatibiliser loading.

Studies are immediately excluded from the screening process if any of the following exclusion criteria is met:

- The study is not in English.
- The full text of the study is not available.
- The publication type is anything other than a peer-reviewed journal article, conference paper, book, book chapter or dissertation. For example, patents and news articles are excluded.
- There are no mechanical properties reported for a variation in the manufacturing methods or conditions.
- No mechanical properties are reported as a function of manufacturing variation, even if other properties (for example, thermal properties, flame retardancy, etc.) are reported. This applies to studies which only investigate creep behaviour.
- The study does not meet the inclusion criteria or is not within the scope of the research question. This will include studies primarily focused on the effect of clay or compatibiliser loading on mechanical properties, which are well represented in literature.

3.2.2 Information sources

Four electronic databases for materials science and engineering were identified: Scopus, Web of Science, EBSCOHost and Engineering Village. The keywords used to search the databases were directly derived from the research question, and included potential synonyms used in the field:

(manuf OR proc* OR extru* OR compound* OR injection OR compress* OR mixing OR ultraso* OR mold* OR mould* OR cast*) AND (mech* OR tensile OR strength OR stiffness OR impact OR fracture OR flexur*) AND (propert* OR character* OR strength OR stiffness) AND (hdpe OR "high density polyethylene") AND (*clay OR *clays OR "layered silicate" OR montmorillonite)*

The keywords were used as presented here in each of the four databases. No limitations or advanced search strategies were included and no start- or end-date limits were used. The search results were exported into a spreadsheet-compatible file, which was used for the data management and screening process. The database search was performed independently by myself (NB) and a collaborator, Mr. David Viljoen (DV), during January 2020 with the

results from the four databases consolidated and stored in a spreadsheet-compatible file, independently for each investigator. In this review, I refer to this spreadsheet-compatible file as a database. Updated searches were performed in September 2021 and June 2022 to ensure no new publications are omitted. Both of these updated searches found that no new publications conformed to the eligibility criteria.

3.2.3 Search strategy and Study Selection

Mr. David Viljoen (DV) and I (NB) removed duplicate entries from the consolidated databases before screening for initial exclusion based on language and publication type. We then independently applied the eligibility criteria in a three-step screening process: screening based first on the title, then on the abstract and finally the full text before providing an initial recommendation for inclusion/exclusion. A new database was created to consolidate the recommended articles and we evaluated the database again to provide a recommendation with our rationale on all studies considered. In cases where no consensus was reached between us, my supervisors Dr. Helen Inglis (HI) and Prof. Johan Labuschagne (JL) considered the recommendations and rationale provided to make a final decision.

3.2.4 Data collection and synthesis

The data collected from the included studies were compiled in a database, and the following data and metadata were collected in an overview table:

- Publication details such as year and publication type.
- The full reference, study focus, material composition (polymer, clay, compatibiliser type and loadings), manufacturing methods and conditions, type of mechanical properties tested (including international standard used and the number of repeated samples tested) and the main conclusions.
- All mechanical properties (tensile, impact, flexural, hardness and dynamic mechanical analysis (DMA)) presented as a function of the manufacturing variation were either extracted from a table or digitised using G3Data (Frantz, 2000) from figures. The method of extraction is indicated in the database.

During the data-collection process the references of included studies evaluating the titles and abstracts against the eligibility criteria were screened. Studies identified for potential inclusion were shared with Mr. David Viljoen (DV) and the same three-step screening process, described earlier, was followed.

A meta-analysis is not viable in this case, as the included studies considered different material compositions, manufacturing methods and conditions—making direct comparison implausible. For this reason, I only considered an exploratory data analysis approach to evaluate

potential trends in the data. The extracted data are presented with no additional processing, apart from ensuring unitary consistency, as the main objective of the study is to present the mechanical properties as recorded in the original studies. This will allow us to gain insight into the mechanical-property trends resulting from manufacturing variations within and across studies. In cases where a study also investigated material system influences I will only report the mechanical properties from the best-performing material system. The focus of this review is on the influence of manufacturing variation, not the material system. The studies were categorised into five categories based on their main focus, namely blending protocol, compounding methods, compounding conditions, processing methods and processing conditions. These categories were chosen as they represent the main phases in the manufacturing process of a polymer-clay composite. The blending protocol describes the process of mixing the components together. Compounding method and conditions is the stage where the polymer-clay composite is mixed together to form a composite compound. The processing method and conditions refers to the stage used to convert the composite into final products, here relevant to mechanical testing. After the data were synthesised and each category written up, I followed a process that included investigator triangulation, with DV providing a detailed review of the data synthesis.

3.2.5 Limitations

There are a few limitations in this systematic literature review. The first relates to the initial search strategy, which was performed during September 2021 and June 2022 using predefined keywords and only four databases, which are considered to be the most prominent in the engineering field. I may, therefore, have omitted studies which could otherwise have been included in this review.

The second limitation is related to the retrieval of the data, where 43 % of the study results had to be digitised, which could introduce slight deviations from the original published results. 28 % of the studies did not report the international testing standard used to obtain the mechanical properties and 39 % did not report the number of samples tested. One study (Merinska *et al.*, 2012) did not provide sufficient information on the polymer considered in their material system. More importantly, several studies (Esteki *et al.*, 2013; Eteläaho *et al.*, 2009; Hwang *et al.*, 2009; Jainal *et al.*, 2014; Lew *et al.*, 2005; Merinska *et al.*, 2012; Nguyen and Baird, 2006; Oliveira *et al.*, 2009) did not provide sufficient information on their manufacturing methods or conditions to replicate their experimental work.

The third limitation is the variation between the material systems and manufacturing- and testing conditions used by the different studies. This resulted in a large variation between the reported mechanical properties, such that I was only able to analyse behavioural trends. 59 % of the studies did not report the standard deviation of the mechanical properties. There was no consistency in the reporting of units for impact strength, for example KJ/m^2, J/m or Kgf.cm. Where possible conversions are made to ensure consistent units are compared.

However, there is no conversion available for J/m to KJ/m^2 unless the cross-sectional area under the notch of the samples were reported (ASTM D256-10, 2018; ASTM D6610-18, 2018).

The last limitation is the reported strain rate. Studies considered different strain rates ranging from 1 mm/min to 100 mm/min with a number of studies not having reported their strain rates. Strain rate is known to have an influence on the mechanical properties (Jo and Naguib, 2008; Botha *et al.*, 2019, 2020). There is an increase in Young's modulus with an increase in strain rate (Jo and Naguib, 2008; Botha *et al.*, 2019, 2020). This increase is due to the polymer chains having more time to adjust at the lower strain rates, resulting in more ductile behaviour. This, of course, is countered by more brittle behaviour at higher strain rates. Results in this review therefore indicate the strain rate at which mechanical properties were obtained.

3.3 Overview of Included Literature

An overview of the 33 studies included in this review is provided here by first reporting the results of the study selection. This is followed by a discussion of the study characteristics which includes an overview of the publication years, the number of papers assigned to each of the five categories, the different components considered in the polymer-clay composite system, the compounding methods and conditions, the processing methods and conditions and the testing standards and number of repeated samples reported. The purpose of this section is to provide a macroscopic view of the included studies.

3.3.1 Study selection

An overview of the study selection process is shown in Figure 3.1. A total of 1633 studies were found during the search of all four databases. After removing duplicate studies, 945 studies remained. The eligibility criteria applied independently by two investigators on the title and abstract resulted in 380 (NB) and 189 (DV) studies for which the full text was evaluated. After evaluation, the independent databases were consolidated—resulting in 312 studies. In cases where a study was included in one database but not the other it was added to the consolidated database.

The full-text studies of this consolidated database were reviewed a second time against the eligibility criteria where the two investigators (NB and DV) agreed on the exclusion of 275 studies. The remaining disagreements were then resolved by two additional investigators (HI and JL), who excluded 4 studies that did not conform to the eligibility criteria. A total of 33 studies are included in this systematic literature review. An overview table reporting key details for each study is provided in Appendix B.

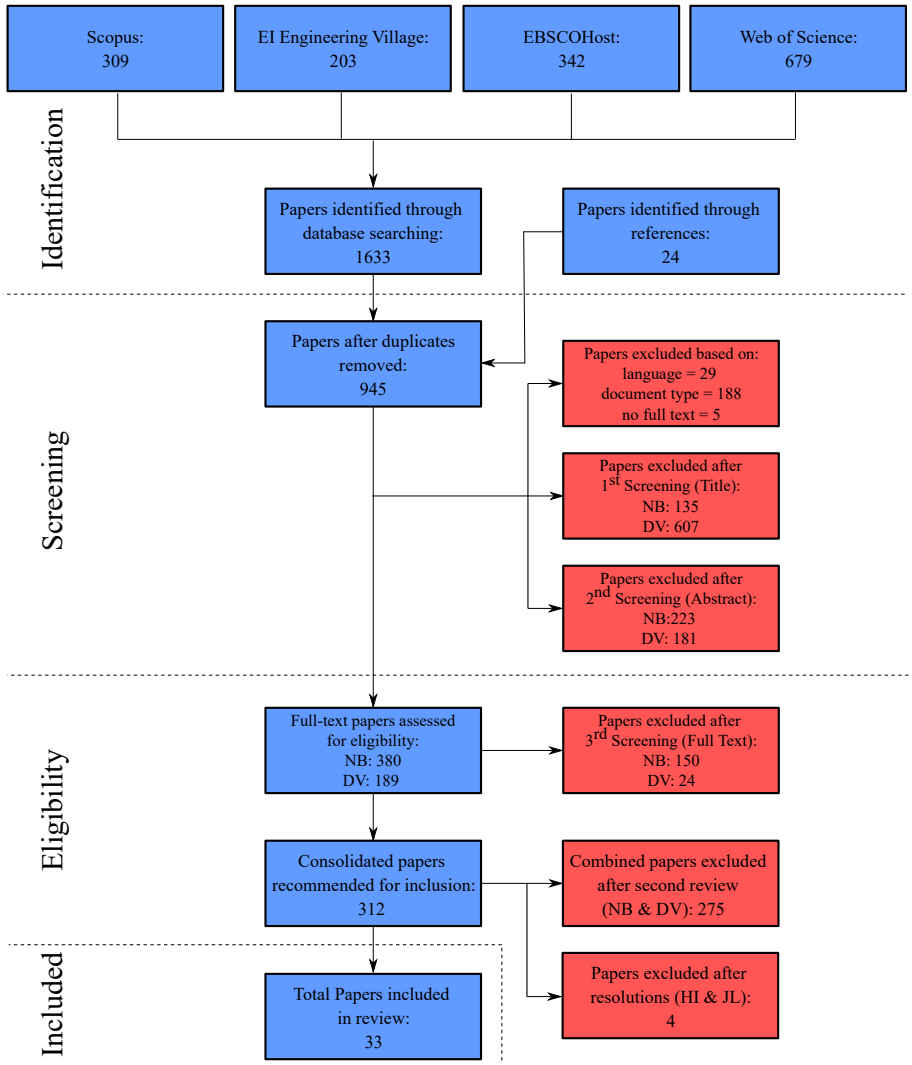

Figure 3.1: The PRISMA (Moher *et al.*, 2009, 2015) flow diagram for the different phases of systematic literature review

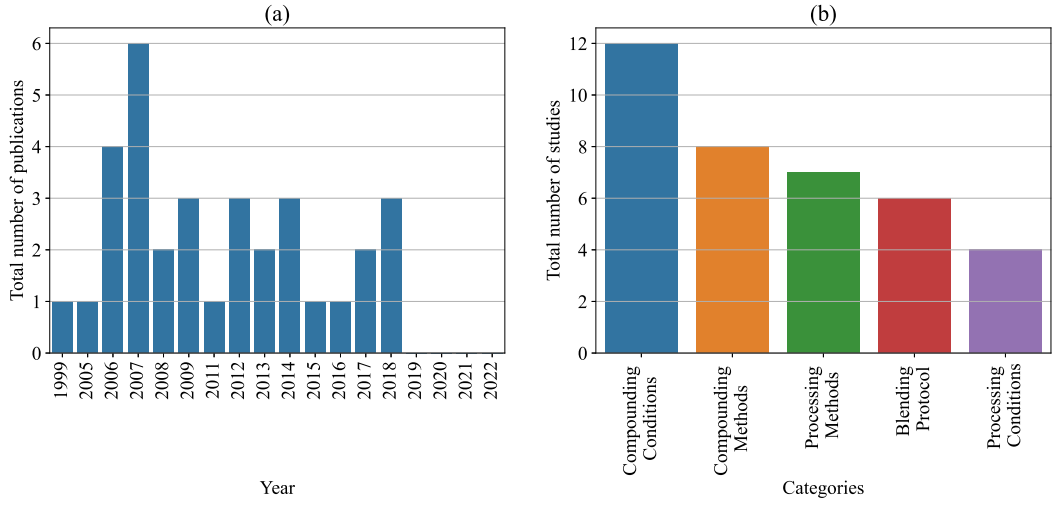

Figure 3.2: An overview of the study characteristics for the 33 studies included in the systematic literature review. (a) provides the total number of publications across the different years and (b) the total number of studies assigned to each defined category.

3.3.2 Study characteristics

A summary of the study characteristics are provided in Figures 3.2 to 3.5. 25 journal publications and 8 conference publications were included. From Figure 3.2(a) note that there is a consistent rate of publication for manufacturing variation-related studies up to 2018. None of the papers published after 2018 met the eligibility criteria. From Figure 3.2(b), compounding conditions seem to be the preferred area of study for manufacturing variation. It should be noted that 4 of the studies were assigned to two categories (Jo and Naguib, 2006, 2007a,b; Mainil *et al.*, 2006).

The different material system elements considered in the included studies are presented in Figure 3.3. Sub-groups are used owing to the large variety of material combinations. Some studies investigated multiple combinations of different clays and/or compatibilisers. Merinska *et al.* (2012) did not specify the type of PE used, as indicated in Figure 3.3(a). From Figure 3.3(b) note the most popular clay type used is Cloisite (especially 20A). The majority of studies did not consider a compatibiliser, as seen in Figure 3.3(c). In cases where a compatibiliser was included, it appears that PE-g-MA was most often used. Similar to the clay type, note that a large variety of compatibiliser types were considered. Finally, two studies considered the use of a secondary filler in their material compositions, namely carbon nanotubes (Brandenburg *et al.*, 2014; Silva *et al.*, 2014), as indicated in Figure 3.3(d).

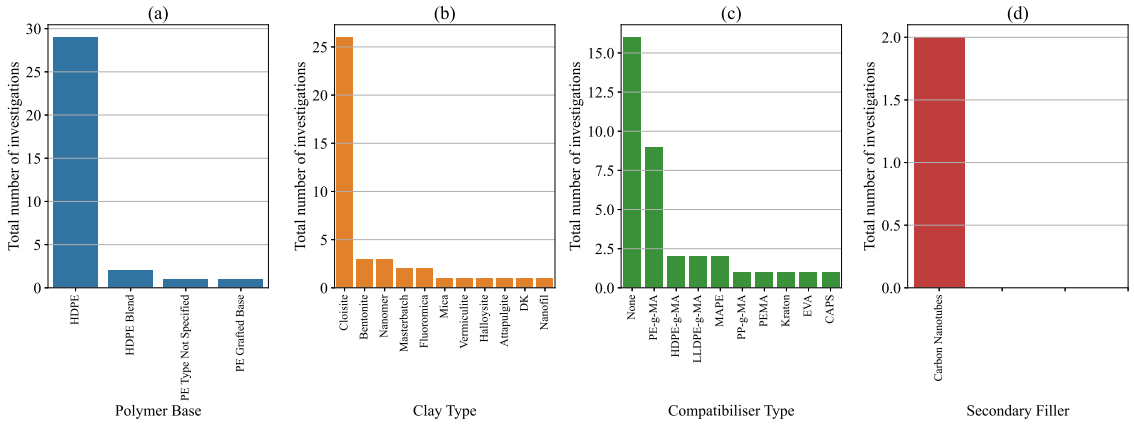

Figure 3.3: An overview of the material compositions characteristics for (a) the polymer base, (b) clay type, (c) compatibiliser type and (d) secondary filler.

An overview of the different compounding methods and conditions considered across the studies is provided in Figure 3.4(a). There are 10 primary methods used for compounding—with extrusion and internal mixing the two dominant methods. The majority of studies used a temperature of between 130 °C and 250 °C with a screw rotation speed of between 30 rpm and 130 rpm and that internal mixing tends to have higher mixing times, with residence times rarely reported for the other methods. Some studies used an assisting device during compounding, for example ultrasound (Lapshin *et al.*, 2008; Li *et al.*, 2007; Swain and Isayev, 2006, 2007) and water (Esteki *et al.*, 2013). From Figure 3.4(b) note that compression moulding is the preferred processing method followed by injection moulding. Typical processing temperatures are between 150 °C and 200 °C, with pressures of, at most, 20 MPa

and a processing time of between 8 min and 16 min. Esteki *et al.* (2013) did not provide any information regarding their processing methods and conditions. It is noteworthy that different variations were considered within the injection moulding category, for example dynamic and static packing (Gao *et al.*, 2012; Xiang *et al.*, 2009).

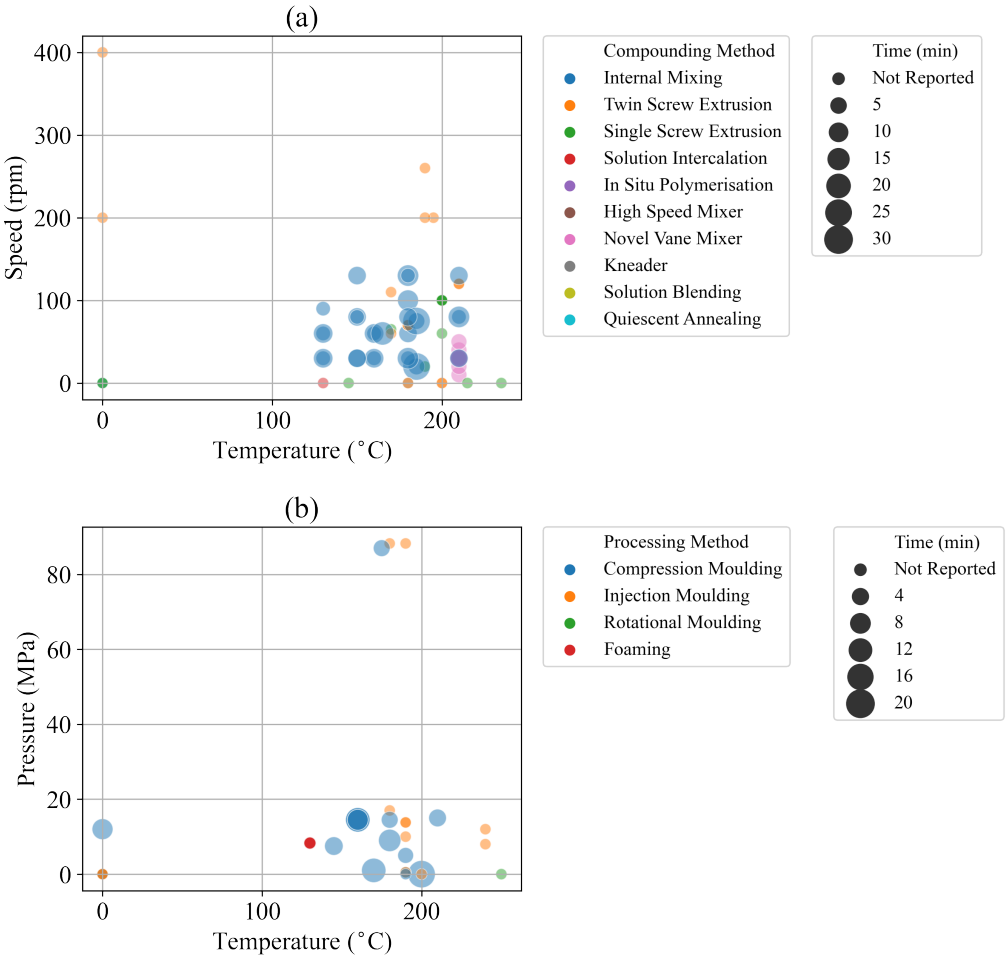

Figure 3.4: An overview of the manufacturing characteristics (methods and conditions) for (a) compounding and (b) processing.

An overview of the mechanical property characteristics is provided in Figure 3.5, where 43 % of the properties were digitised from the studies, 35 % were obtained directly from tables and 22 % were provided both in a table and digitally. Figure 3.5(a) indicates whether a study used an international standard for the mechanical testing. Figure 3.5(b) indicates whether a study considered repeated samples for the mechanical testing. It is clear from Figure 3.5(a) that the majority of studies reported tensile properties with a smaller portion reporting impact, flexural and DMA properties. The majority of studies reported the international standard and number of repeated samples (cf. Figure 3.5(b)) for each test, especially for the tensile, impact and flexural properties. The most commonly used international standards are the ASTM D638 for tensile, ASTM D256 for Izod impact and ASTM D790 for flexural properties. On average, the number of repeated samples considered is 5 for all tests as required by the international testing standards. From Figure 3.5(c) note that 48 % of studies investigating tensile properties reported the use of a strain rate of 50 mm/min which is typical for international standards.

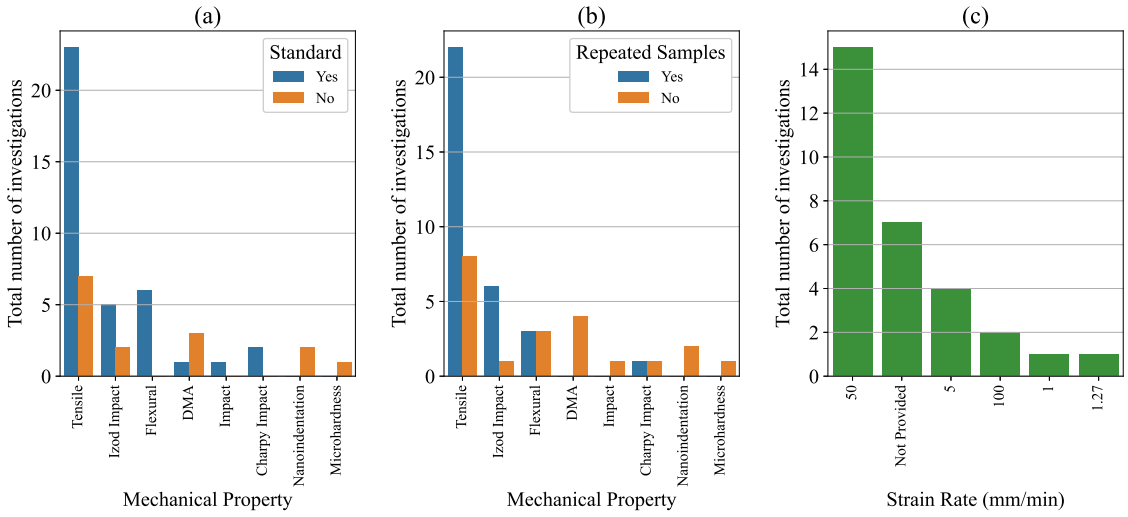

Figure 3.5: An overview of the study characteristics for the mechanical properties for (a) the type of properties reported and whether an international standard was used, (b) the number of studies which indicated the repeated samples used and (c) the strain rate used during tensile testing.

It is concerning that 23 % of studies did not report the strain rate used. There were large variations in the strain rates used, ranging from 1 to 100 mm/min.

3.4 Results and Discussion

The results from the data synthesis are discussed here and are divided into five categories chosen based on the stage of the manufacturing process. These include blending protocol, compounding methods, compounding conditions, processing methods and processing conditions.

3.4.1 Blending Protocol

The method by which clay is dispersed in the polymer matrix has a direct impact on the mechanical properties of the composite. For this reason, understanding the effect that a blending protocol (*i.e.* the order in which components are premixed and compounded together) has on the mechanical properties and composite morphology is important. All of the studies discussed here considered a one-step (direct mixing) and two-step (masterbatching) blending protocol, albeit with different approaches to the two-step blending protocols. A direct mixing protocol is when all material components (polymer, clay and other stabilisers are mixed together at the same time. A masterbatching protocol will first mix two components together (*e.g.* clay and compatibiliser), followed by a second mixing step to mix the masterbatch with the remainder of the components. Six studies considered the effects of blending protocol on the mechanical properties (Asgari *et al.*, 2017; Eteläaho *et al.*, 2009; Lei *et al.*, 2007; Mainil *et al.*, 2006; Passador *et al.*, 2014, 2016).

In the subsequent figures, blending protocols are denoted with acronymns defined at the top of each figure. For ease of reference the acronymns will be displayed in brackets in the text where discussed.

Tensile Properties

Figure 3.6 shows the effect of the different blending protocols on the mechanical properties of the composites. When comparing the intra-study results in Figure 3.6(a), the clay/compatibiliser (C/C) masterbatch tends to improve the Young's modulus when compared to that of direct mixing. For Passador *et al.* (2014, 2016) there is no visible improvement between clay/compatibiliser (C/C) and the polymer/clay/compatibiliser (P/C/C) masterbatches. Adding a compatibiliser provides higher values for Young's modulus as seen with Eteläaho *et al.* (2009) and Passador *et al.* (2014, 2016). This is due to the compatibiliser improving the interaction between the clay and polymer. From Figure 3.6(b) there is no change in First Peak Stress between the different blending protocols. Elongation to failure, Figure 3.6(c), is higher for direct mixing (DM) and reduces by half for a clay/compatibiliser (C/C) masterbatch as observed for both Asgari *et al.* (2017) and Mainil *et al.* (2006).

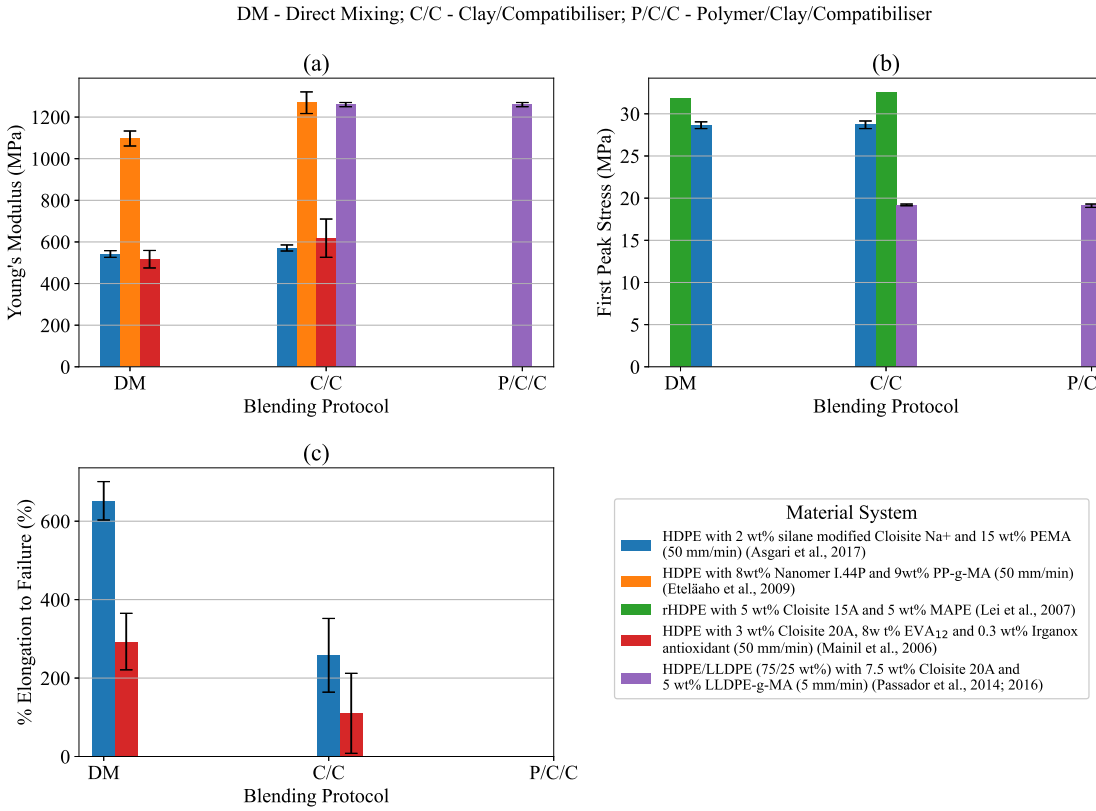

Figure 3.6: Effect of the blending protocol on the tensile properties: (a) Young's modulus, (b) first peak stress and (c) elongation to failure.

Flexural and Impact Properties

The effect of blending protocol on the flexural and impact properties is shown in Figure 3.7. The effects of blending protocol on the flexural properties are small, with only slight changes due to a change in masterbatching protocol. There is a slight increase in impact strength for the clay/compatibiliser (C/C) masterbatch when compared to direct mixing. The general improvement in the flexural and impact properties of the clay/compatibiliser (C/C) masterbatch is due to the clay being properly dispersed and distributed in the polymer matrix which improves clay-polymer adhesion (Passador *et al.*, 2016; Scaffaro *et al.*, 2013). This reduces crack propagation, as the stress transmission between phases is enhanced—thereby improving the toughness of the material (Scaffaro *et al.*, 2013).

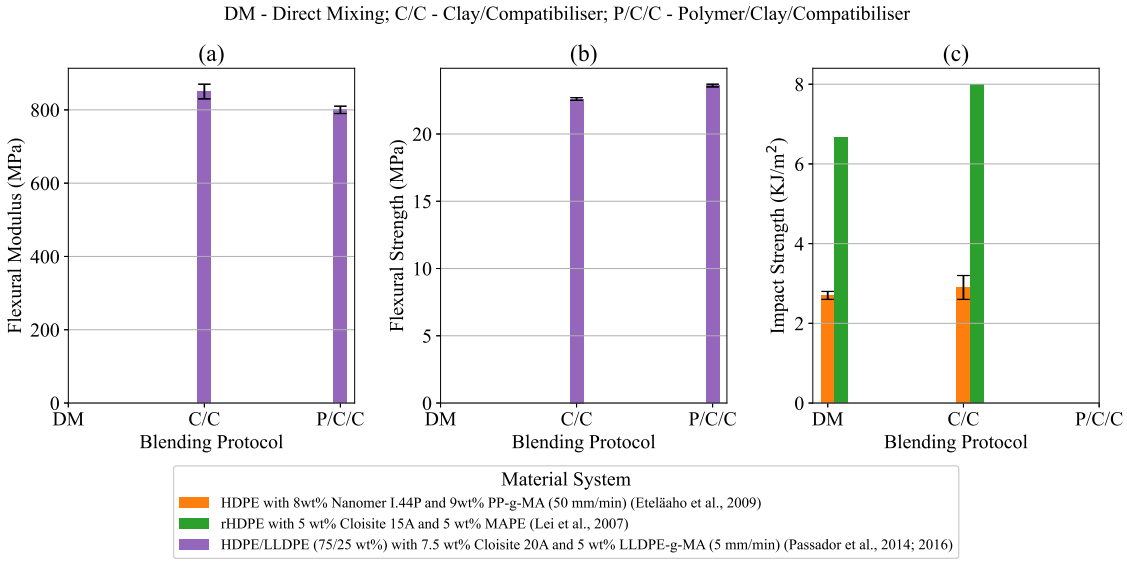

Figure 3.7: Effect of the blending protocol on the flexural and impact properties: (a) flexural modulus, (b) flexural strength and (c) impact strength.

Dynamic Mechanical Analysis

Commonly used measures in rheology to describe the materials deformation response are storage and loss moduli. The storage modulus (also known as the elastic modulus) is defined as the ratio of the elastic stress to strain. It therefore describes the material's ability to store energy elastically. The loss modulus (also known as the viscous modulus) is defined as the ratio of the viscous component to the stress. It describes the material's ability to dissipate stress through heat.

Lei *et al.* (2007) and Passador *et al.* (2016) provided DMA results, which are presented in Table 3.1 and Figure 3.8. From Table 3.1, there is no significant difference between direct mixing and clay/compatibiliser masterbatching in the storage and loss moduli.

In Figure 3.8(a), note that clay/compatibiliser masterbatching results in a higher storage modulus than polymer/clay/compatibiliser masterbatching. This indicates that the poly-

Table 3.1: DMA results based on the effect of blending protocol for rHDPE with 5 wt% Cloisite 15A and 5 wt% MAPE. (Adapted from Lei *et al.* (2007))

Blending Protocol	Storage Modulus (MPa)	Loss Modulus (MPa)
Direct Mixing	1.50	0.166
Clay/compatibiliser	1.43	0.154

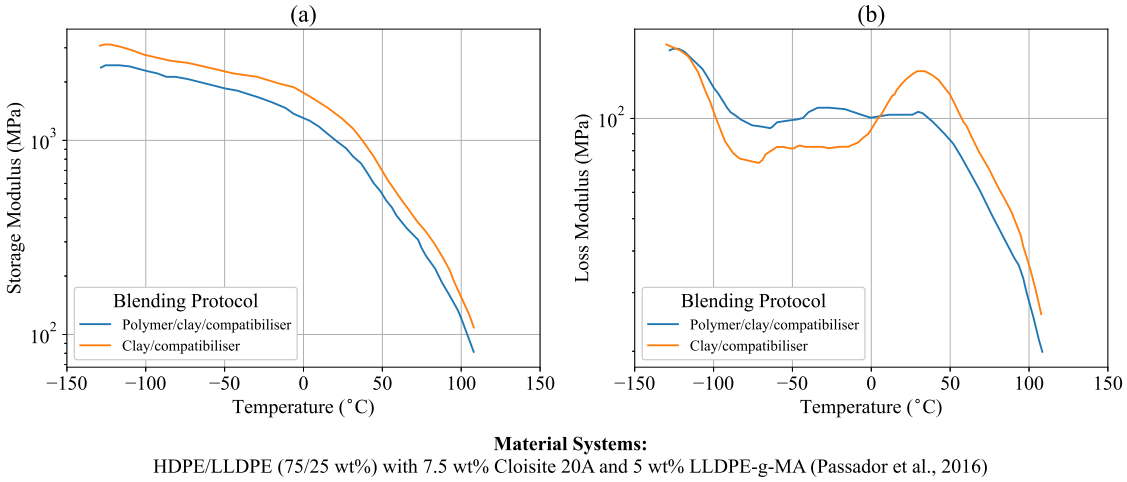

Figure 3.8: Effect of the blending protocol on the DMA properties: (a) storage modulus and (b) loss modulus. (Reproduced with permission from Passador *et al.* (2016))

mer/clay/compatibiliser masterbatching has a reduced energy elastic storage capacity, thereby decreasing the resistance to material deformation. In Figure 3.8(b), the loss modulus for clay/compatibiliser masterbatching tends to be lower than that of polymer/clay/compatibiliser masterbatching at lower temperatures, and higher than that of polymer/clay/compatibiliser masterbatching at higher temperatures with the change-over point just above 0 °C. This indicates that the clay/compatibiliser masterbatching is better able to dissipate stress through heat with increased temperatures. According to Passador *et al.* (2014, 2016) there is crosslinking between the clay and compatibiliser in the clay/compatibiliser masterbatch which is process-induced as a result of matrix degradation. This explains the higher storage modulus while a lower loss modulus is expected compared to the polymer/clay/compatibiliser masterbatch.

The sharp peak around 20 °C (the α relaxation of the matrix), can be ascribed to the increase in amorphous volume in the clay/compatibiliser case, and, potentially, an increase in the ordering present in these volumes owing to mixing effects of the already partially cross-linked masterbatch in the matrix (Danch *et al.*, 2003). The latter must be taken with care, owing to the absence of data for an annealed case of the material prepared using the clay/compatibiliser masterbatch.

Conclusion

Ultimately, the mechanical properties of a composite are affected by the crystallinity of the polymer matrix and the degree of reinforcement from the clay (Passador *et al.*, 2016). The masterbatching approach, therefore, improves the overall composite morphology by improving clay distribution and intercalation (Scaffaro *et al.*, 2013). The clay/compatibiliser masterbatching provides an improvement in composite stiffness compared to direct mixing as it more effectively disperses the clay in the polymer matrix. On the other hand, direct mixing provides better material ductility compared to clay/compatibiliser masterbatching.

3.4.2 Compounding Methods

During compounding, the morphology of the composite changes which ultimately affects the mechanical properties. The different methods used during compounding of the material, that is the phase in the manufacturing process where all the material components are mixed together to form a compound, are considered here. There were 8 studies (Boran *et al.*, 2017; Brandenburg *et al.*, 2014; Silva *et al.*, 2014; Esteki *et al.*, 2013; Heinemann *et al.*, 1999; Höfler *et al.*, 2018; Merinska *et al.*, 2012; Minkova and Filippi, 2011) which compared different compounding methods.

In the subsequent figures, compounding methods are denoted with acronymns defined at the top of each figure. Theses acronymns will be displayed in brackets in the text where discussed.

Tensile Properties

The effects of the different compounding methods on the tensile properties are shown in Figure 3.9. Note that Merinska *et al.* (2012) used DMA to determine the Young's modulus compared to the other studies which used tensile testing. Merinska *et al.* (2012) did not specify the type of PE used, although it is assumed to be HDPE due to the properties obtained.

From Figure 3.9(a), note that internal mixing (IM) offers the highest Young's modulus. From Esteki *et al.* (2013), water-assisted twin-screw extrusion (WA TSE) provides an improvement in Young's modulus over twin-screw extrusion (TSE) as it improves the degree of intercalation. From Boran *et al.* (2017), single-screw extrusion with an extensional-flow mixer (SSE EFM) reduces the Young's modulus slightly but not in a statistically significant way. Solution intercalation (SI) provides a slight decrease in Young's modulus compared to internal mixing. In-situ polymerisation (IP) provides the lowest Young's modulus. This is an interesting observation as it enhances exfoliation which should result in an increased stiffness (Heinemann *et al.*, 1999). In their study, Heinemann *et al.* (1999) found an increase in stiffness with in-situ polymerisation (IP) over internal mixing (IM) when adding 1-octene, which acts as a compatibiliser to improve the dispersion. However, it did reduce the Young's modulus by 61 % for in-situ polymerisation (IP) and 86 % for internal mixing (IM) from that reported

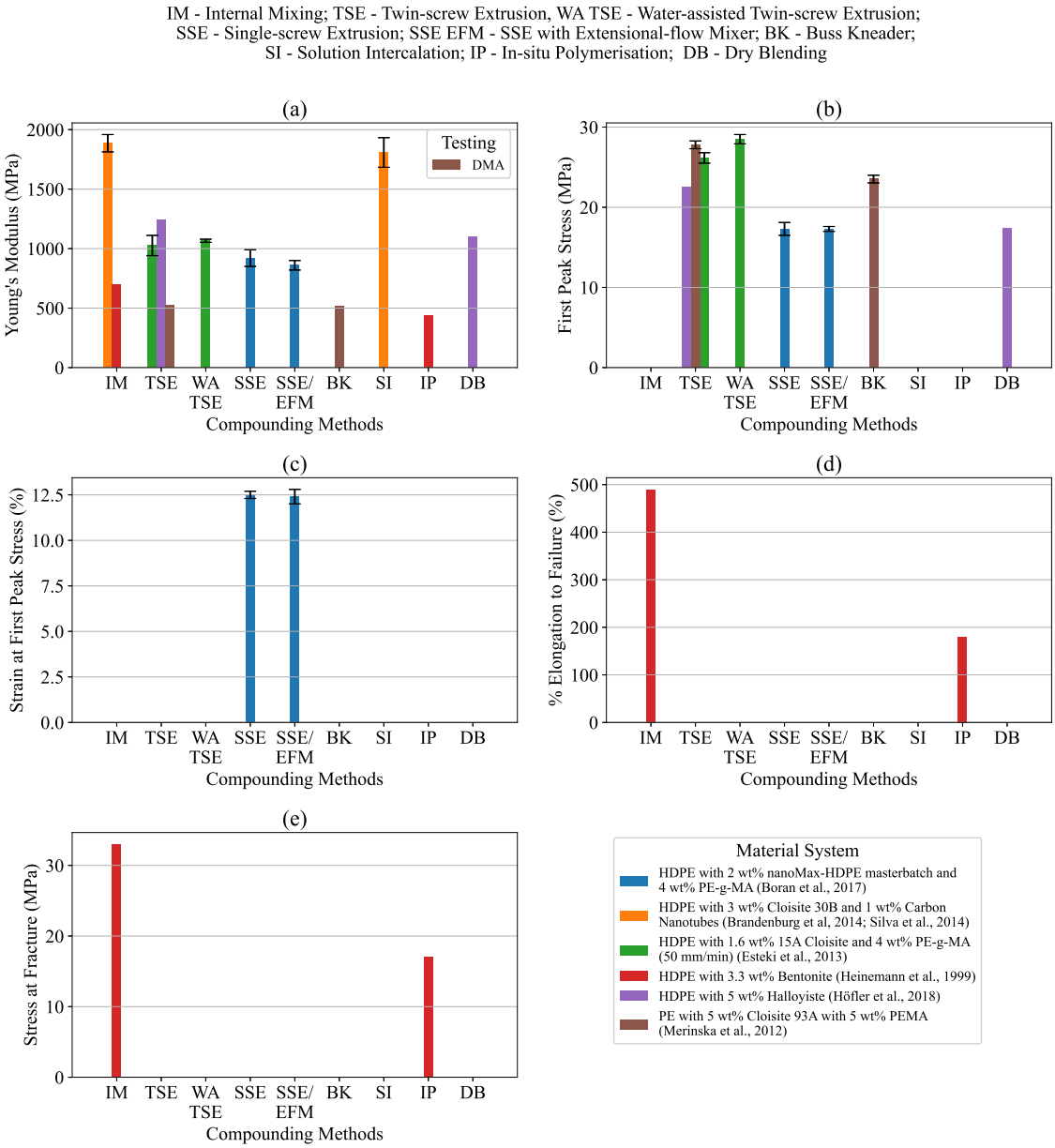

Figure 3.9: Effect of the compounding methods on tensile properties: (a) Young's modulus, (b) first peak stress, (c) strain at the first peak stress, (d) elongation to failure and (e) stress at fracture.

in Figure 3.9(a). Dry blending (DB) in a high-speed mixer will likely result in agglomeration of particles, which is why Young's modulus is reduced, whereas twin-screw extrusion (TSE) provides better mixing and dispersion (Höfler *et al.*, 2018). From Merinska *et al.* (2012) there is no significant change in Young's modulus when using either twin-screw extrusion (TSE) or BUSS kneading (BK).

There are similar trends in the first peak stress, Figure 3.9(b), where twin-screw extrusion (TSE) provides the best overall improvement comparing within the respective studies. BUSS kneading (BK) (Merinska *et al.*, 2012) and dry blending (DB) in a high-speed mixer (Höfler *et al.*, 2018) reduce the first peak stress, and there is no observable change in adding an extensional-flow mixer to the single-screw extruder (SSE EFM) (Boran *et al.*, 2017). A reduced

first peak stress can be explained by stress concentrations during tensile testing caused by agglomerates of clay (Merinska *et al.*, 2012). Adding water to the twin-screw extrusion (WA TSE) process does improve the first peak stress.

It is difficult to draw any overall conclusions from the remaining properties owing to insufficient data. However, there is no change in the strain at first peak stress in Figure 3.9(c). From Figure 3.9(d), the elongation to failure decreases significantly for in-situ polymerisation (IP) (Heinemann *et al.*, 1999). Internal mixing (IM) provides much better stress at fracture compared to in-situ polymerisation (IP) as seen in Figure 3.9(e).

Flexural and Impact Properties

The results for the flexural properties are shown in Figure 3.10. There aren't any significant changes in flexural properties for the different methods within a given study. Owing to differences in material and loading, no conclusions can be drawn between studies in this case.

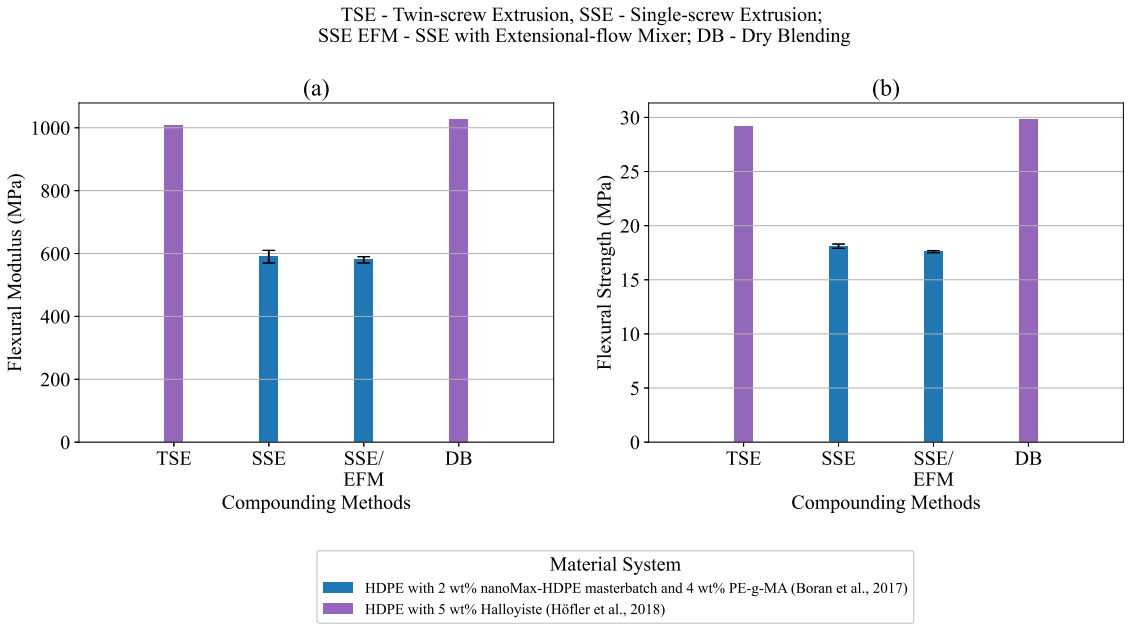

Figure 3.10: Effect of compounding methods on flexural properties: (a) flexural modulus and (b) flexural strength.

The toughness properties are shown in Figure 3.11. Note that for the impact strength in Figure 3.11(a), the studies reported their results in different units. There is an improvement in impact strength for dry blending (DB) in a high-speed mixer compared to twin-screw extrusion (TSE) (Höfler *et al.*, 2018). When adding water to the twin-screw extrusion (WA TSE), the impact strength actually decreases because nano-voids form at the polymer-clay interface, reducing the energy transfer capability (Esteki *et al.*, 2013). In Boran *et al.* (2017), adding an extensional-flow mixer to the single-screw extrusion (SSE EFM) process improves the impact strength as the extensional-flow mixer improves mixing and dispersion. From Figure 3.11(b), the nanohardness improves slightly for solution intercalation (SI) compared to

internal mixing (IM) (Brandenburg *et al.*, 2014; Silva *et al.*, 2014). Solution intercalation (SI) provides a larger interface area allowing for better interaction which increases the resistance to plastic deformation increasing the material toughness (Silva *et al.*, 2014).

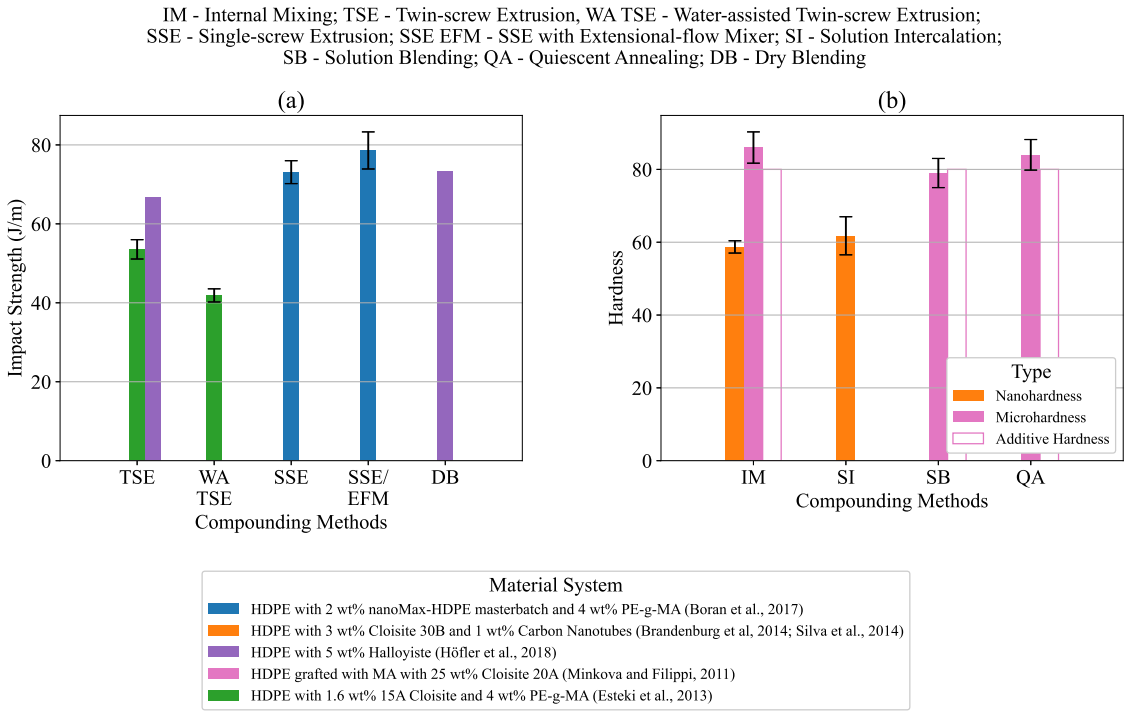

Figure 3.11: Effect of compounding methods on the toughness of the material: (a) impact and (b) hardness.

In Minkova and Filippi (2011), microhardness slightly decreases for solution blending (SB) and quiescent annealing (QA) compared to internal mixing (IM), which provides the highest microhardness. No significant change was found in the additive hardness between the three methods considered. Internal mixing (IM) and quiescent annealing facilitate higher levels of exfoliation and clay dispersion, resulting in improved hardness values. Conversely, poor clay dispersion and agglomeration result in lower values (Minkova and Filippi, 2011). The internal mixing (IM) method provides the best dispersion and therefore the best properties, followed by quiescent annealing (QA) and, finally, solution blending (SB).

Conclusion

Internal mixing and twin-screw extrusion offer the best overall mechanical properties, justifying their frequent use in the literature.

3.4.3 Compounding Conditions

The effects of different compounding conditions such as temperature, time, rotation speed or the use of additional equipment is considered here. This section is subdivided by the type

of compounding condition as opposed to the type of mechanical property as seen in previous sections. This section considers extrusion and internal mixing which are two of the most commonly melt mixing methods employed for polymer-clay composites. A total of 13 studies are discussed which include extruder screw profile (Barbosa *et al.*, 2012), extruder screw speed (Oliveira *et al.*, 2009), extruder temperature profile (Lew *et al.*, 2005), CO_2 treatment (Nguyen and Baird, 2006), ultrasound treatment (Lapshin *et al.*, 2008; Li *et al.*, 2007; Swain and Isayev, 2006, 2007), novel vane mixer(Huang *et al.*, 2015), internal mixer temperature (Gong *et al.*, 2013; Ujianto *et al.*, 2018), internal mixer speed (Gong *et al.*, 2013; Ujianto *et al.*, 2018) and internal mixer time (Gong *et al.*, 2013; Mainil *et al.*, 2006; Ujianto *et al.*, 2018). This is the largest category presented in this review.

Extruder Screw Profile

Barbosa *et al.* (2012) considered two different screw profiles, ROS and 2KB90, as well as a torque rheometer connected to a twin-screw extruder. Details of the screw profiles considered are discussed in Barbosa *et al.* (2012). The results for the mechanical properties are shown in Figure 3.12. The ROS screw profile offered the highest Young's modulus of the three configurations, while the rheometer configuration offered the highest first peak stress, with little difference between the performance of the two screw profiles. The screw profiles are believed to improve dispersion of the composite components, thereby improving the overall material stiffness (Barbosa *et al.*, 2012). However, Barbosa *et al.* (2012) does indicate that sufficient exfoliation was not achieved through these screw profiles as the composite mechanical properties were reduced from the neat HDPE sample.

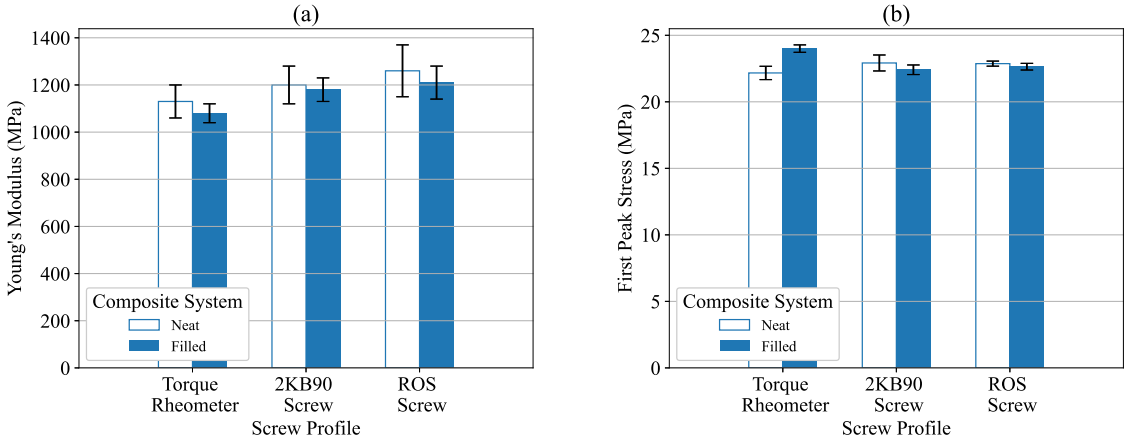

Figure 3.12: Effect of screw profile on the tensile properties: (a) Young's modulus and (b) first peak stress.

Extruder Screw Speed

The effect of the extruder screw-speed on impact strength is shown in Figure 3.13. Oliveira *et al.* (2009) reported the impact strength as 0.12 KJ/m at 200 rpm and 0.13 KJ/m at 400 rpm which is not a significant increase (7 %). An increase in screw speed aids exfoliation, thereby improving mechanical properties but only up to an optimum point before it starts to degrade the properties due to the decreased residence time. A decreased residence time may result in reduced mixing and/or exfoliation, which, in turn, results in the worsening of the properties.

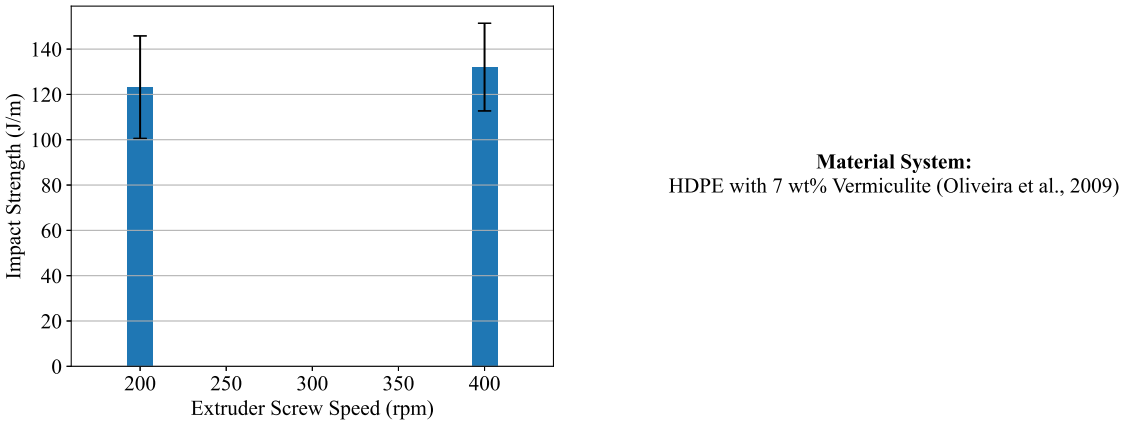

Figure 3.13: Effect of the extruder screw speed on the impact strength.

Extruder Temperature Profile

The effect of varying the temperature profile across all zones is shown in Figure 3.14. Lew *et al.* (2005) considered different temperature profiles with varying combinations of low and high temperatures in the different extruder zones. In Figure 3.14 the different temperature profiles are denoted with TPx where x is a number followed by the extruder temperature profile for each zone.

The higher temperature profiles provided improved mechanical properties with the TP1 (215-215-215-215-215-215-215 °C) and TP5 (215-215-170-170-185-200-215 °C) temperature profiles providing the greatest overall improvement. The authors claim that the initial high temperature aids the interaction of the polymer chains and the clay particles, while the reduced temperature in the latter portions of the extruder will increase melt viscosity and through the ensuing increase in shear, improve exfoliation.

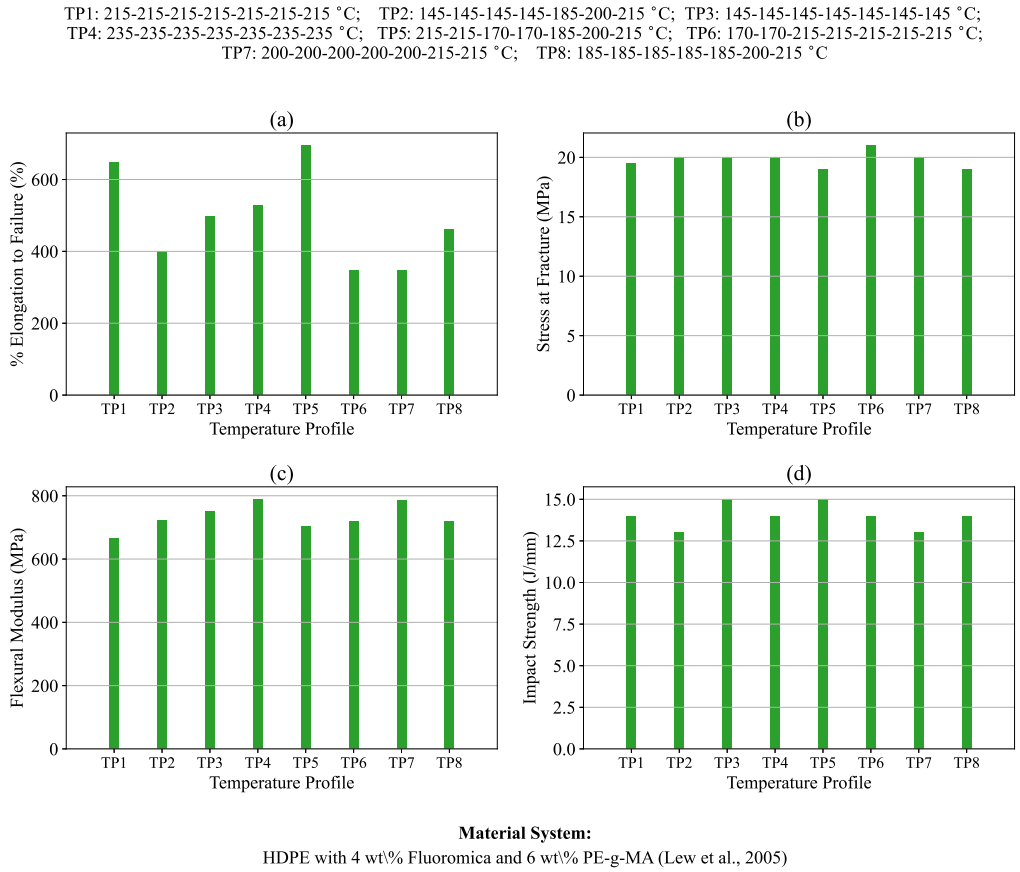

Figure 3.14: Effect of the extruder temperature profile on the mechanical properties: (a) elongation to failure, (b) stress at fracture, (c) flexural modulus and (d) impact strength. Square brackets indicate that a material was recompounded with the letter indicating the starting material. (H - high, L - low, m - mid).

CO_2 Treatment

Nguyen and Baird (2006) used supercritical CO_2 in an attempt to improve the dispersion of the clay particles within the polymer matrix during extrusion. They pressurised the CO_2 before injecting it, through a port, into the extrusion process at the beginning of the second stage of the two stage screw in a single screw extruder.

The tensile properties obtained through CO_2 treatment are shown in Figure 3.15, where the treatment clearly improves the Young's modulus with no significant effect on the first peak stress. This change suggests that the degree of exfoliation is improved for CO_2 treatment during the mixing process (Nguyen and Baird, 2006). Unfortunately, treating the polymer-clay composite with CO_2 during extrusion does lead to a loss of material ductility as seen with the lower elongation to failure. This suggests that while improved exfoliation enhances the material stiffness and strength, it does have the drawback of decreasing material ductility.

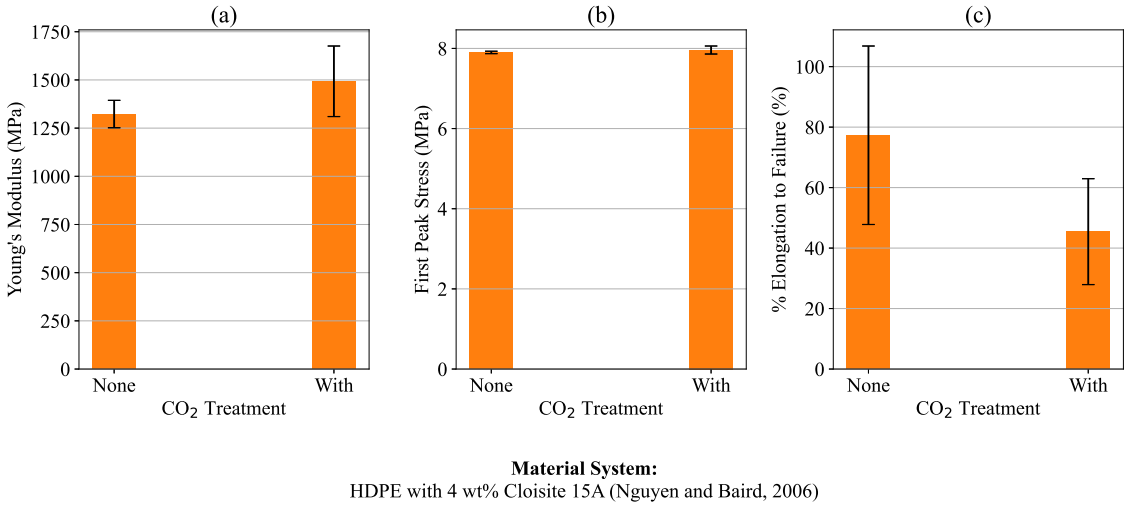

Figure 3.15: Effect of supercritical CO_2 treatment on the tensile properties: (a) Young's modulus, (b) first peak stress and (c) elongation to failure.

Ultrasound Treatment

Ultrasound treatment uses sound waves or vibratory oscillations in an attempt to improve clay dispersion. This is achieved by attaching an ultrasonic device to the slit die at the end of the extrusion process. This allows for continuous treatment of the extrudite as it exits the extruder. (Swain and Isayev, 2006, 2007) and (Lapshin *et al.*, 2008) all used exactly the same ultrasonic device developed in their laboratory with details regarding it published in (Oh *et al.*, 2003). (Li *et al.*, 2007) developed their own ultrasonic device with details regarding it published in (Zhao *et al.*, 2006).

Lapshin *et al.* (2008) considered the effect of the ultrasound flow rate on the tensile properties as shown in Figure 3.16. The ultrasound flow rate refers to the different material flow rates as it exits the extruder and corresponds to the residence time in the treatment zone. In

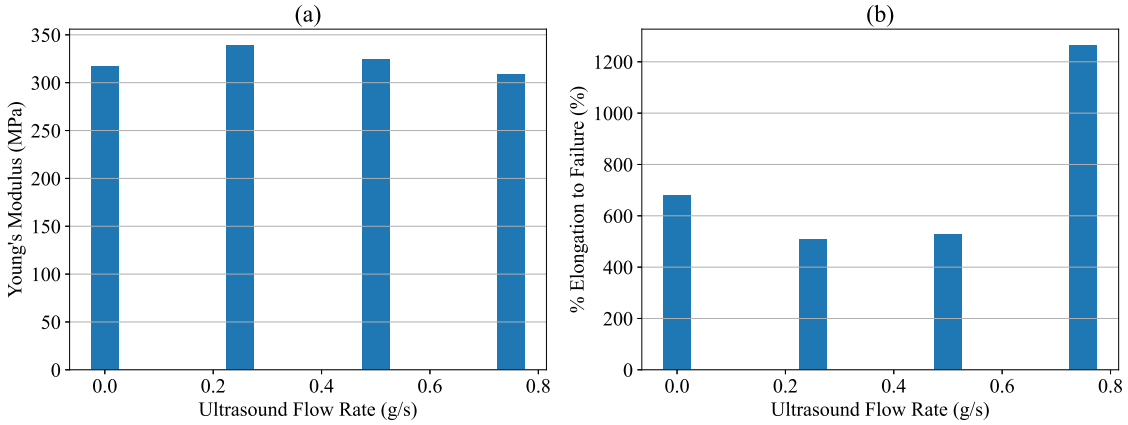

Figure 3.16: Effect of ultrasound treatment on the tensile properties as a function of ultrasound flow rate: (a) Young's modulus and (b) elongation to failure.

Figure 3.16(a) there is an initial increase in Young's modulus up to a flow rate of 0.25 g/s before decreasing as the flow rate increases. The Young's modulus is moderately affected by the ultrasound flow rate with the maximum improvement only 7 % at 0.25 g/s compared to the untreated composite. Lapshin *et al.* (2008) states that this is due to balance of the intercalation or exfoliation of the clay and the polymer-matrix degradation—two competing processes. Elongation to failure, in Figure 3.16(b), has the opposite behaviour: decreasing initially for a flow rate of 0.25 g/s before increasing with an increased flow rate. The increase in elongation to failure is due to the partial exfoliation observed improving the ductility of the material (Lapshin *et al.*, 2008).

The effects of the ultrasound intensity on the mechanical properties are illustrated in Figure 3.17. The ultrasound intensity refers to the power output of the device, *e.g.* at 0 W the ultrasonic device is off and no ultrasound treatment is received, whereas ast 200 W the device is on and the material undergoes ultrasound treatment. There is a general increase in mechanical properties with an increase in intensity, with the exception of the impact strength, which decreases slightly. The general improvement in mechanical properties is due to an improved dispersion of the clay in the polymer matrix, owing to the ultrasound treatment, which breaks down clay agglomerates into smaller stacked tactoids (Li *et al.*, 2007). According to Li *et al.* (2007), this improved dispersion is a reason for the improvement in the elongation to failure.

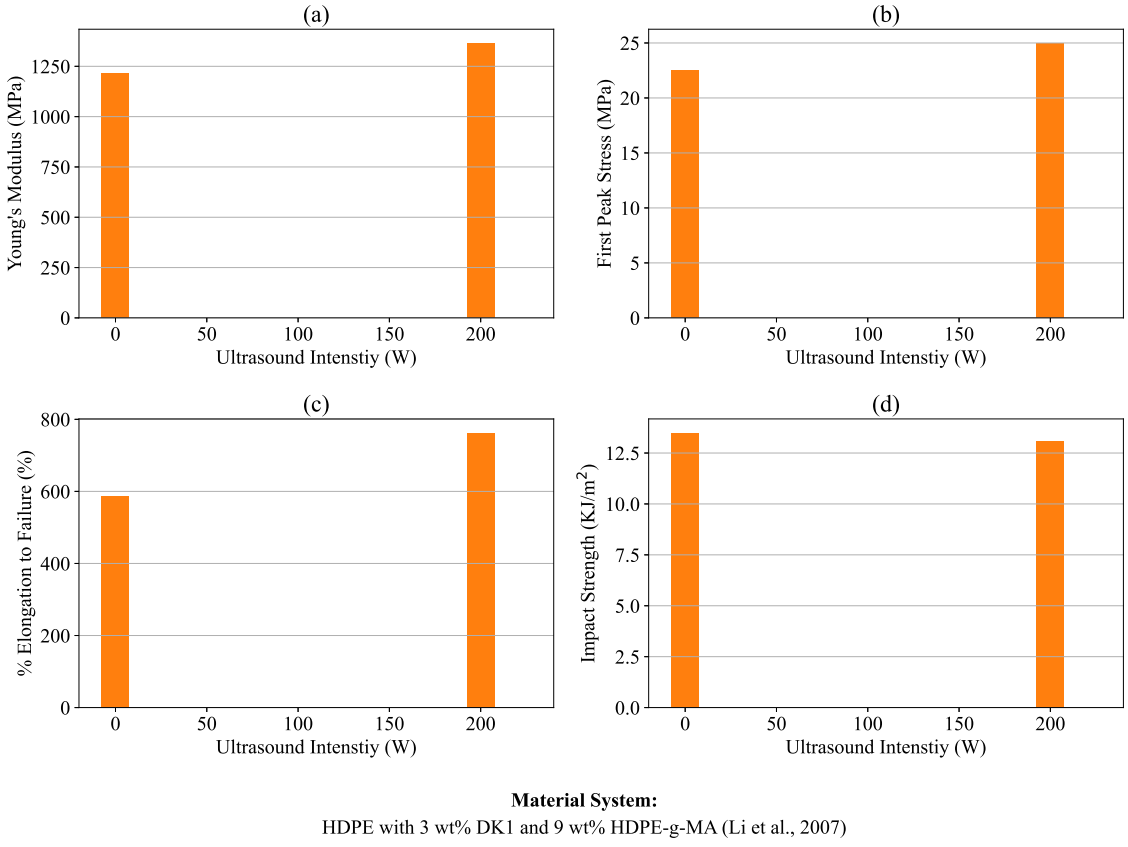

Figure 3.17: Effect of ultrasound treatment on the mechanical properties as a function of intensity: (a) Young's modulus, (b) first peak stress, (c) elongation to failure and (d) impact strength.

Swain and Isayev (2006, 2007) considered the effect of ultrasound amplitude on the mechanical properties, with the results shown in Figure 3.18. The ultrasound amplitude refers to the amplitude of the wave produced by the device. There is a general improvement in the first peak stress, elongation to failure and toughness; while Young's modulus, strain at first peak and impact strength tend to decrease with increased amplitude. Swain and Isayev (2006, 2007) concluded that by applying ultrasound treatment, the clay was better dispersed in the polymer matrix by creating stronger interfacial adhesions, which increased the material ductility.

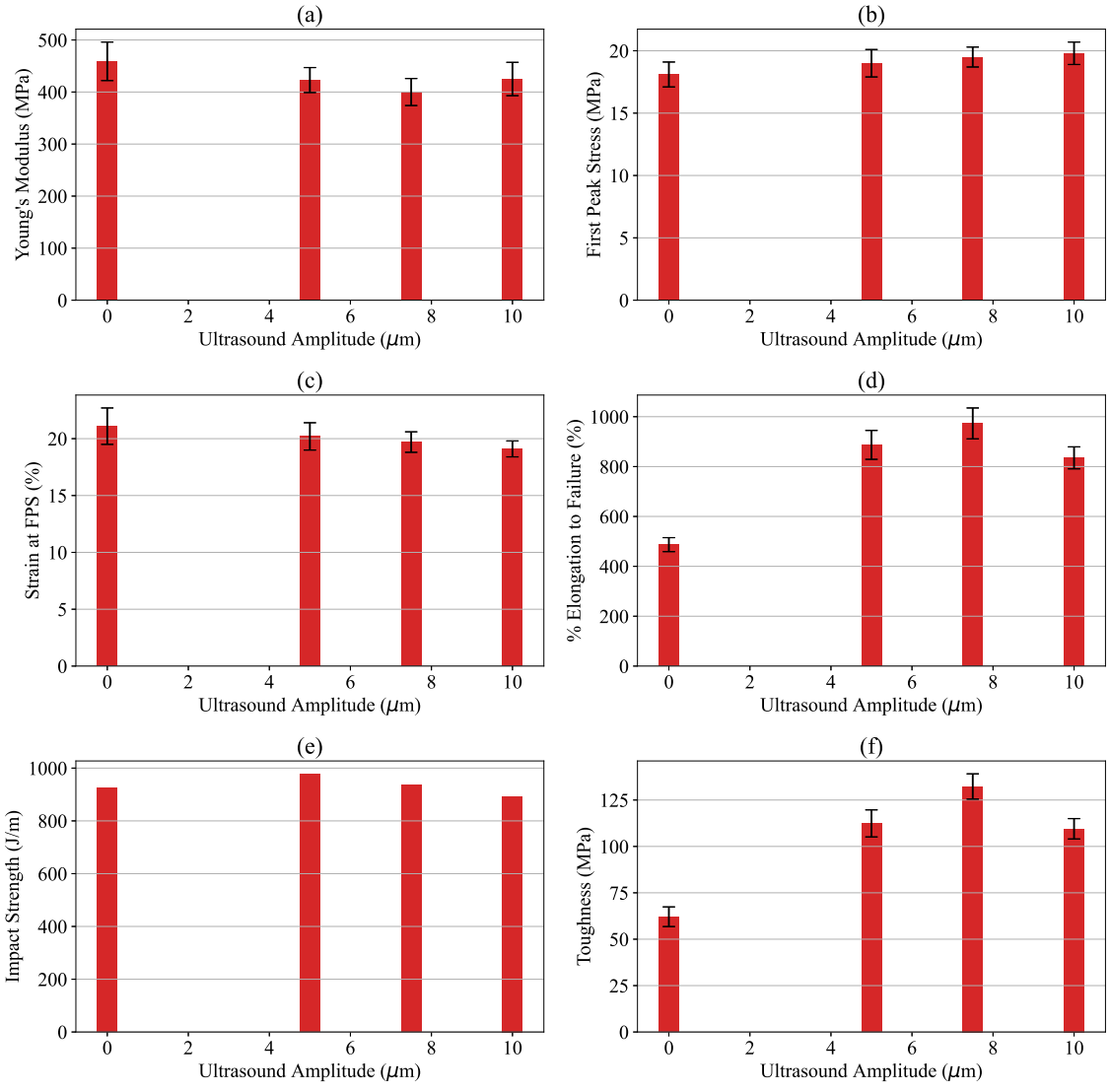

Figure 3.18: Effect of ultrasound treatment on the mechanical properties as a function of amplitude: (a) Young's modulus, (b) first peak stress, (c) strain at first peak stress, (d) elongation to failure, (e) impact strength and (f) toughness.

Novel Vane Mixer

A novel vane mixer is different to the traditional extruder consisting of a feeding unit and two mixing units. This change in structure allows the novel vane mixer to induce elongation flow as opposed to shear flow in traditional extrusion equipment. More details on the novel vane mixer can be found in (Huang *et al.*, 2015).

Huang *et al.* (2015) investigated the effect of rotation speed and mixing time on the tensile properties as shown in Figure 3.19. There is a general increase in first peak stress and elongation to failure up to 40 rpm before decreasing at 50 rpm. The improvement in properties due to rotor speed is attributed to the stress transfer between the polymer matrix and the clay layers (Huang *et al.*, 2015). For mixing time, there is general increase in these properties up to 4 min followed by a decrease at 6 min before increasing again, albeit much more slowly. The initial increase in performance may be ascribed to the improved intercalation that accompanies an increase in mixing time (Huang *et al.*, 2015). It is evident from the results that the optimum conditions for Huang *et al.* (2015) are 40 rpm and 4 min, as these resulted in the highest performance. Huang *et al.* (2015) conclude that the decrease in tensile properties at higher speeds and mixing times is due to the loss of organic cations between the clay platelets, which reduces the stress transfer between the polymer matrix and clay.

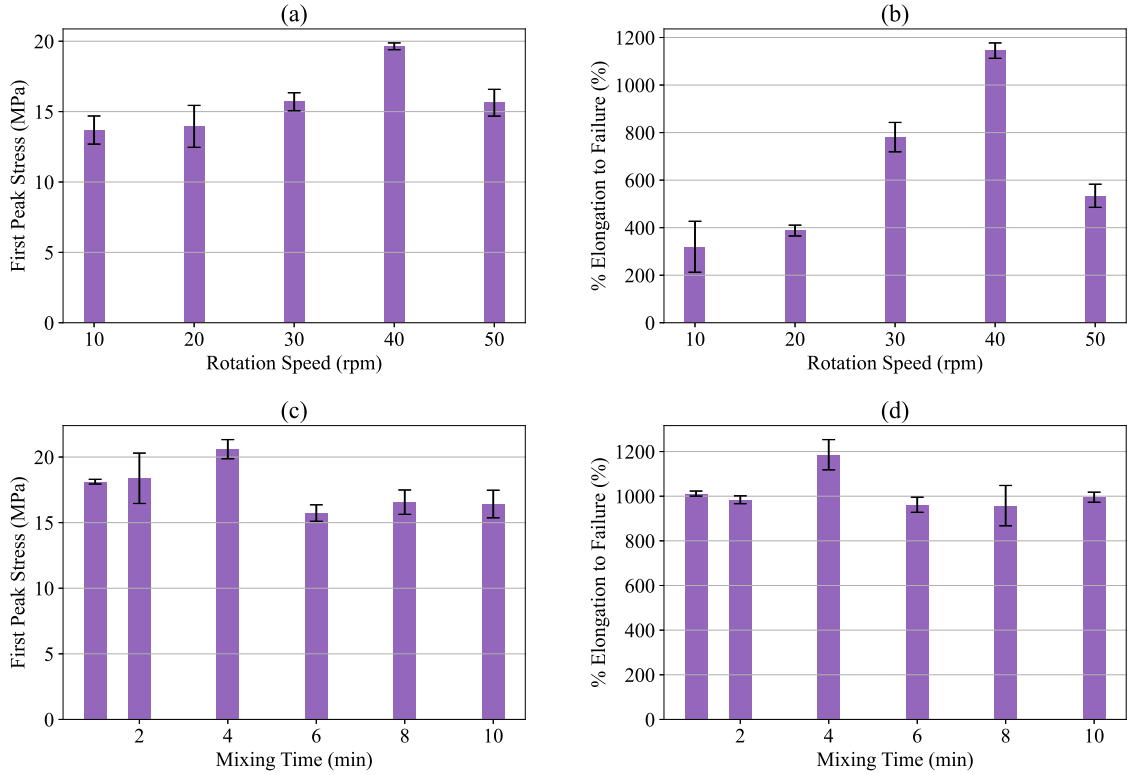

Figure 3.19: Effect of novel vane mixer rotation speed (constant time of 6 min) and mixing time (constant speed of 30 rpm) on the tensile properties: (a,c) first peak stress and (b,d) elongation to failure.

Internal Mixer Temperature

The effect of internal mixer temperature on mechanical properties is illustrated in Figure 3.20. There is a general increase in Young's modulus, albeit small, with an increase in temperature for either a Banbury or Roller rotor, with the Banbury providing the highest modulus. In Figures 3.20(b) and (c), flexural modulus and strength are shown to have a slight negative correlation with temperature in a Brabender mixer.

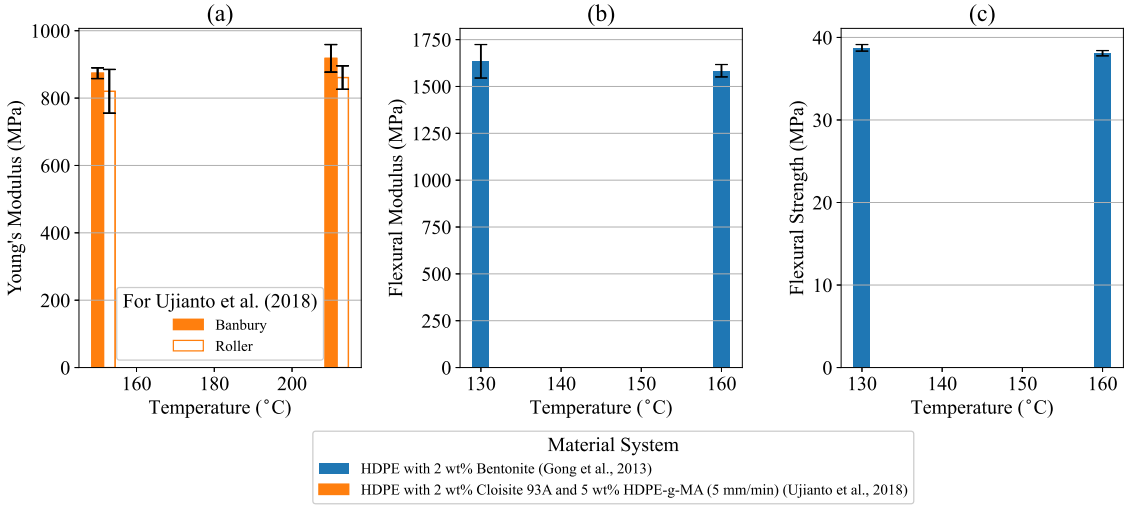

Figure 3.20: Effect of internal mixer temperature on the mechanical properties: (a) Young's modulus, (b) flexural modulus and (c) flexural strength.

Internal Mixer Speed

Figure 3.21 illustrates the influence of internal mixer speed on the mechanical properties. For (Ujianto *et al.*, 2018) there is a decrease in Young's modulus with an increase in rotation speed, with the Banbury rotor providing a higher Young's modulus compared to the Roller rotor. For (Gong *et al.*, 2013) there is no change in the flexural properties. The adhesion between the clay and polymer matrix is improved by increasing the rotor speed (Teymouri and Nazockdast, 2011; Zawawi *et al.*, 2012). This leads to more sufficient exfoliation due to higher shear stress which provides an improvement in composite stiffness and strength. This improvement in stiffness is not observed here which indicates that the increased rotor speed did not provide sufficient exfoliation for the composite systems presented here.

Internal Mixer Time

The effect of internal mixing time on the mechanical properties is shown in Figure 3.22 where a general increase in mechanical properties is observed with an increase in mixing time.

From Ujianto *et al.* (2018) the Banbury rotor provides the most improved Young's modulus compared to the Roller rotor. A longer mixing time allows for a better degree of dispersion

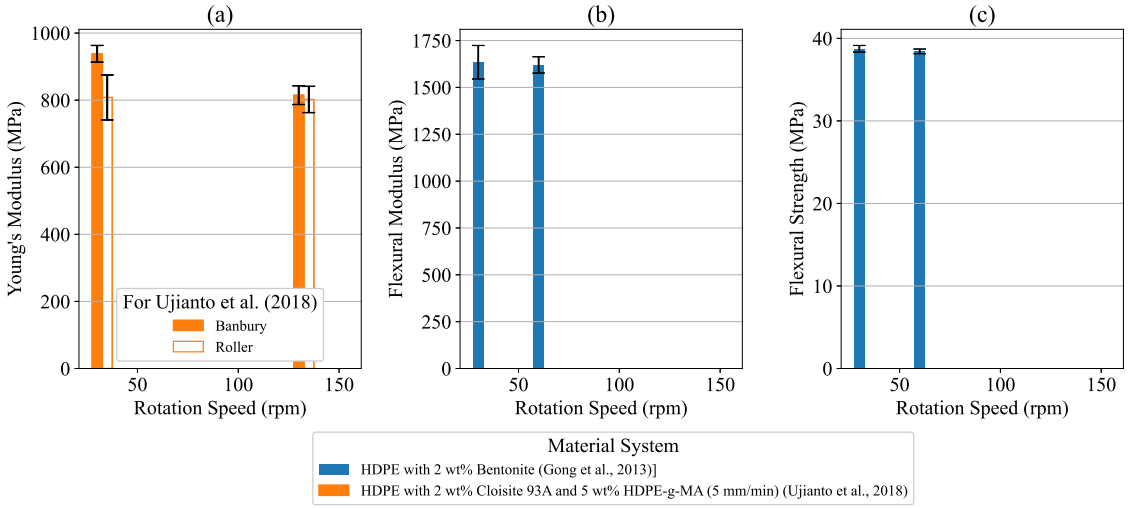

Figure 3.21: Effect of internal mixer rotor speed on the mechanical properties: (a) Young's modulus, (b) flexural modulus and (c) flexural strength.

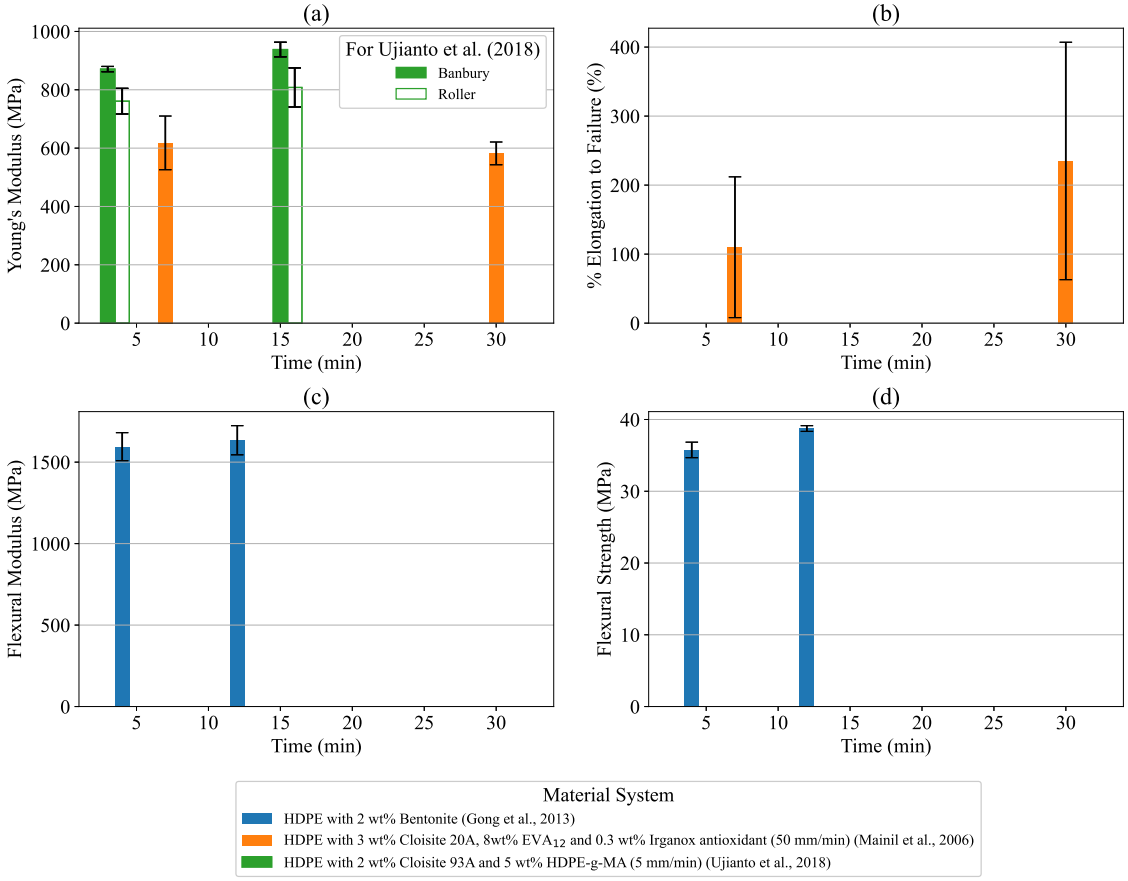

Figure 3.22: Effect of internal mixer time on the mechanical properties: (a) Young's modulus, (b) elongation to failure, (c) flexural modulus and (d) flexural strength.

of the clay in the polymer matrix thereby improving both the tensile (Ujianto *et al.*, 2018; Mainil *et al.*, 2006) and flexural (Gong *et al.*, 2013) properties as seen in Figure 3.22.

Conclusion

For extrusion, the choice of screw type, speed and temperature profile have an impact on the obtained mechanical properties. Including additional treatments such as CO_2 and ultrasound provides an improvement in the polymer-clay exfoliation consequently enhancing the overall mechanical properties. Internal mixing temperature does not have a significant effect, however an increase in rotation speed does have a negative impact on the material stiffness. An increase in mixing time provides improvements in mechanical properties. It is clear that the choices made during compounding of HDPE/MMT composites have an influence on the mechanical properties.

3.4.4 Processing Methods

Processing methods in the context of this study refer to the process subsequent to compounding whereby the samples that are ultimately used to obtain the mechanical properties are produced. Injection and compression moulding are the most commonly used processing methods with injection moulding providing better overall mechanical properties compared to compression moulding. Five studies considered the effects of processing methods (Chu *et al.*, 2007; Gao *et al.*, 2012; Jo and Naguib, 2006, 2007a; Mistretta *et al.*, 2018; Xiang *et al.*, 2009).

In the subsequent figures, processing methods are denoted with acronymns defined at the top of each figure. For ease of reference the acronymns will be displayed in brackets in the text where discussed.

Tensile Properties

The mechanical properties as a function of processing method are shown in Figure 3.23. It is immediately noticeable that injection moulding (IM) results in higher stiffness and strength when compared to compression moulding (CM). This is due to how the processing methods affect the composite morphology. Injection moulding (IM) tends to lead to better separation and dispersion of the clay in the polymer matrix as a result of shear effects, while compression moulding (CM) has a higher likelihood to form agglomerates during melting with the higher compacting times (Chu *et al.*, 2007; Mistretta *et al.*, 2018). It is difficult to make claims regarding the elongation to failure between studies as each study considered a different strain rate. For Mistretta *et al.* (2018) injection moulding (IM) provided a higher elongation to failure compared to compression moulding (CM).

When applying a CO_2 foaming process to compression moulded samples (Foam) as in Jo and Naguib (2006, 2007a), there is a slight decrease in Young's modulus and a significant decrease in elongation to failure. This is due to the clay deteriorating the performance of foamed samples due to poorer dispersion, with little exfoliation and potential agglomeration (Jo and Naguib, 2006, 2007a). Dynamic-packing injection moulding (DPIM) provides a significant

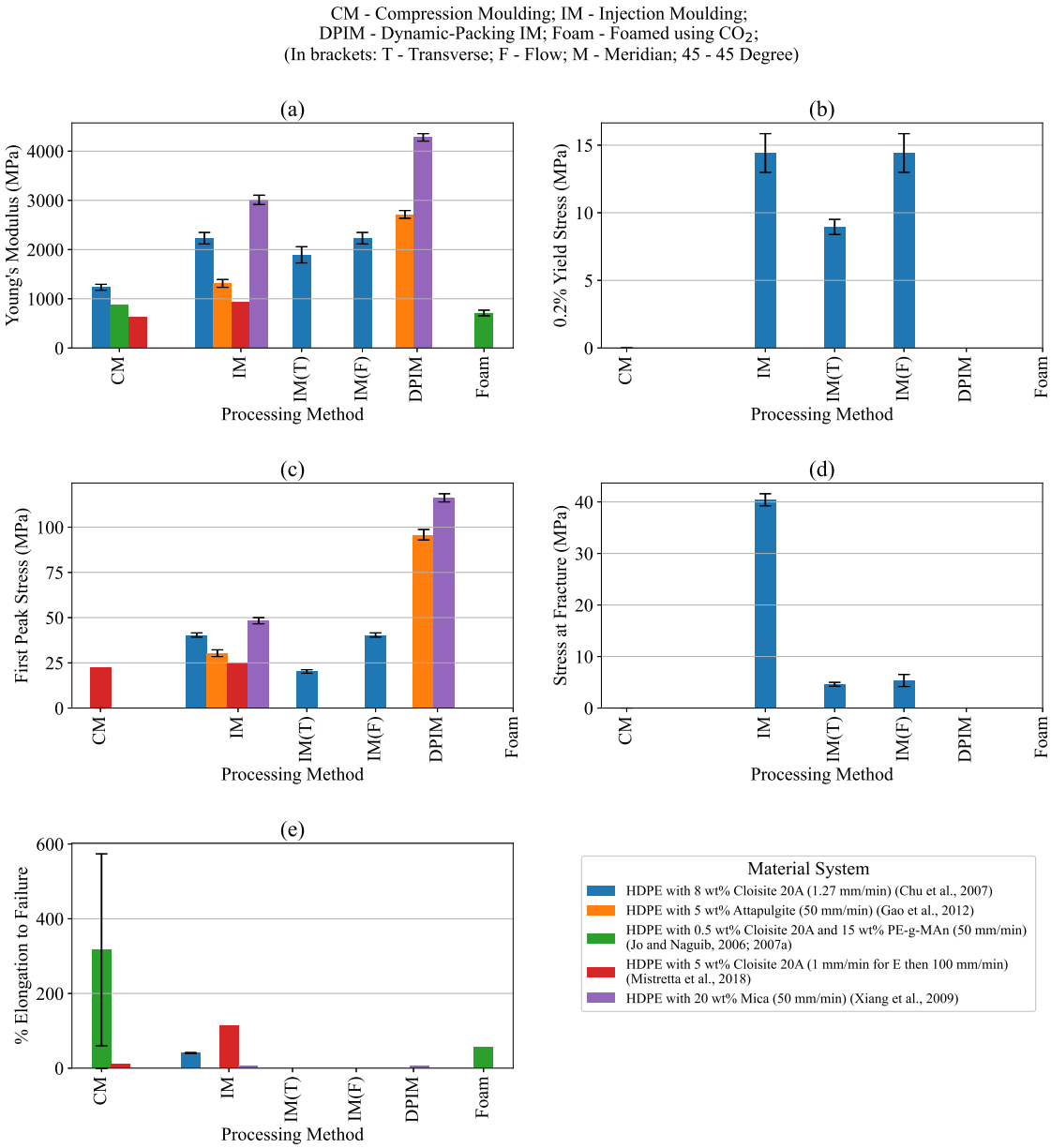

Figure 3.23: Effect of the processing methods on the mechanical properties: (a) Young's modulus, (b) 0.2 % yield stress, (c) first peak stress, (d) stress at fracture and (e) elongation to failure.

improvement in stiffness and strength compared to injection moulding (IM). This improvement is attributed to the improvement in the composite's morphology, where dynamic-packing results in improved dispersion of the clay, clay-polymer interfacial adhesion and orientation of the polymer chains due to the shearing effects (Gao *et al.*, 2012; Xiang *et al.*, 2009).

Chu *et al.* (2007) studied the effect of cutting an injection-moulded sample for testing in either the transverse (IM(T)) or flow (IM(F)) direction. The choice of which direction to cut the samples has a clear influence, with samples cut along the flow direction (IM(F)) providing much better mechanical properties than those cut along the transverse direction (IM(T)). This is due to the polymer matrix being able to transfer greater stress to the clay and the clay particles are oriented in the flow direction (Chu *et al.*, 2007).

Dynamic Mechanical Analysis

Another measure used to describe the materials deformation response in rheology is tan δ. The angle between the storage modulus and loss modulus is referred to as the phase angle, δ. For example, if δ is close to 0 it means that the storage modulus plays a larger role and the material is more elastic. Whereas if it is close to 90 ° the loss modulus has a larger role and the material is more viscous. tan δ is therefore the tangent of the phase angle and defined as the ratio of the viscous to elastic response of a material. In other words, tan δ denotes the energy dissipation potential of the material.

In Figure 3.24, the findings of Xiang *et al.* (2009) on the effects of static and dynamic-packing injection moulding on a material's DMA behaviour may be seen. Dynamic-packing injection moulding provides increases in the DMA storage and loss moduli. The increased storage modulus is due to the shearing effect introduced in dynamic-packing increasing the material stiffness (Xiang *et al.*, 2009), as seen in Figures 3.23(a) and (c). The loss modulus increases due to the enhanced interfacial interactions between the clay and polymer as a result of the shearing effect (Xiang *et al.*, 2009).

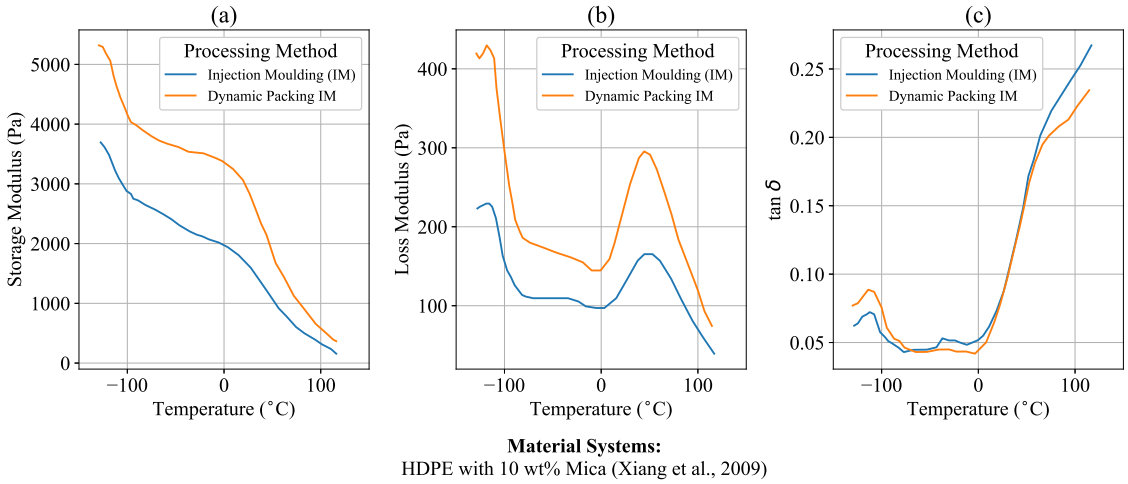

Figure 3.24: DMA results showing the effect of processing methods on the (a) storage modulus, (b) loss modulus and (c) tan δ for HDPE with 10 wt% Mica. (Reproduced with permission from Xiang *et al.* (2009))

Dynamic-packing only results in increased tan δ up to approximately -70 °C. The enhanced shear effect which improves the interaction between clay and the polymer results in proportionally stiffer or more elastic behaviour (due to the higher storage modulus), which is why tan δ is reduced for dynamic packing (Xiang *et al.*, 2009).

Conclusion

Injection moulded samples provide better improvement in mechanical properties when compared to compression moulded samples. For injection moulded samples there is an influence on mechanical properties depending on the direction along which samples are cut. Samples

cut along the flow direction provided better overall properties. Dynamic injection moulding is an improvement on conventional injection moulding as it enhances the material stiffness and strength significantly.

3.4.5 Processing Conditions

Processing conditions are varied during the processing phase where samples for testing are manufactured. Similar to the compounding conditions subdivisions are done according to the type of processing condition. 4 studies are discussed where Jo and Naguib (2006, 2007a,b, 2008) considered the effect of foaming time and sample cooling, while using two different press times between two of the studies.

Foaming Time

The effect of foaming time is illustrated in Figure 3.25. There is a general increase in Young's modulus (absolute and relative) with an increase in foaming time and a decrease in elongation to failure, while there is little change in first peak stress. By increasing the foaming time, the volume expansion ratio first increases before deteriorating at the maximum foaming time of 60 s (Jo and Naguib, 2006, 2007a). The larger volume allows for better clay dispersion, resulting in improved stiffness at the cost of decreased ductility (Jo and Naguib, 2007b).

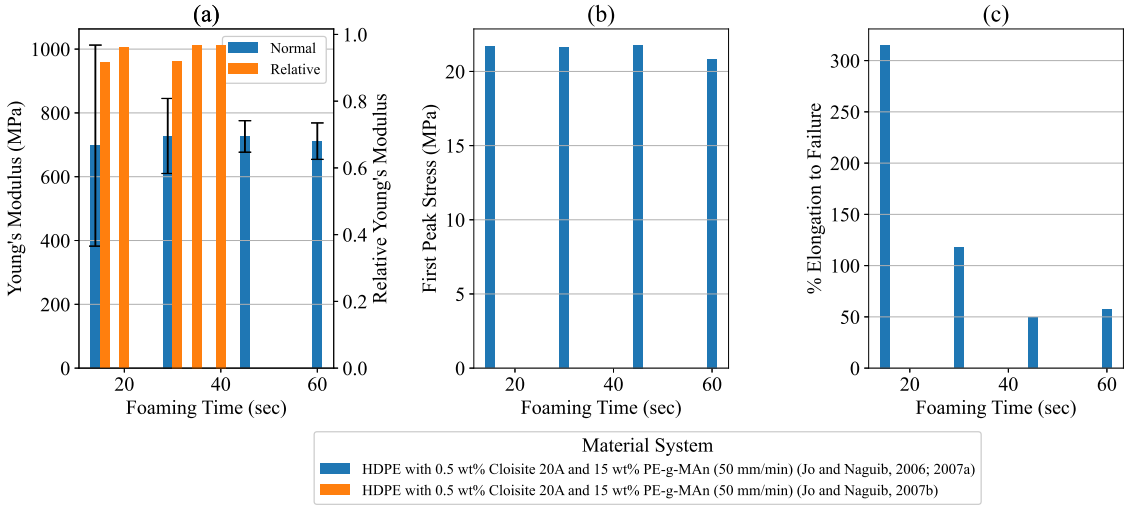

Figure 3.25: Effect of the foaming time on the tensile properties: (a) Young's modulus and relative Young's modulus, (b) first peak stress and (c) elongation to failure.

Compression Moulding Press Time

Jo and Naguib (2006, 2007a,b) inadvertently considered the effect of press time, as they considered different press times in the separate studies. These results are shown in Figure 3.26. It is not possible to directly compare the Young's modulus as Jo and Naguib (2007b) provided

their result only in relative terms. However, converting the provided value for a press time of 15 min (870.06 MPa) with that of the neat HDPE at 15 min which is 797.35 MPa a relative Young's modulus of 1.09 for a press time of 15 min is obtained. When compared to the relative Young's modulus of 1.09 for 10 min there is no effect on the Young's modulus due to press time. This observation corresponds to a previous study (Botha *et al.*, 2020) where press time has no statistically significant effect (c.f. Section 2.4.1).

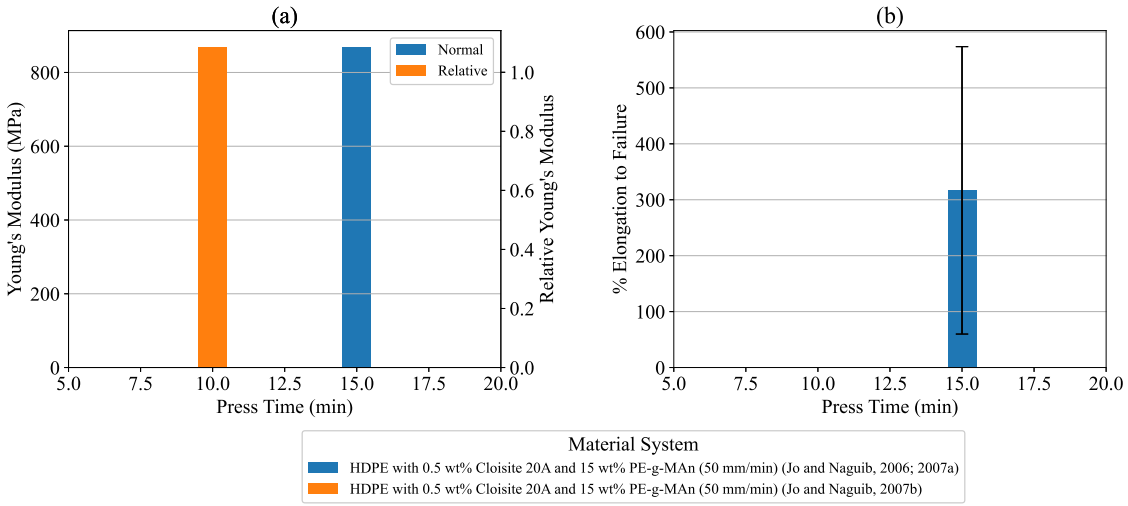

Figure 3.26: Effect of the compression moulding press time on the tensile properties: (a) Young's modulus and (b) elongation to failure.

Sample Cooling Method

Jo and Naguib (2008) conducted an investigation to understand the influence that the sample cooling method has after compression moulding. These results are shown in Figure 3.27 for both conventional and foamed samples. Hot-plate cooling offers the highest Young's modulus and first peak stress, but the lowest elongation to failure. This is followed by air and then water quenching. During sample cooling, the crystallinity of the composite morphology is augmented; where water (65 %) showed the lowest crystallinity, followed by air (71 %) and hot-plate (76 %) cooling with the highest (Jo and Naguib, 2008). Young's modulus and first peak stress increase with increased crystallinity as the cooling rate is decreased (Jo and Naguib, 2008). A previous study (Botha *et al.*, 2020) indicated that air-cooled samples offered better mechanical properties than those quenched in water (c.f. Section 2.3.2). From Figure 3.27(a), conventional compression moulding results in samples with greater Young's modulus than that of those that have been subject to foaming.

Conclusions

An increase in foaming time has a largely negative impact on elongation to failure, while there is a slight increase in Young's modulus. Compression moulding press time has no significant effect on the mechanical properties, while the sample cooling method does have an impact.

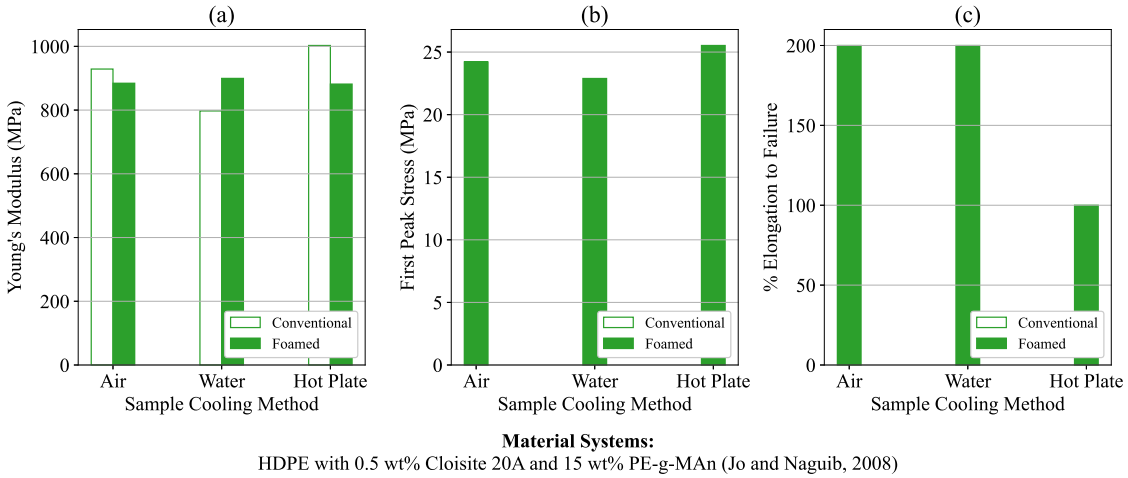

Figure 3.27: Effect of the cooling method after compresson moulding on the tensile properties: (a) Young's modulus, (b) first peak stress and (c) elongation to failure.

The sample cooling method changes the composite crystallinity which affects the mechanical properties.

3.5 Conclusion

In this systematic literature review, I analysed the mechanical properties of 33 studies to determine the influence of different manufacturing variations. The mechanical properties are influenced by the choices made during manufacturing as these affect the composite morphology. The main findings in this review for each of the considered categories are:

- Blending Protocol: The order in which composite components are mixed affects the morphology of the composite which has a significant effect on the degree of exfoliation of the clay, ultimately affecting the mechanical properties. Clay/compatibiliser masterbatching provides the most significant improvement in Young's modulus. However, it does decrease the material ductility. Direct mixing provides the best overall improvement in material ductility but at the cost of material stiffness.

- Compounding Method: Internal mixing followed by solution intercalation offers the best material stiffness, as both methods enhance the degree of intercalation and/or exfoliation of the clay within the polymer matrix. Twin-screw extrusion provided the best material strength followed by Buss Kneader.

- Compounding Conditions: The choice of conditions and combination of these parameters has a large effect on the degree of dispersion. For example, low processing temperatures with high rotational speeds promote high shear, where longer mixing times with medium temperatures promote higher dispersion and higher temperatures and speeds at longer mixing times degrade the clay surface. Mechanical properties can be im-

proved by enhancing exfoliation with additional treatments, such as supercritical CO_2 and ultrasound.

- Processing Methods: Injection moulding offers the best overall improvement in mechanical properties. However, compression moulding is most often the preferred processing method for many researchers (Jordan *et al.*, 2005). This is likely due to it being more cost effective than injection moulding, especially for small scale manufacturing. In this review, 56 % of the studies used compression moulding, with 44 % using injection moulding.
- Processing Conditions: Foaming time and sample-cooling method were found to have an influence on the mechanical properties as these directly affect the composite density and/or crystallinity, while compression-moulding time had no effect at all.

It is quite clear from this review that the choice in not only material system, but the order in which the components are mixed and the decisions made in manufacturing have an important effect on a composite's mechanical properties. In fact, the decisions made during the entire manufacturing process have a direct impact on the final mechanical properties and the type of composite obtained. The main reason for this is that manufacturing has a direct effect on a composite's morphology, crystallinity and the degree of intercalation and/or exfoliation, all of which directly contribute to the mechanical properties. It is, therefore, recommended to take care when choosing and optimising the manufacturing conditions as these should be based on the intended purpose of the final composite.

In general, studies report only the mean and, occasionally, the standard deviation for experimentally determined mechanical properties. This is a limitation to our ability to quantify the variability of associated manufacturing processes. Researchers are encouraged to include statistical techniques in their approaches, such as statistical design of experiments (DoE). Such statistical techniques allow greater insight into the potential effects of design choices.

The influence of manufacturing on mechanical properties has not been as well represented in literature as the influence due to a change in the composite material system. This is even more pronounced for high-density polyethylene/montmorillonite (HDPE/MMT)composite systems. During the screening process I identified 1633 articles of which only 33 conformed to the eligibility criteria. Even within the included articles, most of the studies considered the effects of compounding conditions, while far fewer considered the effects of processing conditions. In fact, all four of the articles where processing conditions were considered were published by the same researchers. This systematic literature review is the first step to bridging this gap by providing a detailed overview of the influence of manufacturing variation on the mechanical properties of HDPE/MMT composite systems.

CHAPTER 4

STATISTICAL DESIGN OF EXPERIMENTS

Statistical design of experiments (DoE) aims to develop a near efficient design while minimising the number of experiments required. This is an optimal approach especially when there is a need to investigate multiple variables. This chapter serves as an introduction to DoE to provide the necessary overview before generating the DoE's required for the experimental portion of this thesis.

Sections of the work discussed in this chapter have been presented as a full length peer reviewed conference paper (Botha *et al.*, 2021).

4.1 Introduction

Experimental work is a key part of any research or industrial project. The engineers and scientists conducting these experiments use some measure of statistical analysis to analyse and report their results. However, not all experimenters have been exposed to statistics during their training. This often results in a lack of knowledge to properly design an experiment and apply the correct statistical tools when there are multiple interacting variables. As a result, experimenters often use the one-factor-at-a-time approach which is commonly taught during their training or practised in industry. (Tanco *et al.*, 2009)

In an experimental design we need to specify the factors, levels and response variables. A **factor** is the manipulated or control variable, also referred to as the input variable of interest. If we consider the example of melt compounding of polymer composites the factors might include temperature and screw speed. The **levels** are the number of different variations (*i.e.* settings or levels) we consider for each factor, for example, with three levels we would consider a low, medium and high temperature. A **response variable** is the output variable of interest, such as material strength.

In a **one-factor-at-a-time approach**, the experimenter varies one factor while keeping the other factors of interest fixed. This is illustrated in Figure 4.1(a) for a design space with

two factors. Such an approach requires a large number of experimental runs, but does not give insight into the interactions between the variables or identify the optimum conditions (Montgomery, 2013).

To mitigate these challenges we consider an approach from the field of statistics, statistical design of experiments (DoE). DoE is the collective name for statistical optimisation techniques which are commonly employed to plan an experimental program with a sufficient number of experiments in order to make sound scientific conclusions from the data (Gündoğdu *et al.*, 2014; Montgomery, 2013). They achieve this by optimising the design process, screening for the most influential factors and determining their interactions while establishing and maintaining quality control (Montgomery, 2013). The goal of a DoE is therefore to provide a near optimal and efficient design which can be performed with the minimum number of experimental runs. DoE's can be grouped into two design classes, factorial designs and response surface method (RSM) designs.

Factorial designs consider all the possible combinations of factors and levels that are being investigated. As a result these tend to rapidly increase the number of experimental runs required as the number of factors increase. A full factorial design will have n^k experiments where n is the number of levels and k is the number of factors. For certain applications, it is possible to do a fractional factorial design which will reduce the number of experimental runs. Fractional factorial designs are generally used when screening the factors that are of interest. An example of factor screening considering a full factorial design is shown in Figure 4.1(b) for two factors and two levels.

RSM designs rely on making an initial assumption about the shape of the response surface. The response surface is the response variable plotted as a function of the factors in the design space. An experiment can be efficiently designed to accurately capture the features of the assumed response surface. RSM is employed after factor screening to optimise the product or system. An example of an RSM design is illustrated in Figure 4.1(c) showing a more focused design region compared to the factorial design. Notice that this is the recommended method which estimates the true optimum.

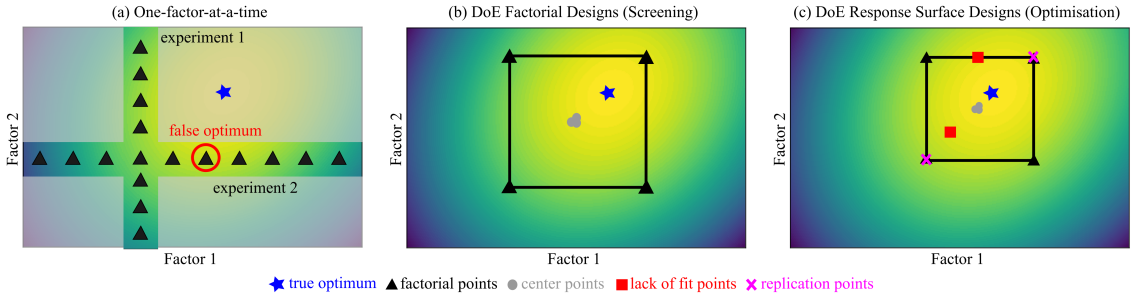

Figure 4.1: Graphical illustration of the (a) one-factor-at-a-time approach, (b) factorial designs for efficient screening and (c) response surface designs for optimisation. The contour colour gradient represents the response variable (yellow = high value and blue = low value). [Redrawn from Bowden *et al.* (2019) under the Creative Commons Attribution 4.0 International License]

In the field of polymer composites, specifically investigating high density polyethylene (HDPE)

or low density polyethylene (LDPE) and clay systems, the standard approach has been one-factor-at-a-time. More recently, researchers have embraced the DoE approach and used techniques such as Taguchi (Akhlaghi *et al.*, 2012; Ibrahim *et al.*, 2014; Najafabadi *et al.*, 2014; Namdeo *et al.*, 2017, 2018a,b; Hafshejani *et al.*, 2019), Box-Behnken (Ramachandran *et al.*, 2012; Shahabadi and Garmabi, 2012a,b; Anjana *et al.*, 2014; Moghri and Dragoi, 2015; Moghri *et al.*, 2016; Rahnama *et al.*, 2017; Moghri *et al.*, 2018; Ujianto *et al.*, 2018), central composite design (CCD) (Campos-Requena *et al.*, 2014; Koodehi and Koohi, 2018) and D-optimal (Mohamadi *et al.*, 2014, 2016). In polymer composites DoE is mainly used to either find the optimum material system (Akhlaghi *et al.*, 2012; Shahabadi and Garmabi, 2012a,b; Anjana *et al.*, 2014; Campos-Requena *et al.*, 2014; Mohamadi *et al.*, 2014; Najafabadi *et al.*, 2014; Moghri and Dragoi, 2015; Mohamadi *et al.*, 2016; Rahnama *et al.*, 2017; Koodehi and Koohi, 2018; Moghri *et al.*, 2018; Hafshejani *et al.*, 2019), manufacturing conditions (Ramachandran *et al.*, 2012; Campos-Requena *et al.*, 2014; Ibrahim *et al.*, 2014; Moghri *et al.*, 2016; Ujianto *et al.*, 2018) or testing conditions (Namdeo *et al.*, 2017, 2018a,b). Finding the optimum conditions is the main consideration, as seen from literature, which is why studies from literature consider designs from the RSM design class. However, none of these studies provided an indication on how or why they chose the desired DoE design. This highlights the need for wider knowledge on the different DoE methods. Choosing the correct method and knowing how to apply it correctly is of the utmost importance, otherwise the data obtained from the study would be meaningless. (Tanco *et al.*, 2009)

There have been introductory review articles which provide a brief introduction to the concept of DoE and the theory behind some of the most used methods. Some of these include general introductory articles (Lundstedt *et al.*, 1998; Telford, 2007), while others are focused on a specific application such as bioengineering (Gündoğdu *et al.*, 2014) or fermentative hydrogen production (Wang and Wan, 2009). Currently there are no such introductory DoE studies in the field of polymer composites.

The aim of this chapter is to provide an introduction to DoE by showcasing and discussing RSM designs. This chapter defines the criteria which will be used to compare these designs in the context of two case studies from the field of polymer composites. The first case study considers only continuous (numerical value) factors and the second considers both continuous and categorical (non-numerical value) factors.

4.2 Theory and Background of Response Surface Methods

The three simplest response surface models are first discussed. This is followed by four classic examples of RSM designs which are then introduced and explained: Taguchi Design, Central Composite Design (CCD), Box-Behnken Design (BBD) and Optimal Designs (with specific focus on D-optimal). Lastly, the criteria for evaluating the efficiency of these methods is defined.

4.2.1 Response Surface Models (RSM)

RSM rely on the assumption of a mathematical relationship between the response variable and the factors. The three simplest assumptions: a linear model, a two-order linear interaction model and a quadratic model, are presented and discussed.

Each model will be considered for continuous and categorical factors. A continuous factor is defined as having a numerical value with an infinite number of values between any two values. For example, the clay weight loading, time or temperature. A categorical factor describes a category or distinct group, for example the clay type or manufacturing method.

In each of these models y represents the response variable, x_i the continuous factors, β are the regression coefficients and z_{il} the categorical factor dummy variables. The dummy variable would be equal to 1 for the n^{th} level of a categorical factor and 0 otherwise. In instances where the regression coefficients have the same subscripts, *cat* is added to indicate that the subscript is assigned to the categorical factors. The purpose of an experiment is to characterise the response surface by solving for the number of regression coefficients, p.

Continuous Factors

The response surface models for continuous variables are illustrated in Figure 4.2 for a model with two factors.

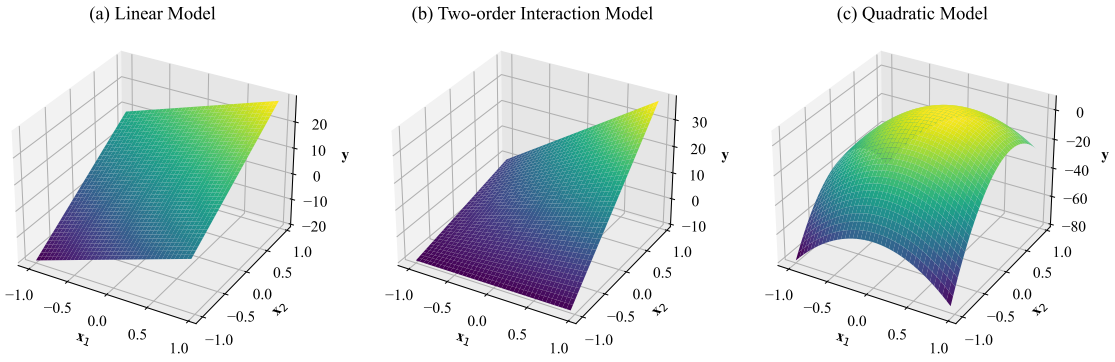

Figure 4.2: Example response surface plots for the (a) linear (regression) model, (b) two-order interaction model and (c) quadratic model with continuous factors.

A **linear model** (also called a linear regression model) for k continuous factors has $p = k + 1$ model parameters and will take the following form:

$$y = \beta_0 + \sum_{i=1}^{k} \beta_i x_i. \tag{4.1}$$

The **two-order interaction model** (also called an interaction model) for k continuous factors

has $p = 1 + (k^2 + k)/2$ model parameters:

$$y = \beta_0 + \sum_{i=1}^{k} \beta_i x_i + \sum_{i=1}^{k} \sum_{j=i+1}^{k} \beta_{ij} x_i x_j. \tag{4.2}$$

A **quadratic model** for k factors has $p = 1 + (k^2 + 3k)/2$ model parameters:

$$y = \beta_0 + \sum_{i=1}^{k} \beta_i x_i + \sum_{i=1}^{k} \sum_{j=i+1}^{k} \beta_{ij} x_i x_j + \sum_{i=1}^{k} \beta_{ii} x_i^2. \tag{4.3}$$

Continuous and Categorical Factors

With the addition of categorical factors a dummy variable, z_{il}, is introduced into the response surface models. This dummy variable would be equal to 1 if the n^{th} level of the categorical factor is active and 0 otherwise. The additional terms describing the categorical factors will therefore result in a numerical value that gets added to the model intercept, β_0. With the inclusion of categorical factors the response surface plots illustrated in Figure 4.2 will therefore shift up or down depending on the updated intercept value for the response variable, y.

A **linear model** for k continuous factors and r categorical factors with n number of levels has $p = k + 1 + r(n - 1)$ model parameters and will take the following form:

$$y = \beta_0 + \sum_{i=1}^{k} \beta_i x_i + \sum_{i=1}^{r} \sum_{l=1}^{n-1} \beta_{il,cat} z_{il}. \tag{4.4}$$

The **two-order interaction model** for k continuous factors and r categorical factors with n number of levels has $p = 1 + (k^2 + k)/2 + r(n - 1)(k + 1)$ model parameters:

$$y = \beta_0 + \sum_{i=1}^{k} \beta_i x_i + \sum_{i=1}^{k} \sum_{j=i+1}^{k} \beta_{ij} x_i x_j + \sum_{i=1}^{r} \sum_{l=1}^{n-1} \beta_{il,cat} z_{il} + \sum_{i=1}^{k} \sum_{j=1}^{r} \sum_{l=1}^{n-1} \beta_{ijl} x_j z_{il}. \tag{4.5}$$

A **quadratic model** for k factors and r categorical factors with n number of levels has $p = 1 + (k^2 + 3k)/2 + r(n - 1)(k + 1)$ model parameters with the following form:

$$y = \beta_0 + \sum_{i=1}^{k} \beta_i x_i + \sum_{i=1}^{k} \sum_{j=i+1}^{k} \beta_{ij} x_i x_j \sum_{i=1}^{r} \sum_{l=1}^{n-1} \beta_{il,cat} z_{il} + \sum_{i=1}^{k} \sum_{j=1}^{r} \sum_{l=1}^{n-1} \beta_{ijl} x_j z_{il} + \sum_{i=1}^{k} \beta_{ii} x_i^2. \tag{4.6}$$

4.2.2 Explanation of Different RSM Design Methods

An overview of four commonly used response surface design methods (RSM) is given. They are illustrated in Figure 4.3, for three factors, in which case the design space is represented

by a cube. For the purposes of this thesis a **replication point** refers to an additional design point which is exactly the same as an existing design point. A **repeated sample** refers to testing multiple samples of the same design point. This is to ensure repeatability and is required to conform to international testing standards.

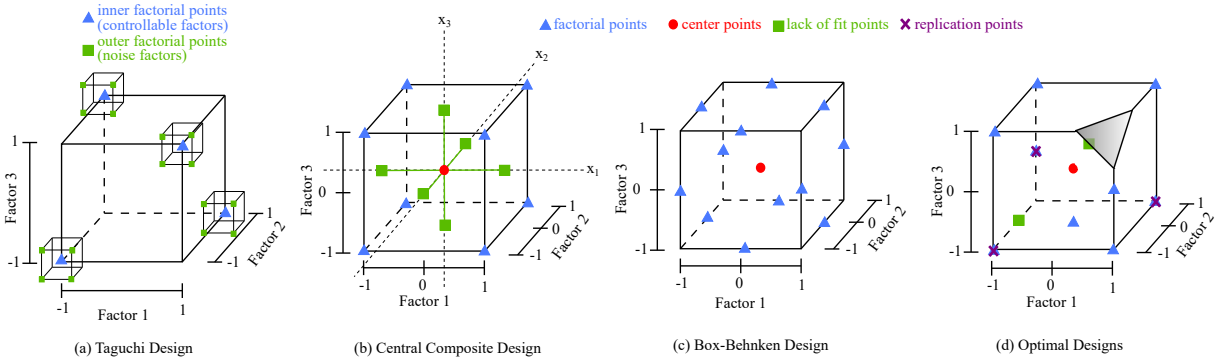

Figure 4.3: Graphical representation of the three-factor design space for the different RSM designs: (a) Taguchi, (b) Central Composite Design, (c) Box-Behnken and (d) Optimal Designs.

Taguchi Design

The Taguchi design originated as a class of factorial design known as robust parameter design (Montgomery, 2013; Myers *et al.*, 2016). A Taguchi design tests all combinations of factors and levels, similar to a factorial design, but uses pairs of combinations to reduce the number of experiments required (Gündoğdu *et al.*, 2014). RSM is applied to the Taguchi design to improve the efficiency of the design by mathematically including both the controllable and noise (or uncontrollable) factors in a single response function to account for uncertainty (Montgomery, 2013). Thus, the effect of two or more levels of the factors on the response variables can be studied (Gündoğdu *et al.*, 2014; Wang and Wan, 2009). The two levels of factors can be seen in Figure 4.3(a) with the inner factorial points denoting the controllable factors and the outer factorial points the noise factors. A disadvantage of Taguchi designs is that they do not account for interaction effects between controllable and noise factors (Myers *et al.*, 2016).

Central Composite Design and Box-Behnken Design

A central composite design (CCD) is a factorial design consisting of factorial points at the edges of the design space, axial points at the midpoint of each level (centers of the faces) and a center point in the middle of the design space. A CCD is illustrated in Figure 4.3(b). The CCD is based on a two level factorial design, 2^k, where k is the number of factors. By adding axial and center points to the design, the CCD requires fewer experimental runs compared to a full factorial design while still producing similar results (Gündoğdu *et al.*, 2014). Axial points are determined by the distance from the design center, α, which provides a measure of rotatability. The rotatability of a CCD *i.e.*, when the design is rotated around the center,

provides an indication of the model's ability to ensure the variance of the predicted response is constant and stable (Montgomery, 2013). This rotatibility measure is dependent on the assumed shape of the response surface. For this study, I consider $\alpha = 1$ which assumes a cuboidal shape resulting in a face-centered CCD. The axial points are then in the center of the cube faces as shown in Figure 4.3(b). Center points are added to the design to estimate experimental error. They provide an indication of curvature, that is detecting quadratic effects (Myers *et al.*, 2016). A CCD is considered to be efficient when fitting a second order model (Gündoğdu *et al.*, 2014; Montgomery, 2013; Wang and Wan, 2009).

An alternative to the CCD is the BBD which is reported to be more economical as it requires fewer experimental runs for the same number of factors (Montgomery, 2013). A BBD is based on a 2^k three level factorial design with an incomplete block design (Gündoğdu *et al.*, 2014; Myers *et al.*, 2016; Wang and Wan, 2009). An incomplete block design considers all combinations for a certain number of factors while keeping the remaining factors at the central levels (Gündoğdu *et al.*, 2014; Montgomery, 2013; Wang and Wan, 2009). The BBD is illustrated in Figure 4.3(c). In comparison with the CCD (Figure 4.3(b)) there are no factorial points at the vertices of the design space. Instead, the factorial points lie along a sphere with radius $\sqrt{k}$. This is similar to where the axial points of a spherical CCD would lie if the design is rotatable with radius $\alpha = \sqrt{k}$. As with the CCD, center points can be added to the BBD to estimate experimental error.

Optimal Designs

Optimal designs are very flexible and are able to handle different user constraints and more complex experimental design problems, such as: constrained design regions; many factors or levels and limits on the total number of experimental runs (Montgomery, 2013; Myers *et al.*, 2016). Optimal designs are numerically generated designs which aim to minimise a specific optimality criterion to select a near optimal design (Montgomery, 2013; Myers *et al.*, 2016). Optimality criteria minimise some mathematical measure which focus on either the estimation of regression coefficients or the prediction of the response variable in the design region (Myers *et al.*, 2016). An optimal design is illustrated in Figure 4.3(d). The constrained design region is represented by a gray triangle in the top right corner, indicating that no design points can be selected above the triangle. As with the CCD and BBD designs center points can be included for estimation of experimental error. For an optimal design, additional design choices can be made which include specifying the number of replicates and lack of fit points. Replications (purple 'x' in Figure 4.3(d)) of certain design points can be added if there is a strong interest in a specific combination of factors and levels (Montgomery, 2013). On the other hand, if there is a need to test the prediction ability of the chosen response surface model, lack of fit points (green squares in Figure 4.3(d)) are included in the design space (Montgomery, 2013). The design is then evaluated based on the response surface model and specified optimality criterion. The optimality criterion is optimised by using a suitable nonlinear optimisation algorithm (Montgomery, 2013; Myers *et al.*, 2016). The computational

algorithm first constructs a full factorial design to create a set of candidate points. An initial design is then selected at random from the candidate points and design weights ($w_i = 1/p$) are assigned to each design point. The points and design weights are then adjusted to optimise the specified criterion. The choice of optimality criterion determines the type of optimal design. For this study, I will consider a D-optimal design as these are the most widely used optimality criteria (Montgomery, 2013). The interested reader is referred to Montgomery Chapter 11 (Montgomery, 2013) or Myers *et al.* Chapter 9 (Myers *et al.*, 2016) for the definitions of other optimality criteria.

A **D-optimal design** aims to find a good estimation of the regression coefficients subject to the constraints on the design region and experimental runs (Myers *et al.*, 2016). The D-optimal design estimates the regression coefficients by maximising the determinant of $|(\mathbf{X}'\mathbf{X})|$, where $\mathbf{X}$ is the model matrix and $\mathbf{X}'$ is the transpose of the model matrix. $\mathbf{X}$ is populated with all the combinations of the factor levels (*i.e.*, -1, 0, 1 for a three level design) for each factor and has columns expanded for all the terms in the response surface model.

Optimal designs can be classified as either continuous (approximate) or exact (discrete) designs (Atkinson *et al.*, 2007). The classification refers to the optimisation approach considered when generating the optimal design. For a continuous design, the aim is to find the minimum number of distinct design points with their assigned design weights ($0 < w_i < 1$) considering the design region (Atkinson *et al.*, 2007). Exact designs specify the number of experimental runs (N) for the optimisation process at the start (Atkinson *et al.*, 2007). The exact design can be approximated by multiplying the design weights w_i ($r_i = w_i N$ is the number of replication points) with the total number of experiments (N) (Atkinson *et al.*, 2007).

Global D-optimal designs are also referred to as continuous or approximate designs. They assign optimum weights to each design point. If the total of number of experiments are specified, the weights can be used to specify the number of replications for each design point, approximately. Therefore, global optimal designs are not always practical since the number of replications must be approximated from the weights. In practice, D-optimal designs are generated from a candidate set, for example n^k experiments, and its efficiency is specified compared to the global D-optimal design. D-optimal designs generated from a candidate set is referred to as exact designs. For a given set of factors, levels and response surface, the global D-optimal design is uniquely defined. This makes the global D-optimal design ideal as a benchmark design. In this study, each of the experimental designs will be compared to the global D-optimal design for the relevant response surface model. Both the required number of experiments and the efficiency of the designs will be compared to the global D-optimal design.

4.2.3 Design Evaluation

I measure the performance of a design by evaluating its efficiency. The efficiency is an indication of whether a design will be able to produce reliable results under a variety of circumstances

(Myers *et al.*, 2016). There are two widely used measures of design efficiency: D-efficiency and G-efficiency (Montgomery, 2013; Myers *et al.*, 2016; Atkinson *et al.*, 2007).

D-efficiency is a measure of the precision of estimation of the regression coefficients, β_{ij} (Myers *et al.*, 2016). Figure 4.4(a), which illustrates D-efficiency in two dimensions. In this simple example the area of the ellipse represents the confidence region of the regression coefficients. D-efficiency is achieved when the area of this ellipse is minimised (Montgomery, 2013; Myers *et al.*, 2016). This is equivalent to maximising the determinant, $|(\mathbf{X'X})|$. Recall that $\mathbf{X}$ is the model matrix containing the factors (x_i) for all levels in the response surface model.

When we want to compare two different designs we need to evaluate the **relative D-efficiency**, which compares the D-efficiency of the current design to that of the global D-optimal design (denoted by subscript *gopt*) by comparing their determinants (Montgomery, 2013; Atkinson *et al.*, 2007):

$$D_{eff} = \left(\frac{|(\mathbf{X'WX})|}{|(\mathbf{X'}_{gopt}\mathbf{W}_{gopt}\mathbf{X}_{gopt})|} \right)^{1/p}, \tag{4.7}$$

where p is the number of regression coefficients, and the matrix $\mathbf{W}$ is a diagonal matrix containing the design weights attached to each design point. $|(\mathbf{X'WX})|$ is the determinant whose inverse provides insight into the variance of the regression coefficients. $\mathbf{W}$ can be included or excluded for exact designs when calculating the D-eff where the design weights $w_i = r_i/N$ for exact designs.

The **G-efficiency** of a design is a measure of the accuracy of the prediction of the response variable in the design region (Montgomery, 2013; Myers *et al.*, 2016). The G-efficiency is defined as (Montgomery, 2013; Atkinson *et al.*, 2007):

$$G_{eff} = \frac{p}{\max(\bar{x}'(\mathbf{X'WX})^{-1}\bar{x})} = \frac{p}{\max(SPV)}. \tag{4.8}$$

The denominator is known as the scaled prediction variance (SPV). SPV is the variance of the predicted response at a point in the design region scaled to the number of experimental runs (Myers *et al.*, 2016).

A simple visualisation of G-efficiency for a linear model with three factors is shown in Figure 4.4(b). Two designs are shown, represented by the red dash-dotted line and the blue dashed line. The y-axis, the SPV, is a measure of how many regression coefficients are required to accurately predict the model response for a given fraction of the design space (FDS), shown on the x-axis. The linear model with three factors has four regression coefficients, *i.e.* $p = 4$. This is represented by the black line for a G-efficiency of 100 %. The red design has $\max(SPV) = 6.5$ giving a G-efficiency of 61.5 %, while the blue design has $\max(SPV) = 5$ resulting in a G-efficiency of 80 %. This means that the red design would require more replications at the specified design points to achieve similar prediction variance as the blue design. Thus it has a lower G-efficiency. To improve the G-efficiency of the design we want to minimise the variance in the response variable prediction, *i.e.* change the design such that

at an FDS of 1 the SPV is minimised (Montgomery, 2013; Myers *et al.*, 2016).

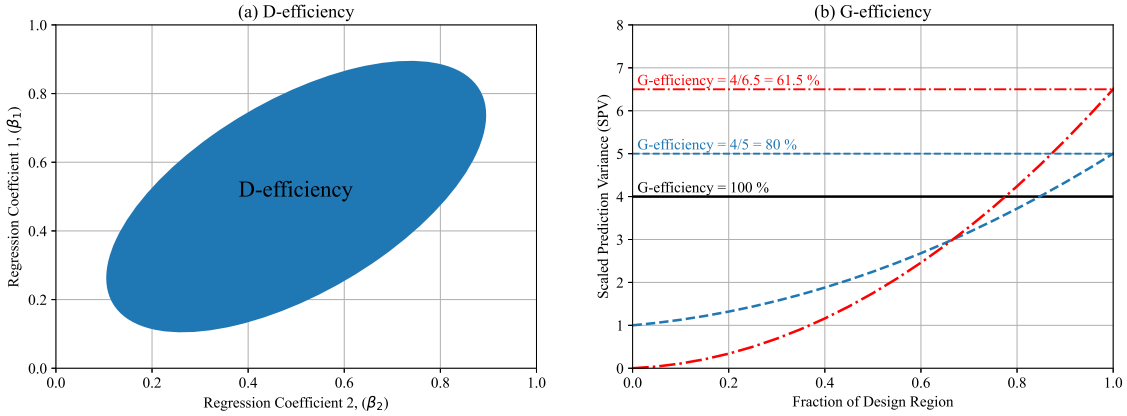

Figure 4.4: Graphical representation of the (a) D-efficiency where the volume of the ellipse denotes the confidence region of the regression coefficients; and (b) G-efficiency where the dashed and dashed-dot curves are examples, for different designs, of the prediction variance across the design region considering a linear model.

4.3 Case Studies

To illustrate the differences between the different experimental designs I consider two case studies. The first only considers continuous (numerical) variables, whereas the second includes categorical (non-numerical) variables. Understanding the use of categorical factors in an experimental design is especially important in polymer composites as the effect of different clay types, polymer types and compatibiliser types are often of interest. Similarly, when investigating different manufacturing methods these are normally indicated as a categorical factor. Each case study is briefly explained. The response surface models are then defined and the global D-optimal and RSM designs generated. Finally, I compare and evaluate the designs in terms of the relative D-efficiency and the G-efficiency, as well as the number of experiments required.

I used Design Expert (Stat-Ease, Inc., 2009) to generate the different RSM designs. To develop the global D-optimal designs and to calculate the D-efficiency and G-efficiency I used R (The R Foundation, 2019) with the AlgDesign Package (Wheeler, 2019).

4.3.1 Case Study 1: Continuous Variables

Ujianto *et al.* (2018) aimed to find the optimum compounding conditions for an HDPE/Cloisite 93A/HDPE-g-MA (93/2/5 wt%) polymer composite using an internal mixer. They investigated the internal mixer temperature, rotor speed and mixing time. They chose the lower and upper boundaries for each factor such that the polymer melts without causing material degradation. This paper has been chosen as the case study as it is well suited for RSM designs, allowing us to illustrate the use of DoE in the design of polymer composite manufacturing

methods. The paper considers only quantitative (*i.e.*, numerically measurable) factors which significantly simplifies the design approach. The three factors and two levels considered are summarised in Table 4.1. The authors used a BBD with three center points, requiring 15 experimental runs. For the response variable analysis they applied a quadratic response surface model.

Table 4.1: Factor and level selection for case study with continuous variables only.

Factors	Low	High
Temperature (°C)	150	210
Rotor speed (rpm)	30	130
Mixing time (min)	4	16

Response Surface Models and Experimental Designs

To compare with the case study design, I generated different experimental designs considering the three response surface models. The Taguchi, CCD and BBD designs are not dependent on the response surface model chosen. In other words, it is not required for the user to specify a response surface model to generate the design. However, the design can still be evaluated for the different response surface models. The global D-optimal and D-optimal designs require the user to define the response surface model and will therefore change depending on the selected model. The full set of designs investigated is summarised in Table 4.2. Notice that the Taguchi design is only considered for the linear model and the same CCD and BBD designs are considered for each of the response surface assumptions. In the modifications column I indicate if it is the base design (*i.e.*, no additional points added) or whether any points are added to the design. For the Taguchi design additional points cannot be added to the design as it is already a complete design considering all the combinations of factors and levels. Center points (CP) provide a measure to estimate the experimental error and are investigated in all the designs except for Taguchi. For the CCD we can add either axial (Ax) or factorial (Fac) points which provides an indication of consistency and stability in the design. For a D-optimal design either replication (Rep) or lack of fit (LOF) points can be added to improve the accuracy of specific factors or the response surface model.

From Equation (4.1) a linear model for three factors will have the following form:

$$y = \beta_0 + \beta_1 x_1 + \beta_2 x_2 + \beta_3 x_3, \tag{4.9}$$

where x_1, x_2 and x_3 are the temperature, speed and mixing time, respectively. The relative D-efficiency compares the generated designs to a global D-optimal design as shown in Equation (4.7). The linear model in Equation (4.9) has four unknown regression coefficients to estimate. Therefore, the global D-optimal design is specified as a 2^{3-1} fractional factorial design with equal weights assigned to the four design points ($w_i = 1/4$). As equal weights are assigned to the design points the global D-optimal is an exact design with the total number of experiments

Table 4.2: Summary of the different RSM designs generated using the linear, interaction and quadratic models for the case study with continuous variables only.

Design Method	Modifications	Number of Experiments for each response surface		
		Linear	Interaction	Quadratic
Taguchi L4	Base design	4	-	-
CCD	Base design	14	14	14
	Add 3 center points (3CP)	17	17	17
	Add 2 factorial points (2Fac)	22	22	22
	Add 2 axial points (2Ax)	20	20	20
	Add 2 factorial and 2 axial points (2Fac, 2Ax)	28	28	28
	Add 3 center, 2 factorial and 2 axial points (3CP, 2Fac, 2Ax)	31	31	31
BBD	Base design	12	12	-
	Add 3 center points (3CP) (Case Study)	15	15	15
D-optimal	Base design	4	7	10
	Add 3 center points (3CP)	7	10	13
	Add 5 replication points (5Rep)	9	12	15
	Add 5 lack of fit points (5LOF)	9	12	15
	Add 5 replication and 5 lack of fit points (5Rep, 5LOF)	14	17	20
	Add 3 center, 5 replication and 5 lack of fit points (3CP, 5Rep, 5LOF)	17	20	23
Global D-optimal		**4**	**8**	**27**

a multiple of 4. A fractional factorial design is very efficient as it covers the whole design region and provides precise estimates for the regression coefficients.

The two-order interaction model for three factors will have the following form based on Equation (4.2):

$$y = \beta_0 + \beta_1 x_1 + \beta_2 x_2 + \beta_3 x_3 + \beta_{12} x_1 x_2 + \beta_{13} x_1 x_3 + \beta_{23} x_2 x_3, \tag{4.10}$$

This model has seven unknown regression coefficients. The global D-optimal design is therefore a 2^3 full factorial design with equal weights assigned to the eight design points *i.e.*, $w_i = 1/8$.

A quadratic model for three factors will have the following form based on Equation (4.3):

$$y = \beta_0 + \beta_1 x_1 + \beta_2 x_2 + \beta_3 x_3 + \beta_{12} x_1 x_2 + \beta_{13} x_1 x_3 + \beta_{23} x_2 x_3 + \beta_{11} x_1^2 + \beta_{22} x_2^2 + \beta_{33} x_3^2, \tag{4.11}$$

where x_1^2, x_2^2 and x_3^2 represent the quadratic terms. The quadratic model has 10 unknown

parameters to estimate. For the global D-optimal design we need to consider three levels to capture the quadratic effects. The global D-optimal design is a fraction of the 3^k full factorial design. However, the design is made up of three parts with different design weights assigned to each. The center point has a weight equal to 0.066, the 2^3 factorial points have a total weight equal to 0.424, and the remainder of the points have total weight equal to 0.510 (see Atkinson *et al.* (2007), Chapter 11, Table 11.6).

Results and Discussion

The relative D-efficiency and G-efficiency for the different designs, including the global D-optimal design, are shown in Figure 4.5, plotted against the number of experiments for all three response surface models. In this case study we considered efficiencies ≥ 90 % to provide an indication of good performance. This threshold is shown with a horizontal line. The vertical line shows the number of experimental runs required by the global D-optimal design. The grey area represents the region for a good design where we have high efficiency with fewer experiments than the global D-optimal design. To differentiate between designs at the same location we have incorporated a slight horizontal perturbation (or jitter) for these data points.

For a linear model the global D-optimal design requires 4 experiments. The Taguchi and D-optimal designs have a relative D-efficiency and G-efficiency of 100 % and only require 4 experiments. These designs are therefore most efficient for estimating the linear regression coefficients. They are equivalent to the global D-optimal design with the exact same number of experiments. However, the D-optimal design with 4 experiments cannot be used to estimate the linear model with 4 parameters, since it has no replicated points for estimating experimental error. BBD has a 100 % G-efficiency, but a less than acceptable relative D-efficiency. It requires three times the number of experiments compared to the global D-optimal, Taguchi and D-optimal designs. BBD is a less than ideal design to consider, but a viable option if the objective of the study is to predict the response variable. CCD provides the worst efficiencies and the highest number of experiments. It is therefore not a viable option when only considering linear effects.

For the two-order interaction model the global D-optimal design requires 8 experiments. It is clear that all the designs are sub-optimal in terms of their efficiencies. However, the D-optimal design is a viable option as they still have relatively high D-efficiencies (approximately 80 %) requiring fewer experiments. Note the D-optimal design with 7 experiments cannot be used to estimate the two-order interaction model with 7 parameters, since it has no replicated design points for estimating the experimental error. BBD has a 100 % G-efficiency, but a very low relative D-efficiency. As with the linear model, it is an option if response variable prediction is the focus. CCD is not a good option to consider for an interaction model as it requires the most experiments and has the worst efficiencies.

To investigate the quadratic effects, the global D-optimal design requires 21 experiments. Some CCD and D-optimal designs require fewer experiments while retaining acceptable effi-

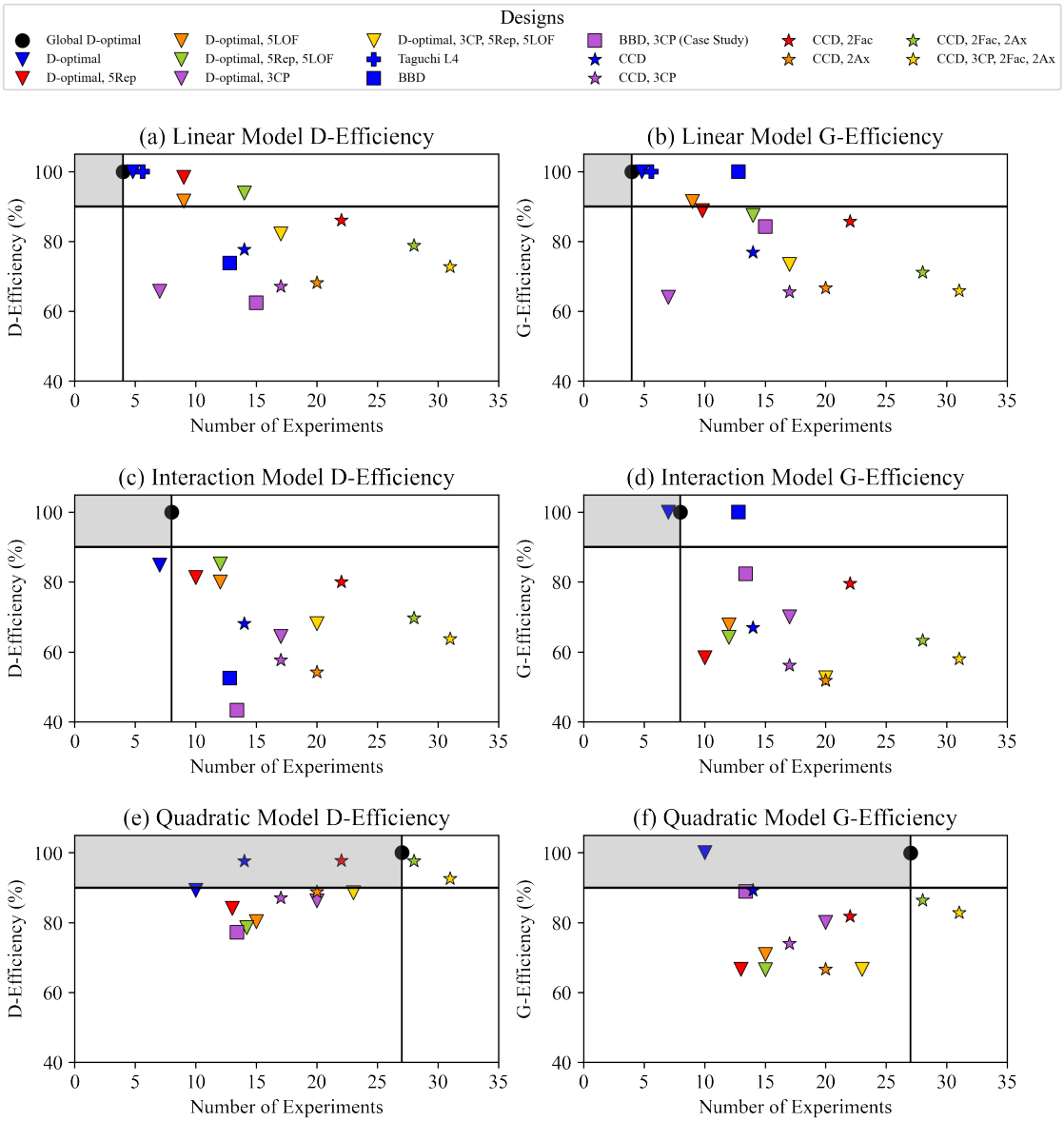

Figure 4.5: Calculated D- and G-efficiencies for the generated designs for case study 1 considering the (a) and (b) linear model, (c) and (d) two-order interaction model, and (e) and (f) quadratic model. The horizontal line indicates a 90 % efficiency and the vertical line denotes the number of experiments required by the global D-optimal design. Data points are slightly perturbed horizontally if they lie at the same location.

ciency measures. Similar to the linear and two-order interaction models, the base D-optimal design with 10 experiments cannot be applied to estimate the quadratic model with 10 parameters, since it has no replications for estimating experimental error. The BBD design is not seen here as the system was found to be computationally singular and the D- and G-efficiencies could not be determined. It is clear from the observed results that CCD designs tend to perform better with a quadratic response surface model, resulting in higher D-efficiencies that are within an acceptable margin. The CCD and BBD have a higher D-efficiency compared to the global D-optimal. Their D-efficiency is lower for the linear model since they use too many experiments for estimating the simple linear regression model.

Adding center points (CP) reduces the relative D-efficiency and G-efficiency for all designs and response surface models, while increasing the number of experimental runs by three. However, there is value in adding center points (CP) as it provides stability in the prediction variance and is a measurement of experimental error (Myers *et al.*, 2016). When adding replication (Rep) and lack of fit (LOF) points to the D-optimal design, the decrease in both relative D-efficiency and G-efficiency is still within the acceptable range with only an additional five experimental runs needed. For CCD we note an improvement in relative D-efficiency and G-efficiency when adding factorial (Fac) points but at the cost of a larger number of experimental runs.

The case study design, a BBD with three center points, provided the worst relative D-efficiency for all three response surface models. This indicates that it is not able to estimate the regression coefficients precisely. On the other hand, it has an acceptable G-efficiency (in the 80 % range). In other words, it is able to predict the response variable with low variance in the design region. The aim of Ujianto *et al.* (2018) was to analyse the effects of the compounding conditions. They would, therefore, have benefited from a design which is able to provide a better estimation of the regression coefficients, such as D-optimal.

4.3.2 Case Study 2: Including Categorical Variables

Mohamadi *et al.* (2014, 2016) aimed to find the optimum material system composition for HDPE/Fluoromica with a compatibiliser. They investigated clay weight loading, compatibiliser type and compatibiliser to clay ratio. For the compatibiliser type the effect of molecular weight was investigated with HDPE-g-MA at two different molecular weights. The three factors and three levels considered are presented in Table 4.3. Mohamadi *et al.* (2014, 2016) was chosen for this case study as they designed an experiment to conduct multiple investigations, *i.e.* effect of molecular weight with the same compatibiliser type and optimising the material system. The authors considered a D-optimal design requiring 16 experimental runs with one repetitive sample to verify repeatability and reproducibility. As this would result in only 13 experimental runs it is assumed that three additional lack of fit points were considered to obtain the total of 16 experimental runs. This is a logical assumption as additional replication points would have replicated design points which is not the case. Adding center points with categorical factors would duplicate the number of center points for the combinations of categorical factors which would require 22 experiments in this case. For the response variable analysis the authors applied a quadratic model, which had to be obtained individually for each compatibiliser type. This is due to the use of a categorical variable as each set of regression coefficients differed for compatibiliser type.

Response Surface Models and Experimental Designs

To compare with the case study design, I generated different experimental designs considering the three response surface models. As discussed in the previous case study, the Taguchi, BBD

Table 4.3: Factor and level selection for the case study with both continuous and categorical variables.

Factors	Type	Low	Mid	High
Clay weight loading (wt%)	Continuous	2	-	6
Compatibiliser to clay ratio	Continuous	3	-	5
Compatibiliser type	Categorical	EVA	HDPE-g-MA 1	HDPE-g-MA 2

and CCD design is not dependent on the chosen response surface model. The same designs will therefore be considered for each response surface assumption. The global D-optimal and D-optimal designs, however, require the user to define a response surface model.

In Design Expert, three continuous factors need to be defined for a BBD design. However, the case study only has two continuous factors. A Taguchi design is only able to construct a design using either continuous or categoric factors, but not a combination of both. To circumvent this, dummy continuous factors are considered for the categorical factors. For example, EVA will be represented by a 1, HDPE-g-MA 1 by a 2 and HDPE-g-MA by a 3. These are then be replaced in the developed design to reflect the true categorical factors before evaluating the designs.

Table 4.4 summarises the full set of designs considered for this case study. Center points (CP) provide a measure to estimate the experimental error and are investigated in all the designs. For the CCD we can add either axial (Ax) or factorial (Fac) points which provides an indication of consistency and stability in the design. For a D-optimal design either replication (Rep) or lack of fit (LOF) points can be added to improve the accuracy of specific factors or the response surface model.

From Equation (4.4) a linear model for two continuous factors and one categorical factor will have the following form:

$$y = \beta_0 + \beta_1 x_1 + \beta_2 x_2 + \beta_{11,cat} z_{11} + \beta_{12,cat} z_{12}, \tag{4.12}$$

where x_1 and x_2 is the clay weight loading and compatibiliser to clay ratio, respectively.z_{11} and z_{12} are the compatibiliser type categorical dummy variables with its second and third levels since the first level is represented by the intercept, β_0. That is, z_{11} denotes HDPE-g-MA 1 and z_{12} HDPE-g-MA 2 where EVA is the first level and therefore represented by the intercept, β_0. z_{11} and z_{12} will take on the value of 1 if the associated compatibiliser type is active and 0 otherwise. Mathematically this is described as:

$$z_{1n} = \begin{cases} 1 & \text{if } n = 1 \text{ (HDPE-g-MA 1) or } n = 2 \text{ (HDPE-g-MA 2)}, \\ 0 & \text{if otherwise (EVA)}. \end{cases}$$

The global D-optimal design is defined in two parts, one for the continuous factors and one for the categorical factor. For the continuous factors the global D-optimal design is specified as a 2^2 full factorial design with equal weights assigned to the design points. For the categorical factors the global D-optimal design considering the continuous factors is replicated for all

Table 4.4: Summary of the different RSM designs generated using the linear, interaction and quadratic models for the case study with the addition of one categorical factor.

Design Method	Modifications	Number of Experiments for each response surface		
		Linear	Interaction	Quadratic
Taguchi L9	Base design	9	9	9
BBD	Base design	12	12	12
	Add 3 center points (3CP)	15	15	15
CCD	Base design	24	24	24
	Add 3 center points (3CP)	33	33	33
	Add 2 factorial points (2Fac)	36	36	36
	Add 2 axial points (2Ax)	36	36	36
	Add 2 factorial and 2 axial points (2Fac, 2Ax)	48	48	48
	Add 3 center, 2 factorial and 2 axial points (3CP, 2Fac, 2Ax)	57	57	57
D-optimal	Base design	5	10	12
	Add 3 center points (3CP)	14	19	21
	Add 5 replication points (5Rep)	10	15	17
	Add 5 lack of fit points (5LOF)	10	15	17
	Add 5 replication and 5 lack of fit points (5Rep, 5LOF)	15	20	22
	Add 3 center, 5 replication and 5 lack of fit points (3CP, 5Rep, 5LOF)	24	29	31
Case Study	D-optimal, add 1 replication point (assume addition of 3 lack of fit points)	-	-	16
Global D-optimal		**12**	**12**	**27**

combinations of the categorical factors. Therefore the global D-optimal design for both the continuous and categorical factors is a $2^2 \times 3^1$ design with equal weights at the design points ($w_i = 1/12$ for an exact design).

The two-order interaction model for three factors will have the following form based on Equation (4.6):

$$y = \beta_0 + \beta_1 x_1 + \beta_2 x_2 + \beta_{12} x_1 x_2 + \beta_{11,cat} z_{11} + \beta_{12,cat} z_{12} + \beta_{111} x_1 z_{11} + \beta_{112} x_1 z_{12} + \beta_{211} x_2 z_{11} + \beta_{212} x_2 z_{12}, \quad (4.13)$$

where $x_1 z_{11}, x_1 z_{12}, x_2 z_{11}$ and $x_2 z_{12}$ represents the interaction between the clay weight loading, compatibiliser to clay ratio and the compatibiliser type categorical factor levels. Similar to the linear model, the global D-optimal design for the two-order interaction model is a $2^2 \times 3^1$ design with equal weights at the design points ($w_i = 1/12$).

A quadratic model for three factors will have the following form based on Equation (4.3):

$$y = \beta_0 + \beta_1 x_1 + \beta_2 x_2 + \beta_{12} x_1 x_2 + \beta_{11,cat} z_{11} + \beta_{12,cat} z_{12} + \beta_{111} x_1 z_{11} + \beta_{112} x_1 z_{12} + \beta_{211} x_2 z_{11} + \beta_{212} x_2 z_{12} + \beta_{11} x_1^2 + \beta_{22} x_2^2, \quad (4.14)$$

where x_1^2 and x_2^2 represent the quadratic terms. For the global D-optimal design we need to consider three levels to capture the quadratic effects. The global D-optimal design is a 3^3 full factorial design. However, the design is made up of three parts with different design weights assigned to each. For a global D-optimal design considering a combination of continuous and categorical factors, the weights at the design points for a quadratic response model are defined as the continuous global optimal design weights (w_i) divided by the number of levels of the categorical factors (b), *i.e.* w_i/b (Atkinson *et al.*, 2007). The design weights for the global D-optimal design were extracted from R (The R Foundation, 2019). For EVA the center point has a weight equal to 0.0047, with the factorial point weights equal to 0.0565 and the remainder of the points have a weight equal to 0.0257. For HDPE-g-MA 1 and HDPE-g-MA 2 the factorial points have a weight of 0.0599 and 0.0600, respectively. The remainder of the points have a design weight equal to 0.0187. The weights are a result of the optimisation algorithm and is done in such a way as to confirm global optimality. The difference in the weights between the design points is due to the quadratic response surface model.

Results and Discussion

The relative D-efficiency and G-efficiency for the different designs considered in this case study are shown in Figure 4.6 plotted against the number of experiments for all three response surface models. For case study 2 efficiencies ≥ 80 % are considered an indication of good performance. This threshold is reduced compared to case study 1 as the inclusion of a categorical factor reduces the design efficiencies. This efficiency threshold is shown with a horizontal line, while the vertical line indicates the number of experiments required by the global D-optimal design. The grey area then represents the region for a good design.

For the linear model, the global D-optimal design requires 12 experiments. Three of the D-optimal designs require fewer experiments namely, the base design, design with 5 replica-

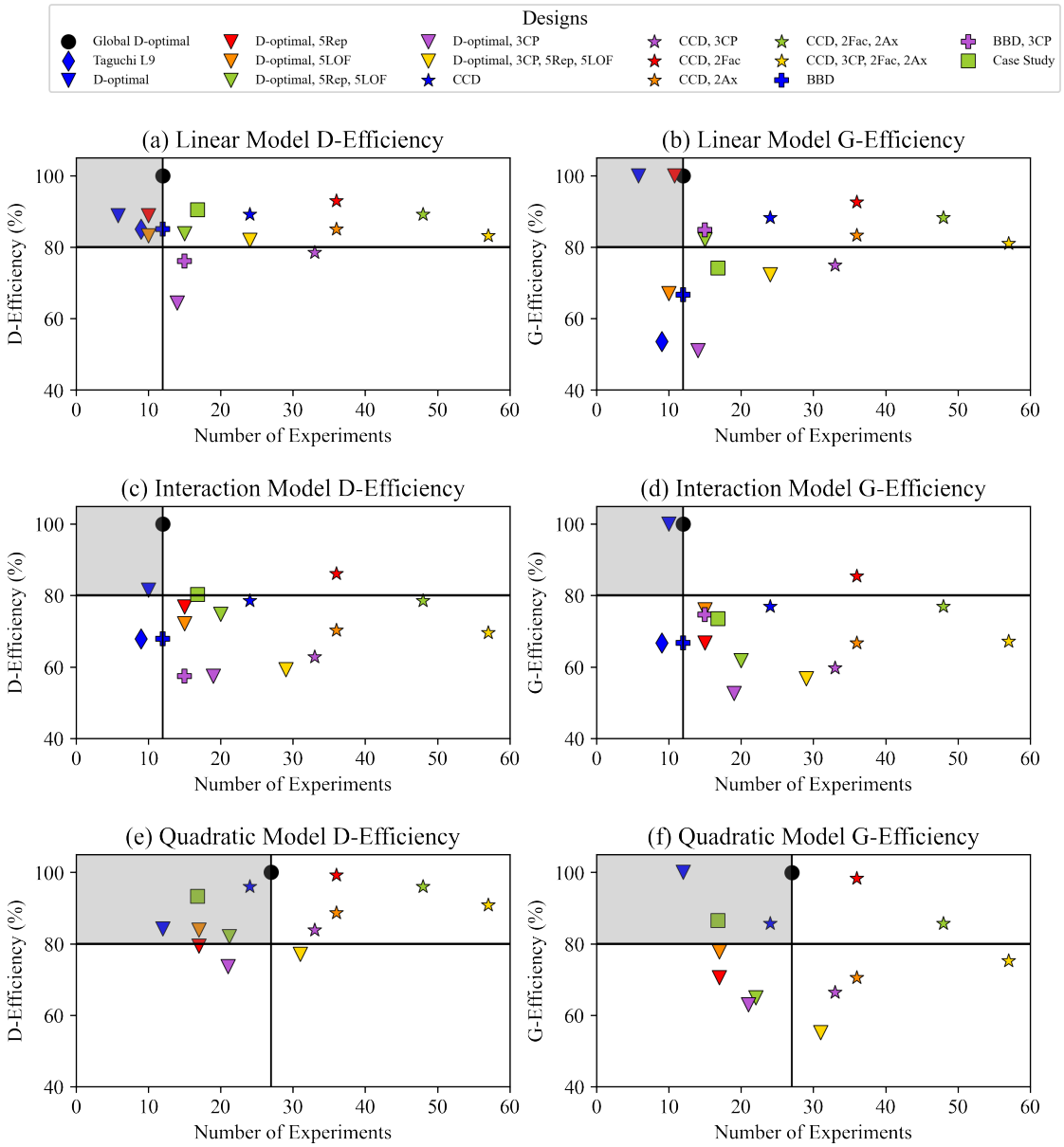

Figure 4.6: Calculated D- and G-efficiencies for the generated designs for case study 2 considering the (a) and (b) linear model, (c) and (d) two-order interaction model, and (e) and (f) quadratic model. The horizontal line indicates a 80 % efficiency and the vertical line denotes the number of experiments required by the global D-optimal design. Data points are slightly perturbed horizontally if they lie at the same location.

tion points and the design with 5 lack-of-fit points. However, the D-optimal design with 5 experiments cannot be used to estimate the linear model with 5 parameters, since it has no replicated points for estimating experimental error. The D-efficiency of the optimal designs are lower than the global D-optimal design, but is within an acceptable range to estimate the linear regression coefficients. These designs are most efficient for estimating the linear regression coefficients. The Taguchi L9 design requires 9 experiments and has a D-efficiency within the acceptable range, although it has a very low G-efficiency. This design would be a viable option if the aim is to accurately estimate the regression coefficients, but at the cost of prediction. The CCD designs require many more experiments while the D-efficiency and G-

efficiency do not provide significant improvement over the global D-optimal design. The base BBD requires the same amount of experiments as the global D-optimal with a D-efficiency within the ideal range and an acceptable G-efficiency. D-optimal designs are the best option if the goal is to only consider linear or main effects between the factors. However, the Taguchi L9 and BBD designs are alternative options if prediction is not of importance.

For the two-order interaction model the global D-optimal design requires 12 experiments. All the designs are suboptimal in terms of their efficiencies, except the D-optimal design with a D-efficiency within an acceptable range and a G-efficiency equal to the global D-optimal design. However, the D-optimal design with 10 experiments cannot be used to estimate the two-order interaction model with 10 parameters, since it has no replicated design points for estimating the experimental error. As with the linear model, the CCD designs require more experiments without providing good efficiencies. If two-order interaction effects are important a base D-optimal design would be the best option. Other designs are not viable requiring more experiments than the global D-optimal with inadequate efficiencies.

For the quadratic model the global D-optimal design requires 27 experiments. Most of the D-optimal designs are viable options requiring fewer experiments than the global D-optimal, while retaining acceptable efficiency measures. Note the base design with 12 experiments cannot be applied to estimate the quadratic model with 12 parameters, since it has no replications for estimating experimental error. The base CCD design performs well requiring less experiments than the global D-optimal, while retaining better efficiencies than the D-optimal designs. Note that the case study performs well with a D-efficiency and G-efficiency within the ideal region. For this case study a quadratic response surface model has the best overall efficiencies for the different designs. Both D-optimal designs and CCD designs can be considered, however the D-optimal designs do require fewer experiments.

Adding center points (CP) or replication points (Rep) reduces the efficiencies for all designs and response surface models. Adding replication points has a larger effect on the efficiency decrease than adding center points, especially for the linear and two-order interaction models. Adding lack of fit points (LOF) does not contribute to the D- or G-efficiency and are mainly used to test model validity. For the CCD designs when adding factorial points there is a general improvement in the D-efficiency and G-efficiency, while the addition of axial points reduces the efficiencies. In both instances the number of experimental runs required is greatly increased.

The case study design was a D-optimal design with 1 center point, 3 lack-of-fit points and developed with a quadratic response surface model. From Figure 4.6 it is clear that the case study design does not provide good efficiencies for the linear and interaction models. This indicates that these models are not able to estimate the regression coefficients precisely (high D-efficiency) or predict the response variable with minimum variance (high G-efficiency). For both cases the design requires more experiments than the global D-optimal while not providing good efficiencies. For the quadratic model the case study design performs well requiring less experiments than the global D-optimal. A D-efficiency of 93 % indicates that

the model is able to estimate the regression coefficients precisely. Similarly a G-efficiency of 87 % provides an indication that the quadratic model can be used to predict the response variable with low variance in the design region. Mohamadi *et al.* (2014, 2016) designed their experiment to find the optimum material system composition. Such a design must be suitable for fitting a response surface model that is able to accurately estimate the regression coefficients. Therefore, Mohamadi *et al.* (2014, 2016) chose a good design for the purposes of their study.

4.4 Conclusion

In this chapter I provided an overview of different RSM designs. I compared and evaluated these designs in terms of their relative D-efficiency and G-efficiency by considering two case studies. The first case study used only continuous (numerical) factors and the second case study included a categorical (non-numerical) factor.

The D-optimal designs were more efficient in estimating the regression coefficients, while minimising the reponse variable prediction variance across the design region. It is considered to be a good design option for all three response surface models. When only considering main or linear effects of the factors, a Taguchi design is a good choice. For quadratic effects, CCD is a viable option although it does require more experimental runs than a D-optimal design.

When adding a categorical factor to the design similar conclusions were observed to the case study only considering continuous factors. The D-optimal design was more efficient in estimating the regression coefficients. For continous and categorical factors a quadratic response surface model performs better in terms of D- and G-efficiency than the linear and two-order interaction models and all designs are viable options.

Additional points (*i.e.* center, lack of fit and replication) can be considered, however, these do negatively impact the designs' relative D-efficiency and G-efficiency. Nevertheless, it is up to the experimenter to decide how many experimental runs are feasible and whether estimation or prediction is more important.

This chapter has clearly shown that considering an experimental design approach is beneficial to reducing the number of experimental runs while obtaining statistically relevant results. It showed the importance of evaluating different designs to determine which one is best suited for the problem of interest. This is especially clear from the two case study designs. Ujianto *et al.* (2018) aimed to analyse the effects of the compounding conditions, that is the temperature, rotor speed and mixing time. A design which is able to precisely estimate the regression coefficients would therefore be the better choice. A BBD is not able to estimate the regression coefficients within a reasonable accuracy, although it is a good design to consider for predicting the response variable with minimum variance in the design region. Ujianto *et al.* (2018) would therefore have benefited from a proper design evaluation. On the other hand, Mohamadi *et*

al. (2014, 2016) aimed to optimise the material system. They chose to utilise a D-optimal design which performed well when compared to the global D-optimal design.

CHAPTER 5

EXPERIMENTAL METHODOLOGY

From the literature review it is clear that variation in manufacturing does have an influence on the mechanical properties of high-density polyethylene (HDPE)/montmorillonite (MMT) composites. Most of the studies in the systematic literature review focused on better understanding the effects of compounding methods and conditions (20 studies) with far fewer investigating the effects of processing methods and conditions (8 studies). This chapter will consider the influence of compression and injection moulding, and the influence of machine variation on layered double hydroxide (LDH) the alternative to MMT. As a synthetic alternative it is theoretically possible to extrapolate the observations for HDPE/MMT and apply them to HDPE/LDH. Since LDH is synthethic it is more tightly controlled.

The manufacturing and experimental work was a multi-site collaborative effort. The compounding and moulding was completed based on a statistical design of experiments developed in this chapter. I completed compounding of all the material required at the Center for Nanocomposites, Council for Science and Industrial Research in South Africa. The compression moulding for the South African samples were completed at the University of Pretoria (UP) by myself. The injection moulding for the South African samples was completed at Tshwane University of Technology (TUT), South Africa. The Leibniz Institute for Polymer Research (IPF) in Dresden, Germany completed both compression and injection moulded samples. The compression moulded samples were pressed as plaques at both sites. The desired sample geometries were then cut from these plaques at the IPF. The IPF conducted all the tensile and impact tests and provided the resulting stress-strain curves to me.

This chapter outlines the experimental methodology followed which includes a description of the materials used, manufacturing methods and conditions, mechanical characterisation, experimental design and statistical analysis.

5.1 Introduction

This experimental study considers the influence of clay type and clay loading on the mechanical properties of HDPE/LDH. Additionally, the influence of compression and injection moulding at different sites is also considered. This multi-site study considers two university laboratories (UP and TUT) and an international state-of-the-art polymer facility (IPF). The effect of manufacturing through different equipment by using the same moulding technique is investigated at different sites. Due to the limitations of the injection moulding tensile moulds available at TUT, the effect of two tensile sample mould types is considered as a sub-study.

A statistical design of experiments approach is considered to develop the experimental designs, thereby ensuring that the fewest amount of experimental runs are required to make reliable inferences. This approach ensures that a near optimal and efficient design is obtained to form reasonable conclusions from the data. To analyse the data various statistical techniques are considered and discussed.

5.2 Materials

Safrene high-density polyethylene (HDPE) grade C7260 was obtained from Safripol, South Africa in pellet form. The HDPE was then pulverised into a fine powder before use. The HDPE has a density of 0.958 g/cm^3, a melt flow rate of 23 g/10 min at 190 °C and an injection moulding temperature range of 200-260 °C. It should be noted that since the inception of this study, Safripol has decommissioned HDPE C7260.

Synthethic LDH clays, DHT-4A (average particle size of 0.5 μm) and Alcamizer 1 (average particle size of 0.7 μm), were obtained from Kisuma Chemicals, The Netherlands. These clays were specifically chosen based on their polymer compatibility. DHT-4A is compatible with polyolefins such as HDPE, whereas Alcamizer 1 is compatible with polyvinyl chloride (PVC). In a previous study (Botha *et al.*, 2019) (c.f. Chapter 2.3.1) Alcamizer 1 showed a higher first peak stress than DHT-4A, which is unexpected given Alcamizer 1's presumed incompatibility with HDPE and therefore needs further investigation.

5.3 Manufacturing

Manufacturing of the HDPE/LDH composite samples occurred in two phases, namely compounding and moulding. During compounding the different materials are mixed together to form a composite. A sample to use for mechanical testing is then manufactured during the moulding phase.

5.3.1 Compounding

The compounding method employed for this study is illustrated in Figure 1.3. The fine HDPE powder was tumble mixed with the desired clay loading in a Jones mixer for 5 min to ensure proper dispersion. The following equation was used to calculate the required mass of the clay (m_c) for a specified mass of polymer (m_p) given the desired clay loading (x):

$$m_c = m_p \left(\frac{x}{1-x} \right) \quad \text{or} \quad x = \frac{m_c}{m_p + m_c} \tag{5.1}$$

The HDPE-clay mixture was then compounded in a TE-30 co-rotating twin screw extruder with a screw diameter of 30 mm, a screw speed of approximately 200 rpm and an extruder temperature profile of 143-170-146-165-199-198-200-201-199-194 °C for the 10 zones. The extruded wire was fed through a chipper to obtain pellets which were then dried overnight at 60 °C. The moisture content affects processability and mechanical properties, especially once clay is introduced. Once the pellets were dried, a second extrusion was performed. From a previous study (Botha *et al.*, 2020) (c.f. Section 2) the exploratory and statistical data analysis indicated that two extrusions are sufficient to obtain a reasonable improvement in mechanical properties.

5.3.2 Moulding Methods

Mechanical testing samples were created by using either compression or injection moulding at different sites. Even though the available equipment at the different sites were not from the same manufacturer or the same model, every effort was made to ensure the moulding conditions were identical.

Injection Moulding

Figure 1.4 provides an illustration of the injection moulding methodology. Injection moulding was done on a TMC30H at TUT, and an ARBURG Allrounder 270S at IPF. It was decided that TUT would determine the optimum injection moulding conditions for neat HDPE C7260 using their equipment. They then shared these conditions with the IPF who used identical conditions as far as possible.

The following optimum moulding conditions were considered at both sites: A mould temperature between 37 °C and 40 °C with no cooling water, a screw speed of 350 rpm, a cooling time of 20 s, an injection pressure of 160 bar, a hold and suck back pressure of 100 bar, a back pressure of 10 bar and a temperature profile from the nozzle to the feed zone of 250-250-230-200-80 °C.

A limitation to consider was the availability of tensile dogbone sample moulds. TUT only had an ISO Type 1A mould available. However, due to the compression moulding equipment

size limitation an ISO Type 1BA will be used for compression mouldedsamples from both UP and IPF. This would result in two different mould sizes considered for each moulding method. Fortunately, the IPF had both an ISO Type 1A and 1BA available. Due to this limitation, the difference in tensile sample mould types is therefore investigated. The sample dimensions for both ISO Type 1A and 1BA are shown in Figure 5.1.

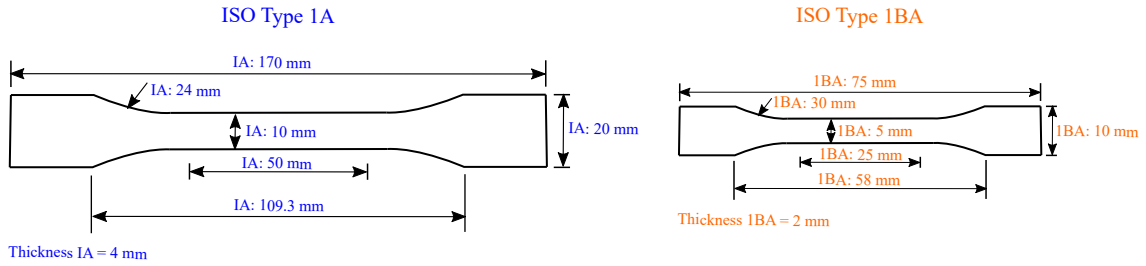

Figure 5.1: Tensile dogbone sample with dimensions for ISO Type 1A (blue) and ISO Type 1BA (orange) (DIN EN ISO 527-2, 2012).

Compression Moulding

The compression moulding methodology is illustrated in Figure 1.5. The methodology that was considered for the historical samples at UP is different to the methodology employed at the IPF. To determine the effect of these two methodologies on the mechanical properties a preliminary experimental study was conducted. The two methodologies are:

- **UP:** Apply a pressure from 0 MPa to 7.5 MPa and hold for 30 s before increasing to 15 MPa and holding for 5 min. Drop the pressure back to 0 MPa and repeat the procedure, this time holding for 19 min at 15 MPa. The total press time is 25 min.
- **IPF:** At 0 MPa hold for 5 min before applying a force of 40 kN and holding for a further 2 min. The total press time is 7 min. The force is converted to pressure, with a piston diameter of 120 mm as provided by the IPF, resulting in a pressure of 3.54 MPa. However, this pressure seems low based on what was observed in literature (c.f. Table B.1), and a pressure of 7.5 MPa (half of the UP pressure) was therefore investigated.

The results are shown in Figure 5.2 with the associated tensile curves in Appendix 7.3.2. There is a 3.65 % difference between the mean σ_{FPS} for the compression moulding method considered at UP (32.33 MPa) and at the IPF with a pressure of 3.5 MPa (33.5 MPa); and a 0.63 % difference between the two pressures considered for the IPF method. In light of this there will be a considerable saving to manufacturing time by adopting the IPF method which has a total press time of 7 min compared to the UP method which is 25 min and had a number of steps where errors could occur. It appears that pressure has no significant influence and we will therefore use a pressure of 3.5 MPa which is comparable to the 40 kN force (applied to a 120 mm diameter piston) which is used at the IPF. There is a 8.26 % decrease in ϵ_f between the UP and IPF (3.5 MPa) methodologies. Given the large variations in ϵ_f, a less than 10 % difference is not considered a significant effect.

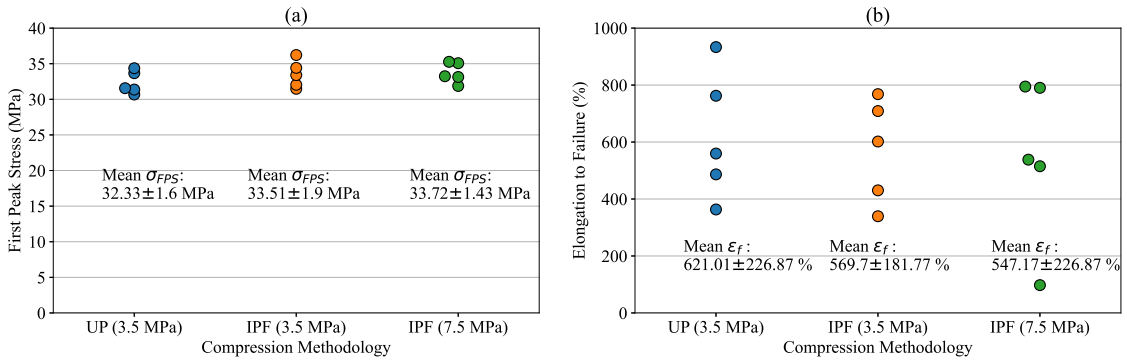

Figure 5.2: Influence of the manufacturing conditions on the (a) first peak stress and (b) elongation to failure for the 2020 data.

Compression moulding was done on a Vertex Hot Press at UP, and a PW40EH (Paul-Otto-Weber GmbH) at IPF. It was conducted at 190 °C with 5 min of heating while no pressure is applied. This is followed with a pressure of 40 kN (equivalent to 3.5 MPa calculated from the cylinder area) for 2 min. The initial heating without pressure applied allows any trapped air in the mould to release, preventing air bubbles from forming in the final sample. Sample moulds were then removed and cooled at room temperature before finishing sample surfaces.

Due to mould restrictions there are differences in the mould thickness. Both sites considered a 100 × 100 mm mould, however the IPF mould was 2 mm thick and the UP mould 3 mm thick. The tensile dogbone (ISO Type 1BA) and impact samples were milled from the plaques at IPF before testing. We do not expect any effect due to the difference in thickness as it is assumed that the mechanical property data is normalised to the sample geometry according to ISO standards. In addition to the differences in thickness, the samples compressed at UP had a wavy or rippled surface (c.f. Figure 5.3) compared to the smooth surface for the IPF samples.

Figure 5.3: Example of the wavy or rippled surface observed for UP compression moulded samples.

5.4 Statistical Design of Experiments

Due to the multi-faceted nature of the experimental study we consider a technique from statistics to develop an experimental design (c.f. Chapter 4). Statistical design of experiments (DoE) allows us to find a sufficient number of experimental runs required while attaining statistically relevant results (Montgomery, 2013).

Based on the evaluation of the case studies from Chapter 4 it is clear that a D-optimal design with a quadratic response surface model would provide the most efficient design. D-optimal designs are able to effectively estimate the effect of different design factors and are best suited for screening purposes and studies which contain categorical variables. In polymer composites, the D-optimal method has successfully been implemented by Mohamadi *et al.* (2014, 2016) to investigate the effects of the material system (*e.g.* clay content, compatibiliser type and compatibiliser to clay ratio) on the mechanical, barrier and rheological properties. These are the only studies where D-optimal has been implemented for HDPE-based composites.

A D-optimal design is therefore considered for this study. The designs were generated using Design Expert (Stat-Ease, Inc., 2009) and are evaluated by comparing their D-effiency and G-efficiency to a global D-optimal design using R (The R Foundation, 2019) with the AlgDesign Package (Wheeler, 2019).

5.4.1 Overview of Factors

Based on the conclusions from both Chapters 2 and 3 the **controllable design factors** considered for the experimental study are clay type, clay weight loading (wt%), strain rate (mm/min), moulding method and site. The **response variables** of interest are the mechanical properties which include tensile and impact properties.

There are several **held-constant factors**, which may have some effect on the response variables but are held at a specific level for this experimental study. These factors include the compounding method, compounding conditions and moulding conditions for each of the moulding methods considered. In other words, the conditions for both moulding methods were kept the same at the different sites, with different operators for each site. The polymer grade is set to HDPE C7260 and the number of extrusions considered during compounding is kept at 2. Testing conditions were also kept constant with a single trained operator conducting all the tests to minimise any potential variation due to the human operator.

Uncontrollable factors are present in all phases of the manufacturing and testing process:

- Laboratory: ambient temperature and humidity.
- Raw Material: initial material properties may differ between batches.

- Compounding: potential contaminants in the feeder, inconsistent diameter of the extrudite, inconsistent size of the chipped pellets after extrusion and the level of clay dispersion.
- Moulding: potential contaminants in the mould, not consistently filling tensile sample moulds with the same amount of material, misalignment of moulding plates, air bubbles trapped in mould and inconsistent cooling depending on laboratory environment.
- Testing: thickness of the compression moulded plaques.

Nuisance factors are unknown and uncontrolled but may have an influence on the results. Potential nuisance factors for this study are different time frames to conduct moulding and testing, machine tolerance, different human operators used during moulding and measurement inaccuracies for mixing of composite material or testing samples.

These different factors are summarised in a cause-and-effect diagram shown in Figure 5.4. A cause-and-effect diagram is often used to assist in planning the experimental design by identifying all factors of interest and those that might have an effect on the experimental study.

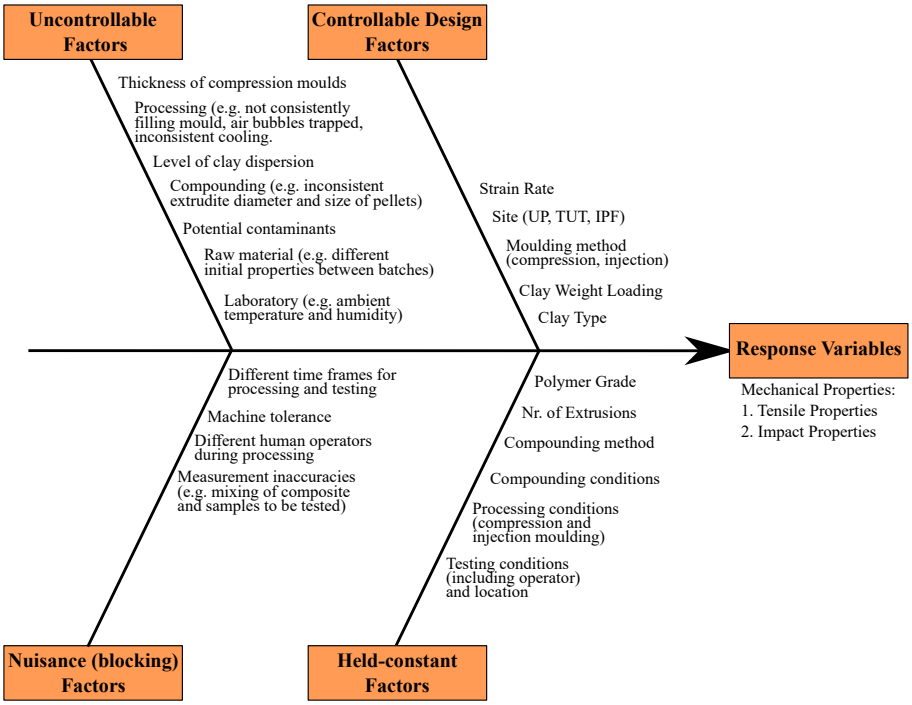

Figure 5.4: Cause-and-effect diagram for the thesis experimental study.

Controllable Design Factors

The controllable design factors shown in the cause-and-effect diagram will be varied in this experimental study. The different factors and associated levels are summarised in Table 5.1.

Table 5.1: Design factors and levels considered for the thesis experimental study.

Design Factor	Type	Levels used	
		Low	High
Clay Type	Categorical	DHT4-A	Alcamizer 1
Clay Loading (wt%)	Continuous	2	10
Strain Rate (mm/min)	Continuous	5	500
Moulding Method	Categorical	Compression	Injection
Site	Categorical	South Africa (UP, TUT)	Germany (IPF)

The historical data analysis indicated that clay type has a statistically significant effect. The interesting result from the exploratory data analysis was that Alcamizer 1 resulted in higher first peak stress than DHT4-A, which is unexpected as Alcamizer 1's surface treatment is not designed for HDPE, whereas DHT4-A is. This observation requires further investigation.

Clay weight loading is known to have an influence on the mechanical properties, although the historical data analysis indicated that there was no statistically significant effect. We want to explore this further to determine if this is due to the material system or the inexperience of the undergraduate students in polymer composite manufacturing. From the historical data analysis we concluded that the clay loading should not exceed 10 wt% as the mechanical properties start to degrade. All previous studies considered 2.5 wt% as the lowest clay loading. For this experimental study we will set this lower bound at 2 wt%.

There is a clear effect on mechanical properties due to strain rate as was shown in the historical data analysis. For this reason it will be further investigated in the experimental study. The lower bound was chosen at 5 mm/min and the upper bound is chosen at 500 mm/min prescribed as the minimum and maximum strain rates in (ASTM D638-14, 2014).

The systematic literature review indicated that the moulding method does have an influence on mechanical properties. Compression moulding is a much simpler and more cost effective method to employ than injection moulding, especially when considering scalability (Azeez *et al.*, 2013; Albdiry *et al.*, 2012) (*i.e.*, from a controlled laboratory to uncontrolled industrial setting). The systematic literature review concluded injection moulding provides better properties than compression moulding as it provides better dispersion of the clay in the polymer.

Finally, we want to determine whether different equipment will influence results even though it performs the exact same moulding method. To do so we compare the manufactured samples from South African university laboratories with that of a state-of-the-art international facility. In South Africa, the compression moulded samples will be manufactured at the University of Pretoria (UP) and the injection moulded samples at Tshwane University of Technology (TUT). Internationally, both samples will be moulded at the Leibniz Institute for Polymer Research (IPF) in Germany.

Table 5.2: D-optimal experimental design for tensile testing. (Gray - removed from design, Orange - missing data points, Green - additional data points not in original design)

Run	Clay Loading (wt%)	Strain Rate (mm/min)	Clay Type	Moulding Method	Site
1	2.8	500	DHT4-A	Compression	UP
2	10	500	Alcamizer 1	Injection	IPF
3	5.12	5	DHT4-A	Compression	IPF
4	10	50	DHT4-A	Compression	UP
5	6	252.5	Alcamizer 1	Compression	UP
6	6	252.5	DHT4-A	Compression	IPF
7	2.8	500	DHT4-A	Injection	IPF
8	6	252.5	Alcamizer 1	Compression	UP
9	3.56	50	Alcamizer 1	Compression	IPF
10	2	5	Alcamizer 1	Compression	UP
11	6	252.5	DHT4-A	Injection	IPF
12	10	5	Alcamizer 1	Injection	TUT
13	6	252.5	Alcamizer 1	Injection	IPF
14	8	500	Alcamizer 1	Injection	TUT
15	10	252.5	DHT4-A	Injection	IPF
16	10	50	DHT4-A	Injection	IPF
17	2	50	DHT4-A	Compression	IPF
18	2.8	500	DHT4-A	Injection	IPF
19	10	500	DHT4-A	Injection	TUT
20	5.2	5	DHT4-A	Injection	TUT
21	6	252.5	DHT4-A	Compression	UP
22	2	500	Alcamizer 1	Compression	IPF
23	3.59	50	Alcamizer 1	Injection	TUT
24	10	50	DHT4-A	Compression	UP
25	10	5	Alcamizer 1	Compression	IPF
26	6	252.5	Alcamizer 1	Compression	IPF
27	2	50	DHT4-A	Injection	TUT
28	2.8	500	DHT4-A	Compression	UP
29	10	500	Alcamizer 1	Compression	UP
30	10	252.5	Alcamizer 1	Compression	IPF
31	6	252.5	Alcamizer 1	Injection	IPF
32	6	252.5	DHT4-A	Injection	TUT
33	2	500	Alcamizer 1	Injection	TUT
34	2	5	Alcamizer 1	Injection	IPF
35	6	252.5	Alcamizer 1	Injection	TUT
36	10	500	DHT4-A	Compression	IPF
Additional Data (AD) — not in original design					
AD	4		Alcamizer	Injection	IPF
AD	8		DHT4A	Injection	IPF
AD	2		DHT4A	Injection	IPF
AD	2		DHT4A	Compression	UP
AD	2		DHT4A	Compression	UP
AD	10		Alcamizer	Injection	IPF
AD	2		Alcamizer	Injection	IPF

5.4.2 Tensile Testing Design

The tensile testing design is the main component of this thesis and requires an efficient design able to predict the response variable. The tensile testing experimental design therefore considered a quadratic response surface model with 11 lack of fit points to test the models prediction ability. There are two instances where the clay loading is close to one another,

namely run 3 and 20 with 5.12 wt% and 5.2 wt% and run 9 and 23 with 3.56 wt% and 3.59 wt%. These are examples of lack of fit points. To account for repeatibility 5 replication points are included (*e.g.* run 7 and 18), while 8 center points are added to account for experimental error (*e.g.* run 6 and 21). This design allowed for a wider representation of clay loading and is shown in Table 5.2. Note that for all individual cases a neat sample is tested as the control sample.

Some of the compounded material was destroyed during shipping. It was therefore necessary to amend the tensile testing experimental plan to accommodate for the material loss. In this amendment the strain rate was removed as a factor and any samples that specifically consider a difference in strain rate were subsequently removed. In Table 5.2 the factor and samples removed due to the loss of material are indicated in gray.

In Table 5.2 samples that are missing, *i.e.* no data was received for them, are indicated in orange. Additional data that was not part of the original DoE are shown in green and the Run number is indicated with an "AD". The missing and additional data are mainly due to a miscommunication and lack of experience working with DoEs.

It must be emphasised that missing data points do not eliminate or reduce the effectiveness of the DoE for estimating the variable effects most precisely. This is clearly illustrated in the discussions of the results that follow. The reason is that the full experimental space in all the design factors is still covered within the amended experimental design program.

5.4.3 Tensile Sample Mould Design

A limitation during tensile testing is the tensile test sample mould type. Due to the equipment restrictions we can only manufacture 100 × 100 plaques for the compression moulded samples which would yield an ISO 1BA tensile sample size (DIN EN ISO 527-2, 2012). For injection moulding TUT only has an ISO 1A tensile sample mould available. The compression and injection moulded samples will therefore be two different tensile sample mould sizes. The influence of this change in size on the mechanical properties needs to be investigated.

For this investigation I considered a quadratic response surface model with 2 replication points, 3 lack of fit points and 8 center points to account for experimental error and repeatibility. The resulting design is summarised in Table 5.3 with additional data, that was not part of the original design, shown in green and the Run number indicated with an "AD". For this design we considered clay type, clay loading and the tensile mould type. All samples will be injection moulded at the IPF as they have both moulds available, and will be tested using a single strain rate. A neat sample is tested for all individual cases as the control sample.

Table 5.3: D-optimal experimental design for tensile testing of ISO 1A and ISO 1BA sample moulds. (Green - additional data points not in original design)

Run	Clay Loading (wt%)	Clay Type	Tensile Mould Type
1	6	DHT4-A	ISO 1A
2	6	Alcamizer 1	ISO 1BA
3	6	Alcamizer 1	ISO 1A
4	2	Alcamizer 1	ISO 1A
5	4	Alcamizer 1	ISO 1BA
6	10	Alcamizer 1	ISO 1A
7	8	DHT4-A	ISO 1BA
8	8	DHT4-A	ISO 1A
9	2	Alcamizer 1	ISO 1BA
10	2	Alcamizer 1	ISO 1A
11	2	DHT4-A	ISO 1BA
12	10	DHT4-A	ISO 1A
13	10	Alcamizer 1	ISO 1A
14	2	DHT4-A	ISO 1A
15	6	DHT4-A	ISO 1BA
16	10	DHT4-A	ISO 1BA
17	10	Alcamizer 1	ISO 1BA
Additional Data (AD) — not in original design			
AD	4	Alcamizer 1	ISO 1A
AD	2.8	DHT4A	ISO 1A
AD	2.8	DHT4A	ISO 1BA
AD	2.8	DHT4A	ISO 1BA
AD	6	Alcamizer 1	ISO 1BA
AD	6	Alcamizer 1	ISO 1A

5.4.4 Impact Testing Design

Similar to the other designs, I considered a quadratic response surface model with 2 replication points, 3 lack of fit points and 4 center points for the impact testing design. The additional points account for experimental error and repeatibility. The resulting design is summarised in Table 5.4 where all design factors, except for strain rate, are considered. Samples that are missing, *i.e.* no data was received for them, are indicated in orange. Similarly, additional data that was not part of the original design are shown in green and the Run number is indicated with an "AD".

5.4.5 Design Evaluation

As discussed in Chapter 4, it is important to evaluate the designs to determine if they are good designs for the intended purpose. As shown in the case studies the generated designs are evaluated against a global D-optimal design. As a quadratic response surface model was considered for all three designs, the global D-optimal design will therefore be a full factorial 3^k, where k is the total number of continuous and categorical factors. The designs are evaluated in terms of their D-efficiency and G-efficiency against the global D-optimal design. The results for the original developed designs and the amended designs are shown in Table 5.5. Note for the tensile testing design an amended global D-optimal design without the strain rate factor is completed otherwise the D-efficiency would be calculated inaccurately due to the mismatch of the number of factors.

Table 5.4: D-optimal experimental design for Charpy impact tests. (Orange - missing data points, Green - additional data points not in original design)

Run	Clay Loading (wt%)	Clay Type	Moulding Method	Site
1	2	Alcamizer 1	Compression	UP
2	2	DHT4-A	Injection	TUT
3	2	DHT4-A	Compression	UP
4	6	DHT4-A	Injection	TUT
5	6	Alcamizer 1	Injection	TUT
6	6	DHT4-A	Compression	IPF
7	6	Alcamizer 1	Compression	UP
8	2	Alcamizer 1	Injection	IPF
9	6	Alcamizer 1	Compression	IPF
10	10	DHT4-A	Compression	IPF
11	2	Alcamizer 1	Compression	IPF
12	2	DHT4-A	Injection	IPF
13	10	Alcamizer 1	Compression	IPF
14	2	Alcamizer 1	Injection	TUT
15	10	DHT4-A	Compression	UP
16	6	DHT4-A	Injection	IPF
17	10	Alcamizer 1	Injection	TUT
18	6	DHT4-A	Compression	UP
19	10	DHT4-A	Injection	TUT
20	10	Alcamizer 1	Injection	IPF
21	6	Alcamizer 1	Injection	IPF
22	10	Alcamizer 1	Compression	UP
23	10	DHT4-A	Injection	TUT
24	2	DHT4-A	Compression	IPF
25	10	Alcamizer 1	Injection	IPF
Additional Data (AD) — not in original design				
AD	3.59	Alcamizer	Injection	TUT
AD	4	Alcamizer	Injection	IPF
AD	2.8	DHT4A	Injection	IPF
AD	8	DHT4A	Injection	IPF
AD	10	DHT4A	Injection	IPF
AD	2.8	DHT4A	Compression	UP
AD	10	Alcamizer	Injection	TUT

Table 5.5: Evaluation of the generated optimal designs for the thesis experimental study.

Design	Type	Nr. Experiments	D-efficiency	G-efficiency
Global D-optimal	D-optimal	72	100	100
Tensile Testing	D-optimal	36	81.16	60.37
Amended Global D-optimal	D-optimal	72	100	92.83
Amended Design	D-optimal	37	84.12	53.97
Global D-optimal	D-optimal	12	100	100
Tensile Sample Mould Evaluation	D-optimal	17	91.50	66.18
Amended Design	D-optimal	23	86.91	55.65
Global D-optimal	D-optimal	72	100	92.83
Impact Testing	D-optimal	25	93.88	75.15
Amended Design	D-optimal	29	89.48	65.29

Both the original and amended tensile testing and impact testing designs require approximately half the number of experiments required for the global D-optimal designs. The original tensile sample mould design requires 5 more experiments than the global D-optimal design, with the amended design requiring about double the amount of runs.

For all the designs the relative D-efficiency is high indicating that the design would be able to efficiently estimate the regression coefficients for the quadratic response surface model. Even though the amended designs see a reduction in D-efficiency, mainly because of the increase in experiments required, it is still considered high being above 80 %.

The G-efficiency indicates that the designs will be adequate at minimising the prediction variance of the response variable. The reason for these lower G-efficiencies is the addition of multiple categorical factors. Again, the additional experiments required with the amended designs adds to the decrease in G-efficiency.

5.5 Mechanical Characterisation

The samples were characterised to obtain the tensile and impact properties. All samples were tested at the IPF, Germany, an internationally accredited polymer testing facility. All necessary calibrations and validations for the testing equipment were done according to the required ISO standards. Due to the material losses discussed in the previous section the number of repeated samples were reduced from 8 to 5.

Tensile properties were measured according to DIN EN ISO 527-2 (2012) for all prepared samples using a Zwick UPM-1456 universal tensile testing machine at a cross-head speed of 50 mm/min.

To calculate the Young's modulus a cross-head speed of 1 mm/min was used. To determine the remainder of the mechanical properties the strain rate was changed to 50 mm/min after the yield point. For each case investigated an average of 5 repeated samples were tested with an extensiometer. For the ISO Type 1A samples the maximum possible traverse movement was often reached. As a result, the elongation to failure and stress at failure could not be determined. To accommodate for this, at least one sample for each case was tested until the maximum traverse movement was reached and all remaining samples were tested to 100 % elongation unless it fractured first.

Charpy impact tests on notched rectangular bar samples were conducted according to DIN EN ISO 179-1 (2010) at a capacity of 0.5 J and impact speed of 2.9 m/s. For each case investigated an average of 5 repeated samples were tested.

5.5.1 Data Processing

The resulting stress-strain curves were already processed using the software of the universal tensile testing machine. The processed tensile curve data was received with the corresponding tensile properties. The maximum stress was reported, however in some instances this related to a stress higher than the first peak stress due to extreme ductility in the material. As a result, the first peak stress and corresponding elongation were extracted from the obtained stress-strain curves. The tensile properties that were provided, along with those extracted, are shown in Figure 5.5 for the ISO Type 1A and ISO Type 1BA moulds.

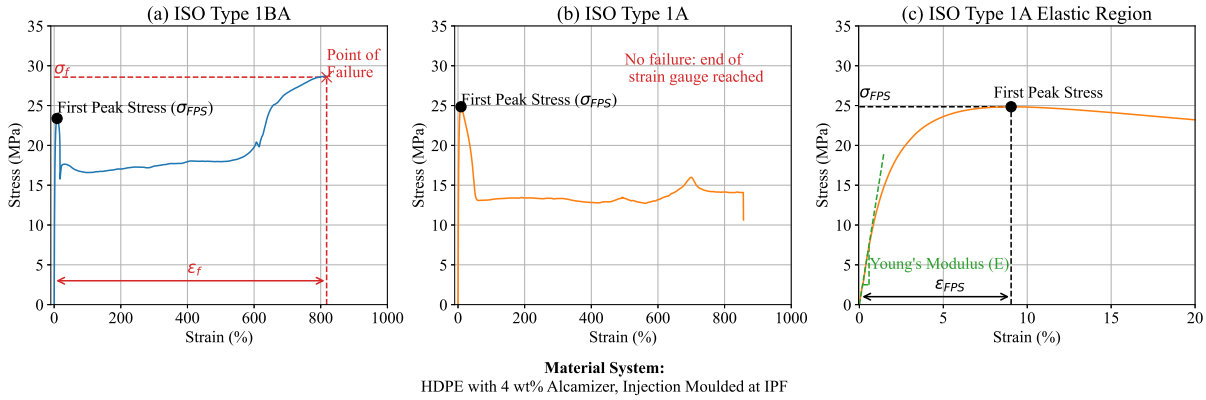

Figure 5.5: Tensile properties defined for the experimental study considering HDPE with 4 wt% Alcamizer 1 injection moulded at IPF as an example. Two cases are illustrated for the (a) ISO Type 1BA and (b) ISO Type 1A mould types, with (c) providing a closer look at the elastic region for the ISO Type 1A mould type.

Figure 5.5(a) represents a case where failure occurred for the ISO Type 1BA sample. The point of failure is denoted with an 'x' and the stress at failure is represented with σ_f and the elongation to failure with ϵ_f. Figure 5.5(b) represents a case where failure was not attained as the ISO Type 1A sample is not only too long for the strain gauges used, but also for the testing area in the universal tensile testing machine.

A zoomed in version of the curve in Figure 5.5(b) is presented in Figure 5.5(c) to view the elastic region. The first peak stress (FPS) is defined as the first peak on the curve where the gradient changes from positive to negative. In polymer composites this is known as the yield point where the material transitions from the elastic region to the plastic region (ASTM D638-14, 2014). It was decided to refer to this point as the FPS rather than the yield point as there were cases where yield was not attained and the value therefore not provided in the reports received. However, in these cases the tensile curve still showed a first peak which could be captured (c.f. Figure 5.6(a)). Young's modulus provides an indication of the material stiffness and is the gradient of the linear elastic region, indicated in green on Figure 5.5(c).

5.5.2 Tensile Properties of Interest

The full set of tensile curves are presented in Appendix A.5. For the purpose of determining the tensile properties of interest, a select few tensile curves are considered as part of the argument for or against a tensile property.

The Young's modulus was calculated using a strain gauge and a cross-head speed of 1 mm/min and can therefore be considered accurate.

In some cases it is not clear if yield was obtained as shown in Figure 5.6(a), for example, and therefore not reported. In addition, some samples tested at a later stage did not report yield at all even though it was reached. As mentioned earlier this point is referred to as the first

peak stress in this thesis as all tensile curves showed a first peak for which a value could be obtained.

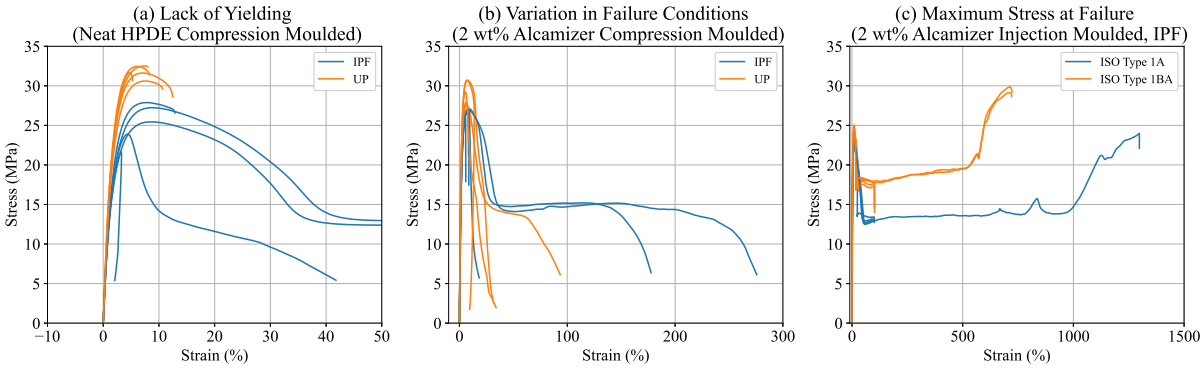

Figure 5.6: Tensile stress-strain curves indicating variation in reported results due to (a) lack of yielding (Neat HDPE - compression moulded), (b) variation in failure conditions (2 wt% Alcamizer - compression moulded) and (c) maximum stress at failure (2 wt% Alcamizer - injection moulded).

The stress at break is not a meaningful property to consider based on the large variation in failure types for the same conditions. An example of this phenomenon is shown in Figure 5.6(b) for HDPE with 2 wt% Alcamizer compression moulded. Even though all samples are compression moulded the stress at break is higher for some breaks and lower for others. In fact, the stress at break was found to be higher than the first peak stress for certain cases as shown in Figure 5.6(c). It should be mentioned that not all samples were tested to failure. Due to this, not all samples have a reported stress or elongation at failure, only those where failure was attained.

The elongation at failure, however, is still a meaningful measure which provides an indication of the material ductility. It is therefore still included even though it is not reported for all cases considered.

The response variables of interest for this study are therefore the Young's modulus, first peak stress, elongation at first peak stress and elongation of failure obtained via tensile testing; and the impact strength obtained from Charpy impact testing.

5.6 Statistical Analysis

Statistical analysis is a powerful tool that can be used to better understand the nuances in the data, determine which factors have any statistically significant effect and quantify these effects. The statistical analysis was conducted using Python's statistical modelling module, statsmodels (Perktold *et al.*, 2010). Some of the information in this section is briefly repeated from Chapter 2 for ease of reference.

5.6.1 Summary Statistics

The summary statistics provides an indication of the important statistical measures for each response variable. These include the mean, standard deviation (SD) and the standard error of the mean (SEM). The SD indicates the variation in the data from the mean, where a lower SD indicates that the data are grouped around the mean and a higher SD that data are spread out. The SEM indicates how far the sample mean of the data is from the true population mean. It will always be smaller than SD with a value close to 0 indicating the sample mean is accurate. The summary statistics therefore provides an indication of the uncertainty, or error limits, related to the obtained data.

5.6.2 Analysis of Variance (ANOVA)

Analysis of variance (ANOVA) is a statistical procedure commonly used to test the equality of several population means (Montgomery, 2013). An F-test compares the variability between two or more groups and is normally used to conduct the ANOVA. The F-value is defined as (Montgomery and Runger, 2007):

$$F = \frac{SS_{between}/Df_{between}}{SS_{within}/Df_{within}}, \tag{5.2}$$

where SS is the sum of squares which describes the total variability of the data from the mean for a specific variable group and Df is the degrees of freedom. The subscript *between* refers to the variability between groups and *within* refers to the variability within the groups. $SS_{between}$ must be greater than SS_{within} to yield significance, that is, a larger F-value is ideal for significance. The probability that a statistically significant effect of a variable on the response is only by chance is indicated by the p-value. The p-value is the probability that the calculated F-value follows the F-distribution under the null hypothesis, which is that the means are equal. Therefore, a p-value smaller than 0.05 indicates a statistically significant effect on the response, with a smaller p-value indicating less probaility that the results are due to chance.

For an ANOVA F-test several assumptions are made, such as a constant variance between the groups and whether the residuals are normally distributed approximately *i.e.*, the data originated from simple random sampling (Montgomery, 2013). It is therefore good practice to perform diagnostics to test these assumptions. The diagnostics are a visual representation of the residuals against the number of observations for the constant variance assumption; residuals against the predicted response variable for the simple random sampling assumption; and a probability plot of the residuals for the assumption of normal distribution.

To quantify the strength of the relationship between the group and response variables, a descriptive statistics variable referred to as ω^2 can be used (Salkind, 2010). ω^2 is defined as a proportion of variation in the response variable that is associated with the group (Salkind,

2010; Olejnik and Algina, 2000). Between-subject analysis ω^2 is calculated as (Olejnik and Algina, 2000):

$$\omega^2 = \frac{(SS_{between} - Df_{between} \times MS_{error})}{SS_{total} + MS_{error}}, \tag{5.3}$$

where $SS_{between}$ is the sum-of-squares between groups, $Df_{between}$ the degrees of freedom between the groups, MS_{error} the mean square error and SS_{total} the total sum-of-squares. These values are easily obtained from the ANOVA table. ω^2 has a value between 0 and 1, where 0 indicates that there is no relationship and 1 indicates that the factor explains the variation in the response variable completely (Salkind, 2010).

5.6.3 Linear Regression and Prediction Model

To determine whether there are any statistically significant differences between the different levels for each factor a linear regression model is considered. This is done by developing a model as a function of the factors using the least squares method. From Section 4.2.1 (Equation 4.4), a linear model with both continuous (k) and categorical (r) variables is defined as:

$$y = \beta_0 + \sum_{i=1}^{k} \beta_i x_i + \sum_{i=1}^{r} \sum_{l=1}^{n-1} \beta_{il} z_{il}. \tag{5.4}$$

The response variable of interest is denoted by y. The intercept is represented by β_0 which includes the first level for variables where a variable consists of more than one level. β_i and β_{il} denote the regression coefficients, x_i the continous variables and z_{il} the dummy categorical variables for each level. The dummy categorical variable is set equal to 1 if the level of the categorical variable is active, and 0 if it is not active.

The ability of a linear regression model to provide a good fit is represented by the R^2 value. R^2 is indicative of the proportion of the total variability in the response variable explained by the model. When the R^2 value is closer to 1 the model provides a good predictability as it would fit the observed data well. When the number of terms in the linear regression model is adjusted, an adjusted R^2 value is considered. As the number of unnecessary terms in the model is increased, the adjusted R^2 value decreases.

As part of the discussion the fitted linear models for the different response variables (or mechanical properties) will be used to predict the response as a function of clay loading. The predicted response, or fitted regression line, is considered for interpretation purposes within the developed statistical design of experiments (DoE) framework. To this end, I will present an example here of how to derive the fitted linear model to predict the desired mechanical properties. For this example I will derive the fitted linear model for the Young's modulus in the tensile testing DoE. In the tensile testing DoE we consider both continuous (*i.e.* clay loading) and categorical (*i.e.* clay type, moulding method and site) variables. Therefore for three categorical variables and one continuous variable the above equation, for a predicted

linear model, will take the following form:

$$\hat{y} = \hat{\beta}_0 + \hat{\beta}_1 x_1 + \hat{\beta}_{11} z_{11} + \hat{\beta}_{12} z_{12} + \hat{\beta}_{21} z_{21} + \hat{\beta}_{31} z_{31} + \hat{\beta}_{32} z_{32}, \tag{5.5}$$

where $\hat{y}$ is the predicted response variable, $\hat{\beta}_0$, $\hat{\beta}_i$ and $\hat{\beta}_{il}$ are the estimated regression coefficients, x_1 denotes the continuous variable clay loading, z_{11} and z_{12} are dummy variables indicating the second and third levels of the clay type, z_{21} is a dummy variable for the second level of the moulding method, and z_{31} and z_{32} the second and third level for the site. The dummy variable is set equal to either 1 or 0 depending on which level of the categorical variable is active. The estimated linear regression coefficient values are obtained from the fitted linear regression model as provided in the Estimate column of Table 5.6. For the fitted linear regression model a t-statistic is used to determine the p-value by determining the difference between the means of two groups. The t-value is therefore determined from (Montgomery and Runger, 2007):

$$t = \frac{\hat{\beta}_i - \beta_i}{SE(\hat{\beta}_i)}, \tag{5.6}$$

where $\beta_i = 0$ under the null hypothesis and the numerator just becomes the estimated regression coefficient $\hat{\beta}_i$. SE is the standard error represented by Std. Error in Table 5.6. For this model the p-value is the probability to obtain a t-distribution value which is greater than the calculated t-value, and is therefore represented as Pr(>|t|) in Table 5.6.

Table 5.6: Tensile testing DoE linear model for Young's modulus.

Nr. Observations	40	R-squared		0.903	
Df Residuals	33	Adjusted R-squared		0.886	
Df Model	6	F-statistic		51.42	
		Residual Standard Error		0.003	
	Estimate	Std. Error	t-value	Pr(> |t|)	
Intercept	0.1513	0.001	105.563	0.000	***
ClayType[T.DHT4A]	0.0009	0.001	0.858	0.397	
ClayType[T.Neat]	-0.0005	0.002	-0.284	0.778	
MouldingMethod[T.Injection]	0.0165	0.001	12.822	0.000	***
Site[T.TUT]	$-8.582e^{-05}$	0.001	-0.057	0.955	
Site[T.UP]	-0.0001	0.001	-0.109	0.914	
ClayLoading	-0.0005	0.000	-2.855	0.007	**

Significance Codes: '***': 0-0.001, '**': 0.001-0.01, '*': 0.01-0.05, '.':0.05-0.1, ' ': 0.1-1.0

An overview of all the variables related to Equation 5.5 with the estimated regression coefficients in Table 5.6 is summarised in Table 5.7 for ease of reference. The response variable of interest for this example is the Young's modulus for the tensile testing DoE.

Next the predicted Young's modulus is determined from Equation 5.5 using the information in Table 5.7 for specific conditions. For example, given that:

Condition 1: The clay type is Alcamizer 1 with tensile sample moulds compression moulded

Table 5.7: Overview of Young's modulus predictive response equation variables. (n denotes the level and $\hat{\beta}_0$ captures the estimated coefficient for the first level of each categorical variable.)

Variable	Variable Type	Description	Value
$\hat{\beta}_0$	Estimated Regression Coefficient	Intercept	0.1513
x_1	Continuous	Clay Loading	0-10 wt%
$\hat{\beta}_1$	Estimated Regression Coefficient	Clay Loading	-0.0005
$\hat{\beta}_{1n}$	Estimated Regression Coefficient	Clay Type	$\begin{cases} 0.0009 & \text{if } n = 1 \text{ (DHT4-A)}, \\ -0.0005 & \text{if } n = 2 \text{ (Neat)}, \\ 0 & \text{if otherwise.} \end{cases}$
z_{1n}	Categorical Dummy Variable	Clay Type	$\begin{cases} 1 & \text{if } n = 1 \text{ (DHT4-A) or } n = 2 \text{ (Neat)}, \\ 0 & \text{if otherwise (Alcamizer 1).} \end{cases}$
$\hat{\beta}_{2n}$	Estimated Regression Coefficient	Moulding Method	$\begin{cases} 0.0165 & \text{if } n = 1 \text{ (Injection)}, \\ 0 & \text{if otherwise.} \end{cases}$
z_{1n}	Categorical Dummy Variable	Moulding Method	$\begin{cases} 1 & \text{if } n = 1 \text{ (Injection)}, \\ 0 & \text{if } n \neq 1 \text{ (Compression).} \end{cases}$
$\hat{\beta}_{3n}$	Estimated Regression Coefficient	Location	$\begin{cases} -8.582\text{e}\hat{}\text{-}05 & \text{if } n = 1 \text{ (TUT)}, \\ -0.0001 & \text{if } n = 2 \text{ (UP)}, \\ 0 & \text{if otherwise.} \end{cases}$
z_{1n}	Categorical Dummy Variable	Location	$\begin{cases} 1 & \text{if } n = 1 \text{ (TUT) or } n = 2 \text{ (UP)}, \\ 0 & \text{if otherwise (IPF).} \end{cases}$

at IPF.

Clay Type	Moulding Method	Site
Alcamizer 1	Compression	IPF
$n = 0$	$n = 0$	$n = 0$
$\hat{\beta}_{10} = 0$	$\hat{\beta}_{20} = 0$	$\hat{\beta}_{30} = 0$
$z_{11} = z_{12} = 0$	$z_{21} = 0$	$z_{31} = z_{32} = 0$

The above is substituted into Equation 5.5 which then reduces it to:

$$\hat{y} = \hat{\beta}_0 + \hat{\beta}_1 x_1, \tag{5.7}$$

$$= 0.1513 - 0.0005 x_1. \tag{5.8}$$

Condition 2: The clay type is changed to DHT4-A while the remaining variables are the same as for condition 1.

Clay Type	Moulding Method	Site
DHT4-A	Compression	IPF
$n = 1$	$n = 0$	$n = 0$
$\hat{\beta}_{11} = 0.0009$	$\hat{\beta}_{20} = 0$	$\hat{\beta}_{30} = 0$
$z_{11} = 1$, $z_{12} = 0$	$z_{21} = 0$	$z_{31} = z_{32} = 0$

Substituting the above into Equation 5.5 results in:

$$\hat{y} = \hat{\beta}_0 + \hat{\beta}_1 x_1 + \hat{\beta}_{11} z_{11}, \tag{5.9}$$
$$= 0.1513 - 0.0005x_1 + 0.0009, \tag{5.10}$$
$$= 0.1522 - 0.0005x_1. \tag{5.11}$$

$\hat{\beta}_{11}$ is the estimated difference between DHT4-A and Alcamizer 1 for compression moulding at IPF. The addition of $\hat{\beta}_{11}$ therefore changes the initial intercept for DHT4-A from 0.1513 to 0.1522.

Condition 3: The moulding method is changed to injection moulding while the remaining variables remain the same as for condition 1.

Clay Type	Moulding Method	Site
Alcamizer 1	Injection	IPF
$n = 0$	$n = 1$	$n = 0$
$\hat{\beta}_{10} = 0$	$\hat{\beta}_{21} = 0.0165$	$\hat{\beta}_{30} = 0$
$z_{11} = z_{12} = 0$	$z_{21} = 1$	$z_{31} = z_{32} = 0$

Substituting the above into Equation 5.5 results in:

$$\hat{y} = \hat{\beta}_0 + \hat{\beta}_1 x_1 + \hat{\beta}_{21} z_{21}, \tag{5.12}$$
$$= 0.1513 - 0.0005x_1 + 0.0165, \tag{5.13}$$
$$= 0.1678 - 0.0005x_1. \tag{5.14}$$

$\hat{\beta}_{21}$ is the estimated difference between injection and compression moulding for Alcamizer 1 at IPF. The addition of $\hat{\beta}_{21}$ therefore changes the initial intercept for injection moulding from 0.1513 to 0.1678.

Condition 4: The site is changed to UP while the remaining variables remain the same as for condition 1.

Clay Type	Moulding Method	Site
Alcamizer 1	Compression	UP
$n = 0$	$n = 0$	$n = 2$
$\hat{\beta}_{10} = 0$	$\hat{\beta}_{20} = 0$	$\hat{\beta}_{31} = -0.0001$
$z_{11} = z_{12} = 0$	$z_{21} = 0$	$z_{31} = 1$

The above is substituted into Equation 5.5 which then reduces it to:

$$\hat{y} = \hat{\beta}_0 + \hat{\beta}_1 x_1 + \hat{\beta}_{31} z_{31}, \tag{5.15}$$
$$= 0.1513 - 0.0005x_1 - 0.0001, \tag{5.16}$$
$$= 0.1512 - 0.0005x_1. \tag{5.17}$$

$\hat{\beta}_{31}$ is the estimated difference between compression moulding at UP and IPF for Alcamizer 1. The addition of $\hat{\beta}_{31}$ therefore changes the initial intercept for the site (*i.e.*, UP) from 0.1513 to 0.1512.

Other iterations for the different variables will result in similar observations considering a linear equation as a function of clay loading with the intercept changed due to the conditions of interest.

This predicted response variable ($\hat{y}$) can be represented by the following generalised equation (Montgomery, 2013):

$$\hat{y}(\mathbf{x_o}) = \mathbf{x_o'}\hat{\boldsymbol{\beta}}, \tag{5.18}$$

where $\mathbf{x_o}$ is a vector of the different points for the factors in the model expanded for all terms in the model. $\mathbf{x_o'}$ is the transpose of the $\mathbf{x_o}$ vector and $\hat{\boldsymbol{\beta}}$ contains the linear regression coefficients for all factor combinations and is expressed as (Montgomery, 2013):

$$\hat{\boldsymbol{\beta}} = (\mathbf{X'X})^{-1}\mathbf{X'y}, \tag{5.19}$$

where $\mathbf{X}$ is the model matrix populated with the different combinations of factors and levels and has columns expanded for all the terms in the linear response surface model. $\mathbf{X'}$ is the transpose of the design matrix and $\mathbf{y}$ contains the observations of the response variable.

5.7 Conclusion

This chapter discussed the experimental methodology that was followed to successfully manufacture and test samples to produce results based on a statistical design of experiments.

A composite consisting of a high-density polyethylene (HPDE) matrix filled with layered double hydroxides (LDH) particulates was considered. The composite was compounded using twin-screw extrusion and processed by means of compression and injection moulding. The processed samples were then characterised with tensile and impact testing according to the relevant ISO standards.

For the experimental designs a D-optimal design was chosen for all three experiments considered: tensile testing, impact testing and evaluation of the two ISO sample mould types. This design was chosen as it provides a good design with acceptable efficiencies. It was decided to include lack of fit, replication and center points in all the designs to ensure we evaluate all aspects. That is, evaluating the model's prediction ability, testing specific combinations of factors and levels and estimating experimental error. Based on the evaluation these designs are adequate and will be able to provide statistically significant observations from the experimental results.

This chapter shows that even when you have a good design, one of the complexities of a large experimental study involving multiple operators is the potential for misinterpretation of

the experimental design. This was experienced during this study where additional data was received that were not part of the initial DoEs. On the other hand, there are missing data which were part of the initial DoEs. Additional work was therefore done unnecessarily due to a lack of explicit communication. Despite the additional and missing data, the DoEs are still effective in estimating the variable effects most precisely, as well as predicting response variables. This is because the full experimental space in all the design factors is still covered within the amended experimental design program. This type of experimental design is obviously still not fully understood within the polymer composite community.

Experimental results will be analysed by means of statistical techniques such as linear regression and analysis of variance (ANOVA). The linear regression line is the best average fit through all the data points, and is used to predict the response for any combination of the factors and levels included in the model. To this end, an example of the linear prediction model for the Young's modulus was provided.

CHAPTER 6

EXPERIMENTAL RESULTS AND DISCUSSION

This chapter presents and discusses the results obtained by following the experimental methodology outline in the previous chapter. This includes the tensile curves, statistical analysis and discussion of key observations which emanated from the results.

6.1 Introduction

The systematic literature review indicated that injection moulded samples have a higher Young's modulus, first peak stress and elongation at break compared to compression moulded samples. Even though this was for high-density polyethylene (HDPE)/montmorillonite (MMT) composites these results can be extrapolated to HDPE/layered double hydroxide (LDH) as LDH is the synthetic equivalent to MMT.

The novel contribution of this thesis, which will be shown in this chapter, is the effect that machine variation (*i.e.*, different sites) and tensile sample mould type have on the mechanical properties. Both of these have not been reported in literature as yet. We would expect that different machines would not have an influence on the properties for the same process with identical moulding conditions. Similarly, the tensile stress and strain results are normalised to the tensile sample geometry and are therefore not expected to have any influence.

In this chapter I will begin by showing all the tensile curves in Section 6.2 and discussing the observable variability. Using statistical analysis methods I will quantify the effect of the design parameters on the response variables of interest in Section 6.3. I will conclude this chapter by discussing the key observations from the data in Section 6.4.

6.2 Tensile Curves

The full set of tensile curves are presented in Figure 6.1. It is most notable that there is a significant increase in stress in the ductile region for the last 100-200 % elongation, especially

for the injection moulded samples. This is the typical stress-strain behaviour expected of soft thermoplastics, such as HDPE. The compression moulded samples did not exhibit this increase in stress with an increase in elongation, but rather a behaviour similar to hard thermoplastics. This indicates that the compression moulding process affects the material ductility significantly more than the injection moulding process. This is likely due to the inconsistent heating process which affects the fusion of two particles creating weaker polymer pellet boundaries (Raghavan and Wool, 1999; Wool *et al.*, 1989; Wu *et al.*, 2002). This could lead to the harder more brittle behaviour observed in the tensile curves for the compression moulded samples.

There are observable differences between the two different sample mould types. ISO Type 1BA has a higher maximum tensile strength at break than ISO Type 1A. ISO Type 1BA elongation to failure is about half the elongation to failure experienced by ISO Type 1A. The tensile strength at break is higher for ISO Type 1BA than ISO Type 1A. These observed differences in mechanical properties between the two sample mould types are unexpected as the data is normalised to the sample geometry.

From these tensile curves it is clear that the elongation at break and consequently the tensile strength at break are sensitive to the moulding method and the sample mould type. There are no easily observable differences for the effect of site, clay type or clay loading. These will be considered by viewing the tensile curves up to an elongation of 50 % to provide more visibility of the elastic region, shown in Figure 6.2. Compression moulded samples are more stiff with a higher linear gradient than injection moulded samples, while having a higher first peak strength. This is contradictory to what was concluded from the systematic literature review where injection moulded samples tend to have a higher stiffness and strength. This is attributed to the changes in composite morphology and clay-polymer interfacial adhesion based on the type of clay and moulding method. In the systematic literature review montmorillonite (MMT), a natural clay, was considered whereas this experimental study considered LDH, a synthetic alternative to MMT. There are differences in the chemical composition of the two clays which could affect the material stiffness and strength. Another factor which affects the composite morphology is the moulding method, where injection moulding tends to consistently heat the material while compression moulding suffers from an inconsistent heating distribution. This can lead to defects such as incomplete fusion of inter-polymer pellet boundaries, which affects the elongation at break, as already noted from Figure 6.1.

There is a potential effect on the mechanical properties due to site where compression moulded samples from UP tend to have a higher first peak stress value and are more brittle than those from IPF. Similarly, for the injection moulded samples those from TUT have a higher FPS than IPF, with both sites producing more ductile samples. For the different sample mould types ISO Type 1BA has a higher FPS although it appears that the stiffness *i.e.*, linear region of the curve is very similar. After investigating the elastic region of the tensile curves we can observe an influence on the mechanical properties due to moulding method, site and sample mould type. The material stiffness and tensile strength are most sensitive to the moulding method and to a lesser degree the site and sample mould type as well. The influence of clay

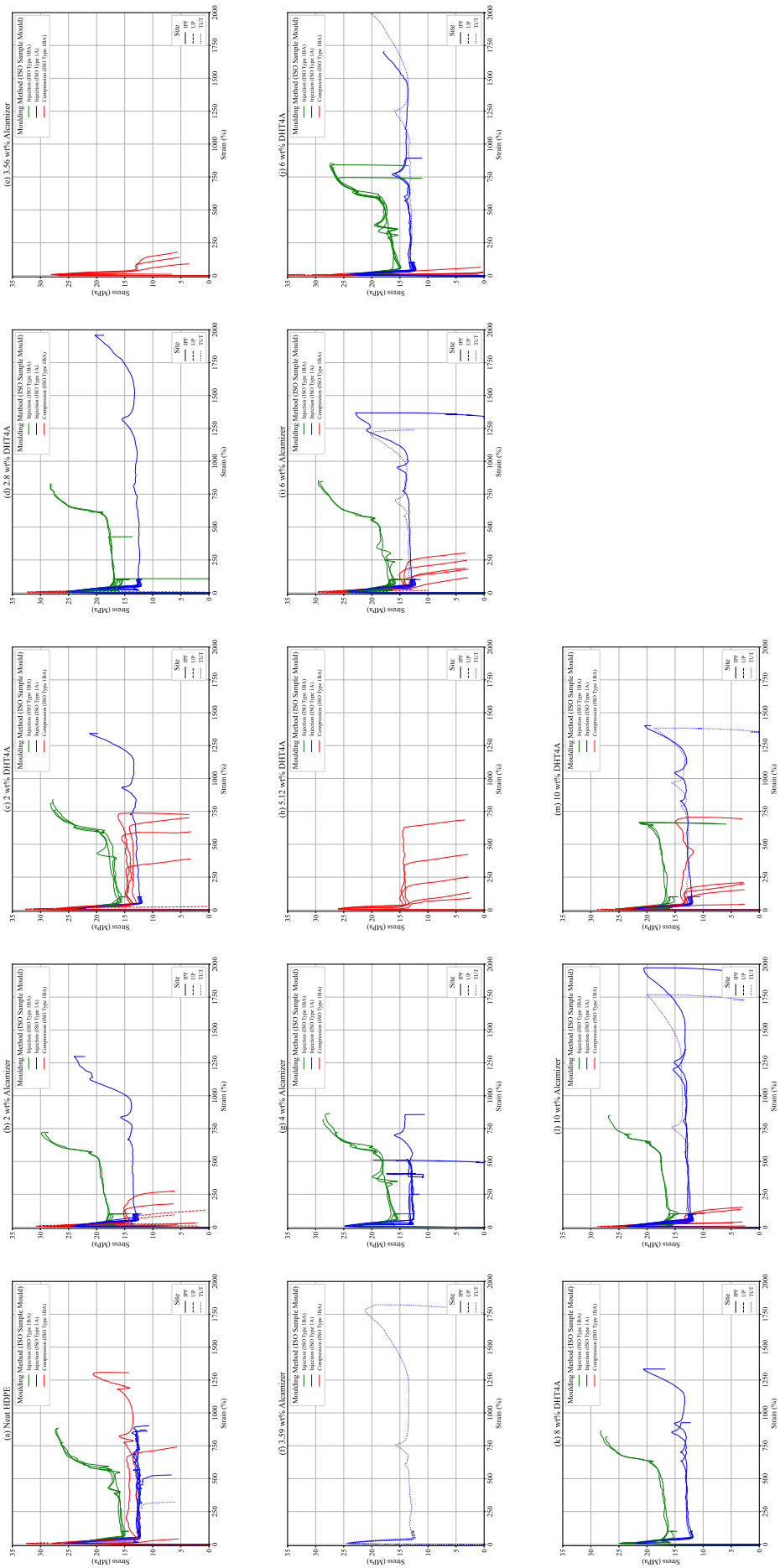

Figure 6.1: Tensile stress-strain curves for HDPE/LDH composites for two different LDH types (Alcamizer 1 and DHT-4A) and different LDH loadings according to the statistical experimental design.

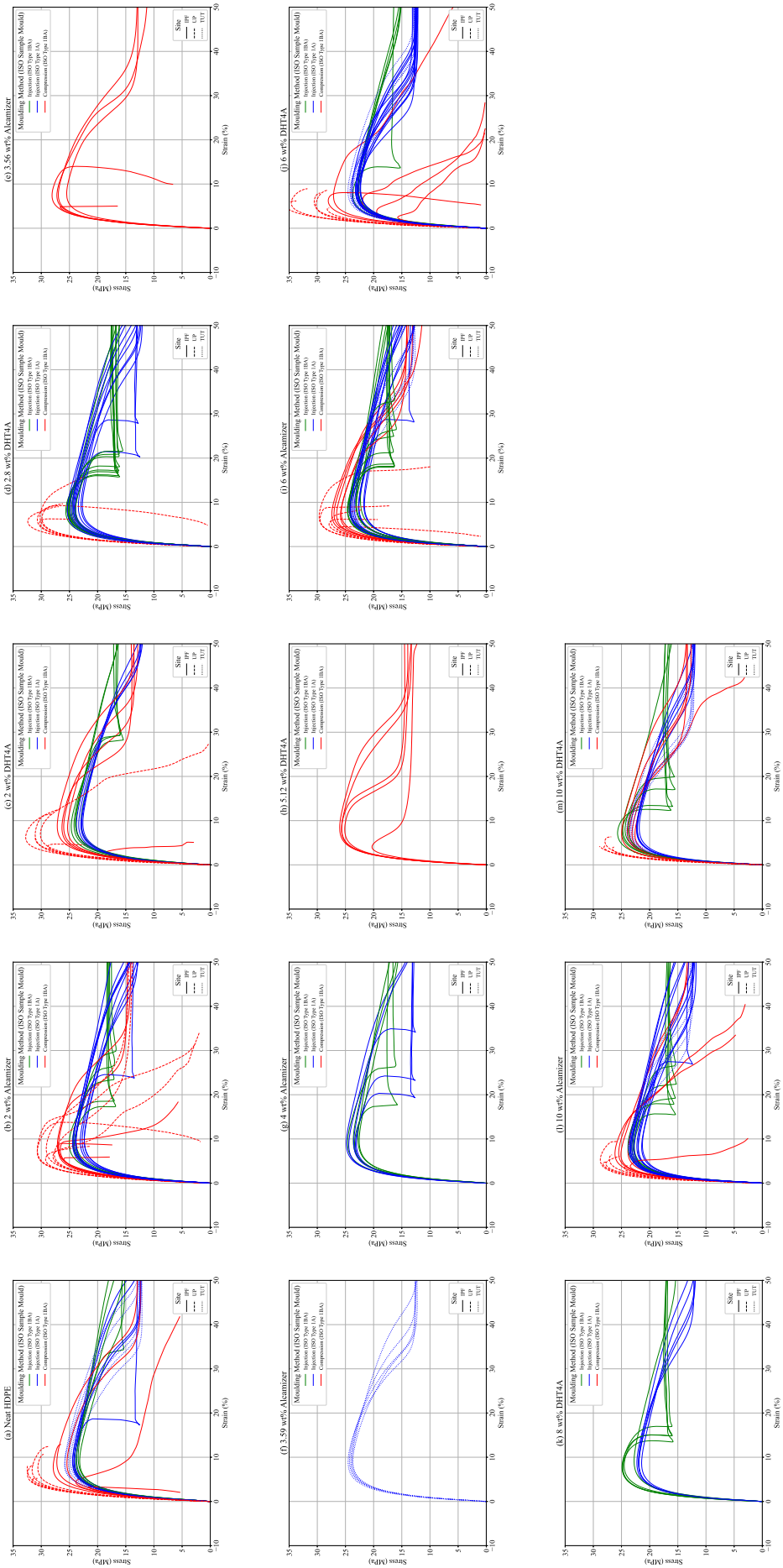

Figure 6.2: Tensile stress-strain curves for HDPE/LDH composites up to an elongation of 50 %.

type and clay loading is not immediately obvious as it appears to have little influence. These influences will be quantified using statistical analysis in Section 6.3.

A very interesting observation in the injection moulded tensile curves is the presence of an artifact, a pronounced step in the response just after yielding occurs. This occurred exclusively in the samples produced at IPF and primarily in the ISO Type 1BA, with a few of the ISO Type 1A samples also exhibiting this behaviour. This artifact effect is illustrated in Figure 6.3 with 4 wt% Alcamizer as an example. This artifact is not something that has been observed in past tensile curves or those presented in literature for polymer-clay composites. As it was not observed for the injection moulded samples manufactured at TUT, this artifact is due to something that exclusively occurs during the injection moulding process at IPF. This could denote a snap-through behaviour or buckling response where the sample cannot bend back into strain *i.e.*, no negative strain values are reported in displacement controlled tensile testing. This behaviour could potentially be due to a thin skin which forms during injection moulding of the samples.

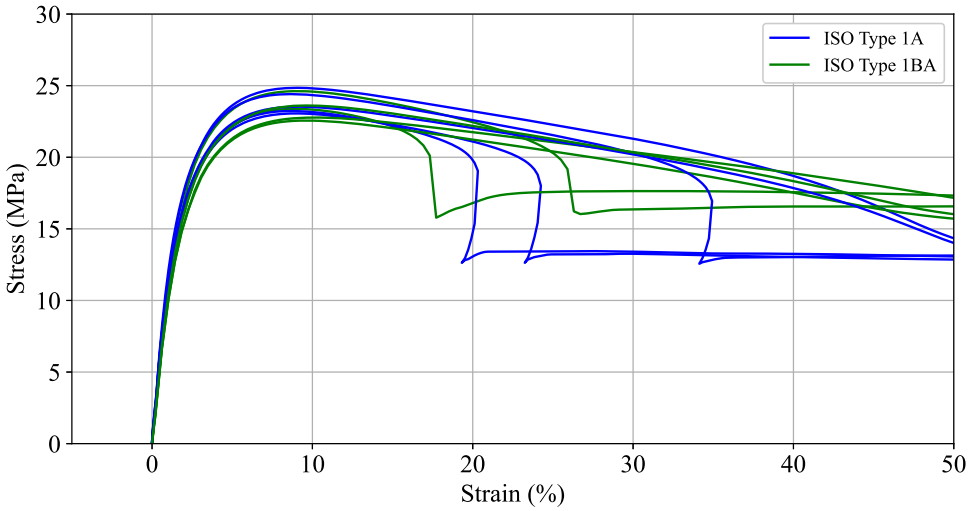

Figure 6.3: Tensile stress-strain curves for 4 wt% Alcamizer injection moulded at IPF for both ISO sample mould types.

6.3 Statistical Analysis

The summary statistics for the mechanical properties of interest are presented for each of the developed statistical design of experiments (DoEs). This is followed by the required diagnostics to verify the assumptions for the analysis of variance (ANOVA). The statistical significance of the different design factors are then discussed in terms of the p-value. Finally, the strength of the relationships are quantified through the ω^2 value to determine which significant factors contribute more to the mechanical properties of interest.

6.3.1 Summary Statistics

The summary statistics for all the mechanical properties of interest are presented here for each of the developed DoEs. The summary statistics include the mean, standard deviation (SD) and the standard error of the mean (SEM), thereby providing a measure of the uncertainty, or error limits, in the data. To study the repeatability of the different DoE's additional points were allocated to the design which replicated certain design points. Ideally, for the design repeatability to be validated the variation within each replicate point should be close together while comparing well with the other replicated points. Replicate points in the designs are indicated in red.

Tensile Testing DoE

The summary statistics for the tensile testing DoE are provided in Table 6.1. The number of observations for the tensile testing DoE's is equal with the majority of cases having 5 observations, with the exception of 2 wt% Alcamizer (compression moulded at UP) with 6 observations, 6 wt% Alcamizer (injection moulded at TUT) with 7 observations and 6 wt% DHT4-A (injection moulded at IPF) with 12 observations. In cases where the majority of cases have an equal number of observations it is said that the design is well balanced.

The mean ranges between 946.96 and 1792.92 MPa for the Young's modulus, 21.81 and 31.86 MPa for FPS, 4.06 and 9.47 % for elongation at FPS, and 4.46 and 1701.68 % for elongation at break.

The SEM is small compared to the mean of the FPS (0.3 - 10.3 % of the mean) and the elongation at FPS (0.5 - 17.6 % of the mean). For Young's modulus the SEM is small when compared to the mean ranging between 0.8 and 6.6 % of the mean value. It is therefore possible to quantify the statistically significant effects of the Young's modulus, FPS and elongation at FPS. For the elongation at break there is a large variation in the SEM ranging between 0 and 62 % of the mean value. This is too large a variation indicating that it will not be possible to quantify statistically significant effects for the elongation at break. Even though the elongation to failure cannot be quantified I will still include it in the statistical analysis and discussion for the sake of completeness.

The SD for FPS ranges between 0.6 and 23% of the mean. Similarly, the SD for elongation at FPS ranges between 1.4 to 39.4 % when compared to the mean. The SD for Young's modulus ranges from 1.8 to 14.7 % of the mean. For all three response variables the variation in SD is small enough indicating that the mean is reliable providing a good measure of the average response. For the elongation at break samples tended to break at different instances within the same sample group where SD ranges from 24.5 to 139.2 % of the mean. This variation is too large and the mean is therefore not reliable.

The repeatability of the design is determined by the replicate points which are shown in Figure 6.4. The error between the means of the two replicate points are shown in the figure.

Table 6.1: Summary statistics of the tensile responses for the different combinations of experimental variables in the tensile testing DoE, where SD is the standard deviation and SEM is the standard error of the mean. Replicate points are indicated in red.

Clay Loading	Clay Type	Moulding Method	Site	Nr. of Observations	Young's Modulus (MPa)			First Peak Stress (FPS) (MPa)			Elongation at FPS (%)			Elongation at Break (%)		
					Mean	SD	SEM	Mean	SD	SEM	Mean	SD	SEM	Mean	SD	SEM
0	Neat	Compression	IPF	5	1570.55	78.24	34.99	25.22	2.54	1.14	6.54	2.58	1.15	420.63	585.41	261.80
0	Neat	Compression	UP	5	1535.46	146.87	65.68	31.78	0.77	0.35	6.60	1.20	0.54	8.93	2.76	1.23
0	Neat	Injection	IPF	5	970.51	78.90	35.28	24.26	0.16	0.07	9.17	0.22	0.10	745.29	183.17	81.92
0	Neat	Injection	TUT	5	984.81	57.13	25.55	25.10	0.87	0.39	9.03	0.47	0.21	5.93		
2	Alcamizer	Compression	IPF	5	1630.86	158.99	71.10	26.74	0.46	0.20	7.47	1.24	0.55	97.26	123.23	55.11
2	Alcamizer	Compression	UP	6	1371.76	94.46	38.56	29.23	1.30	0.53	6.69	0.89	0.36	51.41	50.07	20.44
2	Alcamizer	Injection	IPF	5	946.96	56.45	25.25	22.88	0.63	0.28	9.47	0.17	0.08			
2	Alcamizer	Injection	IPF	5	1055.58	27.59	12.34	24.07	0.26	0.11	9.19	0.25	0.11			
2	DHT4A	Compression	IPF	5	1520.70	105.81	47.32	24.70	3.45	1.54	7.35	2.57	1.15	482.96	298.53	133.51
2	DHT4A	Compression	UP	5	1581.99	179.75	80.39	30.77	1.45	0.65	6.02	1.11	0.50	12.40	9.01	4.03
2	DHT4A	Injection	IPF	5	965.46	30.55	13.66	23.11	0.46	0.20	9.12	0.16	0.07			
2.8	DHT4A	Compression	UP	5	1551.85	107.60	48.12	30.69	0.99	0.44	6.07	0.55	0.24	9.05	4.26	1.90
2.8	DHT4A	Compression	UP	5	1488.70	121.53	54.35	30.22	1.08	0.48	6.11	0.66	0.29	13.09	9.12	4.08
2.8	DHT4A	Injection	IPF	5	999.92	46.11	20.62	23.39	0.57	0.25	8.98	0.38	0.17			
2.8	DHT4A	Injection	IPF	5	1154.37	124.89	55.85	24.63	0.49	0.22	8.57	0.25	0.11			
3.56	Alcamizer	Compression	IPF	5	1556.15	96.38	43.10	26.89	0.95	0.42	7.02	1.26	0.56	84.36	77.01	34.44
3.59	Alcamizer	Injection	TUT	5	1004.32	24.98	11.17	24.08	0.34	0.15	9.11	0.24	0.11			
4	Alcamizer	Injection	IPF	5	1036.29	31.54	14.10	23.82	0.78	0.35	8.89	0.17	0.08			
5.12	DHT4A	Compression	IPF	5	1531.50	119.01	53.22	24.56	2.41	1.08	7.37	1.87	0.84	316.19	242.55	108.47
6	Alcamizer	Compression	IPF	5	1645.88	143.24	64.06	26.53	0.73	0.32	7.32	0.23	0.10	206.01	70.99	31.75
6	Alcamizer	Compression	UP	5	1589.18	71.09	31.79	28.22	1.36	0.61	5.54	1.06	0.47	8.79	5.82	2.60
6	Alcamizer	Compression	UP	5	1480.84	217.35	97.20	28.64	3.24	1.45	6.05	1.03	0.46	10.11	3.50	1.57
6	Alcamizer	Injection	IPF	5	977.57	52.55	23.50	22.27	0.52	0.23	9.23	0.39	0.17			
6	Alcamizer	Injection	IPF	5	1112.96	35.72	15.97	23.92	0.32	0.14	8.54	0.19	0.09			
6	Alcamizer	Injection	TUT	7	1043.09	35.45	13.40	24.11	0.40	0.15	8.93	0.13	0.05	1239.04		
6	DHT4A	Compression	IPF	5	1201.03	123.50	55.23	22.47	5.19	2.32	5.15	1.97	0.88	28.34	21.71	9.71
6	DHT4A	Compression	UP	5	1767.76	145.01	64.85	31.86	3.15	1.41	5.32	0.64	0.28	7.26	1.83	0.82
6	DHT4A	Injection	IPF	12	1005.96	37.18	10.73	22.93	0.42	0.12	8.58	0.31	0.09	1701.68		
6	DHT4A	Injection	TUT	5	1060.72	33.11	14.81	24.07	0.37	0.17	8.45	0.13	0.06			
8	DHT4A	Injection	IPF	5	1006.78	33.39	14.93	21.90	0.30	0.13	8.76	0.16	0.07			
10	Alcamizer	Compression	IPF	5	1792.92	95.89	42.88	24.81	1.13	0.51	6.17	1.34	0.60	74.12	64.46	28.83
10	Alcamizer	Compression	UP	5	1685.94	179.17	80.13	27.29	1.68	0.75	4.56	0.83	0.37	6.13	2.09	0.93
10	Alcamizer	Injection	IPF	5	1044.60	40.27	18.01	21.81	0.43	0.19	8.27	0.25	0.11			
10	Alcamizer	Injection	IPF	5	1232.64	82.97	37.11	23.14	0.35	0.15	8.03	0.28	0.13			
10	Alcamizer	Injection	TUT	5	1122.37	30.33	13.56	23.55	0.23	0.10	8.32	0.12	0.05			
10	DHT4A	Compression	IPF	5	1674.34	133.55	59.73	23.66	0.89	0.40	7.11	0.28	0.13	260.47	250.90	112.21
10	DHT4A	Compression	UP	5	1591.65	209.52	93.70	26.94	2.26	1.01	4.06	0.77	0.34	4.46	1.13	0.51
10	DHT4A	Compression	UP	5	1691.28	161.59	72.27	28.23	1.22	0.55	5.28	0.42	0.19	7.45	2.23	1.00
10	DHT4A	Injection	IPF	5	1098.09	48.30	21.60	22.17	0.19	0.08	8.28	0.27	0.12			
10	DHT4A	Injection	TUT	5	1122.12	20.89	9.34	23.50	0.41	0.18	7.96	0.28	0.12			

For the injection moulded replicate points (left column) the groups are close together showing minimal variability, whereas the compression moulded replicate points (right column) have more variation and therefore a larger SD. For Young's modulus the error between the means of the replicate points is between 10.29 and 15.26 % for the injection moulded samples and between 4.24 and 6.82 % for the compression moulded samples. This error is smaller for FPS (4.94-6.90 % for injection moulded and 1.50 and 4.57 % for compression moulded) and elongation at FPS (2.93-8.10 % for injection moulded and 0.61 and 23.03 % for compression moulded). For elongation at break none of the injection moulded samples reached failure and the error for the compression moulded samples was between 14.93 and 40.02 %. Elongation at break provides higher variations within a group as samples break at different points and it is not guaranteed that the samples in the same group will all break at a similar point. Apart from the larger errors for the elongation at break, the design is still considered repeatable for

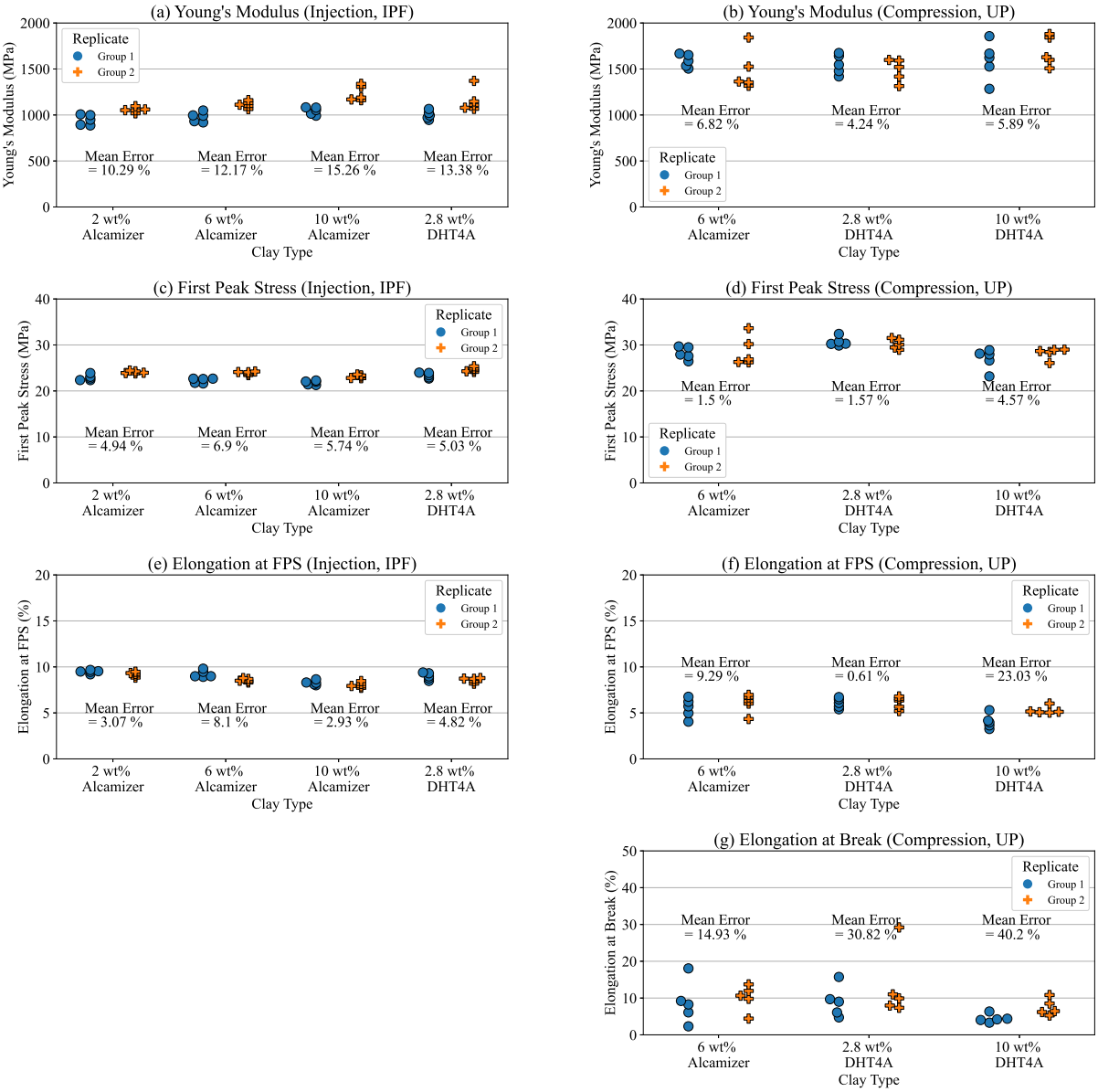

Figure 6.4: Scatter plot of the replicated points in the tensile testing DoE. IPF injection moulded samples are in the first column and UP compression moulded samples in the second column.

the remaining mechanical properties which are within a reasonable margin of error.

Sample Mould DoE

The summary statistics for the sample mould DoE are provided in Table 6.2. The number of observations for the sample mould DoE cases is equal with all cases having 5 observations, with the exception of 6 wt% DHT4-A (ISO 1A) with 12 observations. The design is therefore said to be well balanced as almost all of the cases have an equal number of observations.

The mean ranges between 927.87 and 1521.60 MPa for the Young's modulus, 21.81 and 25.31 MPa for FPS, 7.72 and 9.80 % for elongation at FPS, and 595.04 and 1701.68 % for elongation at break.

For the FPS, elongation to FPS and Young's modulus the SEM is found to be small when compared to the mean. The SEM for FPS is between 0.3 and 1.7 % of the mean, for elongation at FPS it is between 0.8 and 3.7 % of the mean, and for Young's modulus it is between 1 and 5 % of the mean. A small SEM indicates that it is possible to quantify statistically significant effects. Not much can be said for elongation at break regarding the SEM as there are only two values. This is mainly because not all samples reached failure, and as such an elongation at break wasn't available for all five samples in a case and therefore the SEM would not be an accurate representation. Regardless, the elongation at break results will still be presented in the statistical analysis and discussion for the sake of completeness.

A small SD indicates that the mean is reliable and will provide a good measure of the average response. This is the case for FPS, elongation at FPS and Young's modulus. The SD for FPS ranges from 0.6 to 3.7 % of the mean, for elongation at FPS it ranges between 1.7 and 8.2 % of the mean, and for Young's modulus SD ranges from 2.6 to 11 % of the mean). For the elongation at break we observe a much larger variation in SD ranging between 0.1 to 71.7 % of the mean. This variation is too large to consider the mean to be reliable.

Replicate points are included in the design to determine the repeatability. The results are illustrated in Figure 6.5 with the error between the means of the replicate points shown on the figure. The sample points for each group are close together corresponding to the small SD's. The error between the means for Young's modulus ranges between 10.29 and 17.41 %. This error is significantly lower for FPS ranging between 2.94 and 6.9 %, and for elongation at FPS the error ranges between 2.93 and 16.02 %. The overall error between the response variable means for the replicate points is considered acceptable, and the design is therefore repeatable.

Table 6.2: Summary statistics of the tensile responses for the different combinations of experimental variables in the sample mould DoE, where SD is the standard deviation and SEM is the standard error of the mean. Replicate points are indicated in red.

Clay Loading	Clay Type	Mould Type	Nr. of Observations	Young's Modulus (MPa)			First Peak Stress (FPS) (MPa)			Elongation at FPS (%)			Elongation at Break (%)		
				Mean	SD	SEM	Mean	SD	SEM	Mean	SD	SEM	Mean	SD	SEM
0	Neat	ISO 1A	5	970.51	78.90	35.28	24.26	0.16	0.07	9.17	0.22	0.10	745.29	183.17	81.92
0	Neat	ISO 1BA	5	971.33	66.26	29.63	23.67	0.37	0.17	9.50	0.37	0.16	846.61	62.93	
2	Alcamizer	ISO 1A	5	946.96	56.45	25.25	22.88	0.63	0.28	9.47	0.17	0.08			
2	Alcamizer	ISO 1A	5	1055.58	27.59	12.34	24.07	0.26	0.11	9.19	0.25	0.11			
2	Alcamizer	ISO 1BA	5	1287.83	113.14	50.60	24.37	0.44	0.20	9.38	0.40	0.18	721.72	1.20	
2	DHT4A	ISO 1A	5	965.46	30.55	13.66	23.11	0.46	0.20	9.12	0.16	0.07			
2	DHT4A	ISO 1BA	5	1259.49	101.39	45.34	23.93	0.63	0.28	9.28	0.46	0.21	803.83	39.81	
2.8	DHT4A	ISO 1A	5	999.92	46.11	20.62	23.39	0.57	0.25	8.98	0.38	0.17			
2.8	DHT4A	ISO 1A	5	1154.37	124.89	55.85	24.63	0.49	0.22	8.57	0.25	0.11			
2.8	DHT4A	ISO 1BA	5	1407.27	82.79	37.03	25.31	0.26	0.11	8.38	0.23	0.10	824.07	9.19	
2.8	DHT4A	ISO 1BA	5	1031.99	34.01	15.21	24.69	0.54	0.24	8.36	0.43	0.19			
4	Alcamizer	ISO 1A	5	1036.29	31.54	14.10	23.82	0.78	0.35	8.89	0.17	0.08			
4	Alcamizer	ISO 1BA	5	927.87	52.63	23.54	23.39	0.81	0.36	9.54	0.62	0.28	800.87	73.79	
6	Alcamizer	ISO 1A	5	977.57	52.55	23.50	22.27	0.52	0.23	9.23	0.39	0.17			
6	Alcamizer	ISO 1A	5	1112.96	35.72	15.97	23.92	0.32	0.14	8.54	0.19	0.09			
6	Alcamizer	ISO 1BA	5	1236.84	60.35	26.99	23.19	0.69	0.31	9.80	0.57	0.26	849.01	3.62	
6	Alcamizer	ISO 1BA	5	1053.45	48.75	21.80	24.40	0.22	0.10	8.45	0.44	0.20			
6	DHT4A	ISO 1A	12	1005.96	37.18	10.73	22.93	0.42	0.12	8.58	0.31	0.09	1701.68		
6	DHT4A	ISO 1BA	5	961.65	54.64	24.44	22.97	0.50	0.22	8.67	0.70	0.31	820.55	46.98	21.01
8	DHT4A	ISO 1A	5	1006.78	33.39	14.93	21.90	0.30	0.13	8.76	0.16	0.07			
8	DHT4A	ISO 1BA	5	1501.65	165.11	73.84	24.35	0.90	0.40	8.01	0.65	0.29	595.04	426.18	
10	Alcamizer	ISO 1A	5	1044.60	40.27	18.01	21.81	0.43	0.19	8.27	0.25	0.11			
10	Alcamizer	ISO 1A	5	1232.64	82.97	37.11	23.14	0.35	0.15	8.03	0.28	0.13			
10	Alcamizer	ISO 1BA	5	1494.64	42.06	18.81	23.23	0.44	0.20	8.27	0.26	0.12	779.37	99.45	
10	DHT4A	ISO 1A	5	1098.09	48.30	21.60	22.17	0.19	0.08	8.28	0.27	0.12			
10	DHT4A	ISO 1BA	5	1521.60	99.74	44.60	24.71	0.70	0.31	7.72	0.40	0.18	654.68	2.18	

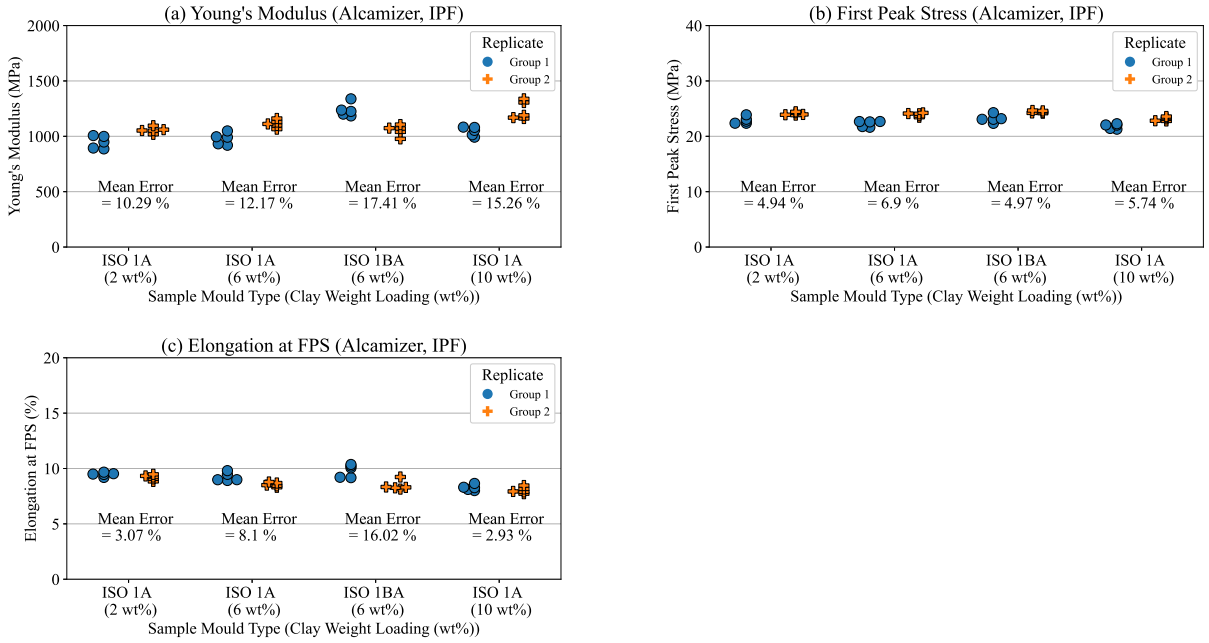

Figure 6.5: Scatter plot of the replicated points in the tensile sample mould DoE. All replicate points are Alcamizer 1 and injection moulded at IPF.

Impact Testing DoE

The summary statistics for the Charpy impact testing DoE are provided in Table 6.3. The number of observations for the impact testing DoE's is equal with cases having either 5 or 6 observations. It is therefore considered to be a well balanced design, as cases have an equal number of observations. The mean for impact strength ranges between 3.5 and 9.3 kJ/m^2.

For impact strength the SEM is between 0.2 and 6 % of the mean. The statistically significant effects can therefore be quantified. The SD ranges 0.6 and 14.6 % of the mean. The small variation is a good indication that the mean is reliable and will therefore provide a good measure of the average response.

There are two replicate points in this design, shown in Figure 6.6, to determine repeatability. Both points are injection moulded at TUT and are grouped closely together. There is a 4.14 % and 3.54 % difference between the replicate point means for 10 wt% Alcamizer and 10 wt% DHT4-A, respectively. This is a small error range and the design is therefore repeatable.

Table 6.3: Summary statistics of the impact response for the different combinations of experimental variables, where SD is the standard deviation and SEM is the standard error of the mean. Replicate points are indicated in red.

Clay Loading	Clay Type	Moulding Method	Site	Nr. of Observations	Impact Strength (kJ/m^2) Mean	SD	SEM
0	Neat	Compression	IPF	5	3.76	0.17	0.08
0	Neat	Compression	UP	6	3.82	0.23	0.09
0	Neat	Injection	IPF	5	5.74	0.17	0.08
0	Neat	Injection	TUT	5	5.92	0.53	0.24
2	Alcamizer	Compression	IPF	5	4.29	0.42	0.19
2	Alcamizer	Compression	UP	6	4.55	0.41	0.17
2	Alcamizer	Injection	IPF	5	9.27	0.49	0.22
2	DHT4A	Compression	IPF	5	3.87	0.13	0.06
2	DHT4A	Compression	UP	6	3.80	0.10	0.04
2	DHT4A	Injection	IPF	5	5.75	0.04	0.02
2.8	DHT4A	Compression	UP	5	3.87	0.41	0.18
2.8	DHT4A	Injection	IPF	5	5.70	0.18	0.08
3.59	Alcamizer	Injection	TUT	5	5.64	0.19	0.08
4	Alcamizer	Injection	IPF	5	5.81	0.15	0.07
6	Alcamizer	Compression	IPF	5	3.91	0.10	0.05
6	Alcamizer	Compression	UP	6	4.16	0.32	0.13
6	Alcamizer	Injection	IPF	5	7.40	0.31	0.14
6	Alcamizer	Injection	TUT	5	6.32	0.33	0.15
6	DHT4A	Compression	IPF	6	4.06	0.39	0.16
6	DHT4A	Compression	UP	6	3.54	0.52	0.21
6	DHT4A	Injection	IPF	5	5.45	0.06	0.03
6	DHT4A	Injection	TUT	6	4.77	0.43	0.18
8	DHT4A	Injection	IPF	5	6.28	0.20	0.09
10	Alcamizer	Compression	IPF	5	4.05	0.13	0.06
10	Alcamizer	Compression	UP	6	3.90	0.49	0.20
10	Alcamizer	Injection	IPF	5	6.21	0.17	0.08
10	Alcamizer	Injection	TUT	5	5.63	0.18	0.08
10	Alcamizer	Injection	TUT	5	5.41	0.14	0.06
10	DHT4A	Compression	IPF	5	3.97	0.20	0.09
10	DHT4A	Compression	UP	6	3.58	0.20	0.08
10	DHT4A	Injection	IPF	5	6.15	0.08	0.04
10	DHT4A	Injection	TUT	5	5.29	0.28	0.12
10	DHT4A	Injection	TUT	5	5.48	0.14	0.06

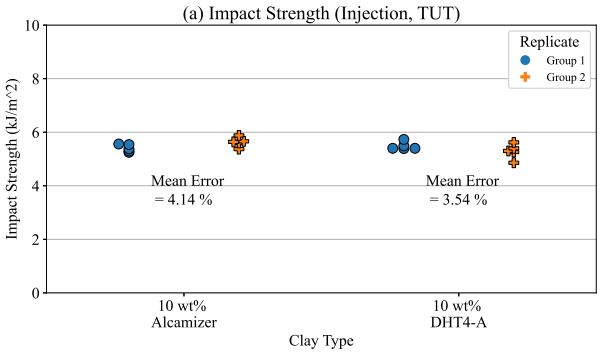

Figure 6.6: Scatter plot of the replicated points in the impact testing DoE. Replicate points are injection moulded at TUT.

6.3.2 Diagnostics

Diagnostics are performed to verify the assumption of normality for linear regression, and constant variance and random sampling for ANOVA (Montgomery, 2013). In the following figures, the normality assumption is in the left column, constant variance assumption in the middle column and assumption of random sampling in the right column. Normality is visualised by means of a probability plot of the residuals and will approximate a straight line, with more emphasis on central values as opposed to values at the edges (Montgomery, 2013). Constant variance considers a plot of the residuals against the number of observations. Ideally a constant variance assumption would have a constant error spread across the number of observations (Montgomery, 2013). Should the assumption be violated the variance spread may be larger on one end than the other (Montgomery, 2013). Random sampling is illustrated with a residuals vs. predicted plot. For the assumption of random sampling to hold this plot should not reveal any structured pattern, but instead appear random (Montgomery, 2013).

Tensile Testing DoE

To determine which response surface model should be considered the R^2 and adjusted R^2 values are determined and summarised in Table 6.4.

Table 6.4: Overview of R^2 and adjusted R^2 for the different response surface models for the tensile testing DoE.

Mechanical	Linear			Two-order Interaction			Quadratic		
Property	R^2	Adjusted R^2	Error (%)	R^2	Adjusted R^2	Error (%)	R^2	Adjusted R^2	Error (%)
Young's Modulus	0.873	0.858	1.673	0.920	0.910	1.000	0.926	0.918	0.907
FPS	0.990	0.989	0.121	0.951	0.946	0.589	0.947	0.941	0.644
Elongation at FPS	0.918	0.908	1.025	0.827	0.808	2.381	0.840	0.821	2.180
Elongation at break	0.913	0.894	2.016	0.749	0.696	7.067	0.830	0.794	4.327

Based on the difference between the R^2 and adjusted R^2 values these are quite close to one another ($\leq$ 3 %) for all mechanical properties and response models. The only exception is the elongation at break for the interaction and quadratic models with a difference of 7.067 % and 4.327 %, respectively. When the R^2 and adjusted R^2 values are close to one another it indicates that the model considered can provide good predictability. This is clearly the case for the all models, except the interaction and quadratic models for the elongation at break. The interaction and quadratic models will therefore not provide good predictability for the elongation at break.

Both the R^2 and adjusted R^2 values decrease when considering an interaction or quadratic model for all properties except Young's modulus which sees an increase in both values. All properties, except Young's modulus, have the highest R^2 and adjusted R^2 values for the linear model. For the linear model, the R^2 value is 0.8726 for Young's modulus, 0.9898 for FPS, 0.9175 for elongation at FPS, and 0.9128 for elongation at break. In all instances the R^2 value is above 0.9 indicating a very good model, except for Young's modulus where a

quadratic model would be better. However, a value of 0.8726 is still a good value, and this can be improved upon by applying a Box-Cox transformation. A Box-Cox transformation applies a power law to the data to better approximate a normal distribution (Montgomery, 2013). By applying this transformation the R^2 value improves from 0.8726 to 0.9041 which is a 3.61 % increase, thereby providing a better fit of the observed data. This is still not as good as the quadratic model, being 2.4 % lower, however it is still an acceptable R^2 value and the linear model will be able to provide good predictability for Young's modulus. A linear model will therefore be considered for all the mechanical properties of interest.

The linear regression and ANOVA diagnostics for the tensile testing DoE are shown in Figure 6.7, with a transformed dataset for Young's modulus. All plots indicate an approximately normal distribution, thereby verifying the normality assumption. The constant variance assumption is within an acceptable range for all mechanical properties with a constant error across the number of observations. The residuals vs. predicted results don't follow any structured pattern for all the mechanical properties, which confirms simple random sampling.

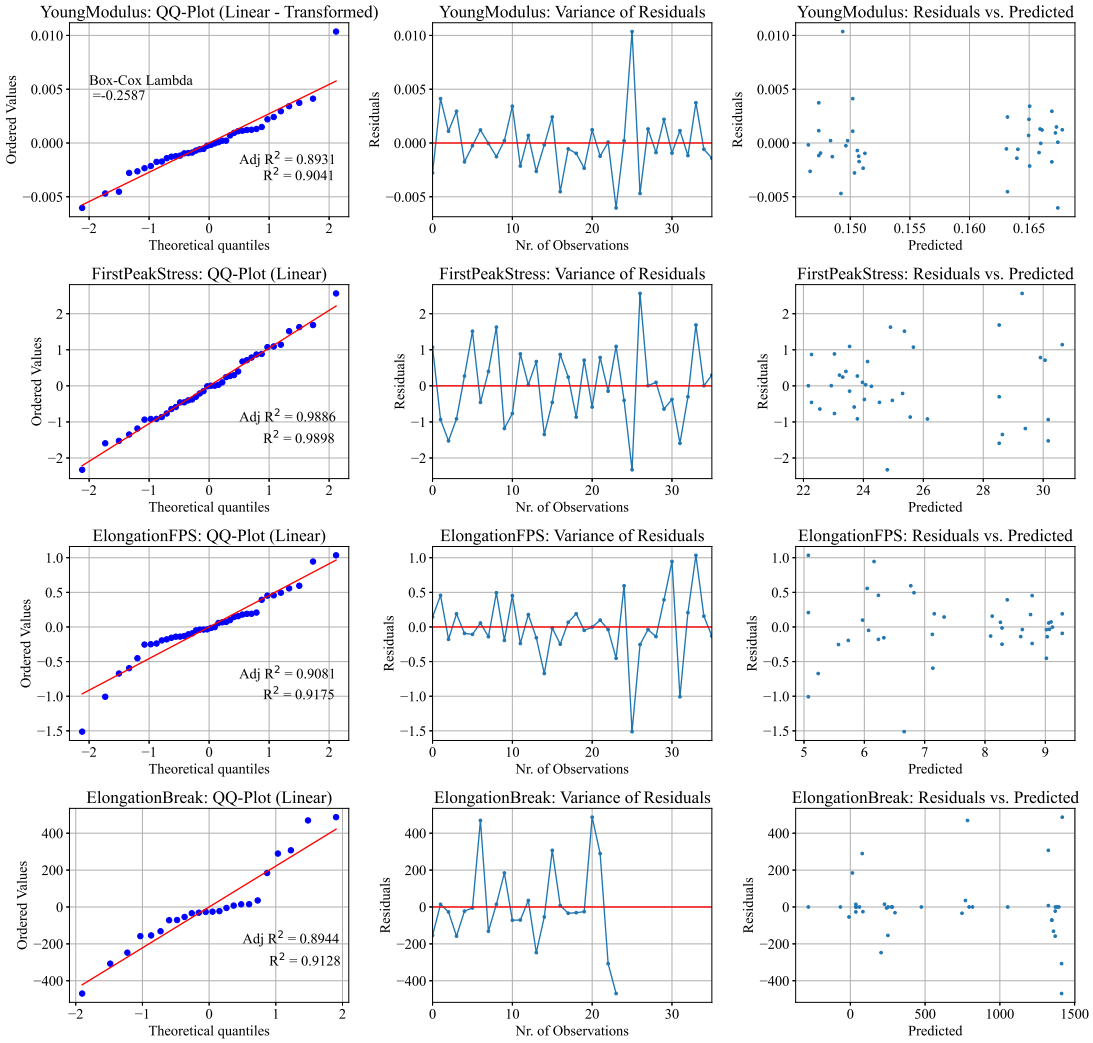

Figure 6.7: Tensile testing DoE ANOVA diagnostics for assumption of normality (left column), constant variance of residuals (middle column) and random sampling (right column).

Sample Mould DoE

Table 6.5 summarises the R^2 and adjusted R^2 values for the different response surface models.

Table 6.5: Overview of R^2 and adjusted R^2 for the different response surface models for the tensile sample mould DoE.

Mechanical	Linear			Two-order Interaction			Quadratic		
Property	R^2	Adjusted R^2	Error (%)	R^2	Adjusted R^2	Error (%)	R^2	Adjusted R^2	Error (%)
Young's Modulus	0.974	0.971	0.359	0.966	0.961	0.487	0.980	0.977	0.276
FPS	0.928	0.919	1.056	0.982	0.979	0.255	0.987	0.985	0.182
Elongation at FPS	0.955	0.949	0.638	0.958	0.952	0.595	0.972	0.969	0.391
Elongation at break	0.919	0.889	3.308	0.962	0.948	1.476	0.784	0.702	10.364

The R^2 and adjusted R^2 values are close to one another (≤ 3.5 %) for all mechanical properties, except elongation at break for a quadratic model. This indicates that the models, except for a quadratic model for elongation at break, can provide good predictability. There is an increase in both R^2 and adjusted R^2 for most mechanical properties for an interaction or quadratic model. The exception is a decrease in both values for an interaction model for Young's modulus, and a quadratic model for elongation at break. An interaction model has at most a 0.89 % decrease in R^2 from the linear model for Young's modulus, 5.75 % increase for FPS, 0.26 % increase for elongation at FPS, and 4.70 % increase for elongation at break. Similarly, for a quadratic model R^2 increases with 0.57 % for Young's modulus, 6.28 % for FPS, 1.78 % for elongation at FPS and decreases with 14.74 % for elongation at break. Both interaction and quadratic models add additional terms to the response surface model which adds an additional complexity to the statistical analysis. The slight improvement in R^2 does not warrant this additional complexity. A linear model will provide good predictability with all R^2 values above 0.9 and is therefore sufficient to consider for all mechanical properties.

The diagnostics for the ANOVA for the sample mould DoE are shown in Figure 6.8. The assumption of normality is verified where all mechanical properties have an approximately normal distribution of the residuals. The assumption of constant variance is verified with a constant error across the number of observations. There is no structured pattern to the residuals vs. predicted results which verifies the assumption of random sampling.

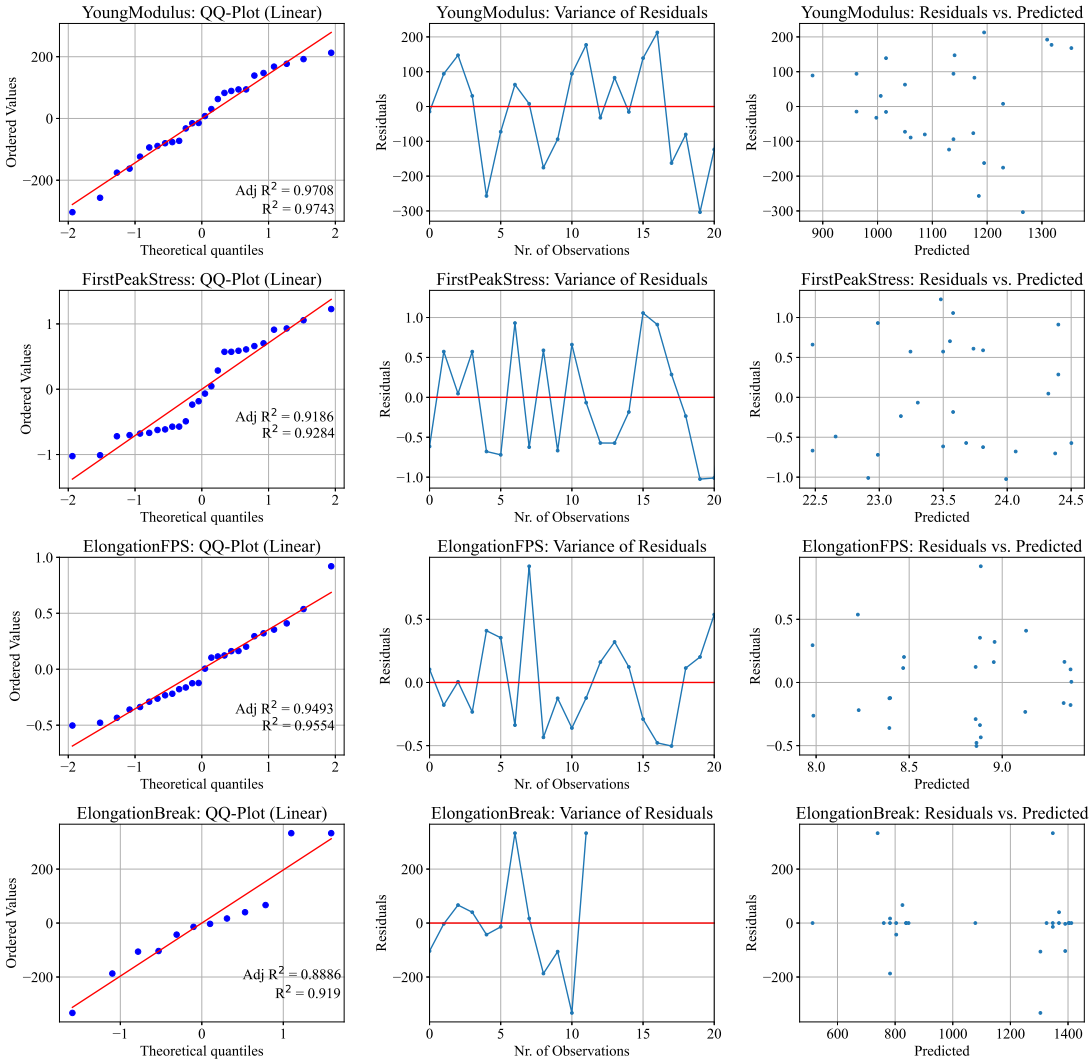

Figure 6.8: Sample mould DoE ANOVA diagnostics for assumption of normality (left column), constant variance of residuals (middle column) and random sampling (right column).

Impact Testing DoE

Similar to the DoE's above, the response surface model is first determined by investigating the R^2 and adjusted R^2 values, summarised in Table 6.6.

Table 6.6: Overview of R^2 and adjusted R^2 for the different response surface models for the impact testing DoE.

Mechanical Property	Linear			Two-order Interaction			Quadratic		
	R^2	Adjusted R^2	Error (%)	R^2	Adjusted R^2	Error (%)	R^2	Adjusted R^2	Error (%)
Impact Strength	0.811	0.784	3.33	0.766	0.732	4.38	0.805	0.777	3.47

Both the R^2 and adjusted R^2 values are relatively close ($\leq$ 3.5 %) except for an interaction model. The linear and quadratic models can therefore provide a good predictability. There is a decrease in the R^2 and adjusted R^2 values for both an interaction and quadratic model when compared to the linear model. The linear model provides the highest value for R^2 and even though 0.811 is an acceptable value being reasonably close to 1, this can be improved by

applying a Box-Cox transformation. By applying this transformation the R^2 value increases from 0.811 to 0.9664 which is a 19.2 % increase. The adjusted R^2 value increases from 0.784 to 0.9616. This transformation reduces the error between the R^2 and adjusted R^2 values from 3.33 % to 0.50 %. A transformed linear model therefore fits the observed data much better than a normal linear model while providing an improvement in the model predictability.

The diagnostics for the ANOVA for the impact testing DoE are shown in Figure 6.9. The normality plot approximates a normal distribution verifying the assumption of normality. The constant variance assumption varies approximately 0.02 units from the mean, except for a few outliers, with a constant error across the number of observations. The assumption of random sampling is verified with no discernible pattern observed in the residuals vs. predicted results.

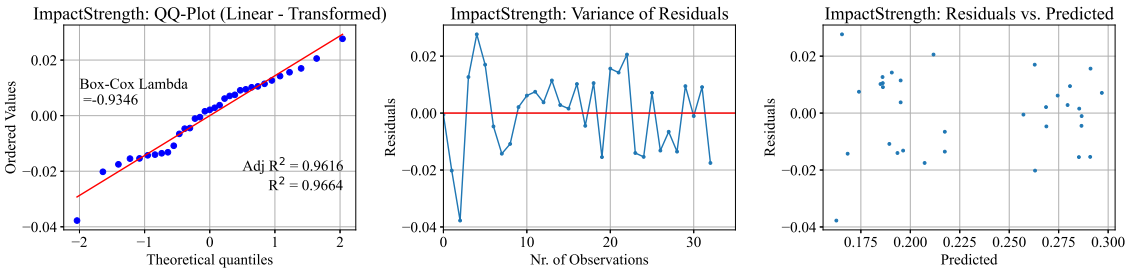

Figure 6.9: Impact testing DoE ANOVA diagnostics for assumption of normality (left column), constant variance of residuals (middle column) and random sampling (right column).

6.3.3 Analysis of Variance (ANOVA)

The complete fitted linear model and ANOVA tabulated results are shown in Appendix C. For simplicity, only the resulting p-value is considered for all the design factors and mechanical properties of interest. A p-value indicates the probability that the effect of the variable on the response is only by chance. A p-value less than 0.05 indicates that the variable has a significant effect on the response with more than 95 % confidence. In Figure 6.10 the results are presented as (1 − p-value) for easier interpretation where the solid black line represents a p-value of 0.05 or (1 − p-value) of 0.95. Therefore any design factor that is above this line is considered to be statistically significant.

From Figure 6.10, the statistically significant influences for the different factors are:

- Clay type (blue) only affects the impact strength for the impact testing DoE. For the sample mould type DoE it affects the elongation at first peak stress.
- Clay loading (orange) was deemed to have a statistically significant effect for all mechanical properties for the tensile testing DoE, except elongation at break. It has no effect on the impact strength. For the sample mould type DoE clay loading is statistically significant for all mechanical properties except elongation at break.
- Moulding method (green) has a statistically significant effect on all mechanical properties of interest for the tensile and impact testing DoE's.

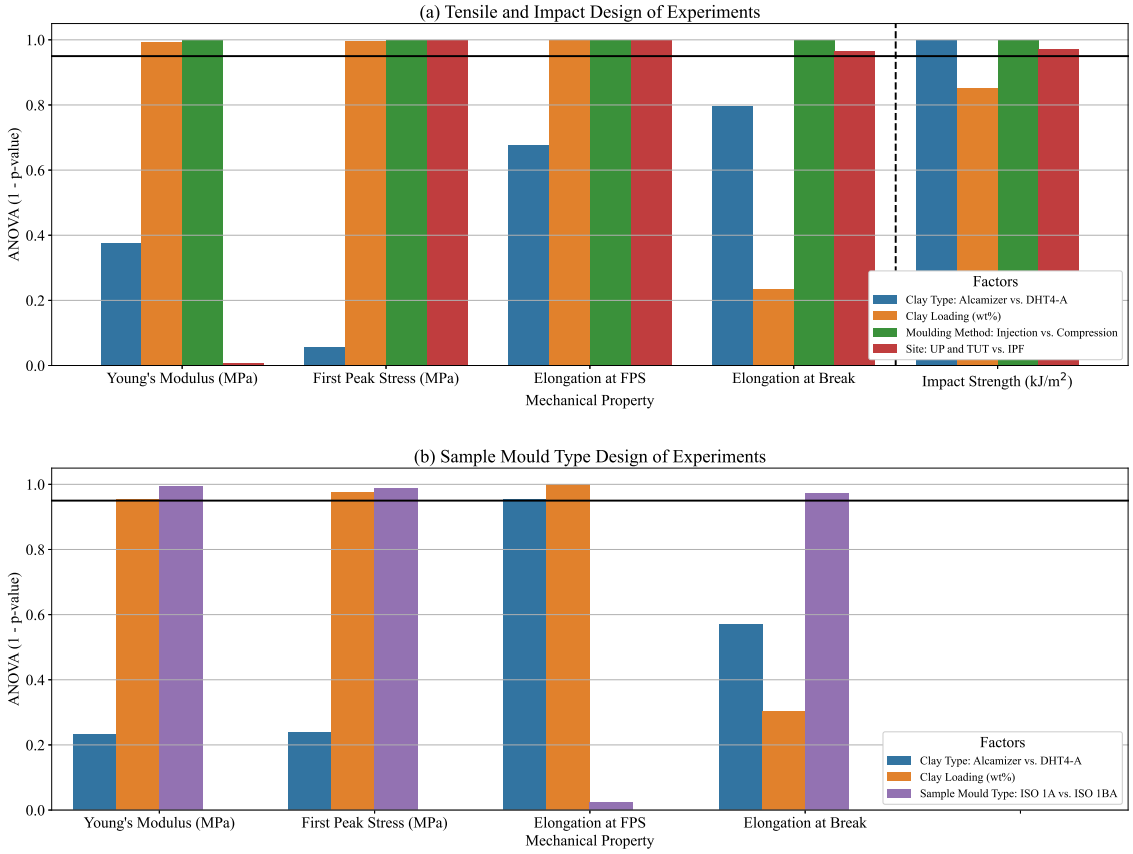

Figure 6.10: Resulting p-value obtained from ANOVA for all mechanical properties of interest represented as (1−p-value) for (a) tensile and impact testing DoE and (b) sample mould type DoE. The solid black line represents a p-value of 0.05.

- Sample mould type (purple) has a statistically significant effect on all mechanical properties except elongation at FPS for the sample mould type design. This indicates that material stiffness is largely influenced by the size of the tensile dog bone sample.
- Site (red) in the tensile and impact DoE has an effect on all mechanical properties except Young's modulus.

6.3.4 Quantify Relationships

To quantify the strength of the relationships between a design variable and the response variable a descriptive statistic known as ω^2 is considered. ω^2 is the proportion of variation in the response variable associated with a specific group. The ω^2 results are shown in Figure 6.11, plotted only for variables which have been shown to have a statistically significant effect on the property.

From Figure 6.11(a) it is clear that moulding method (green) contributes to explaining the variations in the mechanical properties and has a strong effect. Site (red) has a smaller effect contributing less to the variation in mechanical properties. The effect due to site is not as pronounced as the effects of moulding method. The effects due to clay type (blue) and clay

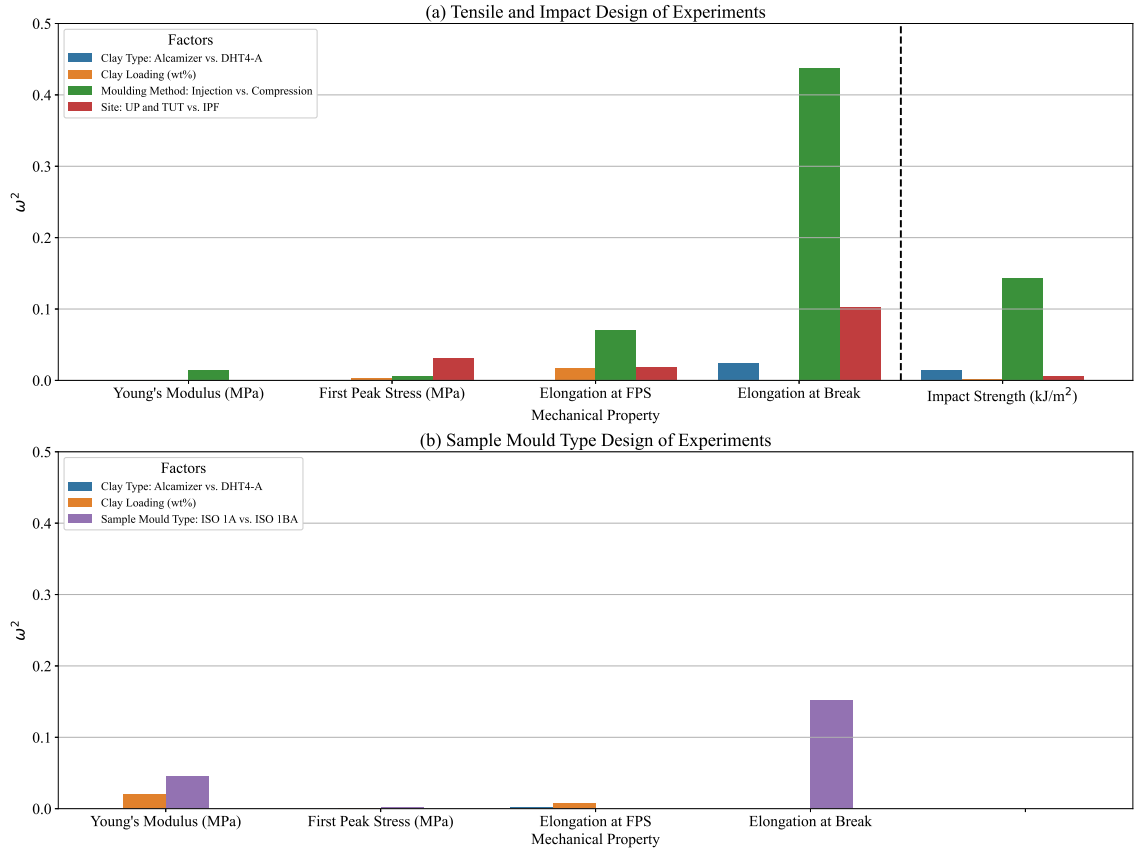

Figure 6.11: ω^2 to quantify the strength of relationships between the different factors and the mechanical properties of interest for (a) tensile and impact testing DoE and (b) sample mould DoE.

loading (orange) are smallest being much closer to 0, indicating the relationship is tenuous at best. Overall, the moulding method has the strongest effect on the mechanical properties followed by the manufacturing site.

From Figure 6.11(b) the effect of sample mould type (purple) is more pronounced for Young's modulus and elongation at break. This indicates that the mould type largely affects the material stiffness and ductility parameters which is exactly what a tensile test determines. Clay loading (orange) has a less pronounced effect although it is still strong, especially for Young's modulus. The effect of clay type (blue) is almost non-existent with very low ω^2 values. For the sample mould type DoE there is a strong relationship with sample mould type.

6.4 Discussion of Key Observations

The key observations from the statistical analysis are discussed here. To complement the discussion an exploratory data analysis approach is considered to present the experimental results. A predicted linear regression line is presented with the experimental results. It is the best average fit through all the data points, and is used to predict the response for any combination of the factors and levels included in the model. The predicted fitted regression

line is represented as a solid straight line and calculated according to the example presented in Chapter 5.

6.4.1 Effect of Moulding Method

For the moulding method I investigated the effect of compression and injection moulding on the mechanical properties of HDPE/LDH. Based on the conclusions of the systematic literature review we expect a difference in mechanical properties between the two moulding methods. In fact, literature often states that injection moulded samples have higher tensile properties than compression moulded samples (Chu *et al.*, 2007; Mistretta *et al.*, 2018). The systematic literature review indicated that Young's modulus, first peak stress and elongation at break is normally higher for injection moulding than compression moulding.

The statistical analysis clearly indicated that moulding method has a statistically significant effect on all the mechanical properties of interest. In fact, based on ω^2 it has the strongest relationship to the mechanical properties. To better understand the effect of moulding method only the data from the IPF is considered here as there is consistency in the mould thickness (at 2 mm) and the sample mould type (ISO Type 1BA) for both injection and compression moulded samples. This ensures that any potential bias due to the other factors of interest which have been shown to have a statistically significant effect (*i.e.*, site and sample mould type) is removed. The resulting data to discuss the effect of moulding method is shown in Figure 6.12. The predicted response based on the fitted linear model is shown as a straight solid line.

From Figure 6.12 it is interesting to note that compression moulding has a higher **Young's modulus** and **first peak stress** compared to injection moulding for both DHT4-A and Alcamizer 1. This is contradictory to what Chu *et al.* (2007) and Mistretta *et al.* (2018) reported and what was observed in the systematic literature review. This is unexpected as injection moulding generally leads to better separation and dispersion of the clay in the polymer matrix, and consequently improved stiffness and tensile strength. It should be noted however that both Chu *et al.* (2007) and Mistretta *et al.* (2018) considered MMT whereas this study considers LDH. Even though the initial assumption was that the observations could be extrapolated as LDH is the synthetic alternative to MMT, perhaps there is a morphological effect due to the chemical differences between the natural and synthetic clay which ultimately affects the composite morphology during compounding and moulding.

The **elongation at break** does perform as expected with higher, more ductile, values for injection moulding compared to compression moulding, which was reported by Mistretta *et al.* (2018). This indicates that injection moulded samples are a lot more ductile than compression moulded samples. This was observed in the tensile curves where UP samples broke at a higher stress and earlier than IPF samples.

By definition **impact strength** is a measure of the material's capability to withstand a sudden applied load. The higher impact strength for injection moulded samples is therefore expected

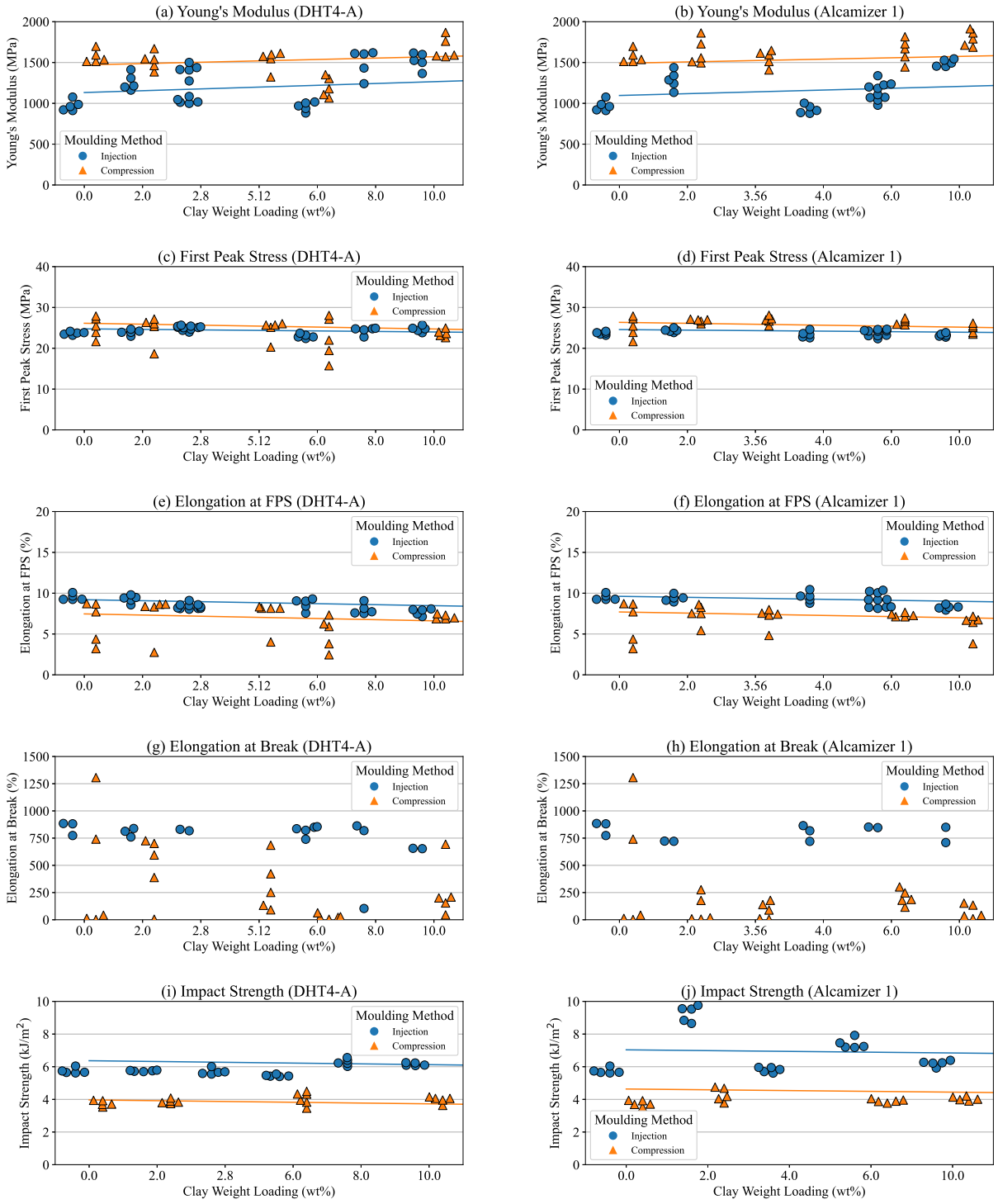

Figure 6.12: Effect of moulding method on the mechanical properties of interest for IPF ISO Type 1BA samples. The first column considers DHT4-A and the second column Alcamizer 1. Predicted values with the fitted linear model are plotted as a straight solid line.

due to the improved processing which leads to a better composite morphology compared to compression moulding. For neat HDPE C7260 the notched Charpy impact strength is 4 kJ/m^2 for compression moulded samples (Safripol, 2018) considering DIN EN ISO 179-1 (2010). Both the UP and IPF compression moulded neat samples have an impact strength of approximately 4 kJ/m^2 which correlates with the published data for HDPE C7260.

Injection moulded samples are grouped closer together, indicating good repeatability. In comparison, compression moulded samples have higher variability. This is likely due to the heating process which is more constant during injection moulding as compounded material is fed through a barrel with a screw and constant heating applied throughout the barrel to melt the material before injecting it into the mould. This allows for better mixing resulting in less agglomeration than compression moulding (Chu *et al.*, 2007; Mistretta *et al.*, 2018). Due to inconsistent heat distribution, the polymer pellet boundaries form inconsistently during compression moulding. A polymer pellet boundary is the interface between two polymer pellets which can affect the overall mechanical properties. Normally during compression moulding the pellet skins around a polymer pellet breaks down with the increased heat and two pellets then diffuse together to form a new continuous melt. This allows the polymer chains to become mobile in the skin zones to form net chain entanglement. (Bucknall *et al.*, 2020; Raghavan and Wool, 1999; Wool *et al.*, 1989; Wu *et al.*, 2002). This could perhaps explain the higher stiffness and strength observed in compression moulded samples. If the polymer chains do not achieve net chain entanglement, but are rather aligned to one another it increases the composite crystallinity resulting in a stiffer material (Khanam and AlMaadeed, 2015). Both the increase in agglomeration and the improper fusing of polymer pellets affect the composite morphology, creating points of stress concentration and reducing the overall material ductility. The ductility is thus more sensitive to the moulding conditions than stiffness and strength (Wu *et al.*, 2002).

These observations are similar for both clay types with very little difference between the properties and identical predicted responses. This was expected from the statistical analysis, which indicated that clay type has no statistically significant effect, except for impact strength where the predicted response for Alcamizer 1 is higher than DHT4-A.

It is clear from these observations, and the statistical analysis, that moulding method has a strong influence on the overall mechanical properties of HDPE/LDH. This was observed in the systematic literature review. It is not an unexpected conclusion as the different moulding processes change and affect the composite morphology, and consequently the mechanical properties, in important ways. This has not been reported often in literature, presumably as it is assumed knowledge within the polymer composite and manufacturing communities. Nevertheless, there is a benefit to explicitly studying these effects to gain more insight into the role of the composite morphology and how it is affected by different manufacturing methods and conditions.

6.4.2 Effect of Machine Variation

In the historical analysis the different clay types did not behave as expected and the effect due to clay loading was almost unobservable. As a result I wanted to compare the results obtained using the available University equipment with those from a state-of-the-art facility. This allows me to better understand whether different equipment will have an influence on the overall mechanical properties even if it performs the exact same moulding method with identical

conditions as far as possible. The only differences are the machine itself (*i.e.*, manufacturer and model) and the human operator's experience level. In the DoE this factor is referred to as site with the levels defined as the three laboratories, UP, TUT and IPF. From the statistical analysis site has a statistically significant effect on all the mechanical properties, except Young's modulus. For the purposes of this discussion the results for all mechanical properties will be presented.

Compression Moulding

First consider the results for the compression moulded samples (ISO Type 1BA) manufactured at UP and IPF shown in Figure 6.13. Note that in this case due to the limitations of the available moulds, the samples from UP were 3 mm thick and had a wavy surface, whereas those from IPF were 2 mm thick with a smooth surface. A straight solid line represents the predicted response based on the fitted linear model.

From Figure 6.13 the **Young's modulus** is not affected by any variation in the machine used or the human operator, or the mould thickness (the blue and orange solid lines are on top of one another visualised here with a slight perturbation for clarity).

Interestingly, the **first peak stress** is higher for samples manufactured at UP than those at IPF. This could allude to an increase in stiffness and strength in the composite morphology which likely results from the polymer pellet boundaries that form during the compression moulding process. It is possible that the increased strength observed is due to the difference in thickness as we now know that the initial assumption i.e., we expect no difference in tensile properties from different sample sizes as they are normalised to the geometry, is flawed. In Section 6.4.3 we show that there is a clear influence on the mechanical properties due to different tensile sample mould sizes. When considering the observations from Figure 6.15 note that the most prominent effect is on the Young's modulus, with very little change to the FPS and elongation at FPS. This is contrary to what we observe here where the Young's modulus has almost no effect and all the variation lies within the FPS and elongation at FPS. One could argue that the effect due to pellet boundaries plays a larger role than the sample thickness. We would need to investigate this more thoroughly to determine the true source of variation.

The **elongation at break** indicates that the samples from UP tend to be much more brittle than those from IPF which have a higher ductility. This is due to the lack of proper fusion between particles during the moulding process which form weaker inter-polymer pellet boundaries. This defect results in a reduction of the material ductility (Wu *et al.*, 2002). This result clearly illustrates that different machines lead to different polymer pellet boundaries which affect the mechanical properties differently, especially the ductility. It appears that the impact strength is not affected by the different sites with very similar values for both UP and IPF.

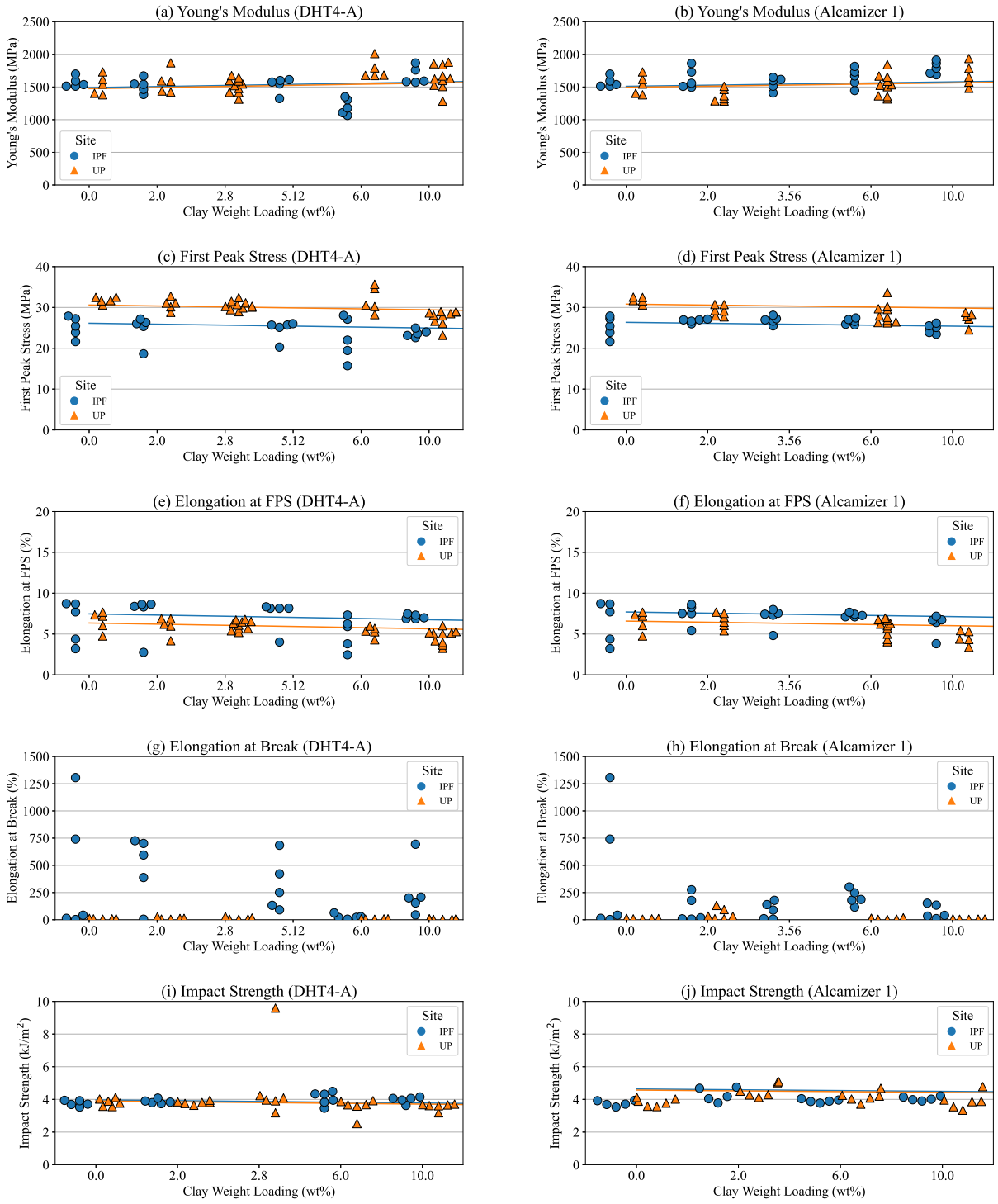

Figure 6.13: Effect of site on the mechanical properties of interest for compression moulded (ISO Type 1BA) samples. The first column considers DHT4-A and the second column Alcamizer 1. Predicted values with the fitted linear model are plotted as a straight solid line.

There is more variability in the samples compression moulded at the IPF than those at UP. While unexpected, this further illustrates the influence of different machines, including the differences in the formation of the polymer pellet boundaries, and how these can affect the repeatability of an experimental design.

Injection Moulding

Now consider the results for the injection moulded samples (ISO Type 1A) manufactured at TUT and IPF shown in Figure 6.14. From Figure 6.14 the **Young's modulus** and **elongation at FPS** are not affected by the site (the blue and orange solid lines are on top of one another with a slight perturbation for visual clarity). Similarly, the **first peak stress** is only slightly higher for TUT samples compared to IPF samples.

Not much can be said regarding the **elongation at break** as very few samples reached failure due to the limitations of the transverse distance of the tensile testing machine. The ISO Type 1A samples were too long for this limitation and therefore did not fail. This is why the predicted response does not appear to match the observed data. The predicted response is based on all the observed data points, but it had very few data points to consider for the IPF and TUT injection moulded levels which influences its predictability. Based on the observed data points and predicted response there is a difference in site for the impact strength. TUT samples tended to have a higher impact strength than IPF samples.

Contrary to the compression moulded samples, there is almost no variability in the injection moulded samples which experience closer groupings. This indicates that the different machines used for the injection moulding process do not affect drastic changes to the composite morphology, and will therefore provide more consistent results and good repeatability.

Similar to moulding method, the observations discussed here (for both the compression and injection moulded data) are the same for both clay types where identical predicted responses are observed, except for impact strength where Alcamizer 1 has a higher predicted impact strength compared to DHT4-A. Again, the statistical analysis did indicate no statistically significant effect for clay type.

There is a clear effect on the mechanical properties due to a change in site, especially for compression moulded samples. It is clear that when you are closer to front end technology the differences would be smaller. That is, for injection moulding a standard injection moulder would still produce similar components to a state-of-the-art injection moulder. However, for compression moulding there is a much larger difference between a state-of-the-art compression moulder and a standard one, hence the larger variation between the sites.

The fact that I have shown that different sites, and by extension different machines, produce differences in the obtained mechanical properties is important. This observation questions our inherent assumptions of similar machines producing similar results and will therefore inevitably have an effect when upscaling or changing a manufacturing process, or even just upgrading existing equipment. This is an observation that has not been discussed in the polymer composites literature and definitely requires further research.

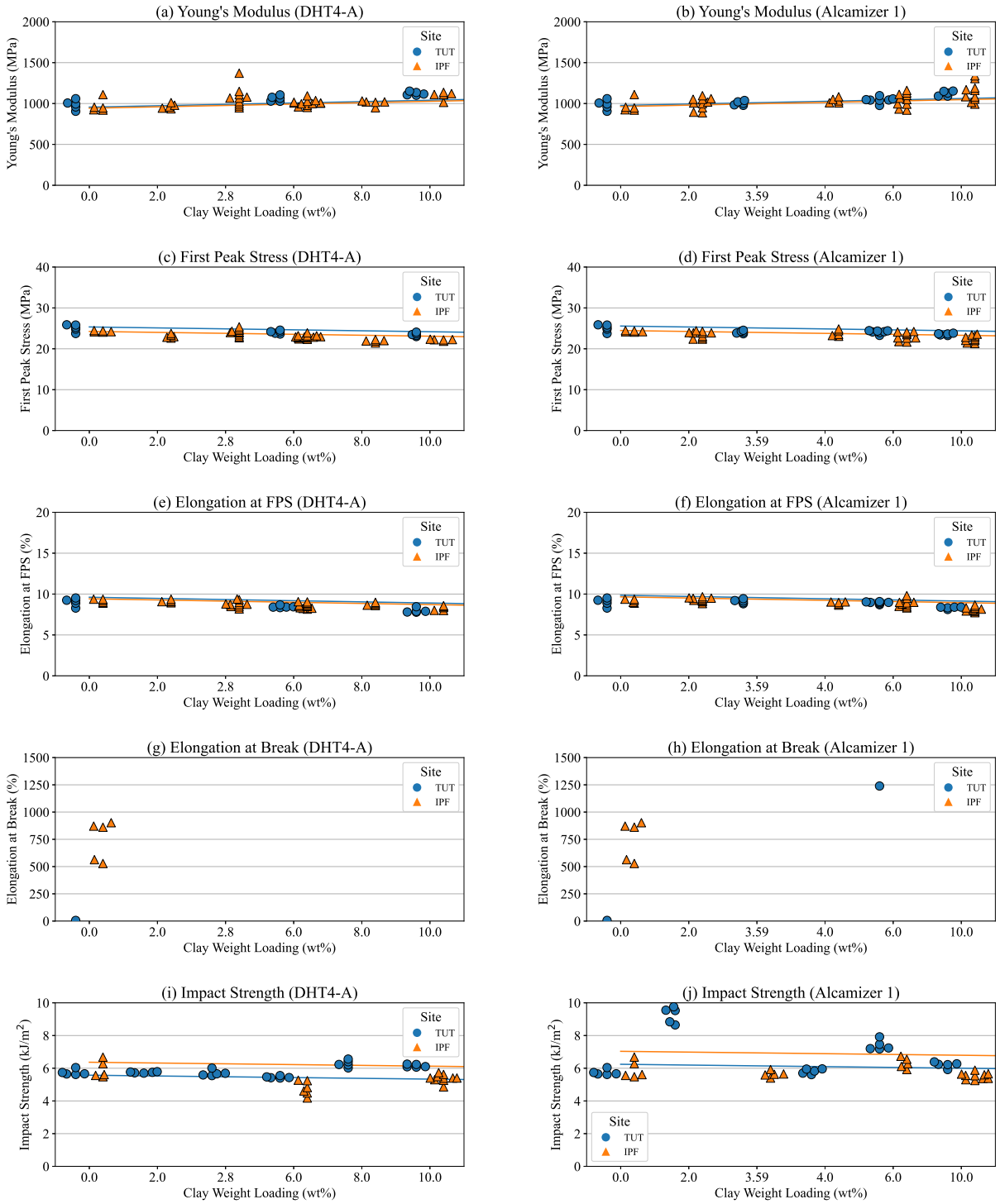

Figure 6.14: Effect of site on the mechanical properties of interest for injection moulded (ISO Type 1A) samples. The first column considers DHT4-A and the second column Alcamizer 1. Predicted values with the fitted linear model are plotted as a straight solid line.

6.4.3 Effect of Tensile Sample Mould Type

For the initial tensile testing DoE a limitation regarding the available tensile sample moulds was identified. The compression moulded samples would only be able to yield an ISO Type 1BA due to the mould size restriction of 100 × 100 mm. On the other hand, TUT only had an ISO Type 1A mould available and therefore the injection moulded samples would be a different size. Fortunately, IPF had both moulds available for injection moulding and I decided to investigate the effect of the different tensile sample mould types to ensure scientific due diligence. Theoretically, the mould type should not affect the mechanical properties as the resulting stress-strain curve is normalised to the specific sample dimensions when following DIN EN ISO 527-2 (2012).

For the purpose of this discussion the injection moulded results from the IPF are presented in Figure 6.15 for all mechanical properties of interest. The statistical analysis indicated that sample mould type has a statistically significant effect on all the mechanical properties, except elongation at FPS. The statistically significant effect is most prominent for the Young's modulus and elongation at break according to ω^2.

From Figure 6.15 ISO Type 1BA has a higher **Young's modulus** than ISO Type 1A, which is interesting as the mechanical properties are normalised for the mould geometry. This indicates that measured material stiffness is influenced by the size of the tensile dog bone sample. A smaller mould (ISO Type 1BA) will therefore yield a higher material stiffness compared to the larger mould (ISO Type 1A). This could potentially be due to the skin effects where a smaller mould will have a larger skin to bulk volume ratio. The ISO Type 1BA has a larger variability in the sample data than ISO Type 1A which has closer groupings. The repeatability for the ISO Type 1A injection moulded samples is therefore good.

There is a small effect of sample mould type on the **first peak stress** which is almost unobservable. This indicates that the tensile strength of the material is not largely influenced by the size of the tensile sample moulds, which is expected as the strength is normalised for geometry. As indicated in the statistical analysis, the sample mould type has no observable effect on the elongation at FPS.

Unfortunately, not all the ISO Type 1A moulds reached failure due to the transverse limitations of the tensile testing equipment. For this reason there are not many data points for the **elongation at break**. The predicted elongation at break is so high for ISO Type 1A as there are just not enough data points available for a good prediction. It is evident that ISO Type 1BA samples all attained a similar point of failure, close to the ISO Type 1A results that were obtained. This indicates that both sample mould sizes would potentially have similar elongations at break. Further work is needed, with a longer traverse area to accommodate the larger ISO Type 1A sample.

For all the mechanical properties there is no change due to clay type, which is corroborated by the statistical analysis.

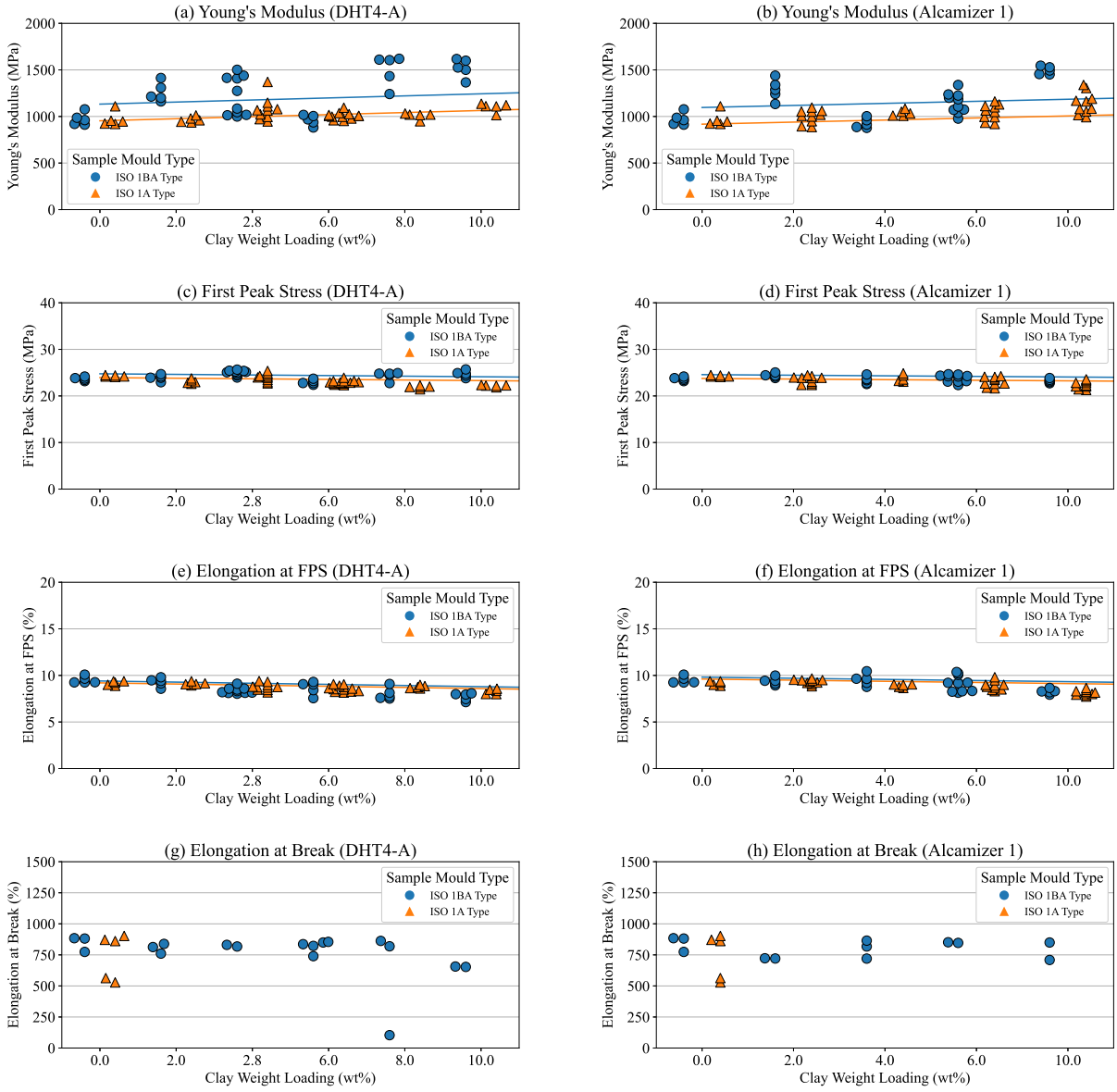

Figure 6.15: Effect of sample mould type on the mechanical properties for IPF injection moulded samples. The first column considers DHT4-A and the second column Alcamizer 1. Predicted values with the fitted linear model are plotted as a straight line.

It is clear from Figure 6.15 (a) and (b) that there are two distinct groupings, especially for the replicate samples. This is more prominent in the ISO 1BA samples. Tensile testing occurred on four different days: 11 November 2021, 26 November 2021, 4 January 2022, and 28 February 2022. It is therefore possible that testing conditions could have an influence. To investigate it as a possibility I include the testing dates for all the data for the two different mould types. Upon closer inspection both replicate sets for 2.8 wt% DHT4-A and 6 wt% Alcamizer were tested on different days as shown in Figure 6.16. There is a possibility that the different testing days have an influence on the mechanical properties which is evident with the different replicate groups, where replicates were tested on different days. However, when only considering the results of samples tested on 11 November 2021, we still see a clear variation in the Young's modulus between the ISO Type 1A and ISO Type 1BA which is

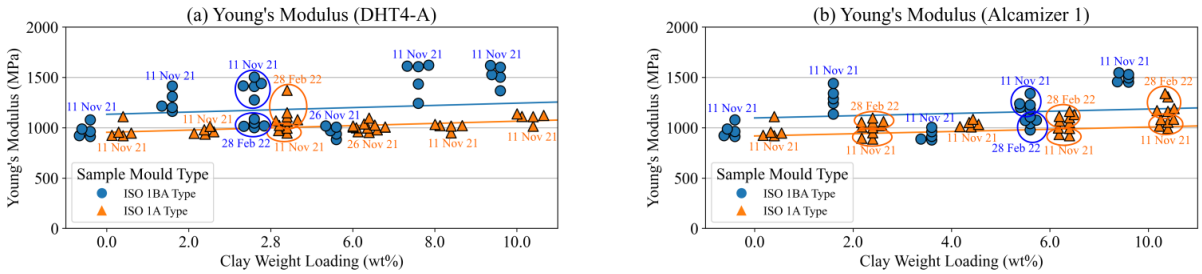

Figure 6.16: Effect of the testing date on the Young's modulus for IPF injection moulded samples for (a) DHT4-A and (b) Alcamizer 1. Predicted values with the fitted linear model are plotted as a straight line.

indicative of a size effect. The different tensile testing days therefore does not detract from the observed conclusion.

The effect of tensile sample mould type was a very unexpected result as tensile results are normalised to the sample geometry. It was observed however that the most prominent effect is on the Young's modulus which was indicated by the statistical analysis. The effect of the tensile sample mould geometry has not been reported previously in literature, most likely due to the same reason I initially thought there would be no effect. Nevertheless, this study has shown that it does have an effect on the mechanical properties. A potential influence could be the skin effects (*i.e.*, surface area to bulk volume of the sample) which form during cooling of the samples. Meister *et al.* (2013) showed that when scaling down the dogbone specimen dimensions from an ISO 1A there is a clear reduction in Young's modulus and yield stress (first peak stress in this thesis). They attributed this behaviour to a change in the polyamide morphology where there is a decrease in crystallinity with a decrease in sample size. Based on the morphological studies of Meister *et al.* (2013) there are clear grain boundaries for the larger sample sizes which reduce due to the accelerated cooling as the sample size reduces. For the very small sample sizes the grain boundaries are no longer visible although the visibility of the sheared and oriented portions based on the injection flow orientation increase. Additional studies are needed to understand the mechanics behind this effect.

6.4.4 Analysing in Isolation

A very interesting overall observation, especially when considering an overview of all the experimental results, is that if I had considered the results in isolation I would have drawn very different conclusions especially with regards to the material system.

Example 1: Analysing different sites in isolation

Consider the compression moulded (ISO Type 1BA) UP samples as shown in Figure 6.17. We observe that Alcamizer 1 has a higher Young's modulus than DHT4-A. This is unexpected as DHT4-A is designed to be compatible with polyolefins such as HDPE, whereas Alcamizer

1 is designed for PVC. There is an increase in stiffness for Alcamizer 1 with an increase in clay weight loading. For DHT4-A there is a sharp decrease at 6 wt% before increasing again. The FPS, elongation at FPS and impact strengths don't reveal much with an increase in clay weight loading. However, DHT4-A does have a larger variation than Alcamizer 1 for FPS and elongation at FPS. Elongation at break indicates a large variation which is expected in compression moulded samples due to the grain boundaries that are formed during the heating process. Wu *et al.* (2002) pointed out that the elongation at break is very sensitive to moulding conditions.

Now, consider the IPF compression moulded samples (ISO Type 1BA) as shown in Figure 6.18. There is a definite increase in Young's modulus with an increase in clay loading. DHT4-A tends to have a slightly higher stiffness and first peak stress than Alcamizer 1. This result is more expected as DHT4-A is designed for compatibility with HDPE, and Alcamizer 1 for PVC. The first peak stress is relatively constant exhibiting a decrease only at 10 wt% for both clay types. Notice that both clays tend to be more brittle with elongation at break being lower than 50 %. The impact strength is relatively constant although Alcamizer 1 tends to be slightly higher than DHT4-A.

If I had only viewed the first data set I would have questioned the validity of the results as I didn't expect Alcamizer 1 to perform better than DHT4-A. In fact, this is exactly what occurred when analysing the historical data in Chapter 2 and the motivation for this thesis.

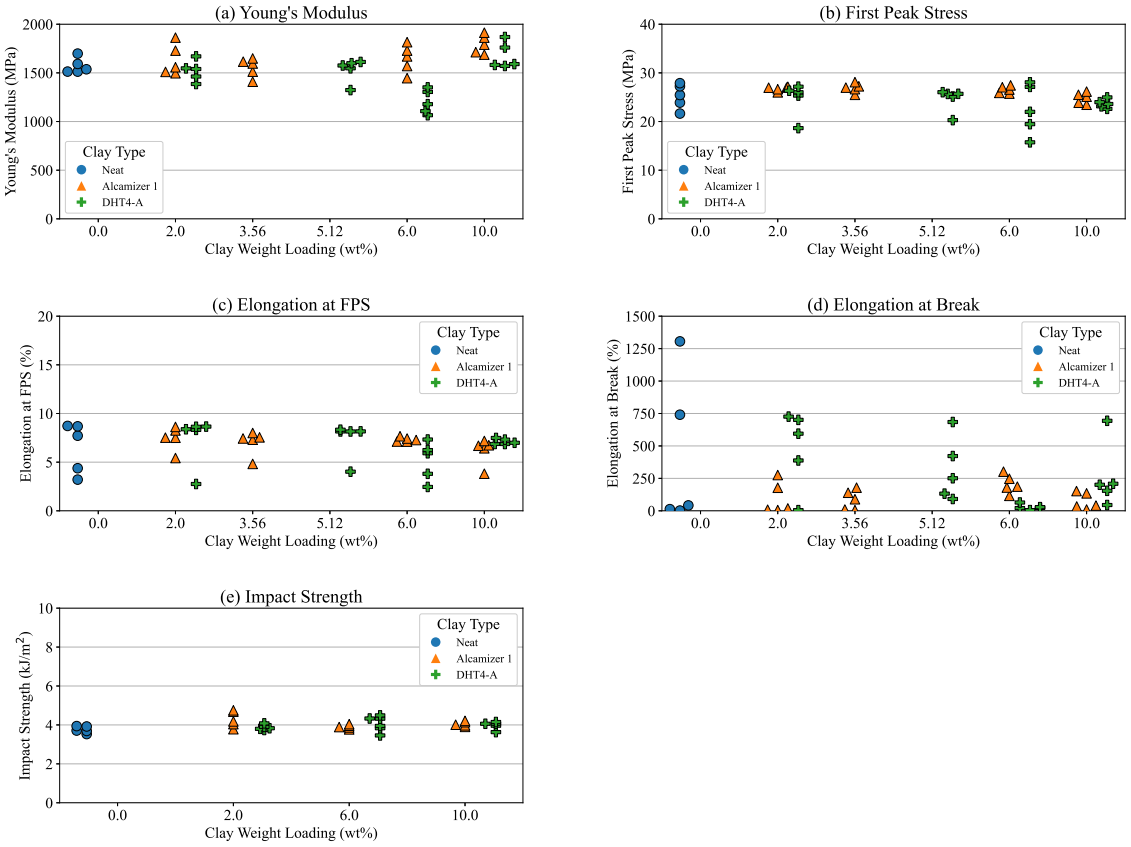

Figure 6.17: Exploratory data analysis of compression moulded (ISO Type 1BA) UP samples.

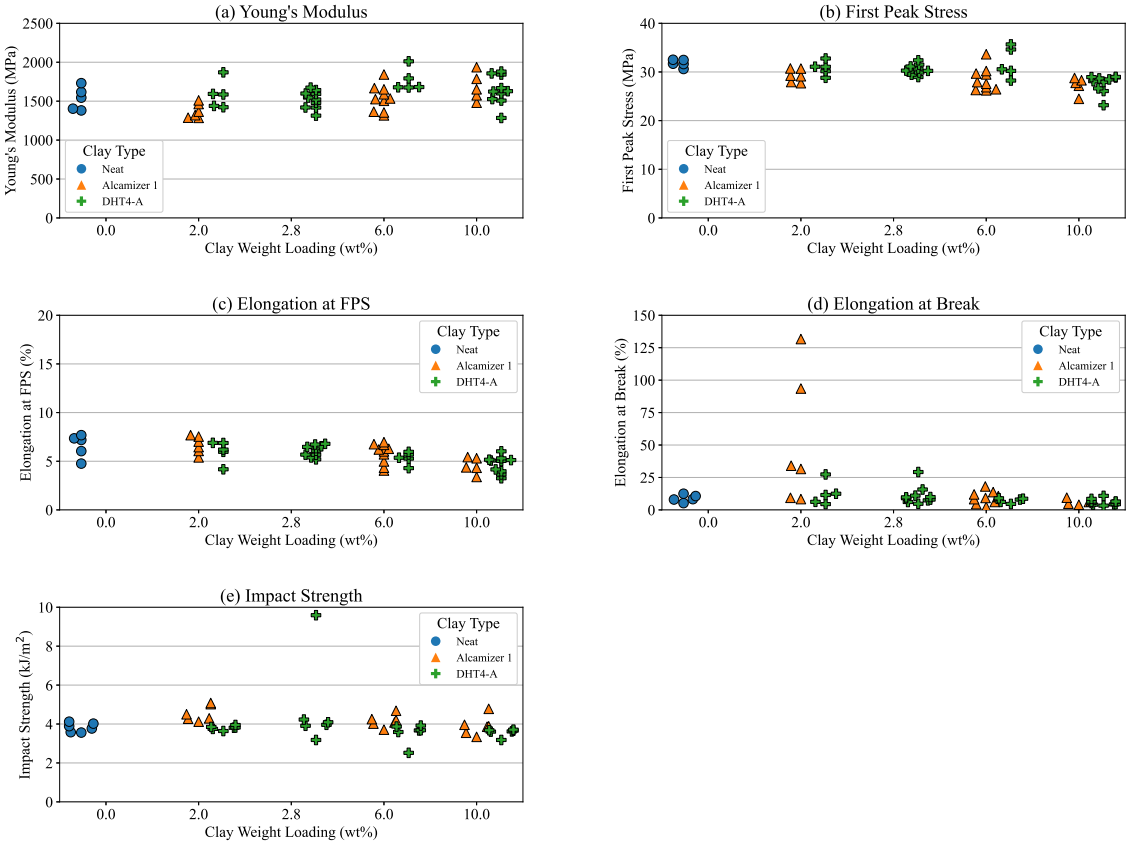

Figure 6.18: Exploratory data analysis of compression moulded (ISO Type 1BA) IPF samples.

On the other hand, if I had only viewed the second data set I would not have questioned the results as the clay performance is exactly as expected. Both experimental methods are identical with the only difference the site of compression moulding. As already observed, site has an influence on the overall mechanical properties, but I would not have been aware as this is not openly discussed in literature.

Example 2: Analysing different sites using different moulds in isolation

Consider injection moulded samples from IPF using the ISO Type 1BA mould shown in Figure 6.19. Clay loading has a clear influence on both Young's modulus and impact strength for both clay types. Alcamizer 1 has a higher impact strength compared to DHT4-A. Clay type is similar for the remaining mechanical properties which is unexpected. As Alcamizer 1 is not compatible with HDPE, I would expect it to have a worse performance compared to DHT4-A which is compatible. I would expect clay loading to have a more pronounced effect on all mechanical properties.

Now, consider injection moulded samples from TUT using the ISO Type 1A mould shown in Figure 6.20. The effect due to clay loading is neglible, except in the impact strength at 6 wt% and Young's modulus at 10 wt%. Both clays have similar performance, except for impact strength at 6 wt% where Alcamizer 1 is a higher strength than DHT4-A. Very few samples

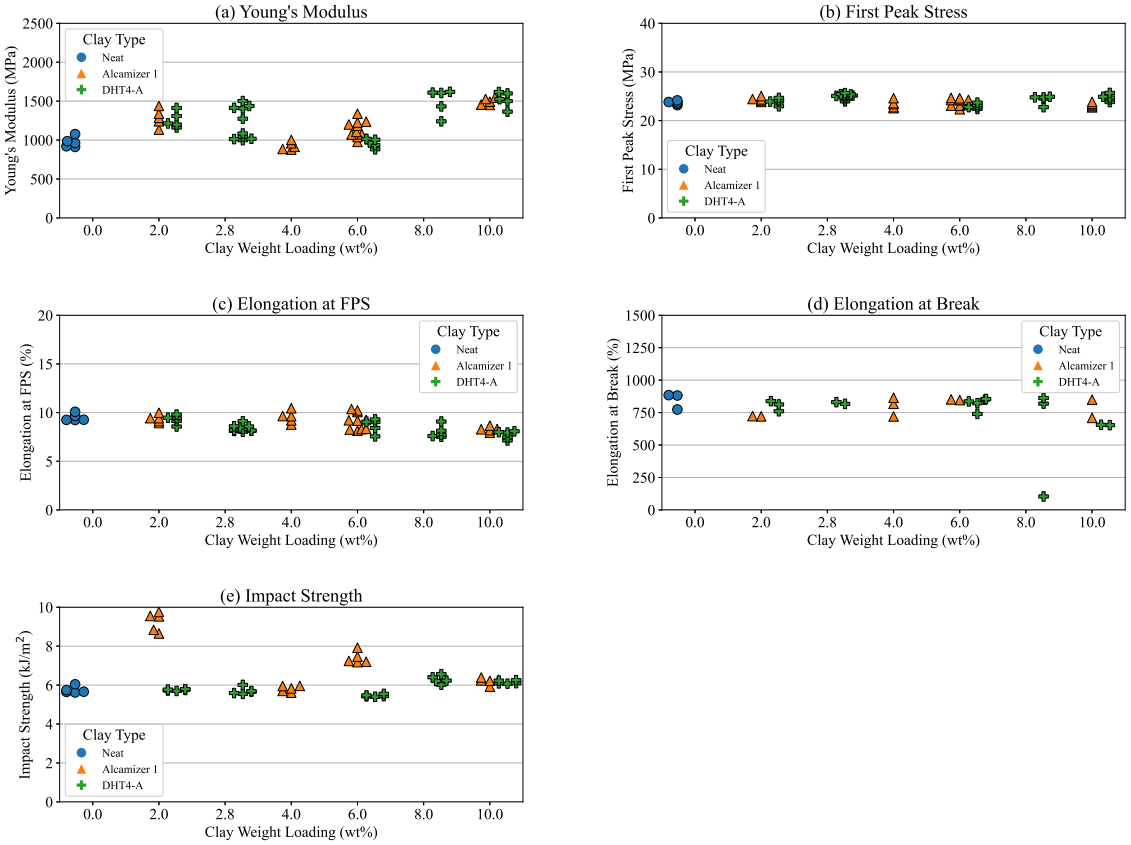

Figure 6.19: Exploratory data analysis of injection moulded (ISO Type 1BA) IPF samples.

reached failure, due to the limitation on the tensile testing machine traverse length. As a result there are only two data points, which do not provide any useful insight.

This example considered injection moulded samples with different sample mould types at different sites. As I've already shown, both the site and sample mould size have an influence on the mechanical properties. For the sample mould size this is most prevalent in the material stiffness, whereas the site influenced the material strength and ductility. This is clear when considering first data set where Young's modulus provided variation in the stiffness as well as higher stiffness values than the second data set. This would not have been noticeable when analysing the data in isolation. Similarly, the first data set illustrated that clay loading does have an effect, which is expected and known. However, the second data set showed no noticeable effects due to clay loading.

It is clear from both examples that analysing results in isolation can result in very different observations and conclusions. Both examples considered the same conditions with variations in either site (Example 1) or site and sample mould type (Example 2). These examples illustrated that the choice of manufacturing can have a larger influence on the mechanical properties than the clay type or clay loading. This is an especially interesting observation as it provides insight into how important it is to consider multi-factor experiments as different conditions (*e.g.* moulding method, site, sample mould type) for the same material system can lead to very different conclusions if considered in isolation.

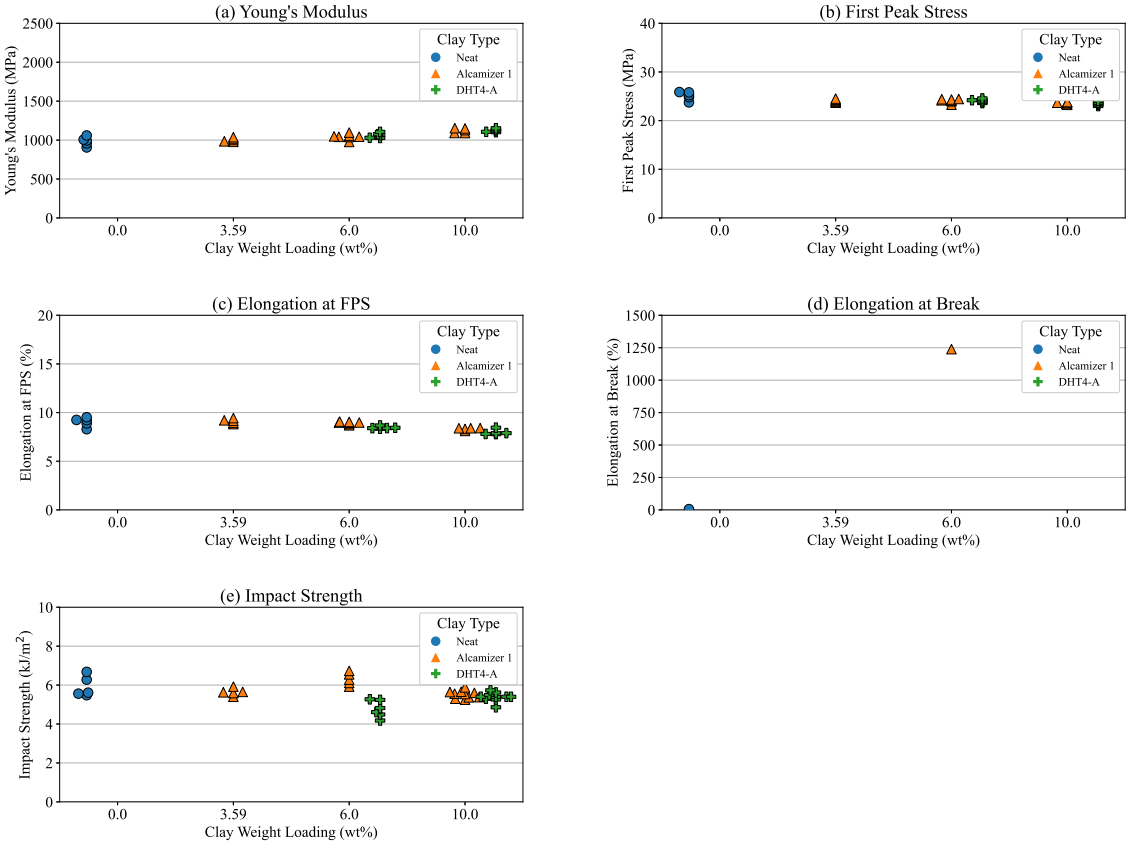

Figure 6.20: Exploratory data analysis of injection moulded (ISO Type 1A) TUT samples.

6.5 Conclusion

This chapter presented the results from the thesis experimental study highlighting the effects of the design factors on the mechanical properties of interest. Through statistical analysis the aim was to better understand the effects of manufacturing choices (*e.g.* moulding method, sample mould type and site) on the mechanical properties of HDPE/LDH composites.

Injection moulded samples were found to be more ductile than compression moulded samples, although compression moulded samples had a larger stiffness and first peak stress. This was observed in the tensile curves and corroborated through the ANOVA which indicated that moulding method has a strong influence on the mechanical properties, especially elongation at break, impact strength and Young's modulus. The higher Young's modulus and first peak stress in compression moulded samples is contrary to literature (which considered MMT) where injection moulded samples had higher values. This is attributed to changes in the composite morphology which ultimately affect the mechanical properties. Firstly, the chemical difference between LDH and MMT can affect the clay-polymer interaction. Secondly, the inconsistent heating distribution of compression moulded samples can lead to agglomerations or weak inter-polymer pellet boundaries with no chain entanglement which could increase material stiffness and strength while decreasing ductility.

The influence of machine variation (or site) was considered by comparing university equipment

to state-of-the-art equipment. The influence of site was more prevalent in the compression moulded samples from UP and IPF, whereas the injection moulded samples from TUT and IPF showed similar mechanical properties. This indicates that mechanical properties from compression moulding are more sensitive to a variation in machine, most likely due to the differences in heating which affect the polymer pellet boundaries. The statistical analysis indicated that elongation at break and first peak stress had the strongest relationship with site.

A more unexpected result was the influence of sample mould type on the mechanical properties, especially elongation at break and Young's modulus. From the tensile curves it was obvious that ISO Type 1A experienced almost double the elongation than ISO Type 1BA. This observation is surprising as the mechanical properties from a tensile curve are normalised for the sample geometry, and it should therefore not have any influence. The size effect can potentially be attributed to the skin effects which form during sample cooling. This is an important result which will have a significant influence when upscaling manufacturing from a laboratory setting to bulk material processing.

Through a detailed statistical analysis and investigation of the mechanical properties this chapter clearly shows that manufacturing variations had a much larger effect on the mechanical properties than the material system in this study. In fact, the results have shown that the mechanical properties are very sensitive to changes in manufacturing.

Two novel contributions to the field of polymer composites emanated from this chapter. These include the influence of tensile sample mould type and site (or machine variation). Both were surprising as intuition would dictate that these do not have any influence.

CHAPTER 7

CONCLUSIONS

7.1 Summary of Findings

The aim of this thesis was to better understand the effects of manufacturing on the mechanical properties of HDPE/LDH composites. By means of a multi-site collaborative experimental study and rigorous statistical analysis, this was successfully demonstrated in the thesis. A summary of the main findings and conclusions for each section of work in this thesis are presented here.

7.1.1 Historical Data Analysis

The motivation for this project was to explain the variability observed in the historical tensile test data, generated by undergraduate students between 2016 and 2018. The question was whether this variability was inherent in the material system, was due to the manufacturing process or was a result of inexperienced operators. To determine the extent of the variability an exploratory data and statistical analysis was conducted on the historical data, with key findings listed below.

- It was found that clay type (Alcamizer 1 and DHT4-A), sample cooling (air, quenched and furnace) and strain rate had a statistically significant effect on both the first peak stress and elongation to failure.
- Interestingly, Alcamizer 1 had a better first peak stress compared to DHT4-A which was very unexpected as Alcamizer 1 is developed for polyvinyl chloride (PVC) and therefore not compatible with poly-olefins such as HDPE.
- The number of extrusions only had a statistically significant effect on the normalised elongation to failure.
- Polymer grade, clay loading and press time had no statistically significant effects.

The historical studies had the goal of investigating the effect of clay loading with a carefully chosen polymer-clay system. However, we found that the material system (*e.g.* polymer grade and clay loading) had very little influence on the mechanical properties compared to manufacturing (*e.g.* sample cooling and number of extrusions) and testing (*e.g.* strain rate) parameters. That is, the composite system is more sensitive to the manufacturing process than expected.

In response to the historical data analysis, the research question of this thesis was developed: *How do variations in manufacturing influence the mechanical properties of polymer-clay composites?* The current study was formulated to carefully investigate the influence of both material and manufacturing parameters on the mechanical behaviour of the composite system.

7.1.2 Systematic Literature Review

For more insight into the manufacturing landscape of polymer-clay composites I conducted an in depth literature review, together with colleagues, using the Preferred Reporting Items for Systematic Reviews and Meta-Analysis (PRISMA) guidelines. The PRISMA guidelines allowed us to present a review which is reliable and reproducible. For this review we considered HDPE/MMT as opposed to HDPE/LDH, simply because it is more commonly used in literature. As LDH is a synthetic alternative to MMT, it should theoretically be possible to extrapolate the observations for HDPE/LDH composites. In this review we considered 33 studies categorised into blending protocol (the order in which material components are premixed or compounded together), compounding method, compounding conditions, processing method and processing conditions.

- For blending protocols it was found that by producing a clay/compatibiliser masterbatch, Young's modulus can be improved although this does decrease material ductility. Conversely, direct mixing (*i.e.*, mixing all the material components together at once) improves the material ductility while decreasing material stiffness.
- For compounding methods the best overall material strength was obtained using twin-screw extrusion. Whereas internal mixing provided the best overal material stiffness. Both these methods enhance the level of dispersion of the clay within the polymer matrix.
- Compounding conditions are very important and affect the degree of dispersion. Low temperatures with high rotational speeds will promote high shear increasing the dispersion of clay within the polymer matrix. Whereas high temperatures and high speeds at longer mixing times will degrade the clay surface, thereby reducing its ability to disperse properly.
- For processing methods it was found that injection moulding offers an improved material stiffness, strength and ductility when compared to compression moulding.

- Processing conditions have an influence on the mechanical properties with foaming time improving the material stiffness at the cost of material ductility. Sample cooling (air, water and hot plate) affect the material stiffness.

The most notable finding from the review is that all these methods and conditions play an important role in the composite morphology. The degree of intercalation of the clay within the polymer matrix is strongly influenced by the blending protocol, compounding method and conditions. Processing methods and conditions, on the other hand, affect the composite crystallinity, potential clay agglomerates and polymer pellet boundaries. These changes in composite morphology, as a result of manufacturing, have a direct effect on the mechanical properties of HDPE/MMT composites. Given that manufacturing has an important influence on mechanical properties it is significant that this is seldom explicitly studied. The remainder of the thesis addresses this gap.

7.1.3 Experimental Methodology and Statistical Design of Experiments

The design of the experimental methodology was informed by the early investigations. The historical analysis indicated that **clay type**, **clay loading** and **strain rate** are potential variables of interest, and these were included as factors in the study. From the systematic literature review it was clear that research into processing methods is needed, therefore **injection and compression moulding** were compared. The effect of **manufacturing equipment** was investigated by comparing university laboratory equipment with equipment at a state-of-the-art facility. This led to the design of the following multi-site collaborative protocol:

- An HDPE/LDH composite system was studied, using Alcamizer 1 and DHT4-A as the LDH clays and HDPE C7260 as the polymer matrix.
- All compounding was performed at the Council for Scientific and Industrial Research (CSIR, South Africa).
- Compression and injection moulding at the Leibniz Institute for Polymer Research (IPF, Germany) was compared with compression moulding at the University of Pretoria (UP, South Africa) and injection moulding at Tshwane University of Technology (TUT, South Africa).
- Tensile and impact testing was done at IPF.
- For each activity, a single operator handled all samples, meaning that operator variability was included in the comparison between sites.
- As far as possible, processing conditions were identical between the different sites, with the only difference the specific machine being used and the operator.

To ensure a rigorous study, I considered a statistical design of experiments (DoE) approach to develop the experimental plan for my research. DoE is an important tool which can be used to design an experiment given a large number of factors to investigate. The aim of statistical DoE is to efficiently study a design space and to allow reliable quantification of the influence of the different design factors.

Statistical DoE is not well known or frequently used in the field of polymer-clay composites. I therefore provided an introduction to the topic comparing different methods in two case studies. Response surface method designs (Taguchi, Central Composite Design, Box-Behnken and D-optimal) were considered. In the first case study I only considered continuous factors (numerical variable) and in the second case study I included a categorical factor (non-numerical variable, normally a name). From these case studies I found that D-optimal designs were more efficient than the other designs, with higher D- and G-efficiencies, while requiring fewer experiments.

A D-optimal approach was therefore employed to design the experiments. Two DoE's, one for tensile and one for impact testing, were initially developed, with clay type, clay loading, moulding method, site (*i.e.* machine variation) and strain rate (for tensile testing) as factors. During the design phase we identified a mismatch between available tensile sample moulds, with TUT only having an ISO Type 1A injection mould, and the compression moulded plaque sizes only allowing for an ISO Type 1BA. A third DoE was therefore designed to investigate the effect of tensile sample mould type during tensile testing. For this DoE, different clay types and loadings as well as different mould types were investigated for injection moulded samples produced at IPF.

Tensile and impact testing were conducted to obtain the mechanical properties of interest (Young's modulus, first peak stress, elongation to FPS, elongation to failure, impact strength), which were then analysed using statistical analysis to provide further insight into the different effects. For the statistical analysis a linear regression prediction model was developed to relate the factors with the mechanical properties of interest. This model was used in an analysis of variance (ANOVA) to determine statistical significance for the different design factors. During implementation, it was discovered that the planned strain rate variation could not be investigated. The strain rate was therefore removed as a factor of interest from the first tensile testing DoE. This serves as an example of the simplicity with which a design can be amended, without compromising the validity of the results obtained.

7.1.4 Experimental Results

The statistical analysis revealed that moulding method and sample mould type had a statistically significant effect on all the mechanical properties. Site (*i.e.* machine variation) had a statistically significant effect on all the mechanical properties, except Young's modulus. Clay loading had a statistically significant effect on all the mechanical properties, except elongation

at break and impact strength. Clay type only had a statistically significant effect on impact strength.

The data showed far less variability than observed in the historical data. This indicates that much of the variability in the historical data can be attributed to the inexperienced operators, as the same material system was considered, using the same university equipment. Both Alcamizer 1 and DHT4-A provided similar mechanical behaviours, with clay type not having a statistically significant effect. It is still interesting that we are not seeing the expected behaviour based on polymer compatibility of the clay types.

This thesis quantified the strength of these relationships through a descriptive statistics variable known as ω^2. These results allow us to clearly demonstrate the influence of manufacturing variation on mechanical properties.

- As expected, **moulding method** has a large influence on both tensile and impact properties. Elongation at break and impact strength, both measures of ductility, are higher for injection moulding. We note an unexpected (but small) effect on Young's modulus in this study, with the compression moulded samples being stiffer than the injection moulded samples. The difference between compression moulded and injection moulded samples can be attributed to the heating distribution of the process. For compression moulded samples an inconsistent heating distribution could lead to improperly fused polymer pellet boundaries which will increase brittleness.
- **Machine variation** was investigated by comparing university equipment to state-of-the-art equipment and was shown to have an effect on the mechanical properties. This effect was most prevalent in the compression moulded samples between UP and IPF, with almost no effect between TUT and IPF for injection moulded samples. For the compression moulded samples, the different sites influenced the first peak stress and elongation at break. This is attributed to the polymer pellet boundaries which are more influenced during compression moulding due to inconsistent heating. This indicates that different compression moulding machines form different polymer pellet boundaries.
- The **tensile sample mould type** had a significant effect on the mechanical properties. The ISO Type 1A is larger than ISO Type 1BA, but otherwise very similar in proportion. Since the mechanical properties are normalised to the sample geometry we did not expect to see an effect. ISO Type 1A had twice the elongation to failure of ISO Type 1BA. Additionally, ISO Type 1BA had a higher stiffness than ISO 1A. This could be due to the skin effects which are formed during sample cooling. The observed size effect is a critically important finding as it brings into question the transferability of mechanical testing results to bulk material processing.

7.2 Limitations and Lessons Learnt

From a practical point of view there were several roadblocks during the execution of the experimental methodology. Firstly, the polymer (HDPE C7260) chosen for this study has since been discontinued by Safripol South Africa. It is therefore not possible to recreate the current study or to conduct the necessary additional morphological studies for further insight. The second roadblock was the onset of Covid-19 and strict lockdown restrictions at the point when experimental work had to be conducted. As a consequence, instead of going to the IPF in Germany myself to conduct the tensile tests, all material and samples were shipped. However, during shipping there were significant material losses as a result of contaminated cases which required an amendment of the developed DoEs. The final roadblock was miscommunication due to assumptions I made about the equipment and processes at the collaborating laboratories. This resulted in additional samples manufactured and tested which weren't required, and some data missing that was originally defined in the DoE. Nevertheless, a major advantage of DoE is that it covers the full design space within the experimental design and is therefore still effective and able to provide statistical insights despite these limitations.

Statistical Design of Experiments (DoE) was a key focus of the study to ensure rigorous scientific study. As such it is important to discuss the practicalities of implementing a DoE. In this study I came across two situations which affected the DoE:

- During shipping of the material from South Africa to Germany a lot of material was lost when customs searched the parcels. This search resulted in contaminated material. I amended the DoE by only removing one of the variables, strain rate and any design points which only varied the strain rate. This exercise showed that it is quite easy to adapt the DoE without having to develop a new one which will potentially change the initial composition of the material (*i.e.* clay type, and clay and polymer weight loadings). This amendment didn't affect the effectiveness of the design.
- During testing of the mechanical properties of interest there was a miscommunication between myself, my collaborators in Germany and the technicians conducting the testing. The developed DoE was not followed exactly and as a result there were some missing data points while also obtaining additional data not in the planned DoE. This did not have a negative influence on the resulting data analysis which provided statistically significant observations. This is due to the main advantage of a DoE approach. The full experimental space in all the design variables is covered within the specified experimental design program and the effectiveness of the developed DoE is therefore not affected. This experience did, however, highlight the fact that the practical implementation of a multi-site DoE requires clear, unambiguous and ongoing communication.

There are clearly benefits to using a statistical experimental design approach even if it is not implemented precisely. The design still provides a more efficient approach to traditional experimentation, where one variable is varied at a time.

7.3 Conclusions

Composite morphology plays a large role in the mechanical properties obtained, and these are significantly affected by our manufacturing choices. The level of dispersion and interaction of the clay and polymer is determined by the compounding methods and conditions. This was clearly illustrated in the systematic literature review. This thesis focussed on processing methods, machine variation (*i.e.*, different sites) and tensile sample mould type. It was found that processing methods significantly affect the composite morphology, ultimately influencing the mechanical properties. During injection moulding the heat distribution is evenly spread throughout the composite as it travels through the barrel before being pressurised into the desired mould. In the mould, the melted composite is evenly spread out with a constant mould temperature which exhibits good interactions between the clay and polymer. The polymer pellet boundaries, which result because of the proper fusion between two polymer pellets to form a new continuous melt, are consistent and strong. This leads to more consistent overall mechanical properties as was observed in the thesis experimental results. For compression moulded samples the heat distribution is uneven often resulting in weaker polymer pellet boundaries due to the improper fusion of polymer pellets and a lack of polymer chain entanglement. This leads to a decrease in material ductility and an increase in material stiffness.

A limitation of this study is that we did not investigate the compression moulding size effect. This was initially assumed to not have an effect, since material properties are normalised to the sample geometry according to ISO standards, we assumed that there would be no difference in properties between different thickness compression moulded samples. There is very little literature which contradicts this assumption (Meister *et al.*, 2013). It was also not convenient at the time to study the size effect with compression moulding as there were limitations with the experimental equipment and availability of different mould sizes. We therefore only studied this effect with injection moulding where these limitations did not exist. Based on these studies we now know that it is possible for a size effect to exist based on manufacturing different size samples. We therefore cannot attribute the observed variability in compression moulding results between sites exclusively to machine variation until we have investigated the potential influence of a size effect."

7.3.1 Key Contributions from the Study

There are two novel contributions to the field from this thesis. The first is the influence of machine variation when manufacturing using the same process with identical settings. This influence is most pronounced in the compression moulded samples. This indicates that the composite morphology is particularly sensitive to variations in the compression moulding process. Different machines inherently result in different heating distributions thereby affecting the polymer pellet boundaries, and consequently the mechanical properties. In comparison, injection moulding, a newer technology, is less sensitive to machine variation. The second

contribution is the identification of a size effect for injection moulded tensile samples. The mechanical properties are clearly influenced by the mould size. The cause of this effect is not yet known, but could be due to differential heating or cooling or to changes in clay-polymer interactions.

A very important observation from the thesis was the care that should be taken when analysing results in isolation, and the importance of multi-faceted studies. This thesis clearly showed that it is possible to draw competing conclusions from the same studies conducted in slightly different circumstances. As scientists, we need to continually question our assumptions and accepted knowledge. This thesis has shown that expected results from the literature will not be obtained without careful control of manufacturing conditions. Clearly, a better understanding of how manufacturing choices affect composite morphology and hence mechanical properties is necessary. This will not only allow for better composite design practices with specific applications in mind, but to make better choices regarding the manufacturing approach for industrial scale manufacturing operations.

7.3.2 Recommendations for Future Research

This thesis opens some important avenues for future research. The immediate next step is a study which investigates changes in composite morphology, especially the level of intercalation of the clay in the polymer matrix, clay-polymer interactions and polymer pellet boundaries using scanning electron microscopy and transmission electron microscopy. This study should compare compression and injection moulded samples for an HDPE/LDH material system similar to the one considered in this thesis, manufactured at one facility.

An important second investigation should determine the true source of variation for the compression moulded samples. In this study a range of different mould sizes should be considered, including varying the mould thickness. These samples should also be manufactured at different sites to investigate machine variation.

It is also important to investigate the potential sources of machine variation considering the same process with identical settings. To isolate the potential sources of error it is recommended to design this new experiment considering a blocking technique. Blocking allows us to remove the effect of nuisance variables such as different operators, different time frames (compounding, moulding and testing) or slight variations in the material properties due to different batches if this source of variability is known and controllable (Montgomery, 2013). An experiment is designed in blocks (or groups) where each block contains some combination of the nuisance factors which are held constant such that only the factor of interest is varied (Montgomery, 2013).

Future investigations should also consider different material systems, where intercalation is attained, to see whether the effects of manufacturing are still as important. It is recommended to consider a polymer grafted with maleic anhydride which already includes compatibilisation to enhance the clay-polymer interactions. This study could also include varying the

compounding method to get better intercalation or exfoliation of the clay in the polymer matrix.

To investigate the size effect of the tensile samples, additional work should compare a range of different compression and injection mould sizes to see if there is a saturation point. A follow up study would then consider bulk processing and how it compares to the laboratory study by cutting tensile samples from the bulk processed component at different locations (*e.g.* near the surface, interior or diagonally).

BIBLIOGRAPHY

360 Research Reports (2022). Global hydrotalcite (cas 11097-59-9) industry research report, competitive landscape, market size, regional status and prospect. Available at: https://www.360researchreports.com/global-hydrotalcite-cas-11097-59-9-industry-research-report-competitive-landscape-market-21903188. Last viewed on 19 January 2023.

Agassant, J., Avenas, P., Carreau, P., Vergnes, B. and Vincent, M. (2017). *Polymer Processing: Principles and Modelling*, second edn, Hanser Publications.

Akhlaghi, S., Sharif, A., Kalaee, M., Elahi, A., Pirzadeh, M., Mazinani, S. and Afshari, M. (2012). Effect of stabilizer on the mechanical, morphological and thermal properties of compatibilized high density polyethylene/ethylene vinyl acetate copolymer/organoclay nanocomposites, *Materials and Design* **33**: 273–283.

Albdiry, M., Yousif, B., Ku, H. and Lau, K. (2012). A critical review on the manufacturing processes in relation to the properties of nanoclay/polymer composites, *Journal of Composite Materials* **47**: 1093–1115.

Anjana, R., Krishnan, A. K., Goerge, T. S. and George, K. E. (2014). Design of experiments for thermo-mechanical behavior of polypropylene/high-density polyethylene/nanokaolinite clay composites, *Polymer Bulletin* **71**: 315–335.

Ardanuy, M., Velasco, J., Maspoch, M., Haurie, L. and Fernández, A. (2009). Influence of emaa compatibilizer on the structure and properties of hdpe/hydrotalcite nanocomposites prepared by melt mixing, *Journal of Applied Polymer Science* **113**: 950–958.

Asgari, M., Abouelmagd, A. and Sundararaj, U. (2017). Silane functionalization of sodium montmorillonite nanoclay and its effect on rheological and mechanical properties of HDPE/clay nanocomposites, *Applied Clay Science* **146**: 439–448.

Asim, M., Jawaid, M., Saba, N., Ramengmawii, Nasir, M. and Sultan, M. (2017). *Hybrid Polymer Composite Materials: Processing*, Woodhead Publishing, chapter Chapter 1: Processing of hybrid polymer composites - a review, pp. 1–22.

ASTM D256-10 (2018). Standard test methods for determining the izod pendulum impact resistance of plastics, *Technical report*, ASTM International, West Conshohocken, PA, United States. www.astm.org.

ASTM D638-14 (2014). Standard test method for tensile properties of plastics, *Technical report*, ASTM International, West Conshohocken, PA, United States. www.astm.org.

ASTM D6610-18 (2018). Standard test method for determining the charpy impact resistance of notched specimens of plastics, *Technical report*, ASTM International, West Conshohocken, PA, United States. www.astm.org.

Ataman Chemicals (2020). Hydrotalcite. Available at: https://www.atamanchemicals.com/hydrotalcite_u25176/. Last viewed on 19 January 2023.

Atkinson, A., Donev, A. and Tobias, R. (2007). *Optimum Experimental Designs, with SAS*, Oxford University Press.

Azeez, A., Rhee, K., Park, S. and Hui, D. (2013). Epoxy clay nanocomposites – processing, properties and applications: A review, *Composites Part B: Engineering* **45**: 308–320.

Barbosa, R., Morais, D., Nóbrega, K., Araújo, E. and Mélo, T. (2012). Influence of processing variables on the mechanical behavior of HDPE/clay nanocomposites, *Materials Research* **15**: 477–482.

Boran, S., Kiziltas, A., Kiziltas, E., Gardner, D. and Rushing, T. (2017). Nanoclay reinforced polyethylene composites: Effect of different melt compounding methods, *Polymer Engineering and Science* **57**: 324–334.

Botha, N., Coetzer, R., Inglis, H. and Labuschagne, F. (2019). Understanding the influence of manufacturing and material parameters on the mechanical properties of polymer-clay composites: An exploratory statistical analysis, *ChemRxiv Preprint*. Available from: https://doi.org/10.26434/chemrxiv.10247522.v1.

Botha, N., Coetzer, R., Inglis, H. and Labuschagne, F. (2020). Understanding the influence of manufacturing and material parameters on the mechanical properties of polymer-clay composites: An exploratory statistical analysis, *AIP Conference Proceedings*, Vol. 2289, pp. 020061(1–5). https://doi.org/10.1063/5.0028759.

Botha, N., Inglis, H. and Labuschagne, F. (2018). Analysis of mechanical property degradation in polymer nanoclay composites, *Advances in Composites, Biocomposites and Nanocomposites*, Vol. 3, pp. 108–120.

Botha, N., Inglis, H., Coetzer, R. and Labuschagne, F. (2021). Statistical design of experiments: An introductory case study for polymer composites manufacturing applications, *MATEC Web of Conferences, 12^th South African Conference on Computational and Applied Mechanics (SACAM2020)*, Vol. 347, pp. 00028(1–12). https://doi.org/10.1051/matecconf/202134700028.

Bowden, G., Pichler, B. and Maurer, A. (2019). A design of experiments (doe) approach accelerates the optimization of copper-mediated ^{18}f-fluorination reactions of arylstannanes, *Scientific Reports* **9**: 11370. https://doi.org/10.1038/s41598-019-47846-6.

Box, G. and Liu, P. (1999). Statistics as a catalyst to learning by scientific method part i - an example, *Journal of Quality Technology* **31**(1): 1–15.

Brandenburg, R., Lofi, A., Lepienski, C., Coelho, L. and Becker, D. (2014). Influence of mixing in mechanical properties of clay and carbon nanotube and high density polyethylene, *AIP Conference Proceedings*, Vol. 1593, pp. 261–264. https://doi.org/10.1063/1.4873777.

Braun, K. T. (2018). A statistical investigation into the effects that additives have on the tensile properties of polymer-clay nanocomposites using a Taguchi's design of experiments, *Final year undergraduate research project (MRN 422)*, Department of Mechanical and Aeronautical Engineering, Faculty of Engineering, Built Environment and Information Technology, University of Pretoria.

Bucknall, C., Altstädt, V., Auhl, D., Buckley, P., Dijkstra, D., Galeski, A., Gögelein, C., Handge, U., He, J., Liu, C.-Y., Michler, G., Piorkowska, E., Slouf, M., Vittorias, I. and Wu, J. (2020). Structure, processing and performance of ultra-high molecular weight polyethylene (iupac technical report). part 2: crystallinity and supra molecular structure, *Pure Applied Chemistry* **92**: 1485—-1501.

Callister, Jr., W. (2003). *Materials Science and Engineering: An Introduction*, sixth edn, John Wiley & Sons, Inc.

Campos-Requena, V., Rivas, B., Pérez, M. and Wilhelm, M. (2014). Application of design of experiments, response surface methodology and partial least squares regression on nanocomposites synthesis, *Polymer Bulletin* **71**: 1961–1982.

Chen, B., Evans, J., Greenwell, H., Boulet, P., Coveney, P., Bowden, A. and Whiting, A. (2008). A critical appraisal of polymer–clay nanocomposites, *Chemical Society Reviews* **37**: 568–-594.

Chen, J., Chen, J., Chen, H., Yang, J., Chen, C. and Wang, Y. (2013). Effect of compatibilizer and clay on morphology and fracture resistance of immiscible high density polyethylene/polyamide 6 blend, *Composites: Part B* **54**: 422–430.

Chen, R., Ahmad, S. and Gan, S. (2017). Characterization of recycled thermoplastics-based nanocomposites: Polymer-clay compatibility, blending procedure, processing condition, and clay content effects, *Composites: Part B* **131**: 91–99.

Cho, J. and Paul, D. (2001). Nylon 6 nanocomposites by melt compounding, *Polymer* **42**(3): 1083–1094.

Choudalakis, G. and Gotsis, A. (2009). Permeability of polymer/clay nanocomposites: A review, *European Polymer Journal* **45**: 967—-984.

Chu, D., Nguyen, Q. and Baird, D. (2007). Effect of matrix molecular weight on the dispersion of nanoclay in unmodified high density polyethylene, *Polymer Composites* **28**: 499–511.

Coetzer, R., Morgan, D. and Maumela, H. (2008). Optimization of a catalyst system through the sequential application of experimental design techniques, *Journal of Applied Statistics* **35**(2): 131–147.

Costa, F., Abdel-Goad, M., Wagenknecht, U. and Heinrich, G. (2005). Nanocomposites based on polyethylene and mg–al layered doublehydroxide. i. synthesis and characterization, *Polymer* **46**: 4447–4453.

Costache, M., Heidecker, M., Manias, E., Camino, G., Frache, A., Beyer, G., Gupta, R. and Wilkie, C. (2007). The influence of carbon nanotubes, organically modified montmorillonites and layered double hydroxides on the thermal degradation and fire retardancy of polyethylene, ethylene–vinyl acetate copolymer and polystyrene, *Polymer* **48**: 6532–6545.

Crosby, A. and Lee, J.-Y. (2007). Polymer nanocomposites: The "nano" effect on mechanical properties, *Polymer Reviews* **47**: 217–229.

Dabrowska, I., Fambri, L., Pegoretti, A. and Ferrara, G. (2013). Organically modified hydrotalcite for compounding and spinning of polyethylene nanocomposites, *eXPRESS Polymer Letters* **7**: 936–949.

Danch, A., Osoba, W. and Stelzer, F. (2003). On the α relaxation of the constrained amorphous phase in poly(ethylene), *European Polymer Journal* **39**: 2051–2058.

Department of Trade and Industry (2018). Industrial policy action plan 2018/19-2020/21: Economic sectors, employment and infrastructure development cluster, *Technical report*, Department of Trade and Industry, Republic of South Africa, Pretoria, Gauteng, South Africa. Available at: http://www.thedtic.gov.za/wp-content/uploads/IPAP.pdf. Last viewed on 8 September 2021.

DIN EN ISO 179-1 (2010). Plastics — determination of charpy impact properties — part 1: Non-instrumented impact test, *Technical report*, Deutsches Institut für Normung e.V. (DIN), Berlin, Germany. [German version].

DIN EN ISO 527-2 (2012). Plastics - determination of tensile properties - part 2: Test conditions for moulding and extrusion plastics, *Technical report*, Deutsches Institut für Normung e.V. (DIN), Berlin, Germany. [German version].

Ding, P. and Qu, B. (2006). Structure, thermal stability, and photocrosslinking characterization of hdpe/ldh nanocomposites synthesized by melt-intercalation, *Journal of Polymer Science Part B: Polymer Physics* **44**: 3165–3172.

Dorigato, A., Dzenis, Y. and Pegoretti, A. (2013). Filler aggregation as a reinforcement mechanism in polymer nanocomposites, *Mechanics of Materials* **61**: 79–90.

El-Fattah, A. A. and ElKader, E. A. (2018). Influence of different clays on the mechanical, thermal, and water absorption properties of recycled high-density polyethylene/wood flour hybrid composites, *Journal of Composite Materials* **52**: 1215–1226.

El-Sheikhy, R. and Al-Shamrani, M. (2015). On the processing and properties of clay/polymer nanocomposites CPNC, *Latin American Journal of Solids and Structures* **12**: 385–419.

Ellis, B. (2017). Statistical study of the mechanical properties of polymer-clay nanocomposites: A Python based analysis of experiments, *Final year undergraduate research project (MRN 422)*, Department of Mechanical and Aeronautical Engineering, Faculty of Engineering, Built Environment and Information Technology, University of Pretoria.

Esteki, B., Garmabi, H., Saeb, M. and Hoffmann, T. (2013). The crystallinity behavior of polyethylene/clay nanocomposites under the influence of water-assisted melt blending, *Polymer-Plastics Technology and Engineering* **52**: 1626–1636.

Eteläaho, P., Nevalainen, K., Suihkonen, R., Vuorinen, J., Hanhi, K. and Järvelä, P. (2009). Effects of direct melt compounding and masterbatch dilution on the structure and properties of nanoclay-filled polyolefins, *Polymer Engineering and Science* **49**: 1438–1446.

Fechter, R. (2016). Modelling and optimisation of flexible PVC compound formulation for mine cables, *Master's dissertation*, Department of Chemical Engineering, Faculty of Engineering, Built Environment and Information Technology, University of Pretoria.

Fechter, R., Sandrock, C., Kühnert, I. and Labuschagne, F. (2018). Modelling and optimisation of a flexible poly(vinyl cholride) compound formulation for mine cables, *Journal of Vinyl and Additive Technology* **25**: E44–E58.

Ferhoum, R., Aberkane, M., Hachour, K. *et al.* (2014). Analysis of thermal ageing effect (hold time-crystallinity rate-mechanical property) on high density polyethylene (hdpe), *International Journal of Materials Science and Applications* **2**(3): 109.

Frantz, J. (2000). g3data (version 1.5.2). https://github.com/pn2200/g3data/.

Fu, S., Sun, Z., Huang, P., Li, Y. and Hu, N. (2019). Some basic aspects of polymer nanocomposites: A critical review, *Nano Materials Science* **1**: 2–30.

Fu, S.-Y., Feng, X.-Q., Lauke, B. and Mai, Y.-W. (2008). Effects of particle size, particle/matrix interface adhesion and particle loading on mechanical properties of particulate-polymer composites, *Composites Part B: Engineering* **39**: 933–961.

Gao, F. (2004). Clay/polymer composites: The story, *Materials Today* pp. 50–55.

Gao, J., Zhang, Q., Wang, K., Fu, Q., Chen, Y., Chen, H., Huang, H. and Rego, J. (2012). Effect of shearing on the orientation, crystallization and mechanical properties of HDPE/attapulgite nanocomposites, *Composites: Part A* **43**: 562–569.

Gündoğdu, T., Deniz, I., Çalışkan, G., Şahin, E. and Azbar, N. (2014). Experimental design methods for bioengineering applications, *Critical Reviews in Biotechnology* pp. 1–21.

Gong, G., Nyström, B. and Joffe, R. (2013). Development of polyethylene/nanoclay masterbatch for use in wood-plastic composites, *Plastics, Rubber and Composites* **42**: 167–175.

Grellmann, W. and Seidler, S. (2013). *Polymer Testing*, second edn, Hanser Publications.

Hafshejani, K., Khorasani, S., Jahadi, M., Hafshejani, M. and Neisiany, R. (2019). Improving mechanical and thermal properties of high-density polyethylene/wood flour nanocomposites, *Journal of Thermal Analysis and Calorimetry* **137**: 175–183.

Hanemann, T. and Szabo, D. (2010). Polymer-nanoparticle composites: From synthesis to modern applications, *Materials* **3**: 3468–3517.

Heinemann, J., Reichert, P., Thomann, R. and Mülhaupt, R. (1999). Polyolefin nanocomposites formed by melt compounding and transition metal catalyzed ethene homo- and copolymerization in the presence of layered silicates, *Macromolecular Rapic Communications* **20**: 423–430.

Hetzer, M. and Kee, D. D. (2008). Wood/polymer/nanoclay composites, environmentally friendly sustainable technology: A review, *Chemical Engineering Research and Design* **86**: 1083–1093.

Heydari-Meybodi, M., Saber-Samandari, S. and Sadighi, M. (2015). A new approach for prediction of elastic modulus of polymer/nanoclay composites considering interfacial bonding: Experimental and numerical investigations, *Composites Science and Technology* **117**: 379–385.

Heymans, D. (2018). Modelling of particulate composites with finite element analysis in CalculiX, *Final year undergraduate research project (MRN 422)*, Department of Mechanical and Aeronautical Engineering, Faculty of Engineering, Built Environment and Information Technology, University of Pretoria.

Höfler, G., Lin, R. and Jayaraman, K. (2018). Rotational moulding and mechanical characterisation of halloysite reinforced polyethylenes, *Journal of Polymer Research* **25**: 132(1–10).

Huang, Z.-X., Zhou, L.-Y., Zhang, G.-Z., Qu, J.-P. and He, H.-Z. (2015). Study on the properties of polyethylene/montmorillonite nanocomposites prepared by a novel vane mixer, *Journal of Applied Polymer Science* **132**: 42600(1–9).

Hussain, F., Hojjati, M., Okamoto, M. and Gorga, R. (2006). Review article: Polymer-matrix nanocomposites, processing, manufacturing, and application: An overview, *Journal of Composite Materials* **40**: 1511–1575.

Hwang, S., Hsu, P., Yeh, J., Yang, J., Chang, K. and Lai, Y. (2009). Effect of clay and compatibilizer on the mechanical/thermal properties of microcellural injection molded low density polyethylene nanocomposites, *International Communications in Heat and Mass Transfer* **36**: 471–479.

Ibrahim, M., Manaff, M., Othman, M., Mustafa, N., Masrol, S. and Rafai, N. (2014). Optimisation of processing condition using Taguchi method on warpage for HDPE-clay composite, *Applied Mechanics and Materials* **660**: 28–32.

Jainal, M., Kamarludin, S., Akhbar, S. and Rahman, M. (2014). Preliminary study of development of HDPE/EVA/MMT/EFB nanohybrid biocomposite by using single screw extruder, *Applied Mechanics and Materials*, Vol. 493, pp. 715–720.

Jo, C. and Naguib, H. (2006). Effect of nanoclay and foaming conditions on the mechanical properties of HDPE/clay nanocomposite foams, *Proceedings of the International Conference on Thermoplastic Foam Processing & Technology, Society of Plastics Engineers*, pp. 134–140.

Jo, C. and Naguib, H. (2007a). Effect of nanoclay and foaming conditions on the mechanical properties of HDPE-clay nanocomposite foam, *Journal of Cellular Plastics* **43**: 111–121.

Jo, C. and Naguib, H. (2007b). Processing, characterization, and modeling of polymer/clay nanocomposite foams, *Journal of Physics: Conference Series* **61**: 861–868.

Jo, C. and Naguib, H. (2008). Modeling the effect of strain rate on the mechanical properties of HDPE/clay nanocomposite foams, *Polymers & Polymer Composites* **16**: 561–575.

Jordan, J., Jacob, K., Tannenbaum, R., Sharaf, M. and Jasiuk, I. (2005). Experimental trends in polymer nanocomposites–a review, *Materials Science and Engineering A* **393**: 1–11.

Khanam, P. and AlMaadeed, M. A. A. (2015). Processing and characterization of polyethylene-based composites, *Advanced Manufacturing: Polymer & Composites Science* **1**: 63–79.

Kisuma (2023). Applications. Available at: https://www.kisuma.com/applications. Last viewed on 19 January 2023.

Koodehi, A. and Koohi, A. (2018). Optimization of thermal stability of high-density polyethylene composite using antioxidant, carbon black and nanoclay addition by a central composite design method: X-ray diffraction and rheological characterization, *Journal of Macromolecular Science, Part B* **57**: 660–678.

Kotal, M. and Bhowmick, A. (2015). Polymer nanocomposites from modified clays: Recent advances and challenges, *Progress in Polymer Science* **51**: 127–187.

Kyowa Chemical Industry (2022). Products: Industrial applications, classified by substance - synthethic hydrotalcite. Available at: https://kyowa-chem.jp/en/products/ind_material03.php. Last viewed on 19 January 2023.

Labuschagne, F., Molefe, D., Focke, W., van der Westhuizen, I., Wright, H. and Royeppen, M. (2015). Heat stabilising flexible pvc with layered double hydroxide derivatives, *Polymer Degradation and Stability* **113**: 46—-54.

Lapshin, S., Swain, S. and Isayev, A. (2008). Ultrasound aided extrusion process for preparation of polyolefin-clay nanocomposites, *Polymer Engineering and Science* **48**: 1584–1591.

Leephakpreeda, T. (2001). Quantitative relation of crystallinity and crystallite's size to mechanical properties of semi-crystalline polymers application to hdpe, *Engineering Journal of Research and Development* **12**(2): 7–14.

Lei, Y., Wu, Q. and Clemons, C. (2007). Preparation and properties of recycled HDPE/clay hybrids, *Journal of Applied Polymer Science* **103**: 3056–3063.

Lew, C., Major, I., Murphy, W. and McNally, G. (2005). Optimise organoclay exfoliation in polymer nanocomposites by customising the extrusion temperature gradient, *ANTEC 2005 Conference Proceedings - Boston, Massachusetts, USA May 1-5, 2005. [Online]. Society of Plastic Engineers*, pp. 249–254.

Li, J., Jiang, G., Guo, S. and Zhao, L. (2007). Effects of ultrasonic oscillations on structure and properties of HDPE/montmorillonite nanocomposites, *Plastics, Rubber and Composites* **36**: 308–313.

Lim, K., Majid, M., Ridzuan, M., Basaruddin, K. and Afendi, M. (2017). Effect of nanoclay fillers on mechanical and morphological properties of napier/epoxy composites, *IOP Conference Series: Journal of Physics* **908**: 012010.

Lundstedt, T., Seifert, E., Abramo, L., Thelin, B., Nyström, A., Pettersen, J. and Bergman, R. (1998). Experimental design and optimization, *Chemometrics and Intelligent Laboratory Systems* **42**: 3–40.

Luo, J.-J. and Daniel, I. M. (2003). Characterization and modeling of mechanical behavior of polymer/clay nanocomposites, *Composites science and technology* **63**(11): 1607–1616.

Mainil, M., Alexandre, M., Monteverde, F. and Dubois, P. (2006). Polyethylene organoclay nanocomposites: The role of the interface chemistry on the extent of clay intercalation/exfoliation, *Journal of Nanoscience and Nanotechnology* **6**: 337–344.

Maniar, K. (2004). Polymeric nanocomposites: A review, *Polymer-Plastics Technology and Engineering* **43**: 427–443.

Meister, S., Vetter, K., Ehrenstein, G. W. and Drummer, D. (2013). Measurement of mechanical material properties for micro parts on injection molded micro tensile bars, *Journal of Plastics Technology* **9**: 74–99. [German].

Merinska, D., Kubisova, H., Kalendova, A. and Svoboda, P. (2012). Processing and properties of polyethylene/montmorillonite nanocomposites, *Journal of Thermoplastic Composite Materials* **25**: 115–131.

Minkova, L. and Filippi, S. (2011). Characterization of HDPE-g-MA/clay nanocomposites prepared by different preparation procedures: Effect of the filler dimension on crystallization, microhardness and flammability, *Polymer Testing* **30**: 1–7.

Mishra, S., Unnikrishnan, L., Nayak, S. and Mohanty, S. (2019). Advances in piezoelectric polymer composites for energy harvesting applications: A systematic review, *Macromolecular Matererials and Engineering* **304**: 1800463:1–25.

Mistretta, M., L. Botta, M. M., Rifici, S., Ceraulo, M. and Mantia, F. L. (2018). Injection molding and mechanical properties of bio-based polymer nanocomposites, *Materials* **11**: 613:1–14.

Mittal, G., Rhee, K., Mišković-Stanković, V. and Hui, D. (2018). Reinforcements in multiscale polymer composites: Processing, properties, and applications, *Composites Part B* **138**: 122–139.

Müller, K., Bugnicourt, E., Latorre, M., Jorda, M., Sanz, Y. E., Lagaron, J., Miesbauer, O., Bianchin, A., Hankin, S., Bölz, U., Pérez, G., Jesdinszki, M., Lindner, M., Scheuerer, Z., Castelló, S. and Schmid, M. (2017). Review on the processing and properties of polymer nanocomposites and nanocoatings and their applications in the packaging, automotive and solar energy fields, *Nanomaterials* **7**: 74(1–47).

Mochane, M., Motaung, T. and Motloung, S. (2018). Morphology, flammability, and properties of graphite reinforced polymer composites. systematic review, *Polymer Composites* pp. 1487–1499.

Modesti, M., Besco, S. and Lorenzetti, A. (2010). *Optimization of polymer nanocomposite properties*, Wiley-VCH Verlag GmbH & Co. KGaA, chapter Chapter 17: Effect of processing conditions on the morphology and properties of polymer nanocomposites, pp. 369–405.

Moghri, M. and Dragoi, E.-N. (2015). Effect of various material parameters on barrier properties of high-density polyethylene/polyamide 6/clay nanocomposites: Experimental and prediction using artificial neural networks, *Journal of Elastomers & Plastics* pp. 1–15.

Moghri, M., Garmabi, H. and Zanjanijam, A. (2018). Prediction of barrier properties of HDPE/PA-6/nanoclay composites by response surface approach: effects of compatibilizer type and the contents of nanoclay, PA-6 and compatibilizer, *Polymer Bulletin* **75**: 2751–2767.

Moghri, M., Shahabadi, S. and Madic, M. (2016). Modeling tensile modulus of (polyamide 6)/nanoclay composites: Response surface method vs. Taguchi-optimized artificial neural network, *Journal of Vinyl & Additive Technology* pp. 29–36.

Mohamadi, M., Garmabi, H. and Keshavarzi, F. (2014). Structural characterization of high-density polyethylene nanocomposites: effect of compatibilizer type and high aspect ratio organoclay platelets, *Polymer Bulletin* **71**: 2709–2731.

Mohamadi, M., Garmabi, H. and Keshavarzi, F. (2016). An investigation of the effects of organomodified-fluoromica on mechanical and barrier properties of compatibilized high density polyethylene nanocomposite films, *Journal of Plastic Film and Sheeting* **32**: 10–33.

Moher, D., Liberati, A., Tetzlaff, J. and Altman, D. (2009). Preferred reporting items for systematic reviews and meta-analyses: The PRISMA statement, *Annals of Internal Medicine* **151**: 264–270.

Moher, D., Shamseer, L., Clarke, M., Ghersi, D., Liberati, A., Petticrew, M., Shekelle, P., Stewart, L. and PRISMA-P Group (2015). Preferred reporting items for systematic reviews and meta-analysis protocols (PRISMA-P) 2015 statement, *Systematic Reviews* **4**: 1–9.

Montgomery, D. (2013). *Design and Analysis of Experiments*, eighth edn, John Wiley & Sons, Inc.

Montgomery, D. and Runger, G. (2007). *Applied Statistics and Probability for Engineers*, fourth edn, John Wiley & Sons, Inc.

Moyo, L., Focke, W., Heidenreich, D., Labuschagne, F. and Radusch, H.-J. (2013). Properties of layered double hydroxide micro- and nanocomposites, *Materials Research Bulletin* **48**: 1218—1227.

Moyo, L., Focke, W. W., Labuschagne, F. J. W. J. and Verryn, S. (2012). Layered double hydroxide intercalated with sodium dodecyl sulfate, *Molecular Crystals and Liquid Crystals* **555**: 51—-64.

Myers, R., Montgomery, D. and Anderson-Cook, C. (2016). *Response Surface Methodology: Process and product optimization using designed experiments*, fourth edn, John Wiley & Sons, Inc.

Najafabadi, M. A., Khorasani, S. N. and Esfahani, J. M. (2014). Water absorption behaviour and mechanical properties of high density polyethylene/ pistachio shell flour nanocomposites in presence of two different UV stabilizers, *Polymers & Polymer Composites* **22**: 409–416.

Namdeo, R., Tiwari, S. and Manepatil, S. (2017). Optimization of high stress abrasive wear of polymer blend ethylene and vinyl acetate copolymer/HDPE/MA-g-PE/OMMT nanocomposites, *Journal of Tribology* **139**: 021610–1–6.

Namdeo, R., Tiwari, S., Manepatil, S. and Chand, N. (2018a). Effect of addition of organomodified montmorillonite nanoclay on three-body abrasive wear behavior of maleic anhydride grafted polyethylene compatibilized ethylene-co-vinyl acetate/high density polyethylene nanocomposites, *Polymer Composites* pp. 3962–3968.

Namdeo, R., Tiwari, S., Manepatil, S. and Chand, N. (2018b). Experimental analysis of dry sliding friction and wear behavior of OMMT nanoclay added EVA/HDPE/MA-g-PE compatibilized polymer blends with parametric study of influencing factors, *Journal of Testing and Evaluation* **48**: 1122–1137.

Nevalainen, K., Vuorinen, J., Villman, V., Suihkonen, R., Järvelä, P., Sundelin, J. and Lepistö, T. (2009). Characterization of twin-screw-extruder-compounded polycarbonate nanoclay composites, *Polymer Engineering and Science* pp. 631–640.

Nguyen, Q. and Baird, C. (2006). Using SC-CO_2 as a processing aid for improving the properties of polymer nanocomposites, *ANTEC 2006 Conference Proceedings - Charlotte, North Carolina, USA May 7-11, 2006. [Online]. Society of Plastic Engineers*, pp. 268–272.

Nichols, G., Byard, S., Bloxham, M. J., Botterill, J., Dawson, N. J., Dennis, A., Diart, V., North, N. C. and Sherwood, J. D. (2002). A review of the terms agglomerate and aggregate with a recommendation for nomenclature used in powder and particle characterization, *Journal of pharmaceutical sciences* **91**(10): 2103–2109.

Nunes, M., Galvão, L., Ferreira, T., Luiz, E., Bastos, Y. and Santos, A. (2016). Reprocessability of high impact polystyrene/clay nanocmposites in extrusion, *Polymer Degradation and Stability* **125**: 87–96.

Oh, J., Isayev, A. and Rogunovab, M. (2003). Continuous ultrasonic process for in situ compatibilization of polypropylene/natural rubber blends, *Polymer* **44**: 2337–2349.

Olejnik, S. and Algina, J. (2000). Measures of effect size for comparative studies: applications, interpretations, and limitations, *Contemporary Educational Psychology* **25**: 241–286.

Oliveira, I., Visconte, L. and Vendramini, A. (2009). Mechanical, thermal and morphological characterization of high-density polyethylene and vermiculate composites, *International Journal of Polymeric Materials* **58**: 489–497.

Osman, M. and Atallah, A. (2004). High-density polyethylene micro- and nanocomposites: Effect of particle shape, size and surface treatment on polymer crystallinity and gas permeability, *Macromolecular Rapid Communications* **25**: 1540–1544.

Parschau, C. (2016). Influence of manufacturing parameters on the tensile properties of clay-polymer nanocomposites, *Final year undergraduate research project (MSC 422)*, Department of Mechanical and Aeronautical Engineering, Faculty of Engineering, Built Environment and Information Technology, University of Pretoria.

Passador, F., Ruvolo-Filho, A. and Pessan, L. (2014). Influence of blending protocol on the thermal and mechanical properties of HDPE/LLDPE blend-based nanocomposites, *AIP Conference Proceedings*, Vol. 1593, pp. 278–281.

Passador, F., Ruvolo-Filho, A. and Pessan, L. (2016). Influence of blending protocol on the thermal and mechanical properties of HDPE/LLDPE blend-based nanocomposites, *International Polymer Processing* **31**: 472–481.

Paul, D. and Robeson, L. (2008). Polymer nanotechnology: Nanocomposites, *Polymer* **49**: 3187—-3204.

Peng, Z., Li, Q., Li, H. and Hu, Y. (2017). Layered nanoparticles modified by chain end functional pe and their nanocomposites with pe, *Chinese Journal of Polymer Science* **35**: 897—-908.

Perktold, S., Perktold, S. and Perktold, J. (2010). statsmodels: Econometric and statistical modeling with python, *Proceedings of the 9th Python in Science Conference*.

Plastics SA (2020). Annual review 2019-2020. Available at: https://www.plasticsinfo.co.za/wp-content/uploads/2020/11/PlasticsSA-Annual-Report-20192020_colour-website.pdf. Last viewed on 8 September 2021.

Quaresimin, M., Schulte, K., Zappalorto, M. and Chandrasekaran, S. (2016). Toughening mechanisms in polymer nanocomposites: From experiments to modelling, *Composites Science and Technology* **123**: 187–104.

Raghavan, J. and Wool, R. (1999). Interfaces in repair, recycling, joining and manufacturing of polymers and polymer composites, *Journal of Applied Polymer Science* **71**: 775—-785.

Rahnama, M., Oromiehie, A., Ahmadi, S. and Ghasemi, I. (2017). Investigation of polyethylene-grafted-maleic anhydride presence as a compatibilizer on various properties of nanocomposite films based on polyethylene/ethylene vinyl alcohol/nanoclay, *Polymers Advanced Technologies* **28**: 449–462.

Ramachandran, A., George, K., George, T. and Krishnan, A. (2012). Optimisation of processing conditions of PP/HDPE/nano kaolinite clay composites by response surface methodology, *International Journal of Plastic Technology* **16**: 136–149.

Romo-Uribe, A. (2017). Polymers in 2D confinement: A nanoscale mechanism for thermomechanical reinforcement, *Polymers Advanced Technologies* **29**: 507–516.

Rong, M., Zhang, M. and Ruan, W. (2006). Surface modification of nanoscale fillers for improving properties of polymer nanocomposites: a review, *Materials Science and Technology* **22**: 787–796.

Rueda, M., Auscher, M., Fulchiron, R., Périé, T., Martin, G., Sonntag, P. and Cassagnau, P. (2017). Rheology and applications of highly filled polymers: A review of current understanding, *Progress in Polymer Science* **66**: 22–53.

Safripol (2018). Safrene technical datasheet: C7260, *Material datasheet*, KAP Diversified Industrial (Pty) Ltd, South Africa.

Salkind, N. (2010). Omega squared, *Encyclopedia of research design*, SAGE Publications, Inc., Thousand Oaks, CA. [Accessed 18 February 2022], DOI: 10.4135/9781412961288.

Sapuan, S., Haniffah, W., Al-Oqla, F., Nukman, Y., Hoque, M. and Sanyang, M. (2016). Effects of reinforcing elements on the performance of laster transmission welding process in polymer composites: a systematic review, *International Journal of Performability Engineering* **12**: 535–550.

Scaffaro, R., Botta, L., Mistretta, M. and Mantia, F. L. (2013). Processing-morphology-property relationships of polyamide6/polyethylen blend-clay nanocomposites, *eXPRESS Polymer Letters* **7**: 873–884.

Shahabadi, S. and Garmabi, H. (2012a). Polyethylene/Na^+-montmorillonite composites prepared by slurry-fed melt intercalation: Response surface analysis of rheological behavior, *Journal of Reinforced Plastics & Composites* **31**: 977–988.

Shahabadi, S. and Garmabi, H. (2012b). Response surface analysis of structural, mechanical, and permeability properties of polyethylene/Na^+-montmorillonite composites, prepared by slurry-fed melt intercalation, *eXPRESS Polymer Letters* **6**: 657–671.

Shamloo, A., Fathi, B., Elkoun, S., Rodrigue, D. and Soldera, A. (2017). Impact of compression molding conditions on the thermal and mechanical properties of polyethylene, *Journal of Applied Polymer Science* pp. 46176 (1–7).

Sheng, N., Boyce, M. C., Parks, D. M., Rutledge, G., Abes, J. and Cohen, R. (2004). Multiscale micromechanical modeling of polymer/clay nanocomposites and the effective clay particle, *Polymer* **45**(2): 487–506.

Silva, B., Nack, F. and Lepienski, C. (2014). Influence of intercalation methods in properties of clay and carbon nanotube and high density polyethylen nanocomposites, *Materials Research* **17**: 1628–1634.

Stat-Ease, Inc. (2009). Design-Expert® Software (version 8.0.0.). https://www.statease.com/software/design-expert/.

Swain, S. and Isayev, A. (2006). Ultrasonic assisted extrusion of HDPE/clay nanocomposites, *ANTEC 2006 Conference Proceedings - Charlotte, North Carolina, USA May 7-11, 2006. Society of Plastic Engineers*, pp. 923–927.

Swain, S. and Isayev, A. (2007). Effect of ultrasound on HDPE/clay nanocomposites: Rheology, structure and properties, *Polymer* **48**: 281–289.

Tadmor, Z. and Gogos, C. (2006). *Principles of Polymer Processing*, second edn, John Wiley & Sons, Inc.

Tanco, M., Viles, E. and Pozueta, L. (2009). *Advances in Electrical Engineering and Computational Science*, Springer Science and Business Media B.V., chapter 52: Comparing Different Approaches for Design of Experiments (DoE), pp. 611–621.

Telford, J. (2007). A brief introduction to design of experiments, *John Hopkins APL Technical Digest* **27**: 224–232.

Teymouri, Y. and Nazockdast, H. (2011). The effect of process parameters on physical and mechanical properties of commercial low density polyethylene/ORG-MMT nanocomposites, *Journal of Materials Science* **46**: 6642–6647.

The R Foundation (2019). The R Project for Statistical Computing (version 3.6.1). https://www.r-project.org/.

Tolinski, M. (2015). *Additives for polyolefins: getting the most out of polypropylene, polyethylene and TPO*, William Andrew.

Ujianto, O., Jollands, M. and Kao, N. (2018). Effect of processing variables on tensile modulus and morphology of polyethylene/clay nanocomposites prepared in an internal mixer, *IOP Conference Series: Material Science and Engineering* **319**: 012019.

Wang, J. and Wan, W. (2009). Experimental design methods for fermentative hydrogen production: A review, *International Journal of Hydrogen Energy* **34**: 235–244.

Wheeler, R. (2019). Package 'AlgDesign' (version 1.2.0). https://github.com/jvbraun/AlgDesign.

Wool, R., Yuan, B.-L. and McGarel, J. (1989). Welding of polymer interfaces, *Polymer Engineering and Science* **29**: 1340—-1367.

Wu, J., Buckley, C. and O'Connor, J. (2002). Mechanical integrity of compression-moulded ultra-high molecular weight polyethylene: effects of varying process conditions, *Biomaterials* **23**: 3773—-3783.

Xiang, Y., Hou, Z., Su, R., Wang, K. and Fu, Q. (2009). The effect of shear on mechanical properties and orientation of HDPE/mica composites obtained via dynamic packing injection molding (DPIM), *Polymers Advanced Technologies* **21**: 48–54.

Zabihi, O., Ahmadi, M., Nikafshar, S., Preyeswary, K. and Naebe, M. (2018). A technical review on epoxy-clay nanocomposites: Structure, properties, and their applications in fiber reinforced composites, *Composites Part B* **135**: 1–24.

Zare, Y. (2016). Study of nanoparticles aggregation/agglomeration in polymer particulate nanocomposites by mechanical properties, *Composites Part A: Applied Science and Manufacturing* **84**: 158–164.

Zare, Y. and Rhee, K. Y. (2019). A simulation work for the influences of aggregation/agglomeration of clay layers on the tensile properties of nanocomposites, *JOM* **71**(11): 3989–3995.

Zawawi, E., Ahmad, S. and Rashid, R. (2012). Effect of melt-blending conditions on the properties of HDPE/NR-blends/organoclay nanocomposites, *Advanced Materials Research*, Vol. 576, pp. 322–325.

Zhang, G., Wu, T., Lin, W., Tan, Y., Chen, R., Huang, Z., Yin, X. and Qu, J. (2017). Preparation of polymer/clay nanocomposites via melt intercalation under continuous elongation flow, *Composites Science and Technology* **145**: 157–164.

Zhao, L., Li, J., Guo, S. and Du, Q. (2006). Ultrasonic oscillations induced morphology and property development of polypropylene/montmorillonite nanocomposites, *Polymer* **47**: 2460–2469.

APPENDIX A: HISTORICAL TENSILE DATA

This appendix contains additional information with regards to the historical tensile data analysis discussed in Chapter 2. That is, all the unprocessed vs. processed tensile (stress-strain) curves from the historical studies. If you are interested, more details regarding the experimental work for a specific year can be found in Parschau (2016), Ellis (2017), Braun (2018) and Heymans (2018). In addition to this, in 2020 I conducted a preliminary experimental study to test the compression moulding equipment and differences in procedure between University of Pretoria and Leibniz Institute of Polymer Research Dresden (IPF).

A quick overview of all the available historical data is provided in Table A.1. The Type V dogbone sample size was used in 2020 because of the sizing limitations on the compression moulding equipment at the IPF. The dogbone geometry with relevant dimensions is shown in Figure A.1 for both Type I and V.

Table A.1: Overview of the available historical tensile data.

Year	Design Variables	Tensile Conditions	Sample Mould Type	Type of Data	Nr. of Samples
2016	clay loading, number of extrusions	Up to failure without clip gauge	ASTM D638-14 (2014) Type I	No raw files available, digitized from report	79
2017	clay loading, clay type, polymer grade, press time	Up to elongation of 30 % with clip gauge	ASTM D638-14 (2014) Type I	Raw data available	410
2018	clay loading, number of extrusions, sample cooling, strain rate	Up to failure without a clip gauge	ASTM D638-14 (2014) Type I	Raw data available	85
2020	number of extrusions, compression moulding method, compression moulding pressure	Up to failure without a clip gauge	ASTM D638-14 (2014) Type V	Raw data available	20

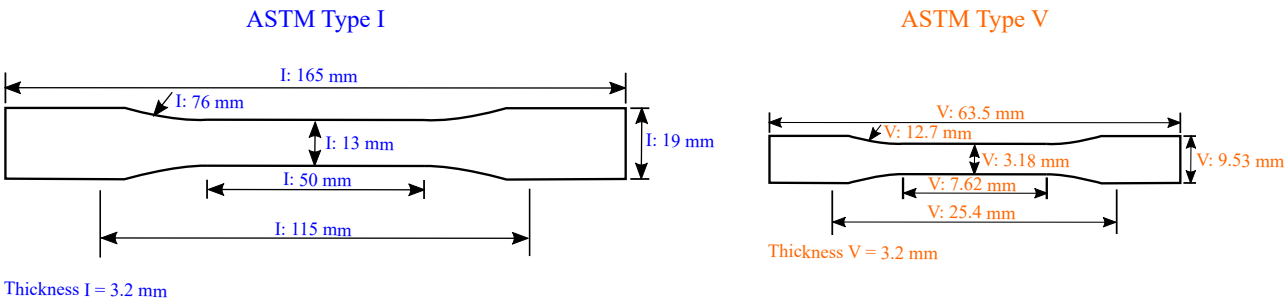

Figure A.1: Tensile dogbone sample dimensions for ASTM Type I (blue) and ASTM Type V (orange) (ASTM D638-14, 2014).

A.1 Tensile Data Processing: Machine Stiffness

When not using a clip gauge the machine displacement is normally accounted for by calculating the machine stiffness using a few samples which were tested with a clip gauge. This was done during the experimental studies in 2018 where a single sample was tested with a clip gauge and the machine stiffness (k) was calculated to be 195 N/mm (Heymans, 2018). The machine displacement ($d_{measured}$) is then corrected ($d_{corrected}$) by means of:

$$d_{corrected} = d_{measured} - \frac{F}{k} \tag{1}$$

To determine whether the displacement values are trustworthy it is necessary to quantify the error due to the machine stiffness. This is done by considering different stiffness values.

Through trial and error it was determined that a machine stiffness lower than 150 N/mm resulted in corrected displacement values which are negative. For the sensitivity study, this value was therefore chosen as the lower bound. The upper bound was chosen to be twice the original calculated machine stiffness of 195 N/mm.

The resulting tensile curves from the sensitivity study are shown in Figure A.2. The blue curve in each figure represents the sample tested with a clip gauge.

From Figure A.2 it is clear that there is no effect on the σ_{FPS} when applying a machine stiffness. This is to be expected as σ_{FPS} is not a function of the strain. When considering a lower stiffness (c.f. Figure A.2(b)) the average change in ε_f is 11.76 % which decreases as the machine stiffness increases. Applying the machine stiffness as calculated by Heymans (2018) (c.f. Figure A.2(c)) results in a 9.04 % change in ε_f and finally doubling the stiffness ((c.f. Figure A.2(d)) results in a change of 4.53 % in ε_f.

In Chapter 2 it was noted that there is a lot of variation in ε_f. To determine the effect of applying the machine stiffness correction on ε_f consider the mean ε_f for all datasets, except 2017 which used a clip gauge and therefore no correction is necessary. These results are shown in Table A.2 where it is noted that there is an average error in ε_f of 3.75 % for 2018 and 0.48 % for 2020. Compared to the large variations of ε_f in a dataset, this is such a small error. Therefore, there is no need to perform a machine correction on the 2018 or 2020 datasets.

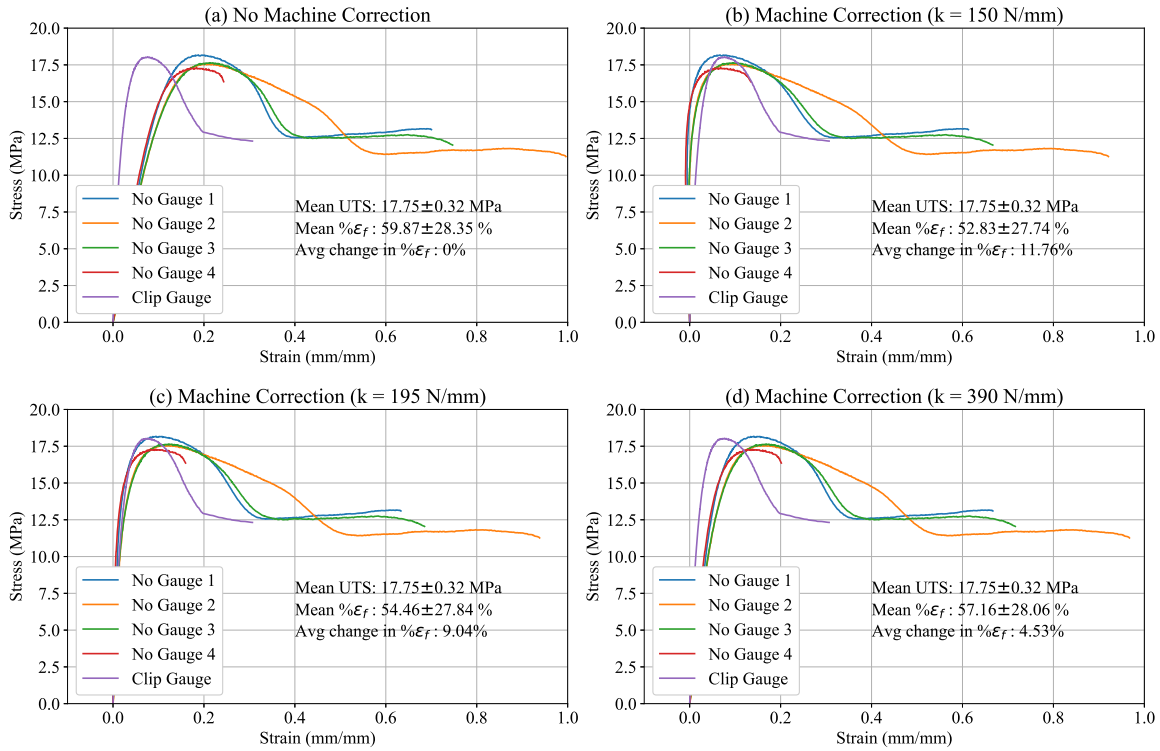

Figure A.2: Tensile curves for (a) no machine correction applied and applying a machine stiffness of (b) 150 N/mm, (c) 195 N/mm and (d) 390 N/mm.

Table A.2: Mean, standard deviation and average error (based on the mean) of ε_f for the 2018 and 2020 data sets where no clip gauge was used.

Year	No correction	With Correction	Average Error
2018	$121.25 \pm 135.24\%$	$116.71 \pm 135.24\%$	3.75%
2020	$494.32 \pm 252.99\%$	$491.95 \pm 252.61\%$	0.48%

A.2 2016 Data

In 2016 the primary design variable under consideration was to investigate the influence of the number of extrusions on the resulting material system (Parschau, 2016). HDPE A7260 was chosen for the polymer and Alcamizer 1 for the clay. The raw data was no longer available and as such the data was digitized from the report of Parschau (2016) with the digitized tensile stress-strain curves shown in Figure A.3 for the three different extrusions considered.

The unprocessed data is shown in the top row and the processed data in the bottom row for each figure.

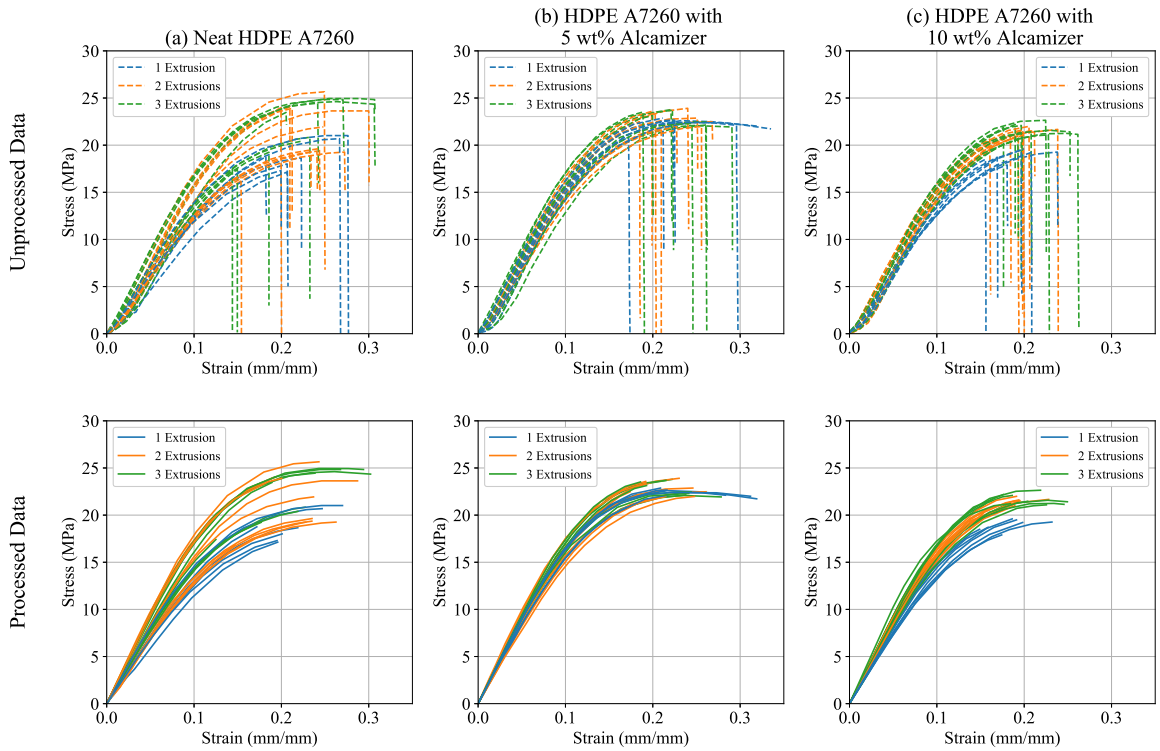

Figure A.3: Digitized tensile stress-strain curve for HDPE A7260 with Alcamizer 1 considering the influence of the number of extrusions.

A.3 2017 Data

During 2017 the influence of different polymer grades and clay types were investigated, along with the the total time the sample moulds spent in the Vertex Hot Press (Ellis, 2017). HDPE B7750, C7260 and D7255 were considered for the polymer grades; and Alcamizer 1, Uncoated Alcamizer 1 and DHT4-A for the clay types. The raw vs. processed tensile stress-strain curves are shown in Figures A.4 through A.12 on pp. A5-A13 for the different material compositions and the four different pressing times considered.

The unprocessed data is shown in the top row and the processed data in the bottom row for each figure.

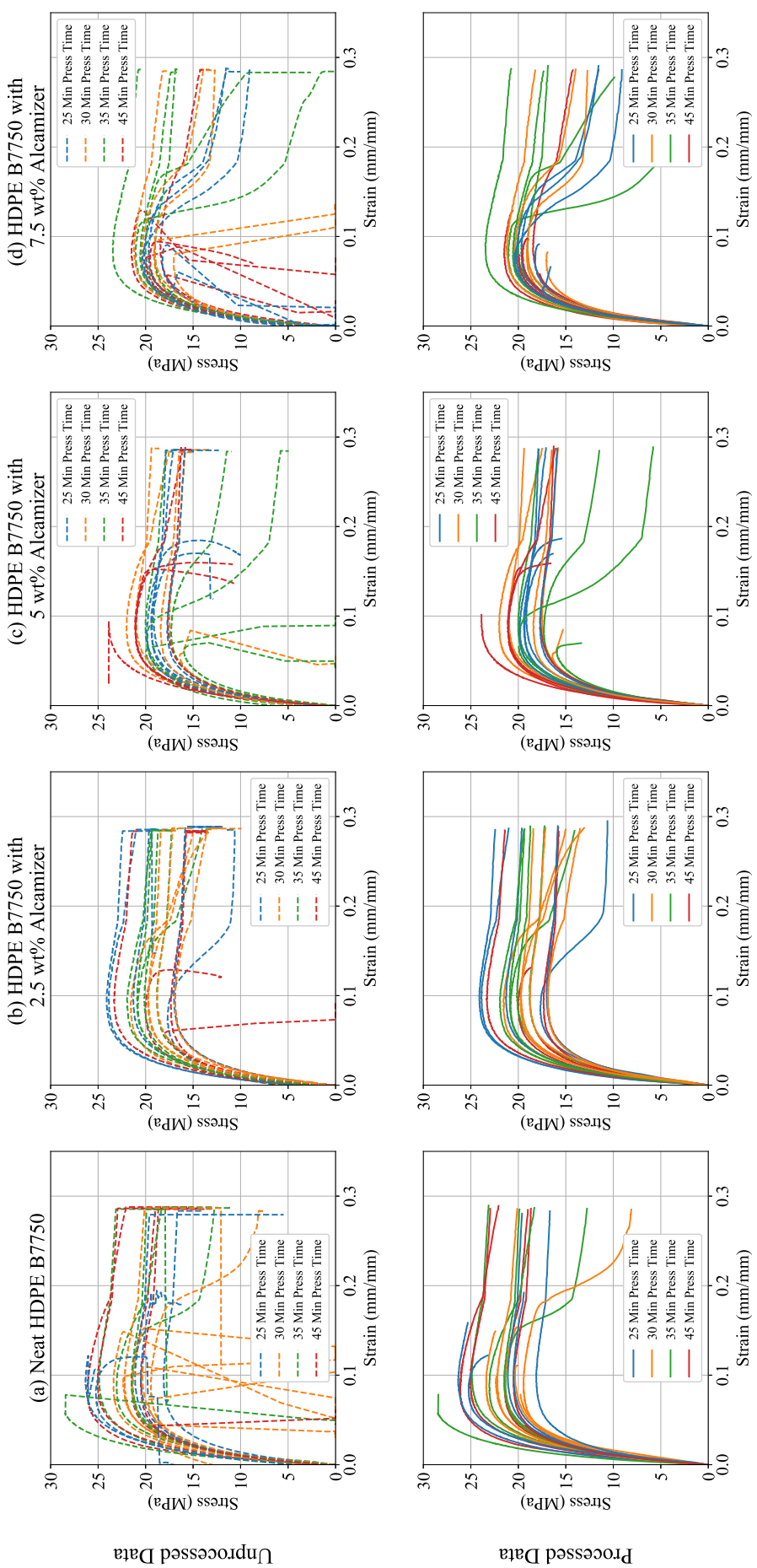

Figure A.4: Unprocessed (top row) vs. processed (bottom row) tensile stress-strain curve for HDPE B7750 with Alcamizer 1 considering the influence of the tensile sample pressing times.

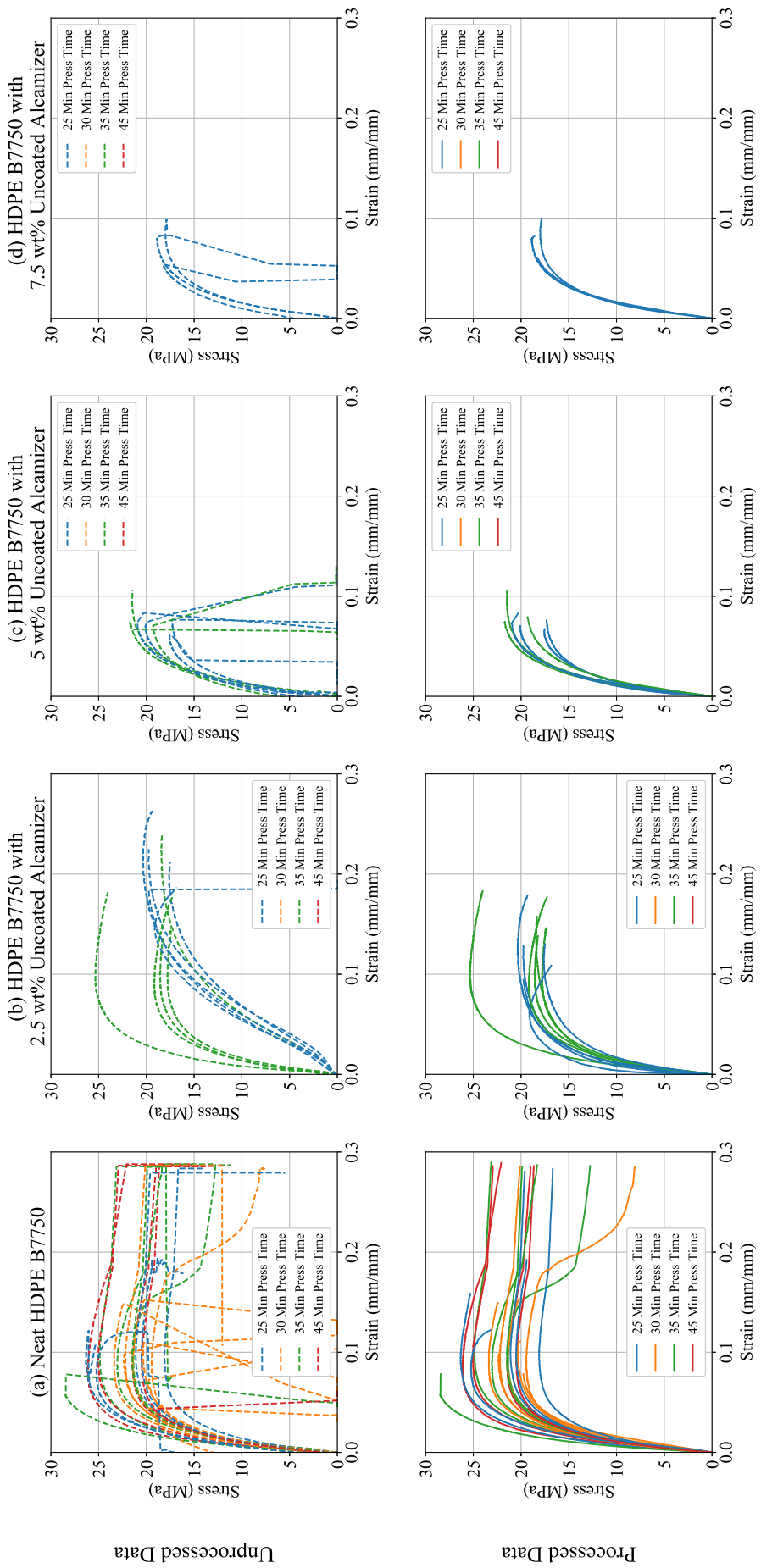

Figure A.5: Unprocessed (top row) vs. processed (bottom row) tensile stress-strain curve for HDPE B7750 with Uncoated Alcamizer 1 considering the influence of the tensile sample pressing times.

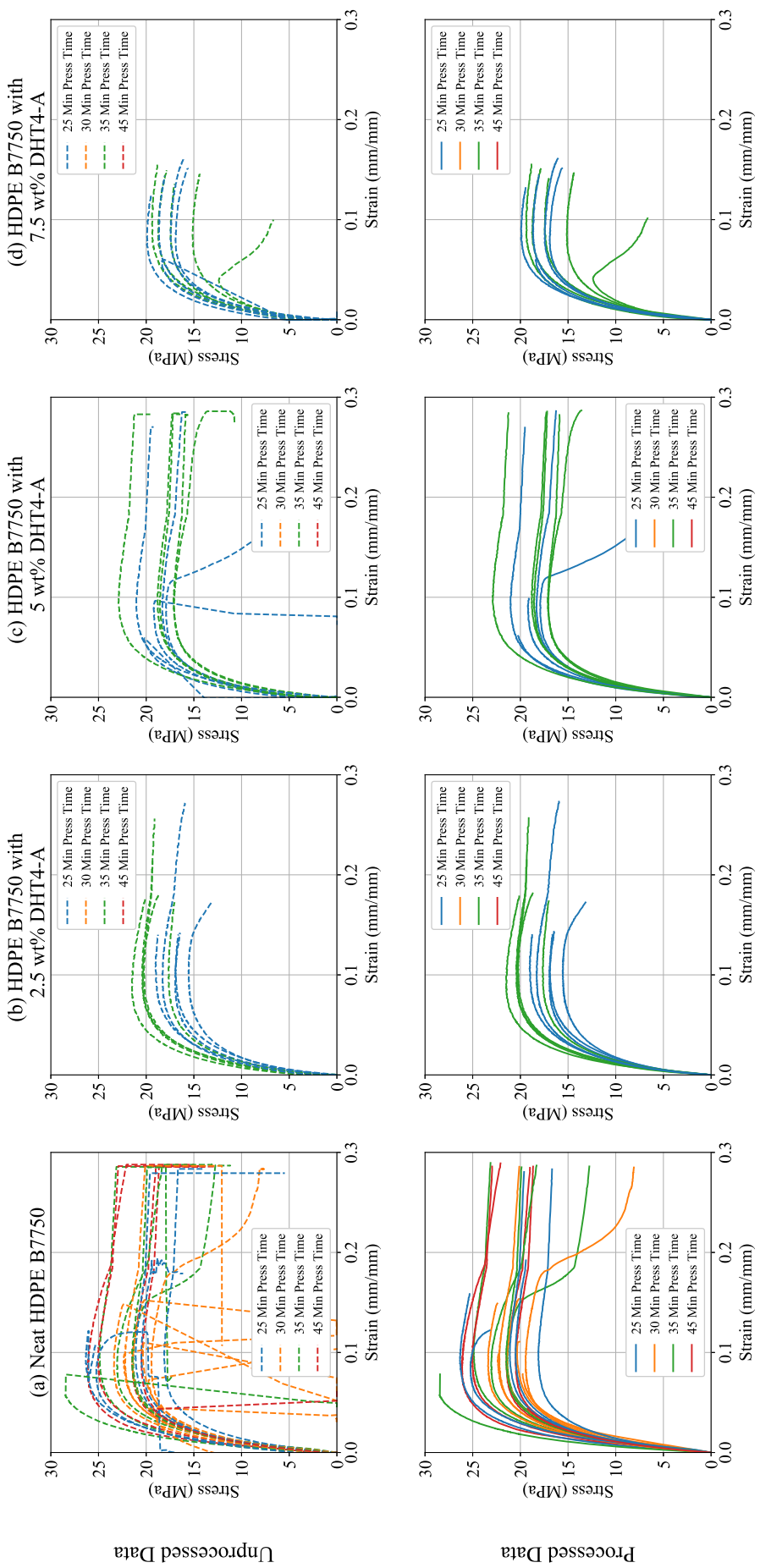

Figure A.6: Unprocessed (top row) vs. processed (bottom row) tensile stress-strain curve for HDPE B7750 with DHT4-A considering the influence of the tensile sample pressing times.

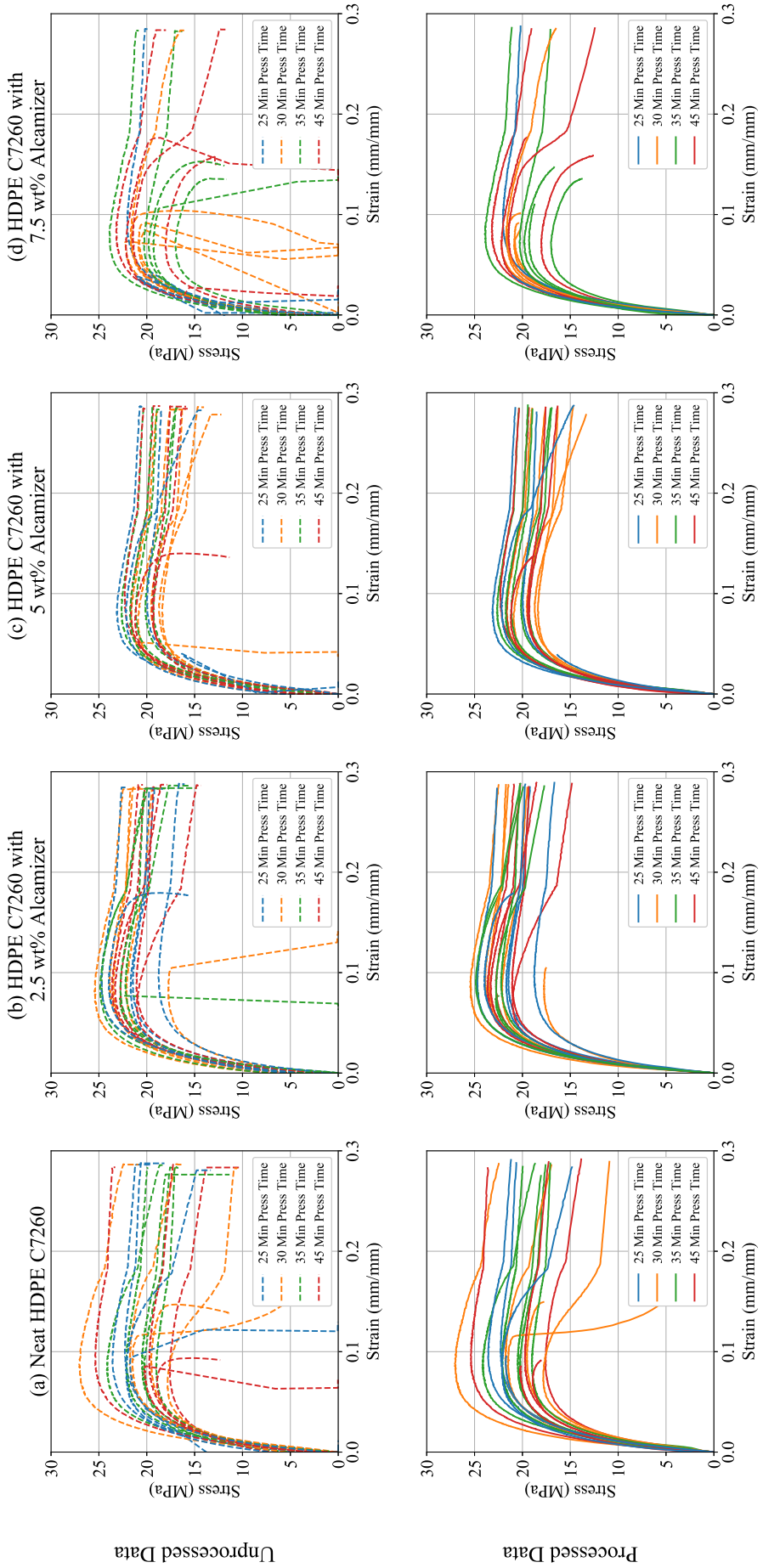

Figure A.7: Unprocessed (top row) vs. processed (bottom row) tensile stress-strain curve for HDPE C7260 with Alcamizer 1 considering the influence of the tensile sample pressing times.

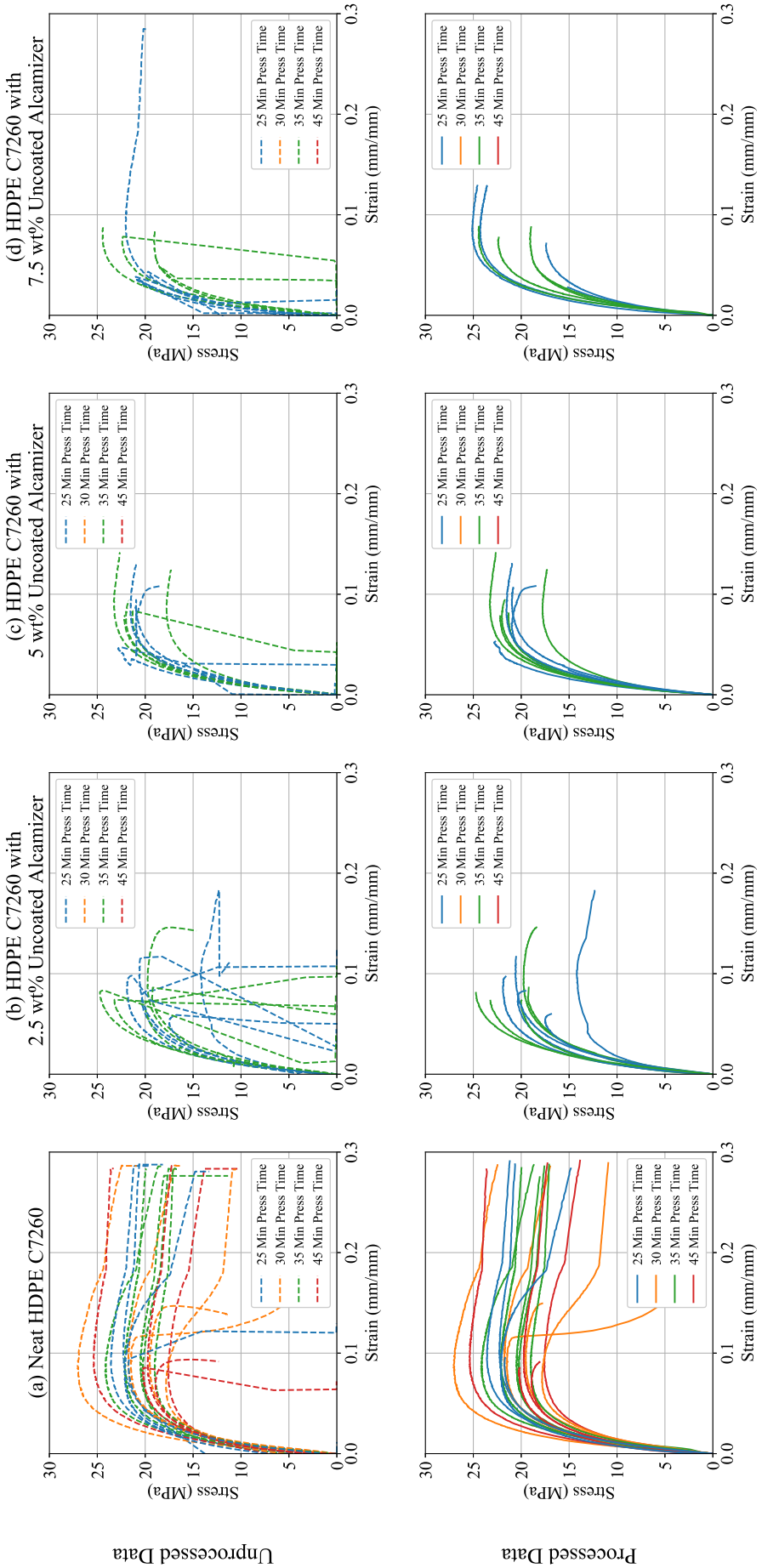

Figure A.8: Unprocessed (top row) vs. processed (bottom row) tensile stress-strain curve for HDPE C7260 with Uncoated Alcamizer 1 considering the influence of the tensile sample pressing times.

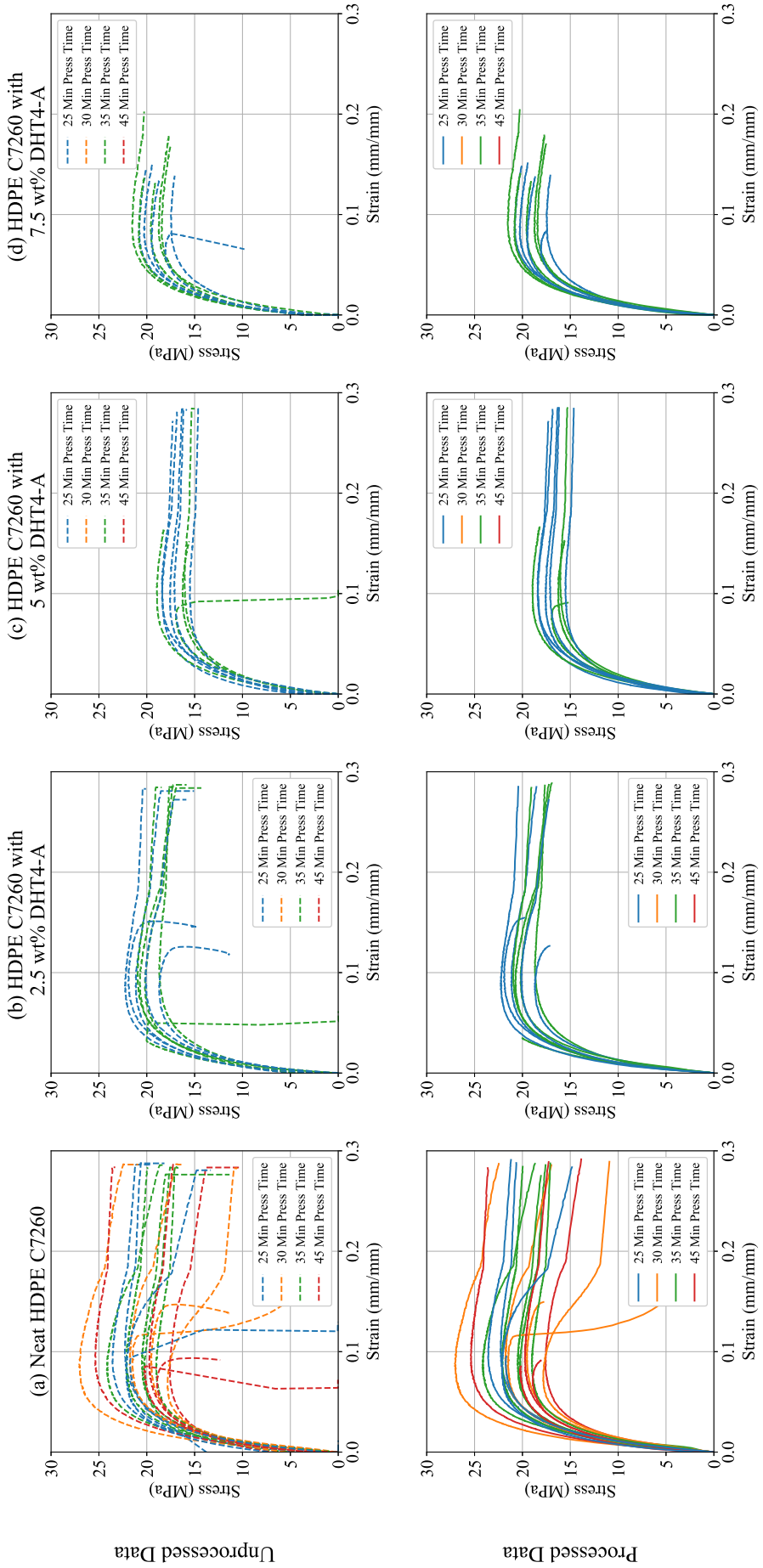

Figure A.9: Unprocessed (top row) vs. processed (bottom row) tensile stress-strain curve for HDPE C7260 with DHT4-A considering the influence of the tensile sample pressing times.

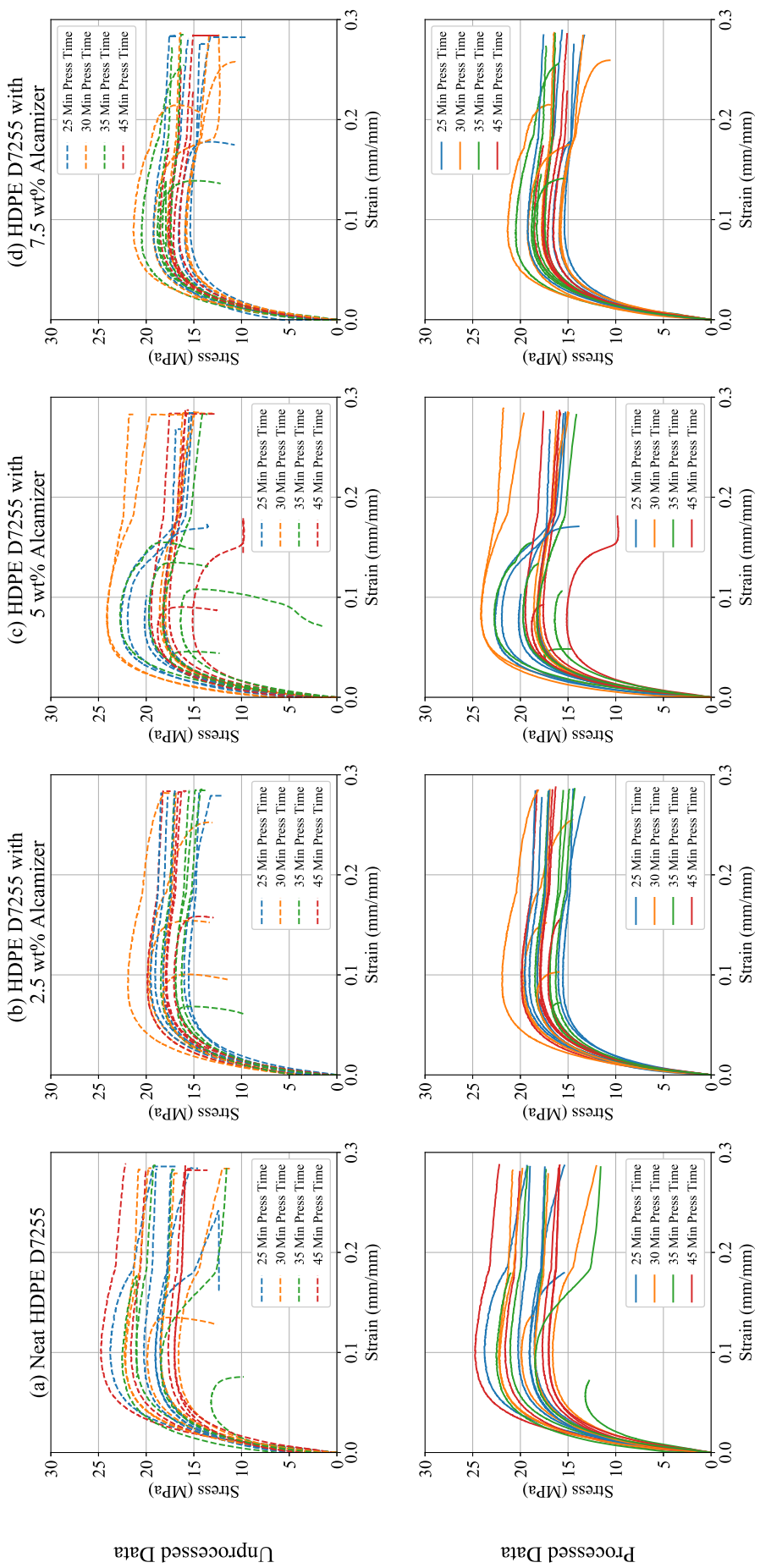

Figure A.10: Unprocessed (top row) vs. processed (bottom row) tensile stress-strain curve for HDPE D7255 with Alcamizer 1 considering the influence of the tensile sample pressing times.

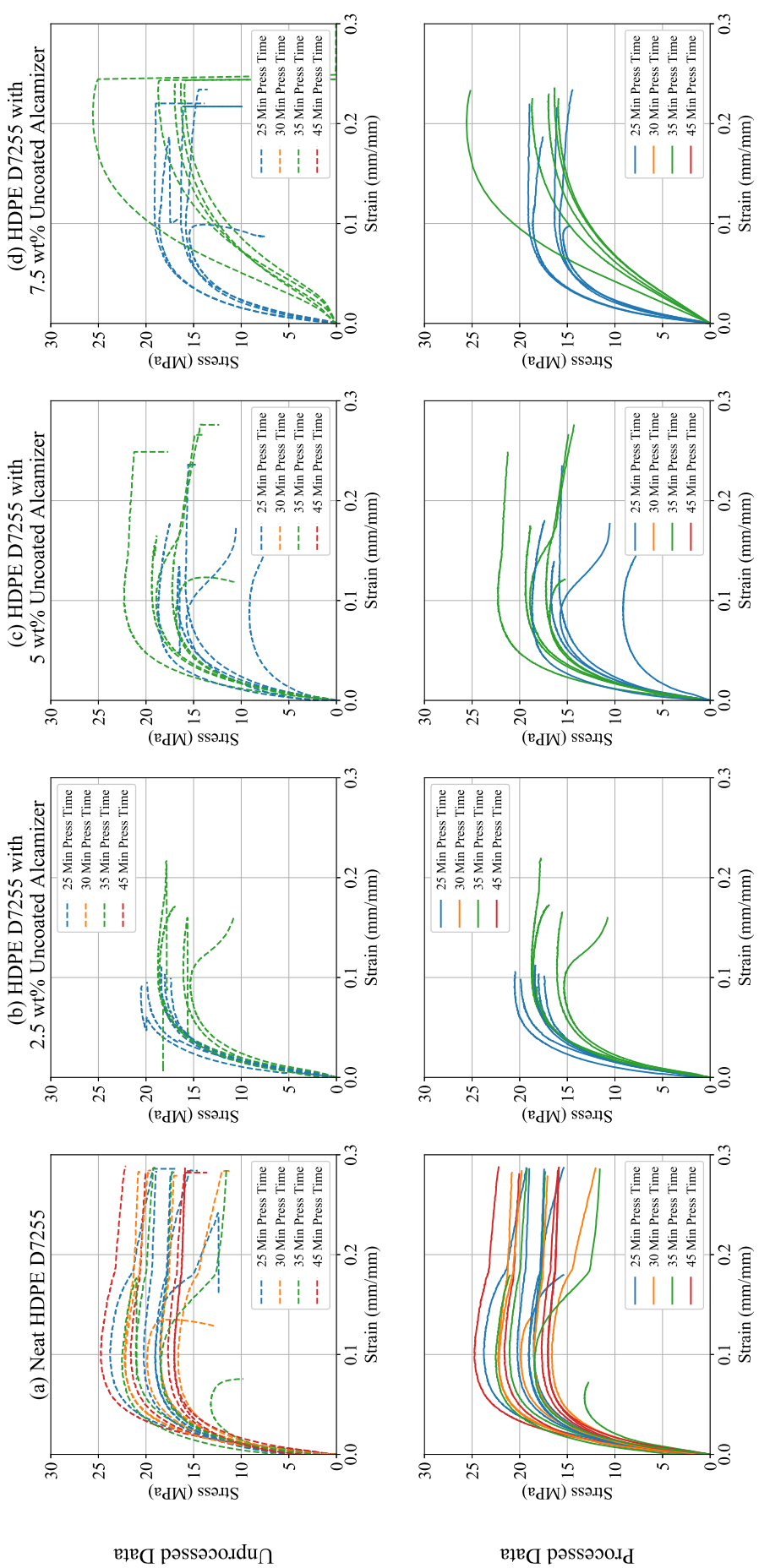

Figure A.11: Unprocessed (top row) vs. processed (bottom row) tensile stress-strain curve for HDPE D7255 with Uncoated Alcamizer 1 considering the influence of the tensile sample pressing times.

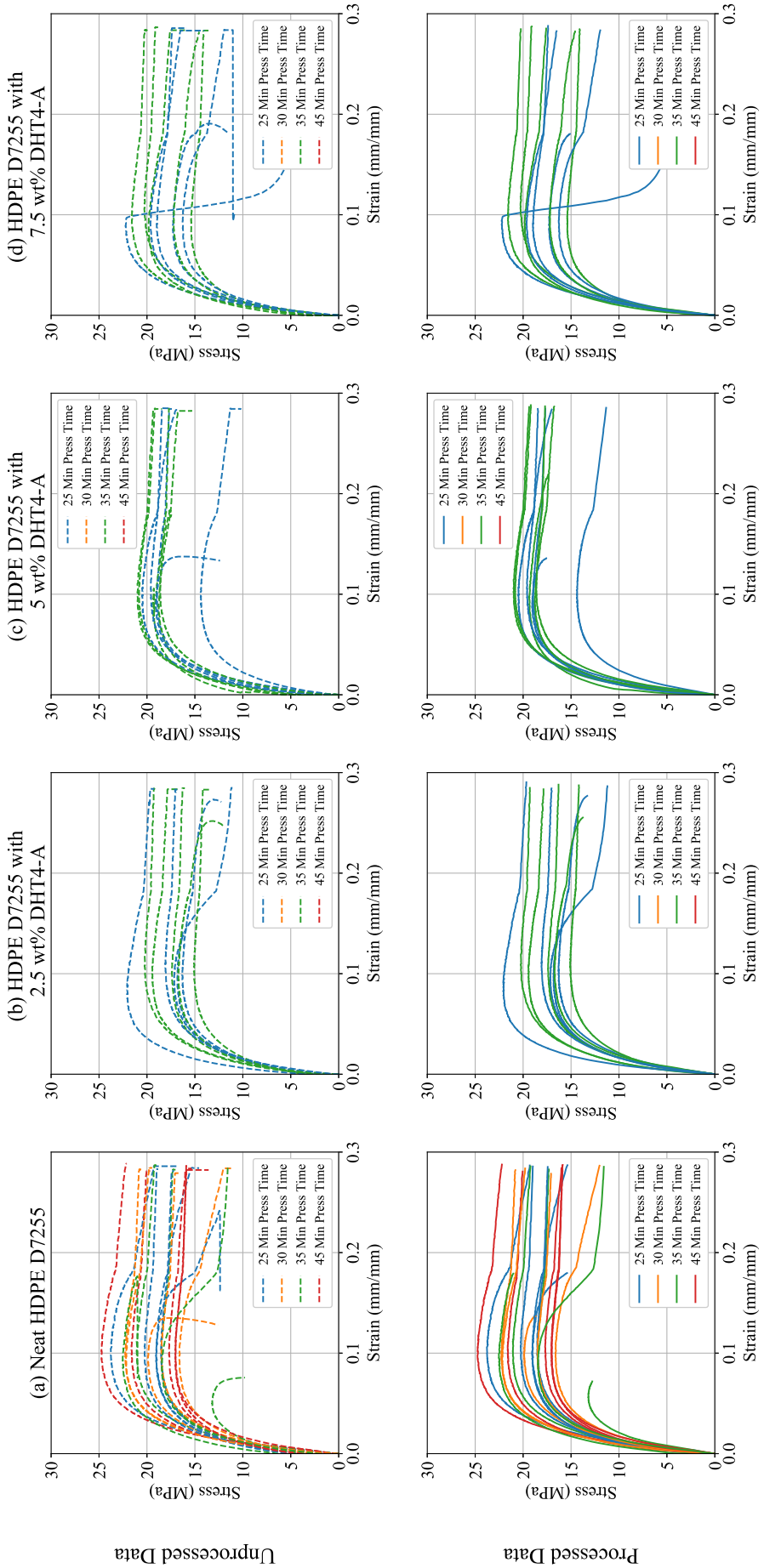

Figure A.12: Unprocessed (top row) vs. processed (bottom row) tensile stress-strain curve for HDPE D7255 with DHT4-A considering the influence of the tensile sample pressing times.

A.4 2018 Data

During 2018 the influence of the number of extrusions was investigated at higher clay weight loadings Heymans (2018), as well as the influence of the sample cooling method and the applied strain rate during tensile testing Braun (2018). HDPE B7750 with DHT4-A was considered for the first investigation and due to polymer supply and equipment failures Neat HDPE C7260 was considered for the second investigation. The raw vs. processed tensile stress-strain curves are shown in Figures A.13 and A.14 on pp. A14-A15 for the two different extrusions and three different cooling methods and strain rates considered.

The unprocessed data is shown in the top row and the processed data in the bottom row for each figure.

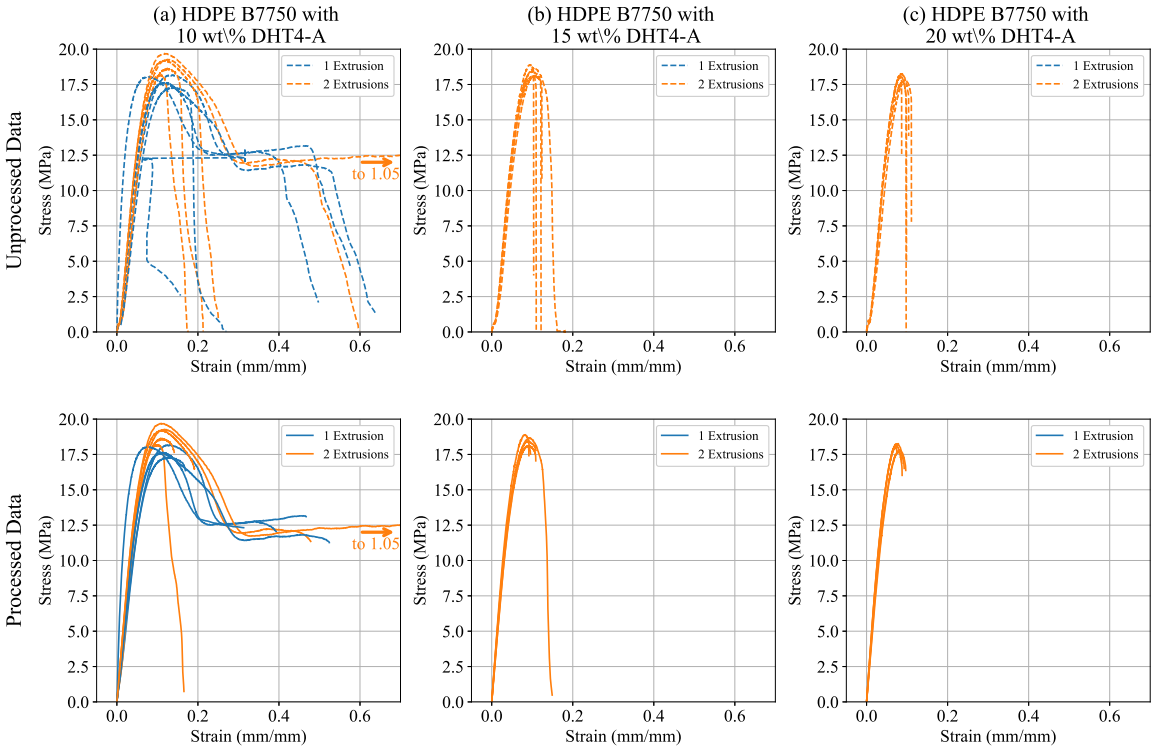

Figure A.13: Unprocessed (top row) vs. processed (bottom row) tensile stress-strain curve for HDPE B7750 with DHT4-A considering the influence of the number of extrusions at higher clay weight loadings.

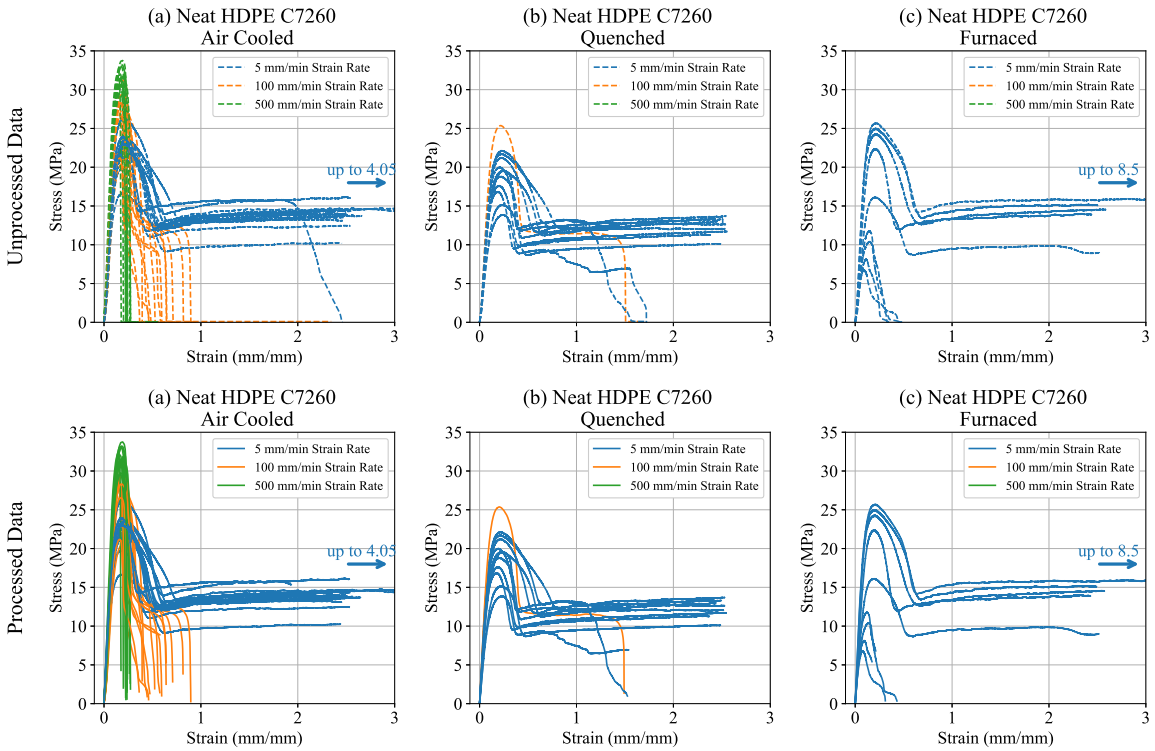

Figure A.14: Unprocessed (top row) vs. processed (bottom row) tensile stress-strain curve for Neat HDPE C7260 considering the influence of the tensile sample cooling methods and different strain rates during tensile testing.

A.5 2020 Data

Before conducting the primary experimental study for this thesis a preliminary experimental study was required to test:

1. the manufacturing equipment and procedure as the 2019 results were not at all what is expected with all of them having a brittle failure even when ductile behaviour was expected and hence not reported in this thesis; and

2. the difference between our compression moulding procedure and the one used at the Leibniz Institute of Polymer Research Dresden (IPF), our international collaborators. In both cases a melting temperature of 190 $°C$ was considered.

Only neat HDPE C7260 was considered at 1 and 2 extrusions. The unprocessed data is shown in the top row and the processed data in the bottom row in Figure A.15.

For the number of extrusions there is a 5.62 % increase in mean σ_{FPS} from 30.61 MPa (1 extrusion) to 32.33 MPa (2 extrusions). As was shown in Sections 2.3.2 and **??** we know that the number of extrusions has a statistical significant effect especially from 1 to 2. The material also exhibits higher ductile behaviour for 2 extrusions compared to 1 extrusion.

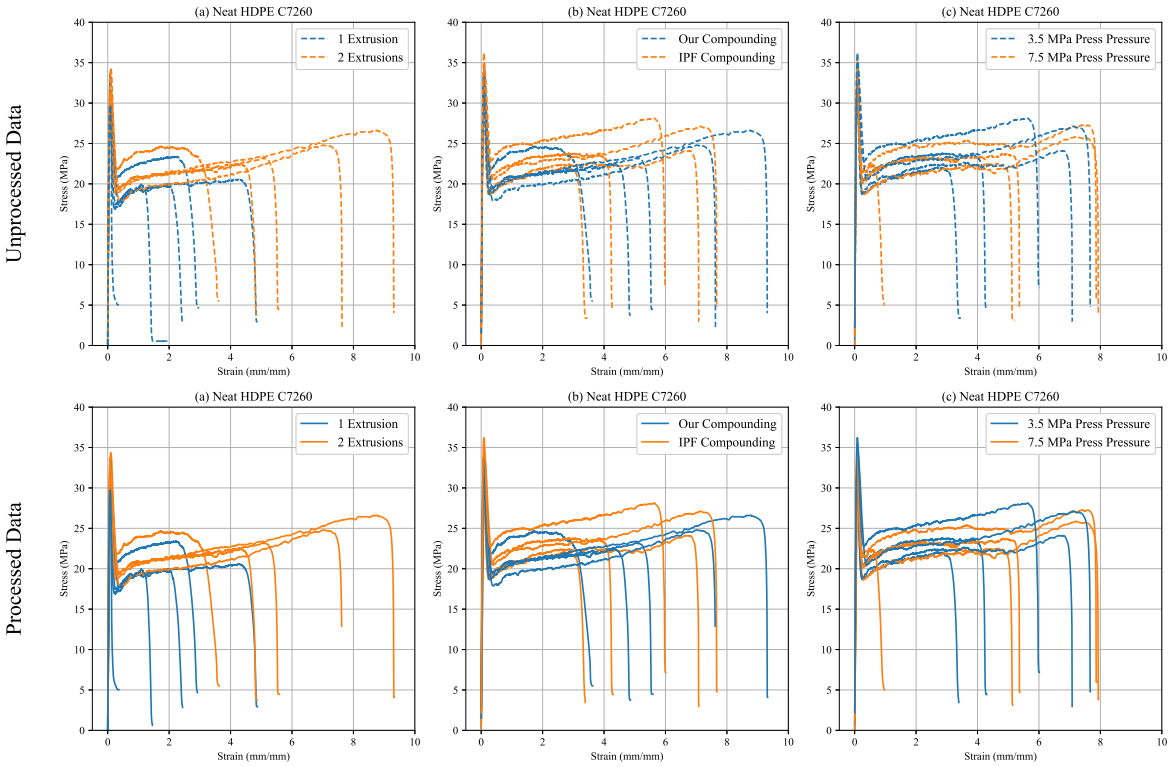

Figure A.15: Unprocessed (top row) vs. processed (bottom row) tensile stress-strain curve for Neat HDPE C7260 considering the influence of (a) the number of extrusions, (b) the compression moulding method and (c) the compression mouling pressure.

There is a 3.65 % difference between the mean σ_{FPS} for the compression moulding method considered at UP (32.33 MPa) and at the IPF with a pressure of 3.5 MPa (33.5 MPa). And a 0.63 % difference between the two pressures considered for the IPF method. There is a 8.26 % decrease in $\%\varepsilon_f$ between the compression moulding at UP (621 %) and the IPF (569.7 %). Given the large variations in these values, a less than 10 % difference is not considered a significant effect.

APPENDIX B: DETAILED OVERVIEW OF SYSTEMATIC LITERATURE REVIEW STUDIES

A detailed overview of the study characteristics and main conclusions for each of the 33 studies included in the systematic literature review is provided in Table B.1. The studies are sorted alphabetically for ease of reference and studies where work was done together (e.g. same material system and manufacturing conditions, same collaborators, etc.) are grouped together.

Also of note is that only one of the studies (Ujianto *et al.*, 2018) included in the systematic literature review actually performed a statistical experimental design. Ujianto *et al.* (2018) considered a Box-Behnken design.

Table B.1: Detailed overview of all the studies included in the systematic literature review.

Reference	Paper Classification	Paper Focus	Material System				Manufacturing System		Mechanical Properties					Main results	DoE Used
			Polymer	Clay	Compatibiliser	Other	Compounding Method	Processing Method	Tensile	Impact	Flexural	DMA/DMTA	Other		
Asgari et al. (2017)	Blending Protocols	Different blending protocols and effect of adding compatibiliser	HDPE	Cloisite Na+ (2 wt%, silane modified)	PEMA (15 wt%)		Silane functionalisation (1.4, 2.7, 3.6, 4.5, 9 and 15 mmol/g clay)) followed by internal mixing (temperature: 180 C, speed: 100 rpm, time: 15 min) considering: 1. Masterbatching (clay/compatibiliser) 2. Direct mixing	Compression moulding (temperature: 200 C, Time: 20 min)	ASTM D638 Type V 50 mm/min (5 replicates) (Table)					Masterbatching provides higher Young's modulus with a lower yield stress and no affect to strain at break. General increase in Young's modulus and yield stress and almost no change in strain at break when adding compatibiliser. Statistical analysis indicated that the blending protocol has significance.	N
Barbosa et al. (2012)	Compounding Conditions	Two different screw profiles for compounding and effect of adding clay and compatibiliser	HDPE	Bentonite (3 wt%)	PE-g-MA (6 wt%)		Twin screw extrusion by two methods: 1. coupled with torque rheometer 2. considering two different screw profiles (ROS and 2KB90)	Injection moulding (Barrel temperature: 200 C, mould temperature: 40 C, cooling time: 25 s)	ASTM D638 50 mm/min (Digitised and Table)					Screw 2 provided an increase in Young's modulus and tensile strength.	N
Boran et al. (2017)	Compounding Methods	Different compounding methods and effect of masterbatch vs individual components and adding compatibiliser	HDPE	Nanomer I.44P (2 wt%) or Masterbatch (50 wt% clay diluted to 2 wt%)	PE-g-MA (4 wt%)		1. Single screw extruder (Temperature profile: 145-145-150-150-160-170 C, speed: 65rpm) 2. Twin screw extruder (Temperature profile: 145-145-150-150-160-170 C, speed: 60rpm) 3. Single screw extruder and extensional flow mixer (Temperature profile: 190-200- 200 C, speed: 60rpm) 4. Bowl mixer masterbatch method (Temperature: 180 C, speed: 60rpm, time: 10min) – diluted the mixture using 2 or 3	Injection moulding (Barrel and mould temperature: 180 C, pressure: 17 MPa, holding and cooling time: 10 s)	ASTM D638 (3 replicates) (Table)	Izod ASTM D256 (3 replicates) (Table)	ASTM D790 (3 replicates) (Table)			Overall masterbatch compounding methods provided the best improvement to mechanical properties. Mechanical properties are improved with the addition of compatibiliser.	N
Brandenburg et al. (2014) and Silva et al. (2014)	Compounding Methods	Different compounding methods and effect of clay type and a secondary filler	HDPE	Cloisite Na+ or Cloisite 30B (3 wt%)		Carbon Nanotubes (1 wt%)	1. Solution Intercalation (130 C followed by sonication for 30 min at 150 W and precipitation at 6 C for 8h) 2. Internal Mixer (temperature: 180 C, speed: 50 rpm, time: 10 min)	Compression moulding (temperature: 180 C, pressure: 14.5 Mpa (5T), time: 5 min). Cooled in water.					Nanoindentation – provided E from this as well (Digitised)	Solution intercalation provided highest improvement in Young's modulus. In general melt intercalation provided the best improvement in nanohardness. Adding carbon nanotube improved Young's modulus. Cloisite 30B also provided best improvement.	N
Chu et al. (2007)	Processing Methods	Different processing methods and effect of clay loading, polymer molecular weight and direction in which sample was cut	HDPE at low, middle and high molecular weights	Cloisite 20A (0, 2, 4, 8 wt%)			Single screw extrusion (temperature profile: 130-160-160-190 C, speed: 20 rpm, L/D: 18)	1. Compression moulding (temperature: 190 C, pressure: 0.5 MPa) 2. Injection moulding (Barrel temperature: 190 C, mould temperature: 70 C, holding pressure: 0.5 MPa, speed: 200 rpm) Clay at 8 wt% for all three polymer molecular weights.	ASTM D638 With Extensometer 1.27 mm/min (5 replicates) (Digitised and Table)			1 Hz 30 to 140 C (only for polymer type)		Injection moulding provided higher mechanical properties. Injection moulded samples cut from the transverse direction generally provided higher mechanical properties as opposed to samples cut from the flow direction. High molecular weight HDPE provided the best mechanical properties. DMTA results only consider the difference in molecular weight, not the different processing methods.	N
Esteki et al. (2013)	Compounding Methods	Compounding with or without water assistance and effect of clay type and adding compatibiliser	HDPE	Cloisite Na+ (0, 1.6 wt%) or Cloisite 15A (0, 0.1, 1.6, 3.1, 4.6 wt%)	PE-g-MA (0, 4 wt%)		Twin screw extrusion (temperature profile: 150-180-185-190-185-170 C, speed: 180 rpm, L/D: 40) assisted with or without water at a feeding rate of 340 g/h and a screw speed of 260 rpm.	Not mentioned	ASTM D638 50 mm/min (Table)	Izod ASTM D256 (Table)				Mechanical properties are improved with water assisted extrusion. Compatibiliser does improve mechanical properties as does Cloisite Na+.	N
Eteläaho et al. (2009)	Blending Protocols	Different blending protocols and effect of clay loading	HDPE	Nanomer I.44P (0, 3, 6, 8 wt%) or Nanoblend MB 2201 (with clay content of 40 wt%)	PP-g-MA (9 wt%)		Twin screw extrusion (temperature profile: 170-170-170-170-170-170-180-180-180-195 C, speed: 200 rpm) considering: 1. Direct mixing 2. Masterbatching using commercial compound diluted to the desired clay concentration 3. Masterbatching using an in-house compound	Injection moulding	ISO 527 50 mm/min (Table)	Charpy (Notched and Unnotched) ISO 179 (Table)				Mechanical properties generally improved considering the masterbatch method with in-house better for lower clay loadings (<= 3 wt%) and commercial for higher. Notched and unnotched impact tests were performed, however for PE based results only the notched impact strength was reported.	N
Gao et al. (2012)	Processing Methods	Different injection moulding methods and effect of clay loading	HDPE	Attapulgite (0, 1, 3, 5 wt%)			Twin screw extrusion (temperature profile: 130-155-165-170-170-145 C, speed: 110 rpm)	Injection moulding (barrel temperature: 180 C, pressure: 88.26 MPa (900 kg/cm2)) considering: 1. Conventional injection moulding 2. Dynamic packing injection moulding	GB/T1040 50 mm/min (5 replicates) (Digitised)					Dynamic packing injection moulding provides better mechanical properties.	N

Table B.1. continues on the following page

Table B.1. continues on from the previous page

Reference	Paper Classification	Paper Focus	Material System				Manufacturing System		Mechanical Properties					Main results	DoE Used
			Polymer	Clay	Compatibiliser	Other	Compounding Method	Processing Method	Tensile	Impact	Flexural	DMA/DMTA	Other		
Gong et al. (2013)	Compounding Conditions	Different mixing conditions and effect of compatibiliser type and clay and compatibiliser loading	HDPE	Bentonite (0, 2, 6 wt%)	3 different MAPE – E100, E265, M603 (MAPE/clay ratio: 0, 1, 3, 6, 9)		Internal mixer (temperature: 130, 160 C, time: 4, 12 min, speed: 30, 60, 90 rpm)	Pressed into sheets and plates			ASTM D790 (4 replicates) (Digitised)			Increase in rotation speed decreases mechanical properties. Lower temperature and higher time improves the properties. Ideal is 60 rpm, 160 C and 12 min. Adding compatibiliser improves the properties with E265 providing the highest.	N
Heinemann et al. (1999)	Compounding Methods	Different compounding methods	HDPE	Bentonite or Fluoromica			1. In situ polymerisation 2. Internal mixer (temperature: 190 C, time: 5 min)	Compression moulding (temperature: 170 C, pressure: 1 MPa, time: 15 min)	Yes (Table)					In-situ polymerisation provided better Young's modulus while internal mixing provided better stress and elongation at break.	N
Höfler et al. (2018)	Compounding Methods	Different compounding methods and effect of polymer type and clay loading	LMDPE (VP305 or VX567) or HDPE	Halloysite (0, 2, 5, 10 wt%)			1. Dry blended with high speed mixer 2. Twin screw extrusion (temperature profile: 140-200 C)	Rotational moudling (temperature: 250 C, cooling from 180 C). Samples cut from side walls for testing.	ASTM D638 (5 replicates) (Digitised)	Charpy ASTM D6110 (5 replicates) (Digitised)	ASTM D790 (5 replicates) (Digitised)			Extrusion provided better mechanical properties. HDPE provided best mechanical properties.	N
Huang et al. (2015)	Compounding Conditions	Different compounding conditions	HDPE	Nanomer I.44P (3 wt%)			Novel vane mixer (temperature: 210 C, speed: 10, 20, 30, 40, 50 rpm, time: 1, 2, 4, 6, 8, 10 min)	Compression moulding (temperature: 210 C, pressure: 15 MPa, time: 6 min)	GB/T1040 50 mm/min (5 replicates) (Digitised)					Increase in mechanical properties up to 40 rpm before they decrease. Similar observation for an increase in time up to 4 min.	N
Jo and Naguib (2006, 2007a, 2007b)	Processing Conditions and Processing Methods	Different foaming times during processing and effect of clay loading.	HDPE	Cloisite 20A (0, 0.5, 1, 2 wt%)	PE-g-Man (15 wt%)		Twin screw extrusion (temperature profile: 140-180 C, speed: 70 rpm, L/D: 10)	Compression moulding (temperature: 160 C, pressure: 14.5 MPa, time: 15 min for 2006/2007a and 10 min for 2007b). Apply CO2 to compression moulded samples (pressure: 8.3 Mpa) and immerse in glycerin bath for foaming (temperature: 130 C, time: 15, 30, 45, 60 s for 2006/2007a and 15, 20, 30, 35, 40 s for 2007b) after releasing the pressure and immediately quenched in cold water to prevent cell deterioration.	Not mentioned, but assumed ASTM D638 as it was indicated in Jo and Naguib (2008) 50 mm/min (5 replicates) (Digitised)					Improvement in mechanical properties with the addition of clay for both HDPE/clay and HDPE/clay foams. Volume expansion ratio increases with an increase in foaming time, but decreases with an increase in clay loading.	N
Jo and Naguib (2008)	Processing Conditions and Testing Conditions	Effect of sample cooling and strain rates	HDPE	Cloisite 20A (0, 0.5, 1, 2 wt%)	PE-g-Man (15 wt%)		Twin screw extrusion (temperature profile: 140-180 C, speed: 70 rpm, L/D: 10)	Compression moulding (temperature: 160 C, pressure: 14.5 MPa, time: 10 min). Apply CO2 to compression moulded samples (pressure: 8.3 Mpa). Considered three cooling rates: room temperature, quenched in cold water and cooled slowly on a hot pressing plate. Compression samples were then immersed in glycerin bath for foaming (temperature: 130 C, time: 20, 30, 40, 50 s) after releasing the pressure and immediately quenched in cold water to prevent cell deterioration.	ASTM D638 1, 5 and 50 mm/min (5 replicates) (Digitised)					Results presented were for a foaming time of 20s which resulted in the highest volume expansion ratios. Results are presented as a function of percentage crystallinity which indicated that hot plate cooled samples provided the highest crystallinity. Foaming degree increased with an increase in crystallinity. Mechanical properties generally increased with an increase in crystallinity and strain rate.	N
Lapshin et al. (2008) and Swain and Isayev (2006, 2007)	Compounding Conditions	Different compounding conditions with and without ultrasound treatment and the effect of clay loading	HDPE	Cloisite 20A (0, 2.5, 5, 10 wt%)			Single screw extrusion (temperature profile: 180-190-200-200 C, speed: 100 rpm) with ultrasound (frequency: 20 kHz, amplitude: 5, 7.5, 10 micom) at the die at varied flow rates (0.25, 0.5, 0.75 g/s) for different residence times (21, 10, 7 s)	Injection moulding (Barrel temperature: 190 C, mould temperature: 25 C for 2008 and 40 C for 2006/2007, injection speed: 40 mm/s, pressure: 10 Mpa for 2008 and 13.8 Mpa for 2006/2007, holding and cooling time: 20 s)	ASTM D638 50 mm/min (5 replicates) (Digitised and Table)	Izod (5 replicates) (Digitised and Table)				Improved mechanical properties with ultrasound treatment at lower residence time of 7s. Higher residence times causes property degradation. Increase in ultrasound amplitude generally improves mechanical properties, with 7.5 microm being optimal.	N
Lei et al. (2007)	Blending Protocols	Different blending protocols and effect of clay and compatibiliser loading and compatibiliser type	rHDPE	Cloisite 15A (0, 1, 3, 5, 7 wt%)	MAPE or CAPS (0, 2.5, 5, 10 wt%)		Internal mixer (temperature: 165 C, speed: 60 rpm) considering: 1. Masterbatching (MAPE/clay) at 20 min 2. Direct mixing at 15 min	Compression moulding (temperature: 175 C, pressure: 87 MPa (30T), time: 5min)	ASTM D638 (6 replicates) (Table)	Izod ASTM 256 (5 replicates) (Table)		Yes (Table)		Masterbatching provides higher mechanical properties. Compatibiliser improves mechanical properties, but decreases loss and storage modulus.	N
Lew et al. (2005)	Compounding Conditions	Different compounding conditions	HDPE	Fluoromica (4 wt%)	PE-g-MA (6 wt%)		Single screw extrusion (L/D: 30) considering 12 different temperature gradient profiles. Refer to paper for details on the profiles.	Injection moulding	ASTM D638 (Digitised)	ASTM D5628 (Digitised)	ASTM D590 (Digitised)			Mechanical properties are improved at all temperature profiles with the best improvement found with HHLL (215-215-170-170-185-185-200-215)	N
Li et al. (2007)	Compounding Conditions	Different ultrasound conditions and effect of adding clay and compatibiliser	HDPE	DK1 (0, 3, wt%)	HDPE-g-MA (0, 9 wt%)		Single screw extrusion with ultrasound (power: 0, 200 W) at the die	Compression moulding (pressure: 12 MPa, time: 10 min)	100mm/min (5 replicates) (Table)	Izod GB/T1843 (5 replicates) (Table)				Ultrasound treatment improves mechanical properties. Compatibiliser improves mechanical properties.	N

Table B.1. continues on the following page

Table B.1. continues on from the previous page

Reference	Paper Classification	Paper Focus	Material System				Manufacturing System		Mechanical Properties					Main results	DoE Used
			Polymer	Clay	Compatibiliser	Other	Compounding Method	Processing Method	Tensile	Impact	Flexural	DMA/DMTA	Other		
Mainil et al. (2006)	Blending Protocols and Compounding Conditions	Different blending protocols and effect of compatibiliser type	HDPE	Cloisite 20A (0, 3 wt%)	PE-g-MA or EVA12 or Kraton (8 wt%)	Irganox antioxidant (0.3 wt%)	Internal mixer (temperature: 185 C, speed: 20, 75 rpm, time: 7, 30 min) considering: 1. Masterbatching (compatibiliser/antioxidant/clay) 2. Direct mixing	Compression moulding (temperature: 145 C, 7.5 MPa, time: 7 min).	ASTM D638 Type V 50 mm/min (3 replicates) (Table)					Masterbatching provides higher mechanical properties. Compatibiliser improves mechanical properties, with EVA12 providing best results.	N
Merinska et al. (2012)	Compounding Methods	Different compounding methods and effect of clay type and adding compatibiliser	PE (type not specified)	Cloisite 25A, 30B, 93A or Nanofil 5 (5 wt%)			1. KO Buss Kneader (temperature profile: 180 C, L/D: 18) 2. APV MP19-25 TC Twin screw extrusion (L/D: 18, temperature profile: 180 C)	Compression moulding	Yes (Digitised)			30 C (Digitised and Table)		Twin screw extrusion provided best mechanical properties. Cloisite 93A provided best mechanical properties.	N
Minkova and Filippi (2011)	Compounding Methods	Different compounding methods and effect of clay loading	HDPE grafted with MA	Cloisite 20A (0, 6.2, 10, 15, 25 wt%)			1. Solution blending to create a fine powder 2. Internal mixer (temperature: 150 C, speed: 30 rpm, time: 10min) 3. Quiescent Annealing where the powder from the solution blending process was compressed to prepare tablets before placing them in a mould to heat at different times and then quenched in ice-water	Compression moulding (temperature: 190 C)					Micro-hardness (Table)	Internal mixer provides the best mechanical properties.	N
Mistretta et al. (2018)	Processing Methods	Different processing methods and effect of adding clay	HDPE	Cloisite 20A (5 wt%)			Twin screw extrusion (temperature profile: 120-130-140-150-160-170-190 C, speed: 200rpm, L/D: 35)	1. Compression moulding (temperature: 190 C, pressure: 5 MPa, time: 4 min) 2. Injection moulding (Barrel temperature: 235-235-235-240 C, injection pressure: 8 MPa, holding pressure: 4.5 MPa)	ASTM D882 1 mm/min up to 3% and then 100 mm/min Injection and compression moulded samples tested on different machines (Digitised)	Charpy (no recorded value for processing methods) (Table)				Injection moulding provided better improvement in mechanical properties. Impact properties are for injection moulded samples only where no break occurred and no value is therefore reported. It also does not compare with compression moulded samples.	N
Nguyen and Baird (2006)	Compounding Conditions	With and without CO2 treatment and effect of polymer type and adding clay	HDPE (Paxon or HHM)	Cloisite 15A (4 wt%)			Single screw extrusion (L/D: 30) with CO2 injection port	Injection moulding	Yes (Table)					CO2 treatment improves the mechanical properties. Paxon polymer provides higher mechanical properties.	N
Oliveira et al. (2009)	Compounding Conditions	Different compounding conditions and effect of clay loading	HDPE	Vermiculite (0, 7, 10, 15, 20 wt%)			Twin screw extrusion (speed: 200, 400 rpm)	Injection moulding		Izod ASTM D256 (6 replicates) (Digitised)				Mechanical properties improve with an increase in screw speed.	N
Passador et al. (2014, 2016)	Blending Protocols	Different blending protocols and effect of clay loading	HDPE/LLDPE (75/25 wt%)	Cloisite 20A (0, 2.5, 5, 7.5 wt%)	LLDPE-g-MA (5 wt%)		Internal mixer (temperature: 180 C, speed: 80 rpm, time: 10 min) followed by twin screw extrusion (temperature profile: 180-190-190-200-210 C, speed: 120 rpm, L/D: 25) considering: 1. Masterbatching 1 (LLDPE/compatibiliser/clay) 2. Masterbatching 2 (compatibiliser/clay)	Injection moulding (Barrel temperature: 225-230-235-240-240 C, mould temperatuer: 45 C, injection pressure: 190 MPa, holding pressure: 12 Mpa)	ASTM D638 5 mm/min (5 replicates) (Digitised and Table)		ASTM D790 (Digitised and Table)	ASTM D648 1 Hz -130 to 110 C 2 C/min (Digitised)		Masterbatching method 2 provides higher mechanical properties.	N
Ujianto et al. (2018)	Compounding Conditions	Different mixing conditions and two different rotors	HDPE	Cloisite 93A (2 wt%)	HDPE-g-MA (5 wt%)		Internal mixer (temperature: 150, 180, 210 C, speed: 30, 80, 130 rpm, time: 4, 10, 16 min) with a roller or banbury rotor	Compression moulding (temperature: 180 C, pressure: 9 MPa, time: 12 min)	ASTM D638 5 mm/min (4 replicates) (Table)					Roller rotor provides higher mechanical properties. The optimal mixing conditions are dependent on the rotor. For the Roller rotor a medium temperature and speed provides the best mechanical properties, whereas for the Banbury rotor it is a low temperature and high speed.	Y
Xiang et al. (2009)	Processing Methods	Different injection moulding methods and effect of clay loading	HDPE	Mica (0, 1, 3, 5, 10, 20 wt%)			Twin screw extrusion (temp profile: 165-180-190-200-200-195 C)	Injection moulding (barrel temp: 190 C, injection pressure: 88.26 MPa (900 kg/cm2)) considering: 1. Dynamic packing injection to introduce oscillatory shear at 1 Hz and a rate of 10s-1. 2. Static packing without shearing.	GB/T1040 50 mm/min (5 replicates) (Digitised)			-130 to 120 C 3 C/min (Digitised)		General improvement in mechanical properties (tensile and DMA) for dynamic packing when compared to static packing.	N

APPENDIX C: ANOVA AND LINEAR REGRESSION MODEL RESULTS

In this appendix the full set of tabled results from the analysis of variance (ANOVA) and linear regression model are presented as only a summary of the p-values and ω^2 values are presented in the main text. Statistical significance is determined by obtaining a p-value of less than 0.05. The level of significance is indicated in each table using the list of significance codes presented at the bottom of the table as reference.

C.1 Tensile Testing DoE

C.1.1 Young's Modulus

Table C.1: ANOVA results for Young's Modulus for the tensile testing DoE.

	Sum Sq	Df	F-value	Pr(>F)	ω^2	
Intercept	$1.014e^{-01}$	1.0	11143.633	$2.502e^{-43}$	0.982	***
ClayType	$8.749e^{-06}$	2.0	0.481	$6.225e^{-01}$	-0.000091	
MouldingMethod	$1.495e^{-03}$	1.0	164.391	$2.287e^{-14}$	0.014	***
Site	$1.377e^{-07}$	2.0	0.008	$9.925e^{-01}$	-0.000175	
ClayLoading	$7.412e^{-05}$	1.0	8.149	$7.390e^{-03}$	0.000630	**
Residual	$3.002e^{-04}$	33.0	NaN	NaN	NaN	

Significance Codes: '***': 0-0.001, '**': 0.001-0.01, '*': 0.01-0.05, '.':0.05-0.1, ' ': 0.1-1.0

Table C.2: Linear model results for Young's Modulus for the tensile testing DoE.

Nr. Observations	40	R-squared		0.903	
Df Residuals	33	Adjusted R-squared		0.886	
Df Model	6	F-statistic		51.42	
		Residual Standard Error		0.003	
	Estimate	Std. Error	t-value	Pr(> |t|)	
Intercept	0.1513	0.001	105.563	0.000	***
ClayType[T.DHT4A]	0.0009	0.001	0.858	0.397	
ClayType[T.Neat]	-0.0005	0.002	-0.284	0.778	
MouldingMethod[T.Injection]	0.0165	0.001	12.822	0.000	***
Site[T.TUT]	$-8.582e^{-05}$	0.001	-0.057	0.955	
Site[T.UP]	-0.0001	0.001	-0.109	0.914	
ClayLoading	-0.0005	0.000	-2.855	0.007	**

Significance Codes: '***': 0-0.001, '**': 0.001-0.01, '*': 0.01-0.05, '.':0.05-0.1, ' ': 0.1-1.0

C.1.2 First Peak Stress (FPS)

Table C.3: ANOVA results for first peak stress (FPS) for the tensile testing DoE.

	Sum Sq	Df	F-value	Pr(>F)	ω^2	
Intercept	3005.562	1.0	2446.243	$1.554e^{-32}$	0.944	***
ClayType	0.141	2.0	0.057	$9.442e^{-01}$	-0.0007	
MouldingMethod	19.087	1.0	15.535	$3.972e^{-04}$	0.006	***
Site	103.756	2.0	42.224	$7.999e^{-10}$	0.032	***
ClayLoading	12.526	1.0	10.195	$3.090e^{-03}$	0.004	**
Residual	40.545	33.0	NaN	NaN	NaN	

Significance Codes: '***': 0-0.001, '**': 0.001-0.01, '*': 0.01-0.05, '.':0.05-0.1, ' ': 0.1-1.0

Table C.4: Linear model results for first peak stress (FPS) for the tensile testing DoE.

Nr. Observations	40	R-squared		0.874	
Df Residuals	33	Adjusted R-squared		0.851	
Df Model	6	F-statistic		38.03	
		Residual Standard Error		1.108	
	Estimate	Std. Error	t-value	Pr(> |t|)	
Intercept	26.0513	0.527	49.460	0.000	***
ClayType[T.DHT4A]	-0.1061	0.374	-0.283	0.779	
ClayType[T.Neat]	0.0860	0.705	0.122	0.904	
MouldingMethod[T.Injection]	-1.8696	0.474	-3.941	0.000	***
Site[T.TUT]	1.0404	0.551	1.889	0.068	.
Site[T.UP]	4.4993	0.500	8.998	0.000	***
ClayLoading	-0.1912	0.060	-3.193	0.003	**

Significance Codes: '***': 0-0.001, '**': 0.001-0.01, '*': 0.01-0.05, '.':0.05-0.1, ' ': 0.1-1.0

C.1.3 Elongation at FPS

Table C.5: ANOVA results for elongation at FPS for the tensile testing DoE.

	Sum Sq	Df	F-value	Pr(>F)	ω^2	
Intercept	253.890	1.0	1006.001	$2.675e^{-26}$	0.859	***
ClayType	0.588	2.0	1.165	$3.244e^{-01}$	0.0003	
MouldingMethod	20.953	1.0	83.023	$1.577e^{-10}$	0.070	***
Site	5.827	2.0	11.545	$1.581e^{-04}$	0.018	***
ClayLoading	5.337	1.0	21.149	$5.986e^{-05}$	0.017	***
Residual	8.328	33.0	NaN	NaN	NaN	

Significance Codes: '***': 0-0.001, '**': 0.001-0.01, '*': 0.01-0.05, '.':0.05-0.1, ' ': 0.1-1.0

Table C.6: Linear model results for elongation at FPS for the tensile testing DoE.

Nr. Observations	40	R-squared	0.904
Df Residuals	33	Adjusted R-squared	0.887
Df Model	6	F-statistic	51.87
		Residual Standard Error	0.502

	Estimate	Std. Error	t-value	Pr(> |t|)	
Intercept	7.5716	0.239	31.718	0.000	***
ClayType[T.DHT4A]	-0.1627	0.170	-0.959	0.345	
ClayType[T.Neat]	-0.4359	0.320	-1.364	0.182	
MouldingMethod[T.Injection]	1.9589	0.215	9.112	0.000	***
Site[T.TUT]	-0.0265	0.250	-0.106	0.916	
Site[T.UP]	-1.0888	0.227	-4.804	0.000	***
ClayLoading	-0.1248	0.027	-4.599	0.000	***

Significance Codes: '***': 0-0.001, '**': 0.001-0.01, '*': 0.01-0.05, '.':0.05-0.1, ' ': 0.1-1.0

C.1.4 Elongation at Break

Table C.7: ANOVA results for elongation at break for the tensile testing DoE.

	Sum Sq	Df	F-value	Pr(>F)	ω^2	
Intercept	2.244e+05	1.0	3.377	0.084	0.039	.
ClayType	2.334e+05	2.0	1.755	0.203	0.025	
MouldingMethod	1.840e+06	1.0	27.687	0.000064	0.438	***
Site	5.509e+05	2.0	4.144	0.034	0.103	*
ClayLoading	6.094e+03	1.0	0.092	0.766	-0.015	
Residual	1.130e+06	17.0	NaN	NaN	NaN	

Significance Codes: '***': 0-0.001, '**': 0.001-0.01, '*': 0.01-0.05, '.':0.05-0.1, ' ': 0.1-1.0

Table C.8: Linear model results for elongation at break for the tensile testing DoE.

Nr. Observations	24	R-squared		0.733	
Df Residuals	17	Adjusted R-squared		0.639	
Df Model	6	F-statistic		7.775	
		Residual Standard Error		257.815	
	Estimate	Std. Error	t-value	Pr(> |t|)	
Intercept	262.8967	143.069	1.838	0.084	.
ClayType[T.DHT4A]	47.2624	121.273	0.390	0.702	
ClayType[T.Neat]	-329.0666	194.613	-1.691	0.109	
MouldingMethod[T.Injection]	1118.6623	212.598	5.262	0.000	***
Site[T.TUT]	-577.3708	264.850	-2.180	0.044	*
Site[T.UP]	-214.4825	116.604	-1.839	0.083	.
ClayLoading	-5.7233	18.902	-0.303	0.766	

Significance Codes: '***': 0-0.001, '**': 0.001-0.01, '*': 0.01-0.05, '.':0.05-0.1, ' ': 0.1-1.0

C.2 Sample Mould DoE

C.2.1 Young's Modulus

Table C.9: ANOVA results for Young's Modulus for the tensile sample mould DoE.

	Sum Sq	Df	F-value	Pr(>F)	ω^2	
Intercept	$3.174e^{+06}$	1.0	136.965	$1.154e^{-10}$	0.787	***
ClayType	$1.241e^{+04}$	2.0	0.268	$7.677e^{-01}$	-0.009	
MouldType	$2.056e^{+05}$	1.0	8.870	$7.168e^{-03}$	0.046	**
ClayLoading	$1.023e^{+05}$	1.0	4.415	$4.787e^{-02}$	0.020	*
Residual	$4.867e^{+05}$	21.0	NaN	NaN	NaN	

Significance Codes: '***': 0-0.001, '**': 0.001-0.01, '*': 0.01-0.05, '.':0.05-0.1, ' ': 0.1-1.0

Table C.10: Linear model results for Young's Modulus for the tensile sample mould DoE.

Nr. Observations	26	R-squared		0.430	
Df Residuals	21	Adjusted R-squared		0.322	
Df Model	4	F-statistic		3.967	
		Residual Standard Error		152.24	
	Estimate	Std. Error	t-value	Pr(> |t|)	
Intercept	917.3448	78.384	11.703	0.000	***
ClayType[T.DHT4A]	36.1812	62.492	0.579	0.569	
ClayType[T.Neat]	-35.9247	130.759	-0.275	0.786	
MouldType[T.ISO 1BA]	179.0038	60.103	2.978	0.007	**
ClayLoading	22.1186	10.527	2.101	0.048	*

Significance Codes: '***': 0-0.001, '**': 0.001-0.01, '*': 0.01-0.05, '.':0.05-0.1, ' ': 0.1-1.0

C.2.2 First Peak Stress (FPS)

Table C.11: ANOVA results for first peak stress (FPS) for the tensile sample mould DoE.

	Sum Sq	Df	F-value	Pr(>F)	ω^2	
Intercept	2128.521	1.0	3588.250	$5.851e^{-25}$	0.990	***
ClayType	0.327	2.0	0.276	$7.618e^{-01}$	-0.0004	
MouldType	4.341	1.0	7.318	$1.326e^{-02}$	0.002	*
ClayLoading	3.403	1.0	5.737	$2.602e^{-02}$	0.001	*
Residual	12.457	21.0	NaN	NaN	NaN	

Significance Codes: '***': 0-0.001, '**': 0.001-0.01, '*': 0.01-0.05, '.':0.05-0.1, ' ': 0.1-1.0

Table C.12: Linear model results for first peak stress (FPS) for the tensile sample mould DoE.

Nr. Observations	26	R-squared		0.412	
Df Residuals	21	Adjusted R-squared		0.299	
Df Model	4	F-statistic		3.671	
		Residual Standard Error		0.770	
	Estimate	Std. Error	t-value	Pr(> |t|)	
Intercept	23.7540	0.397	59.902	0.000	***
ClayType[T.DHT4A]	0.1801	0.316	0.570	0.575	
ClayType[T.Neat]	-0.2016	0.662	-0.305	0.764	
MouldType[T.ISO 1BA]	0.8225	0.304	2.705	0.013	*
ClayLoading	-0.1276	0.053	-2.395	0.026	*

Significance Codes: '***': 0-0.001, '**': 0.001-0.01, '*': 0.01-0.05, '.':0.05-0.1, ' ': 0.1-1.0

C.2.3 Elongation at FPS

Table C.13: ANOVA results for elongation at FPS for the tensile sample mould DoE.

	Sum Sq	Df	F-value	Pr(>F)	ω^2	
Intercept	348.425	1.0	2431.171	$3.392e^{-23}$	0.979	***
ClayType	1.014	2.0	3.537	$4.743e^{-02}$	0.002	**
MouldType	0.000	1.0	0.001	$9.769e^{-01}$	-0.0004	
ClayLoading	3.098	1.0	21.618	$1.377e^{-04}$	0.008	***
Residual	3.010	21.0	NaN	NaN	NaN	

Significance Codes: '***': 0-0.001, '**': 0.001-0.01, '*': 0.01-0.05, '.':0.05-0.1, ' ': 0.1-1.0

Table C.14: Linear model results for elongation at FPS for the tensile sample mould DoE.

Nr. Observations	26	R-squared		0.601	
Df Residuals	21	Adjusted R-squared		0.525	
Df Model	4	F-statistic		7.915	
		Residual Standard Error		0.379	
	Estimate	Std. Error	t-value	Pr(> |t|)	
Intercept	9.6106	0.195	49.307	0.000	***
ClayType[T.DHT4A]	-0.4126	0.155	-2.655	0.015	*
ClayType[T.Neat]	-0.2806	0.325	-0.863	0.398	
MouldType[T.ISO 1BA]	0.0044	0.149	0.029	0.977	
ClayLoading	-0.1217	0.026	-4.649	0.000	***

Significance Codes: '***': 0-0.001, '**': 0.001-0.01, '*': 0.01-0.05, '.':0.05-0.1, ' ': 0.1-1.0

C.2.4 Elongation at Break

Table C.15: ANOVA results for elongation at break for the tensile sample mould DoE.

	Sum Sq	Df	F-value	Pr(>F)	ω^2	
Intercept	$1.430e^{+06}$	1.0	25.130	0.002	0.565	**
ClayType	$1.085e^{+05}$	2.0	0.954	0.430	-0.002	
MouldType	$4.253e^{+05}$	1.0	7.476	0.029	0.152	*
ClayLoading	$9.388e^{+03}$	1.0	0.165	0.697	-0.020	
Residual	$3.983e^{+05}$	7.0	NaN	NaN	NaN	

Significance Codes: '***': 0-0.001, '**': 0.001-0.01, '*': 0.01-0.05, '.':0.05-0.1, ' ': 0.1-1.0

Table C.16: Linear model results for elongation at break for the tensile sample mould DoE.

Nr. Observations	12	R-squared		0.541	
Df Residuals	7	Adjusted R-squared		0.278	
Df Model	4	F-statistic		2.059	
		Residual Standard Error		238.521	
	Estimate	Std. Error	t-value	Pr(> |t|)	
Intercept	1411.8641	281.642	5.013	0.002	**
ClayType[T.DHT4A]	21.3143	157.935	0.135	0.896	
ClayType[T.Neat]	-333.4609	274.181	-1.216	0.263	
MouldType[T.ISO 1BA]	-564.8989	206.604	-2.734	0.029	*
ClayLoading	-10.7679	26.507	-0.406	0.697	

Significance Codes: '***': 0-0.001, '**': 0.001-0.01, '*': 0.01-0.05, '.':0.05-0.1, ' ': 0.1-1.0

C.3 Impact Testing DoE

C.3.1 Impact Strength

Table C.17: ANOVA results for impact strength for the Charpy impact testing DoE.

	Sum Sq	Df	F-value	Pr(>F)	ω^2	
Intercept	0.203	1.0	832.240	$2.846e^{-21}$	0.802	***
ClayType	0.004	2.0	8.438	$1.500e^{-03}$	0.014	**
MouldingMethod	0.037	1.0	149.893	$2.684e^{-12}$	0.144	***
Site	0.002	2.0	4.044	$2.956e^{-02}$	0.006	*
ClayLoading	0.0005	1.0	2.208	$1.493e^{-01}$	0.001	
Residual	0.006	26.0	NaN	NaN	NaN	

Significance Codes: '***': 0-0.001, '**': 0.001-0.01, '*': 0.01-0.05, '.':0.05-0.1, ' ': 0.1-1.0

Table C.18: Linear model results for impact strength for the Charpy impact testing DoE.

Nr. Observations	33	R-squared		0.917	
Df Residuals	26	Adjusted R-squared		0.898	
Df Model	6	F-statistic		47.78	
		Residual Standard Error		0.0156	
	Estimate	Std. Error	t-value	Pr(> |t|)	
Intercept	0.2543	0.009	28.849	0.000	***
ClayType[T.DHT4A]	0.0223	0.006	3.820	0.001	**
ClayType[T.Neat]	0.0264	0.011	2.471	0.020	*
MouldingMethod[T.Injection]	-0.0946	0.008	-12.243	0.000	***
Site[T.TUT]	0.0211	0.008	2.737	0.011	*
Site[T.UP]	0.0059	0.008	0.725	0.475	
ClayLoading	0.0014	0.001	1.486	0.149	

Significance Codes: '***': 0-0.001, '**': 0.001-0.01, '*': 0.01-0.05, '.':0.05-0.1, ' ': 0.1-1.0